

**WEATHERING AND SOIL PROPERTIES ON OLD GRANITIC CATENAS
ALONG CLIMO-TOPOGRAPHIC GRADIENTS IN KRUGER NATIONAL
PARK**

**By
LESEGO KHOMO**

**A dissertation submitted to the Faculty of Science, University of the Witwatersrand,
Johannesburg, South Africa, in partial fulfillment of the requirements for the degree
Doctor of Philosophy**

Johannesburg 2008

DECLARATION

I declare that this dissertation is my unaided work being submitted for the degree of Doctor of Philosophy in the University of the Witwatersrand, Johannesburg. It has not been submitted elsewhere for any degree or examination.

_____ Day of _____, 2008

ACKNOWLEDGEMENTS

This project was funded by the Andrew W. Mellon Foundation. Thanks to South African National Parks for granting permission to work in the Kruger National Park.

I am grateful to:

- Professor Kevin Rogers, Dr Anthony Hartshorne and Professor Oliver Chadwick, my supervisors. Kevin introduced me to catenas and sodic sites in Nylsvlei all that time ago and has put up with me since 1999. Tony has been a constant inspiration since the beginning, and I owe him so much. Oliver's help, especially most of this year since April can't be repaid, and I thank him for making me one of his priorities.
- Wendy Midgley for all the support needed to help me concentrate on the research aspect of the degree. And the rest of the CWE.
- Melissa Parsons for encouraging help and motivational speeches during my MSc into the PhD.
- Members of the Geography department in Santa Barbara and the whole UCSB campus where I has privilege to spend time. I am very thankful to all the UCSB students and staff who helped with labwork, Val Bullard, Natalie Boes, Kevin Braton, and Katie Lindenburg.
- Game guards Wilsonii Dinda, Million Cossa and Samuel Nkuna for protection in the field.
- All my field assistants for help digging soils.
- South African Wildlife College for accommodation during fieldwork.
- My Family, my mother Shirley Khomo, my brother Kgomotso, my granny Mapheleki and all my uncles, aunts and cousins.

VITA OF LESEGO KHOMO

Born in Tladi, Soweto, 26 August 1977

Ph. D. in Soil Science, U. Witwatersrand, South Africa, 2003-present
M.Sc. in Botany (With distinction), U. Witwatersrand, South Africa, 2003
B.Sc. (Hons.) (First class) in Botany, U. Witwatersrand, South Africa, 1999
B.Sc. in Botany and Zoology, U. Witwatersrand, South Africa, 1998

Grants and awards

2000-2001 National Research Foundation Prestigious merit award for M.Sc.
1999 National Research Foundation merit award for B.Sc. (Hons.), U.
Witwatersrand Postgraduate merit award, Certificate of first class, Plant
ecology award

Publications

L. Khomo and K.H. Rogers. Proposed mechanism for the origin of sodic patches in Kruger National Park, South Africa. *African journal of Ecology* 43(1), 29-34, 2005

L. Khomo. The influence of geomorphic gradients on physical and vegetation heterogeneity in a savanna drainage network. M.Sc. thesis, U. Witwatersrand, 2003

L. Khomo. Spatial distribution of patch types and change in their landscape position between 1942 and 1989 along the Phugwane River drainage network, northern Kruger National Park, B.Sc. (Hons.) thesis, U. Witwatersrand, 1999

L. Khomo and K.H. Rogers. Stream order controls geomorphic heterogeneity and plant distribution in a savanna landscape, *Austral Ecology*, in press, 2008

Employment

Research assistant in the Geography department, University of California, Santa Barbara.
Teaching Assistant in the APES department, U. Witwatersrand.

ABSTRACT

Weathering and soil properties on old granitic catenas along climo-topographic gradients in Kruger National Park

By

Lesego Khomo

Catenas, the geomorphologically and hydrologically linked soils on hillslopes between crests and toeslopes, are arguably the best heuristic tool to underpin pedological work for understanding soil landscape evolution. Under this pretext, I investigated the expression of soil forming factors in shaping weathering and soil development in Kruger National Park's diverse granitic landscapes. The quantitative investigations in four data chapters are preceded by narrative on how the soil landscape can most compellingly be viewed in pedological research. This synthetic perspective provides an interdisciplinary framework derived from the fusing long-standing pedological, geological and geomorphological thinking. Briefly, the framework articulates (1) the origin and fate of rock derived soil constituents; (2) how those constituents, primarily clay minerals and soil's dissolved load, interact and react to the soil forming factors *viz.* climate, rock type and topography and (3) the distribution of soil properties along gradients of soil forming factors.

My field sites were located in Kruger National Park, on the eastern seaboard of South Africa, nestled between the Great Escarpment to the west and the Lebombo Mountains to the east along the Mozambican border. Kruger affords an opportune test-case to study the interaction of climate, topography and geology on soil landscape patterns in a model ecosystem that acts as a natural laboratory. Kruger functions as a model ecosystem for earth scientists because

physiographic gradients are well demarcated and can be studied iteratively by focusing on the variation in one gradient while others are kept constant. For example, the north-south axis of the park separates granite from basalt; and rainfall increases from north to south. Therefore the park has four well-bounded blocks within which the interaction of rainfall and geology can be investigated. Also, the influence of rainfall on soil properties can be isolated by fixing geology and varying climate, as illustrated in the first data chapter of the thesis.

There, I used new and established tools to set boundaries on granitic weathering and soil development. In addition to constraining geology along the 400 to 700 mm mean annual rainfall gradient, the topographic dial on weathering was also set to zero by restricting sampling to crest soils. In this way, the sole impact of increasing rainfall on weathering and soil development was examined in exclusion of added complications imposed by geology and topography. Results suggested by geochemical mass balance, cosmogenic ^{10}Be concentrations as an erosion proxy, soil exchange properties and clay amount and mineralogy all demonstrated indiscriminant loss of rock-derived constituents as rainfall increases from north to south. This means that granitic crests in Kruger are losing material under all climatic regimes, from dry in the north to wet in the south. The next question then was: what is the destiny of the material lost from crests? Does the material remain on the catenas or is it lost to the rivers for transport towards the ocean? How are the patterns different on catenas in distinct topographic contexts? These questions were the subjects of subsequent chapters in the thesis.

Therein, analyses for crests were extended to capture patterns between those crests and toeslopes across three relief classes in each of three climate zones for a nested matrix of nine catenas. Material removal from crest soils was evident across all nine catenas, but was nuanced by depletion and accumulation zones whose extents were context-dependent within the topo-

climatic matrix. Depletion zones invariably occurred at or near crests whereas accumulation zones were near toeslopes in all catenas across climate and relief. Depletions were most expressed by base cation and silicon losses while zones of accumulation were of heightened concentrations of aluminium and titanium. In terms of concrete soil properties, the depleted soils were clay-poor with low exchangeable base cation concentrations whereas soils at distal ends of catenas were high in both clay and exchangeable base cations. These general patterns were modified by the amount of rainfall and hillslope relief. Clay-rich zones were narrow in both high and low rainfall areas but widest at intermediate rainfall. Similarly with relief, it appeared that intermediate steepness facilitated the retention of material on catenas. Hence, coupled rainfall-topography interactions provide a thrust on material transfers on catenas resulting in a spectrum of catena types across gradients in soil forming factors. Hence, the catena is far from the static entity it is commonly imagined to be, but is dynamic if quantified across gradients of variation in soil forming factors.

TABLE OF CONTENTS

Abstract		v
Chapter 1	Introduction.....	1
Chapter 2	Weathering and soil properties on crests in arid to semi-arid Kruger National Park.....	23
Chapter 3	Clay and base cation distribution along catenas in different climo-topographic settings of Kruger National Park.....	66
Chapter 4	Chemical mass balance on geologically complex catenas along gradients of relief and climate I: parent material and index element choice.....	129
Chapter 5	Chemical mass balance on geologically complex catenas along gradients of relief and climate II: strain and major element loss/gain.....	167
Chapter 6	Conclusions.....	200
References		211

CHAPTER 1: INTRODUCTION

1. DISTRIBUTION OF SOIL PROPERTIES IN LANDSCAPES

Soil preserves a record of landscape evolution and climate that can be interpreted by quantifying numerous chemical and physical properties accumulated in soil profiles. This thesis investigates variations in soil properties developed on ancient catenas along gradients of arid to semi-arid climate and topography in Kruger National Park. Weathering extent is a soil property that indexes the degree to which soil mineral chemistries diverge from the chemistry of soil's parent material, which can either be the underlying rock, exogenous material such as dust, or a combination. Departures of soil from parent material composition are a function of how appreciably soil has evolved away from its starting material. The divergence of soil from its mineral precursors in parent material is mediated by soil forming factors such as climate and topography which vary geographically (Jenny, 1941), and serve to modify the intensity of soil forming processes, such as chemical weathering and leaching (Bridges, 1978). Consequently, weathering extent and the emergence of unique soil properties will vary spatially in landscapes by geographic location.

Hillslopes are a convenient scale to view locally interacting factors and processes that impinge on soil formation because they are delimited by a hillcrest and a basal stream. Beyond the boundaries demarcated by crests and streams, hydrological connectivity ceases. The predictable relationship among soils that make up a hydrologically connected hillslope is defined as a catena (Milne, 1935). A catena is a series of physically, chemically and morphologically distinct soils on a hillslope linked by topographically mediated transfers of material. This study analyzes differences in local soil patterns along catenas sampled from different topographic and climatic settings in Kruger National Park. Since effective moisture,

slope length and hillslope relief control the amount of water and mass transmitted through catenas, the central question is how weathering and soil properties change along catenas in different relief classes across an arid to semi-arid climate gradient. Answering this question will enhance understanding of pedogenesis and landscape evolution pathways in arid and semi-arid climates underlain by granite and inform efforts to conserve and manage them.

Kruger National Park lies across a north-to-south climate gradient whose western half is predominantly underlain by granitoid lithologies (Barton et al., 1986) upon which topographic variation is limited by relatively quiescent tectonics (Partridge and Maud, 1987) and the plant community is savanna (Gertenbach, 1983). Such constrained controls on soil development enable us to isolate specific variables for study while others remain constant. Thus the main objective of this study is to understand the role of climate and topography in determining pedological patterns as they are distributed across Kruger National Park.

1.1 The nature of soil

The nature of soil requires multidisciplinary research for a full comprehension of its complexity, and there has been recent advocacy for such approaches (Brantley et al., 2007). Fragmentary views will always fail to garner overarching understanding of soil complexity and will thereby limit integrated views on how soil develops and is spatially arranged in landscapes. The disciplinary framework in this study therefore spans soil science, geomorphology and geology to more effectively probe and explain complexities in soil landscapes.

Soil is complex because it forms at the boundary of the lithosphere, atmosphere, hydrosphere and biosphere (Brady and Weil, 2002), the interface recently termed the Critical Zone, due to its importance for the functioning of terrestrial ecosystems (Chorover et al.,

2007). Soil is a multiphase mixture of solids derived from primary minerals in the lithosphere; gases unique from and continuous with the atmosphere; water containing dissolved and suspended material; and organisms and their by-products. Soil complexity can hence best be understood in the context of geological material open to spatially heterogeneous biological, hydrological and geochemical exchanges at the Earth's surface.

Inputs to soil are via addition of organic matter, rain water, rock-derived minerals, plus atmospheric deposition of gaseous and particulate matter. Outputs from soil occur by physical erosion, leaching of solutes and colloids, incorporation of soil constituents into biomass and emission of volatiles to the atmosphere. Therefore, the complex nature of soil requires many cross-disciplinary excursions including an appreciation of the geological inheritance of soil and the role that geomorphic setting plays in determining water flow through soil landscapes.

1.2 Scales of soil variation

There are various scales at which patterns in soil property distribution emerge in landscapes. Variations span microscopic (micrometers) to vast regional (square kilometers) scales. To yield pedological utility, an investigation must take place at scales commensurate with the spatial domains of pedological pattern. In this study, research questions pertain to changes in weathering and soil properties on catenas as influenced by differences in climate and topography. Therefore, the spatial domain encompasses scales where topographic and climatic variations are expressed in soil properties. Consequently, the study's spatial domains are: (1) Kruger National Park at the broadest scale for which climate varies; (2) the drainage network at which scale hillslope relief varies *viz.* high and low relief hillslopes in the upper and lower reaches of drainage networks respectively; (3) the catena for which there is rising

contributing area with increased distance from crest; (4) the pedon in which soil properties and weathering vary with depth and (5) the soil horizon at the smallest scale which demarcates the unit for measuring soil properties in the study. Between the extremes of Kruger National Park and a soil horizon, patterns in weathering extent and soil properties are governed by factors of soil formation that lead to differences in the intensity of soil forming processes.

1.3 Organization of soil

A soil profile is composed of near-horizontal layers (horizons) distributed vertically from the soil surface to rock or sediment, a differentiation driven by vertical penetration of biotic products and percolation of water. Thus, the gradual transition from soil to rock coincides with lower concentrations of clay and organic matter and more gravel to cobble size rock material. Not all soil processes lead to strong horizonation. For example, horizons can be destroyed by biological mixing; too much water flowing through a soil can lead to uniformly leached horizons and limited water flux can arrest soil formation leading to indistinct horizon development.

An individual soil profile lies in a mosaic of others indexed by a measure referencing its location between a crest and basal stream *e.g.* distance from crest or upslope contributing area. A single catena is part of a drainage network of streams ranging from small depressions in headwaters to progressively larger channels downstream. In the context of hydrological fluxes along hillslopes, catena properties vary with topographic attributes such as slope gradient, relief, catchment size, *etc.* The soil landscape thus cascades in scale from a horizon, to a soil profile, to a series of profiles coalescing into pattern at the catena scale, to a

spectrum of catenas abutting streams at bigger scales and to drainage networks in different climate zones.

1.4 Soil differentiation

Horizon properties themselves suggest mechanisms for profile differentiation through intra-profile processes. These inter-horizon processes operate vertically from surface soil to rock in response to infiltrating water. Gravity induces water to percolate through the soil skeleton bearing a load of dissolved and colloidal material, which are removed from near-surface horizons and re-deposited as plasma at depth resulting in horizonation or soil profile differentiation. The pattern of soil profiles down a catena likewise is linked by downslope water flow that redistributes mass as solution or colloidal flow.

The degree to which a soil profile or catena are differentiated from the source-rock is a function of soil forming processes and pedological state factors, which are scale dependent. For example, at the hillslope scale, geology is generally uniform from crest to base, but at larger scales, geology shapes weathering and soil properties on geo-topographic platforms in landscapes.

2. CONTROLS ON WEATHERING AND SOIL PROPERTIES BY PARENT MATERIAL AND TOPOGRAPHY

The intensity of material fluxes across catenas depends on parent material and topography which are in turn ultimately shaped by tectonic activity. Variation in tectonic forcing on continents leads to geo-tectonic soil provinces distinguished by dominant lithospheric material, seismicity, volcanism and topography (Paton et al., 1995). Thick soil

develops on continental plate centres characterized by low seismicity, low volcanism, gentle topography and granitic rock. In the absence of significant geothermal control, topography and rock type emerge as major thrusts on pedogenesis and soil landscape evolution. Since Kruger is set in a continental interior with low seismicity, weathering and soil properties there will hinge primarily on juxtaposed climate, parent material and topographic variation.

2.1 Parent material control

Parent material is the raw input of primary minerals for pedogenesis at time zero (Schaetzl and Anderson, 2005). The parent material of a soil may be rock, dust, alluvium or another soil. A soil inherits its parent material's primary minerals, chemistry and physical properties. These parent material attributes become initial soil properties until the soil is divorced from its genetic origin by soil forming processes. For example, coarse-grained granite produces an initially coarse-grained soil. However, mobilization and illuviation of plasma may modify a downslope soil's granitic inheritance by supplementing it with material from upslope. Felsic landscapes exemplify the discrepancy between soil and parent material far more than other geo-terrains. If downslope illuviation occurs on a mafic catena, for example, extra plasma downslope will not result in a sharp texture contrast because the soil was clay-rich to begin with. In granite, by contrast, a coarse matrix aids relatively unimpeded movement of plasma through pores down soil profiles and laterally across catenas. Therefore granitic landscapes are ideal for studying catena differentiation in various factorial contexts because potential clay augmentation is most readily identified in coarse-grained lithologies.

But within granite itself, soil development is nuanced by internal heterogeneity in rock composition which alters the degree of catena differentiation. Rock variation is

pervasive in landscapes and occurs even in apparently uniform stretches. Often, landscapes are in reality compositionally heterogeneous at scales too fine for most geological maps.

2.2 Topographic control

Weathering on a geologically varied catena culminates in relief as a result of localized differences in rock resistance. Relief is thus partly due to variation in geology as evident in hillcrests underlain by resistant rocks and down-warn toeslopes underlain by more susceptible rocks. Scholten et al. (1997) show that soils in high-lying ground are rich in resistant K-feldspar relative to easily weathered plagioclase. Therefore, geology plays a crucial role in topographic development and acts as a template for catena differentiation.

Once established, topography is a passive soil forming factor, modifying weathering and soil properties indirectly via its influence on water and mass movements (Jenny, 1941). Topographic variation can be viewed at many scales; ranging from the contrast between inland plateaus and coastal escarpments; to variation in the relief of a drainage network's stream-catena systems and to the topographic contrasts on a hillslope between crest and toeslope. Geomorphic changes along the cross section of a hillslope induce material transfers down gradients of decreasing potential energy from high to low ground, whether liquid, solute, plasma or solid. Therefore in addition to the genetic link that a soil has with its underlying parent material, the soil can also have a hydrological link with an upslope soil through material redistribution mediated by topography.

Geo-topographically controlled variation in soil properties on hillslopes forms regular and repeated catena patterns from crest to toeslope (Milne, 1935). Greene (1947) saw the catena's resemblance to a soil profile rotated to its side in how soils down a profile or catena are hydrologically connected. Milne acknowledged the veracity of geologic variation in

landscapes and suggested there should be catenas developed on uniform parent and those traversing various geologies (Milne, 1935). He attributed catena differentiation to translocation of plasma and solutes, as well as particulate transport by soil erosion. Thus, unlike most of his North American contemporaries, who viewed the soil-topography relationship as a curious modifier of climatic control, Milne recognized the geomorphic process of erosion as central to pedogenesis (Brown, 2006). Far from being surrogate to climate in controlling weathering and soil properties, topography and geology are the template upon which climate acts.

3. IMPACT OF CLIMATE AND TIME ON WEATHERING THE GEO- TOPOGRAPHIC TEMPLATE

The control that climate exerts on weathering and soil properties was first highlighted by the pedological pioneer, Prof. Vasily Dokuchaev's observation of rainfall induced morphological changes in Russian chernozems (Humphreys and Wilkinson, 2007). Global variation in rainfall provides another instance of climate's significance for soil formation and properties. For example, in the Atacama Desert, where annual rainfall dips below 21 mm, weathering and soil formation almost cease as a result of insufficient acid inputs into soil due to low plant cover and persistence (Ewing et al., 2006). By contrast, when rainfall approaches 4000 mm annually, soil becomes so weathered and nutrient-depleted that exogenous inputs like dust must compensate the limited reserves to support normal plant growth (Vitousek, 2002). Outside these spectacular minima and maxima in global rainfall distribution, climate's influence on weathering and soil properties is less dramatic, but occurs nonetheless. Under arid to semi-arid rainfalls exceeding 100 mm but less than 1000 mm, soils carry the imprint of balancing dry and wet conditions in sporadic episodes that may be short or long lasting.

This balance results in some of the most well differentiated soil profiles and catenas (Young, 1976), examples of which are presented in this study.

In flat landscapes where topography bears minimal control over soil formation and properties, rainwater falls uniformly across the land. More commonly though, water falling on the geo-topographic template is partitioned and routed through catenas resulting in water-shedding crests and water basins at the toeslopes. The relative proportions of collector and shedder zones on a catena will depend on long-term climate. Where water is abundant, the collector zone will be smaller than the shedding zone because material is forced further downslope. At some threshold in water availability, both collector and shedder zones occur, and this threshold represents Young's (1976) proposed maximum catena expression to be found in semi-arid areas.

3.1 Time intensifies factor impact

The footprint of climate and other soil forming factors requires time to be fully expressed. Time intensifies signatures of climate, geology and relief in soil landscapes. At time zero, soil resembles the raw assemblage of water, plant material and rock, and is not the emergent product of these ingredients. Once weathering has begun along gradients of soil forming factors in catenas, soil age determines weathering extent and soil properties.

The relative youth of soil landscapes, as compared to underlying bedrock age, is due to erosion and/or burial, which episodically reset time zero for pedogenesis. Exhumed surfaces and deposits act as fresh substrate on which new cycles of weathering and soil production begin (Schaetzl and Anderson, 2005). Age is thus the time taken to form a soil where erosion and deposition are slower than the rate of soil production. Soils on a catena thus cannot be given an absolute and uniform age because erosion and deposition rejuvenate

them (Yoo et al., 2005). In Hawaii's Kauai island for example, only 2 % of a 4 Ma landscape is preserved on the original basalt, with most reworked by erosion and deposition many times (Porder et al., 2005). Thus the geomorphic processes of erosion and deposition complicate soil age determination.

Soil age determination on hillslopes, which form the vast majority of terrestrial surfaces, has been improved greatly by advanced mass spectrometry able to measure minute concentrations of cosmogenic isotopes (Heimsath et al., 1997). Cosmogenic nuclide analysis records the long-term exposure age and erosion rates of Earth surfaces (Cockburn and Summerfield, 2004). When cosmic rays encounter mineral-bound oxygen, $^{10}\text{beryllium}$ is produced and accumulates as a function of its production, decay and removal via erosion (Bierman and Clapp, 1996; Heimsath et al., 1999). Soil production rate is measured by quantifying ^{10}Be concentration at the soil-saprolite interface which can be used to provide an erosion rate and a soil residence time. Hence, soil age can be constrained in eroding landscapes to isolate the impact of soil forming factors on weathering and soil properties.

4. WEATHERING AND DIFFERENTIAL ELEMENT MOBILITY ON CATENAS

Once the factorial and process dynamics of a catena have been established, the flux of rock-derived elements downslope by mass, solute and colloidal transport controls soil horizon differentiation. For example, a clay-rich soil has a higher proportion of aluminium than a clay-depleted soil. Hence a catalogue of major element composition from crest to base can be interpreted in the context of depletion and accumulation zones of a catena and compared across gradients of soil forming factors.

The release of an element from primary minerals and its subsequent flux through soil are due to the element's interaction with water (Birkeland, 1999). If attraction to water's O^{2-}

is weak as in sodium, the ion is engulfed by water, remains in solution, and is leached from soil. If attraction to O^{2-} is strong as in iron, hydrogen is expelled from the water molecule and the element precipitates as a hydroxide e.g. $FeOOH$. Ionic potential (IP), the ratio of valence charge to radius in Angstroms, can be used to predict an element's behavior in soil. Elements with an IP between 4 and 10 \AA such as Si, Al and Fe will hydrolyze water creating relatively insoluble hydroxides or oxyhydroxides. Aluminium has an IP of 6 \AA and is immobilized as gibbsite or clay, but is mobile in acid soil and where organic ligands abound. Ferric iron has an IP of 4 \AA and precipitates as ferrihydrite, hematite or goethite, and as with Al, Fe is mobile in the presence of organic chelates or in acid soil. Reduced Fe has an IP of 2 \AA and is thus relatively mobile. Silicon has an IP of 9 \AA and precipitates as opal or forms clay minerals. Silicon is mobile even under neutral pH due to its greater electropositivity compared with Al and Fe. Larger, low-charge ions, with IP's less than 4 \AA , are maintained in solution by hydrated shells and are relatively mobile (Railsback, 2003). These include Ca, Mg, K and Na. Their low charge density precludes formation of stable mineral complexes; rather they attract shells of water which keep them soluble under neutral and acid conditions. Calcium precipitates as carbonate under alkaline conditions and magnesium substitutes into 2:1 clays under neutral to acid conditions.

Therefore, IP determines how easily an element leaches once released from primary minerals and the element's interaction with other soil material alters its fate in soil profiles and catenas. A typical scenario on a catena is mobile element depletion in crest positions and additions downslope. Quantifying these redistributions requires mass balance approaches that provide specific indexing of elements to parent material concentrations and correct for volume changes occurring during pedogenesis.

4.1 Geochemical mass balance

Geochemical mass balance quantifies weathering by exploiting the incongruent weathering of primary minerals which fractionates the ratio of immobile to mobile elements by loss of low IP mobile elements (Brimhall and Dietrich, 1987). Parent material has both weatherable and resistant minerals, and the mass of resistant minerals remains constant as weatherable minerals are lost. On the basis of volume change and parent material composition, the mass change of any rock-derived element due to chemical weathering can be calculated (Birkeland, 1999; Brimhall et al., 1991). Geochemical mass balance is thus enabled by the split fates of rock-derived elements following their release from primary minerals into soil. As chemical weathering proceeds, the concentration of elements housed in resistant minerals is residually increased relative to their concentration in rock (Muir and Logan, 1982). By contrast, elements that reside in soluble minerals are depleted relative to concentrations in rock and either accumulate in place or are redistributed elsewhere in the landscape (Sommer et al., 2000). The mass balance of rock forming elements thus provides a quantity for long-term flux of elements in a landscape (Brimhall et al., 1991; Brimhall and Dietrich, 1987). For mass balance to be most effective, parent material has to be absolutely uniform in the soil profile and this may not be the case; and second, some element must be immobile in soil and this is often not so (Stiles et al., 2003). Mass balance quantifies chemical weathering and provides clues about mechanisms responsible for observed distributions of soil properties in different factorial contexts.

5. SOIL PROPERTY DISTRIBUTION ALONG CATENAS IN DIFFERENT CONTEXTS

To illustrate how I will use soil properties recorded at sample locations to interpret weathering and soil formation along gradients of climate, topography and parent material, I use texture, structure and colour for now but consider other properties in subsequent chapters. Soil texture, structure and colour are three of the more self-evident soil properties easily perceived in the field or in hand samples.

Soil texture depends on the relative abundances of sand (2.0-0.05 mm), silt (0.05-0.002 mm) and clay (<0.002 mm) sized particles. The size distribution of particles is originally inherited from parent material and subsequently modified by atmospherically derived dust and chemical weathering, leading to a slow and progressive skewing of the size distribution toward smaller particles. Superimposed on these determinants of soil texture are redistribution processes whereby clays are removed from upper and to lower horizons or from catena apices to low lands.

Texture contrasts among soil horizons generally reflect differences in pedogenic processes (Bridges, 1978), but may also denote biological, geological or geomorphic discontinuities (Schaetzl and Anderson, 2005). For example, bioturbation by macrofaunal agitation of soil may obliterate any horizons resulting in homogenization of texture. Also, mining of fine soil from deep horizons by mesofauna such as termites can also produce a texture contrast in soil (Jones, 1990; Nye, 1955b). In yet other situations, a lithological discontinuity as exists in layered sedimentary rock can be inherited by a soil resulting in texture contrast.

As with texture, systematic changes in soil structure attest to differentiation down a soil profile or along a catena. Structure encapsulates size, shape and integrity of individual

soil aggregates. Structure can range from small granules that disintegrate on touch to hard blocks depending on the carbon content and soil texture (Schoeneberger, 1998). High concentrations of organic matter promote granular structure whereas blocky structure reflects high clay with less organic matter. Since clay tends to accumulate in the distal ends of catenas, strong, blocky structures are common in downslope positions.

Colour is a compound soil property due to relative amounts of soil components such as organic matter, iron oxides, salts such as calcium carbonates and primary minerals. The important colorants in soil are dark brown to black organic matter, red to yellow iron oxides, and whitish salts. By contrast, primary minerals have subdued colours that are only evident under conditions which suppress the more colourful soil components. Overall, soil colour is a balance between the amount of organic matter and the abundance and extent of grain coating by various species of oxidized iron or calcium carbonate. Therefore, parts of a granitic catena with abundant primary minerals in an unweathered state will have the light colours of quartz and feldspar whereas downslope, where organic matter and iron oxides accumulate, soils commonly have darker colours. Soils that lie near water seeps along catenas where redox processes are common have light colours that betray the absence of oxidized iron.

All soil properties have a systematic landscape distribution under factorial (Jenny, 1941) and process domains (Bridges, 1978) specific to the soil's location. If the factors and processes of soil formation are known, weathering and soil properties can be explained. This study presents analyses of chemical weathering, erosion and soil properties in Kruger National Park to unravel how soil forming factors and processes shape soil landscapes.

6. SCOPE AND SCIENTIFIC UTILITY

This thesis provides a detailed account of variations in soil properties on a stable, passive continental margin underlain by ancient granitoid rocks along an arid to semi-arid climate gradient.

Why is this setting important?

- Unlike significant parts of the temperate northern hemisphere where most soil research has been conducted; low elevation tropical areas in much of Africa, Australia and South America escaped ice sheets in the last glacial maximum. Pedogenesis in the northern latitudes often has a time zero under 20 Ka, whereas most austral soils and geomorphic surfaces have been subject to pedogenesis for much longer – in fact I show that the Kruger soils have residence times at least 10 times greater than this. Research on these globally significant soils will provide insights into undocumented pedogenic pathways.
- The field sites in this study are arrayed on an arid to semi-arid climate in the relatively narrow 400-750 mm range of mean annual rainfall. While many climosequences cover sharper gradients in rainfall, recent findings suggest that fundamental thresholds in pedogenesis are breached within narrow MAP ranges (Ewing et al., 2006). In Kruger, the range in rainfall superimposed on gradients in other soil forming factors brackets a suite of pedogenic regimes. The dry end of the rainfall gradient preserves arid pedogenesis while the wet end bears the signatures of intensive leaching on soil development. A critical interval in the rainfall allows maximum expression of catena differentiation at the barrier between arid and semi-arid climate. The rainfall gradient in Kruger and antiquity of its landforms produce what are possibly the most varied

and well-differentiated (“classic”) catenas in the world, and these are yet to be investigated from a purely pedogenic and landscape evolution perspective.

What is the value of this study?

For pedology – The manuscripts generated here will be the first comprehensive catalogue of African catenas across climate and relief using extensive field and laboratory data to describe soil patterns. Catena studies are usually restricted to isolated hillslopes from which generalizations are made. While this has borne much heuristic worth since Geoffrey Milne’s treatise in east Africa, new tools from laser altimetry, surface dating using cosmogenic isotopes and major/trace element geochemistry offer an unprecedented opportunity to re-evaluate the catena concept. This study is not just descriptive; the theoretical framework employed here is process-oriented and encompasses traditional soil science perspectives, geomorphology and geology.

For ecosystems science – A landscape is the expression of spatial heterogeneity at any scale (Pickett and Cadenasso, 1995). Ecological studies must therefore have a scale domain that directs where sampling occurs. The immensity of ecosystems makes it difficult to sample efficiently and representatively. This work will identify major processes that shape soil landscapes which ecologists often overlook when designing their sampling protocols. One of the glaring oversights by ecologists is to blanket “granites” under a single banner as garnered from very coarse geological maps. If a patch in the “granite” contains significant mafic “contamination”, variation in some ecological process driven by soil may be wrongly attributed to something other than geology. Hence this thesis challenges ecologists to consider the extent to which relief, geology, climate and catena position matter for particular questions. Furthermore, the detailed soil data in this study can be used to parameterize soil

modules in ecological models, which often lack the rigour required to make reasonable predictions. For example, hotspots for ecologically important processes such as nutrient cycling are ultimately contingent upon morphometry and soil properties in landscapes (McClain et al., 2003). Thus if soils are disregarded, there will be very limited understanding of the where and why of ecological hotspots.

7. THESIS STRUCTURE AND CHAPTER OUTLINE

Chapter 1: Setting the stage, literature and framework

The focus of chapter 1 is on soil forming factors and how they mediate soil processes resulting in catenas with particular soil properties. Many pedological works assume that geology and geomorphology are beyond the confines of soil science (Nikiforoff, 1949). On the contrary, pioneering pedological concepts began with 19th century geology and geography but were obscured by soil science's allegiance to agriculture in the last century (Anonymous, 1940, in his obituary to pedology; Humphreys and Wilkinson, 2007). Currently however, there is a resurging link between soil science and its more natural sister disciplines of geology and geomorphology. Water permeates all surfaces whether geological, pedological or geomorphic and presides as the principal agent of alteration at all levels in soil landscape organization (Paton et al., 1995). Hence this study includes geological and geomorphic perspectives in addition to traditional soil science. The introductory chapter presents these major themes and provides the conceptual framework for the whole study.

Chapter 2: Weathering and soil properties on crests in arid to semi-arid Kruger National Park

In this chapter, I probe how water-shedding crests lacking significant inflow respond to an effective rainfall gradient by quantifying soil properties including carbon, clay mineralogy, clay amount, exchange properties (pH, cation concentration and CEC), soil erosion and losses of rock forming elements using geochemical mass balance. To ensure that sampling sites are crests indeed, I measure the contributing area (Moore et al., 1991) of each sample point using accurate topographic data obtained from GPS (Gessler, 1996b).

Chapter 3: Clay and base cation distribution along catenas in different climo-topographic settings of Kruger National Park

The second chapter is followed by an investigation into the landscape ramifications of material loss from crests with a focus on the most significant morphological expression of primary mineral weathering, clay. The third chapter examines clay distribution in Kruger along gradients of climate, relief and hillslope position. The physiographic settings of the study catenas are presented as detailed terrain attributes which are then related to where clay is in the landscape under factorial and process influences. Since clay acts as the binding agent for the nutrients that fuel ecosystems, its quantification along catenas holds value for nutrient and associated plant distribution. Clay inventories are described as clay %, clay on an aerial basis and maximum clay in soil profiles. The clay distribution is also related to clay mineralogy and concentration of base cations along catenas.

Chapter 4: Chemical mass balance on geologically complex catenas along gradients of relief and climate I: parent material and index element choice

In chapter 2, geochemical mass balance uses average parent material composition for the crest soils. It is reasonable to assume that granitic crests have relatively uniform rock across the park since they are the landscape's most resistant anchors. Positions outside crests are lower because of mineralogical/ chemical variations in rock that facilitate weatherability resulting in elevation troughs. The assumption of parent material uniformity is thus more risky when applied to mass balance across catenas. Chapter 4 shows how much error propagates in assuming uniformity in parent material within a soil, across catenas and between catenas. Also, the immobile element for carrying out mass balance in Kruger is chosen using multiple sources of evidence for the recalcitrance of Zirconium and Titanium. The evidence includes a qualitative assessment of dust accretion and the association of candidate elements with clay along catenas and soil profiles.

Chapter 5: Chemical mass balance on geologically complex catenas along gradients of relief and climate II: strain and major element loss/gain

Following the selection of the appropriate parent material and index element, chemical weathering fluxes across catenas will then be quantified. In this chapter, I evaluate the weathering extent of soils along catenas in relation to climate, length of the hillslope and the location of the soil between crest and toeslope. The element-by-element weathering nuances are also examined against each element's expected behavior based on the element's interaction with the soil environment *i.e.* leacheability, adsorption to colloids, nutrient uptake, *etc.*

Chapter 6: Conclusion

In the concluding chapter, all findings of the study are set within an integrated whole and assessed for their contribution and implication for the field of pedology.

8. STUDY AREA

Kruger National Park covers about 2 million ha in the South African lowveld with an unparalleled mammalian diversity under crucial conservation status (Mabunda et al., 2003). Kruger's geology is summarized in Barton et al. (1986). Most granites in the park are Precambrian with gneissic to migmatitic composition. Ecologists tend to blanket Kruger's granites into a single unit, a reasonable assumption for some ecosystems work. However, soil's varied geologic origin must be appreciated to understand landscape evolution and its contemporary legacy on soil properties.

In a geotectonic context, the Lowveld is a passive margin landscape created by tectonics associated with rifting and continental breakup (McCarthy and Rubidge, 2006). Today, the Lowveld lies between the Drakensberg Escarpment and the Lebombo Mountains (Fig. 1).

The classic path of landscape evolution in the Lowveld is parallel scarp retreat proceeded by long-term planation as King (1944) proposed, and based on correlating erosion surfaces at different elevations and designating relative exposure ages (King, 1976; Partridge and Maud, 1987). The King model suggests a scarp retreat rate around 1000 -1500 m/ Ma since the break-up of Gondwanaland 140 My ago, which places retreat to 60-100 km since the split (Venter et al., 2003). Recent studies with more precise backwearing and denudation

estimates contradict scarp retreat as the dominant mode for landscape evolution, placing retreat rates at a modest 50 to 95 m/ Ma (Cockburn et al., 2000; Fleming et al., 1999).

Kruger is arid to semi-arid with a high variability in rainfall (Dollar et al., 2007). Summer rains originate from alternating low pressure cells in the Indian Ocean and inland anticyclones. Less commonly, northern low pressure troughs cause prolonged low intensity rains. Unusually high rainfall years are caused by late summer cyclones from the Mozambique Channel moving inland (Chappel, 1992).

The sample sites used in the study fall along a gradient of increasing rainfall with the maximum at Pretoriuskop, minimum in Shingwedzi and intermediate water availability in Skukuza. Pretoriuskop has a mean annual rainfall of 736 mm, a mean annual temperature of 21 °C and the altitude is up to 780 m above sea level (asl) (Venter, 1990). Pretoriuskop's vegetation is a broadleaf deciduous bush savanna co-dominated by *Terminalia sericea* and *Sclerocarya birrea* (Gertenbach, 1983).

The Skukuza area lies east of Pretoriuskop over an identical host pluton. However, rocks in Skukuza have more ferromagnesian minerals due to intrusive dolerite, migmatite and amphibolite giving Skukuza catenas greater geological heterogeneity. Skukuza vegetation is a moderately dense bush savanna dominated by *Combretum apiculatum*, *Acacia nigrescens* and *Sclerocarya birrea* (Gertenbach, 1983). The Skukuza area is lower than Pretoriuskop at 260 m asl; with a mean annual rainfall of 550 mm and a mean annual temperature of 22 °C.

Shingwedzi, to the north of Skukuza, consist of gneiss, migmatite, granite and remnants of greenstone rocks with mafic properties. The frequency and size of dolerite dykes is greater than in Skukuza (Venter, 1990). Shingwedzi receives less than 500 mm of rain annually, with a mean annual temperature of 23 °C and an altitude of 215 m asl. The Shingwedzi is dominated by a seemingly endless expanse of *Colophospermum mopane* with *C. apiculatum* on crests (Gertenbach, 1983).

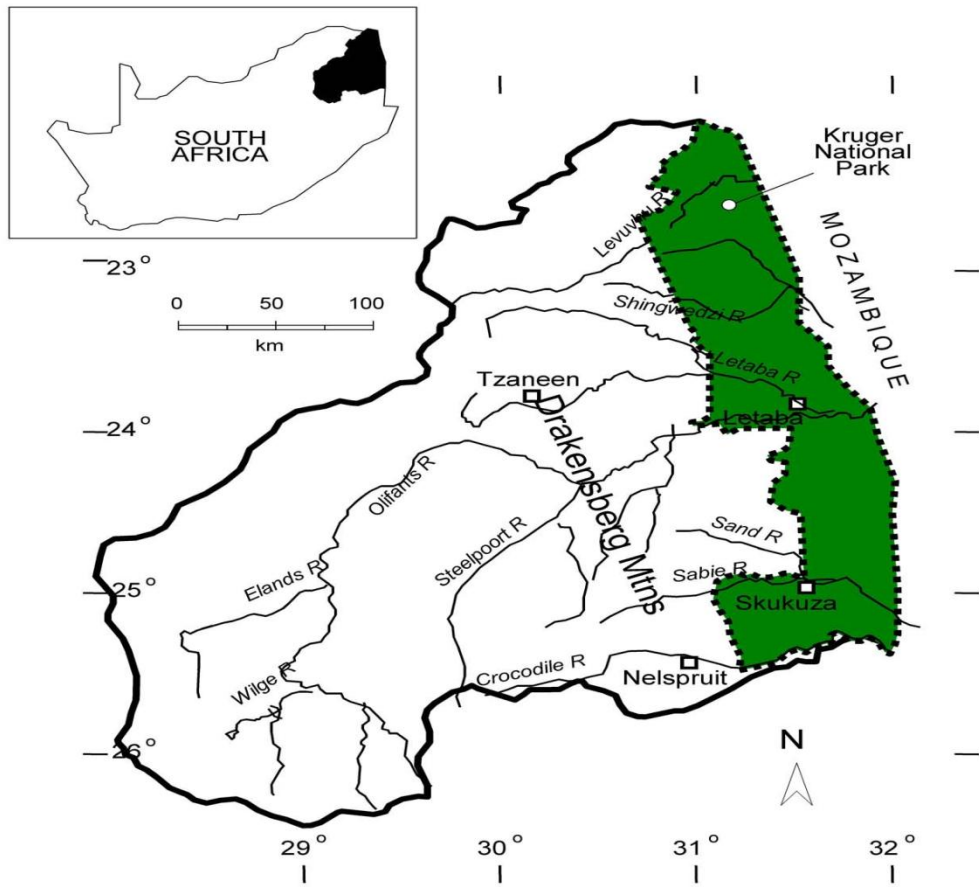


Figure 1. Study site map showing Kruger National Park in the South African Lowveld

CHAPTER 2: WEATHERING AND SOIL PROPERTIES ON CRESTS IN ARID TO SEMI-ARID KRUGER NATIONAL PARK

1. INTRODUCTION

Soil is the delicate veneer between the atmosphere and lithosphere forming a porous conduit for plants to pump organic acids into rocks facilitating primary mineral dissolution by chemical weathering. Residues of rock weathering are eventually returned to Earth's asthenosphere in subduction zones where they are recycled. This epic biogeochemical reaction sets the pace for soil landscape evolution and pattern at large scales (Burbank and Pinter, 1999; Raymo and Ruddiman, 1992).

Over smaller spatio-temporal scales, the rock-derived products of chemical weathering are redistributed in local soil landscapes demarcated by an apical crest and a basal stream on catenas linked by material exchanges. The pedogenic pattern expressed on catenas is conditioned by the magnitudes of soil forming factors (Jenny, 1941), which drive chemical weathering and soil formation leading to unique soil patterns in different physiographic settings.

Because net primary productivity and associated organic acid inputs are fuelled by water availability, climate is one of the more important soil forming factors that impinge on chemical weathering and soil properties. Water left over following evapotranspiration, during a limited period in arid and semi-arid areas, controls the leaching flux of soil constituents within profiles and across catenas. The volume of water and its leaching its power increase systematically with mean annual temperature and precipitation globally (Riebe et al., 2004) and with increasing contributing area downslope along catenas (Chamran et al., 2002).

Here I investigate the impact of increasing arid to semi-arid rainfall on chemical weathering and soil formation. My study area, Kruger National Park in the Lowveld of Southern Africa, lies on a stable and ancient continental plate centre underlain by granite secluded from recent tectonic activity and/or rejuvenation of base level (Partridge and Maud, 1987). The local landscape is composed of gently rolling hills that exhibit well developed catenas (Munnik et al., 1990; Venter, 1990) not unlike those described further north in Africa by Milne (1935) originally and more recently by Brown et al. (2004).

Catenas interact with rainfall to enhance or dissipate water and its stimulating impact on weathering by altering contributing area. High points on a catena have low contributing area and shed water, whereas low points have high contributing area and collect water, leading to accelerated weathering in the low points. Spatial variation in water availability and weathering occurs on catenas in spite of a uniform climate regime. Therefore catenas have multiple soil forming environments within their spatial extents between streams and watersheds. In addition to this local variation in pedogenic pattern on catenas, climate provides a further source of variation in soil formation on catenas in different climates (Birkeland, 1999). In this chapter, however, I focus on climate independent of material redistribution on catenas to emphasize the climatic influence outside the added complication of topography.

I therefore sampled crest soils to minimize the impact of water run-on from surrounding areas. In order to ensure consistent and representative sample locations, I used DEM analysis to select relatively broad crests at three points along Kruger's climate gradient. Soils in crest locations are sandy, highly bioturbated and support rapid infiltration resulting in little overland flow (Venter, 1990). Therefore downslope water-movement is through the sandy matrix or along the shallow bedrock contact,

and both flowlines act as conduits for mass transfer from crest source zones to sink positions further downslope along catenas.

I quantified the impact that increasing effective rainfall has on chemical weathering and soil properties in crests by characterizing soil morphological, physical and geochemical and mineralogical attributes. To constrain soil residence times, I quantified long-term erosion rates using cosmogenic ^{10}Be . Differences in weathering, leaching losses, and mineral transformations were used to infer the role of climate in soil profile development in crests.

2. METHODS

2.1 Study area

Kruger National Park lies in the lowveld on the east coast of Southern Africa (Fig 1). The lowveld is an old planation surface formed after the break-up of Gondwanaland and subsequent rifting on the subcontinent (Partridge and Maud, 1987). Elevation inside Kruger averages ~400 m above sea level, and the regional terrain is mostly flat except along the Lebombo Mountains to the east and towards the Great Escarpment in the west (Venter and Bristow, 1986). Kruger can be broadly divided into a western granitic half composed of gently rolling hills and a much flatter basaltic plain in the east. My focus here is the granitic segment that extends about 300 km from Shingwedzi in the north to Pretoriuskop in the south.

2.2 Climate, rainfall style and an aridity index for Kruger's climate gradient

The climate in Kruger and Southern Africa in general is principally controlled by west-easterly anticyclones that result in wet conditions where the escarpment generates orographic precipitation. Less frequently, cyclones penetrate inland from the ocean bringing rainfall. The easterly dip in precipitation is associated with decreased altitude away from the Great Escarpment which experiences up to 1200 mm of rain annually (Schulze, 1997). The east-to-west increase in rainfall is especially pronounced in the south of Kruger where the escarpment is nearest and orographic rise the greatest. Mean annual rainfall in the park also increases from north to south in association with closer proximity to the escarpment.

Most rainfall events in Kruger are powerful convective storms, and these may deliver up to half the mean annual rainfall in a single episode on exceptional occasions (Venter et al., 2003). Figure 2 depicts the rainfall style for the 2005/06 rainfall year using daily and cumulative rainfall in Shingwedzi (dry), Skukuza (intermediate rainfall) and Pretoriuskop (wet). Figure 2 also shows maximum daily, maximum monthly and maximum annual rainfalls between 1960 and 1990 in the three climate zones. Daily and monthly maxima between 1960 and 1990 were highest in Skukuza (Fig. 2), but lower temperatures imply lower ET in Pretoriuskop and on balance produce wetter conditions. The rainfall style testifies that a large proportion of mean annual rainfall, up to 80 % in some years, fall in five to seven summer months between October and April (Gertenbach, 1980) (Fig. 2). There can be unexpected oscillations in rainfall across Kruger associated with the highly heterogeneous rainfall regime typical of arid and semi-arid areas. For example, during

2005/06, Skukuza was even wetter than Pretoriuskop with a much higher than average rainfall that actually exceeded the record year between 1960 and 1990.

Kruger's climate within Southern Africa's regional context has tracked global climate through Earth history (Gilchrist et al., 1994). Following Gondwanaland's fragmentation during the Cretaceous, the lowveld was uplifted during the Miocene and Pliocene (Hobbs et al., 1998). The fragmentation of Gondwanaland and uplifts were responsible for present-day Lowveld location relative to the Indian Ocean and the interior (Tyson and Partridge, 2000). The warm-and-dry to cool-and-wet climate gradient from north to south has probably held through time without a reversal (Tyson and Partridge, 2000).

2.2.1 Aridity index for the climate gradient

I calculated an aridity index to proxy water remaining following evapotranspiration. The index is a ratio of potential evapotranspiration and mean annual rainfall termed effective rainfall (Birkeland, 1999). Average annual rainfall for Shingwedzi in the north is 468 mm, Skukuza is 550 and Pretoriuskop furthest south has an annual rainfall of 734 mm. Average temperature in Shingwedzi is 24 °C, 22.5 °C in Skukuza and 21.7 °C in Pretoriuskop (Venter et al., 2003). Potential evapotranspiration was estimated using Linacre's (1977) Penman-Monteith derived equation which computes potential evapotranspiration using only temperature data:

$$E_0 = \frac{700T_m / (100 - A) + 15(T - T_d)}{(80 - T)} \text{ mm day}^{-1} = \text{potential evaporation rate} \quad (1)$$

where $T_m = T + 0.006h$, h is the altitude in meters, T is the mean temperature, A is the latitude (degrees) and T_d is the mean dew point. The factor $(T - T_d)$ is estimated with the equation $(T - T_d) = 0.0023h + 0.37T + 0.53R + 0.35R_{\text{ann}} - 10.9$ °C where R is the

mean daily range of temperature and R_{ann} is the difference between the mean temperatures of the hottest and coldest months. The effective rainfall index for the field sites were therefore 0.15 in Shingwedzi, 0.2 in Skukuza and 0.27 in Pretoriuskop (Table 1). Kruger's effective rainfall is nearly four times less than 1 in wet Pretoriuskop, meaning that potential evapotranspiration exceeds rainfall by a factor of four. Therefore, the increasing effective rainfall in the north-south axis of Kruger is entirely in the arid to semi-arid range by UNESCO standards (Tilahun, 2006).

2.3 Crest selection

Crests occur on catena apices from which material is lost and transported downslope, but not gained from upslope for lack of contributing area. Kruger crests have flattened tops with gentle slopes, exposed bedrock in rare cases and broad leafed trees dominated by *Combretum apiculatum* (Venter, 1990). Relative to locations further downslope, crests have a minimum upslope contributing area so that displacement of mass in any direction leads downslope. Therefore, crests receive the least material augmentation from upslope positions resulting in potentially greater leaching losses than elsewhere on catenas. Crests are ideal sampling locations for isolating climatic impacts on weathering because their contributing areas vary modestly from catena to catena within and between climate zones.

I evaluated uniformity in crest size by constructing high resolution DEMs for 13 crests across Kruger's arid to semi-arid climate gradient. Elevation data were collected by Airborne Laser Solutions using an ALTM (Optech, Canada) sensor with a 25 kHz frequency. The sensor was anchored at 500 m above ground in a fixed-wing plane to achieve a 0.1 m vertical and 0.5 m horizontal accuracy. The elevation data

were processed into 1 m raster DEMs in ArcGIS 9.1 with the inverse distance weighted method based on the eight nearest neighbours (ESRI, 2005). Prior to calculating contributing area, slope gradient and flow routing were computed using the D-8 algorithm in Taudem (Tarboton, 1997). D-8 is a single direction flow algorithm which allocates flow from a centre cell to neighbours with the steepest downslope gradient. Slope gradient and flow direction were then used to calculate the area contributing runoff to each grid cell in the watersheds containing the 13 sampled crests (Moore et al., 1990).

2.4 Estimating soil erosion and residence time using cosmogenic ^{10}Be

To constrain residence time for soil development, I (with help from Arjun Heimsath) measured soil production rates, or the rate at which bedrock is converted to soil at the base of the soil profile at three representative crests, one in each climate zone (Heimsath et al. 1999). Higher abundances of cosmogenic ^{10}Be imply slower soil production rates. Because crests cannot receive remobilized soil from upslope, a soil residence time can then be calculated as the ratio of soil depth and the inverse of soil production rate.

I collected ~1 kg of saprolite at the boundary with soil to a 1 – 10 cm depth to ensure samples were retrieved from regolith's immobile zone (Heimsath et al., 1999). The boundary was marked by C-horizon properties such as an increased rock fragment and loss of soil structure. The rock/soil sample was crushed, sieved through a 1 mm mesh and purified according to Kohl and Nishiizumi (1992) to isolate quartz. ^{10}Be was then extracted from the dissolved quartz using ion exchange chromatography and its concentration measured at the Lawrence Livermore National

Laboratory by Accelerator Mass Spectroscopy. Appendix III provides a more detailed description of the method.

2.5 Soil sampling and laboratory analysis

I sampled four crest pedons in Shingwedzi, five in Skukuza and four in Pretoriuskop for a total of 13 crests across Kruger's climate gradient. Soils were described with standard methods (Soil Survey Staff, 1996) and excavated from morphological horizons along pit faces for chemical, physical and mineralogical analyses. Bulk density samples were collected as intact clods for measuring using the saran coated clod method or in a ring of known volume. Routine soil analyses on the <2 mm fraction were performed at the University of California, Santa Barbara.

Particle size was determined by the hydrometer method after hydrogen peroxide pre-treatment to remove organic matter and soil dispersal with sodium hexametaphosphate (Soil Survey Staff, 1996). Exchangeable base cations and cation exchange capacity (CEC) were extracted with NH_4OAc and KCl respectively, both buffered at pH 7. The concentration of base cations was measured with an atomic absorption spectrometer and the CEC (as NH_4^+) was measured colorimetrically using a Lachat autoanalyser. Soil pH was measured in a 1:1 water solution and carbon with a CN analyzer. Total elemental analysis on soils' fine-earth fraction and rocks was measured by ICP-MS on a borate fusion for Zirconium and X-ray fluorescence for all major elements at ALSChemex in Sparks, Nevada. Loss-on-ignition (LOI) was measured by mass loss following incineration in a muffle furnace at 1000°C for 1 hour.

Mineralogical analyses were completed on the fine-earth fraction (<2 mm) through selective separation by particle size. Samples were air-dried, dispersed in sodium hexametaphosphate, and the <2 μm (clay) fraction isolated by repeated centrifugation and decantation following settling in a cylinder. X-ray diffraction (XRD) spectra were obtained for smear mounts between 2 and 35 $^{\circ} 2\theta$ on a Scintag PAD-V Diffractometer (Department of Chemistry and Biochemistry, University of California, Santa Barbara) configured at: 45kV, 35mA, a step size of 0.05, and a dwell time of 0.5 seconds.

Diffraction patterns of the clays were obtained following standard pretreatment to allow identification (Theissen and Harwars, 1962). For each sample, a K and Mg saturated slide was prepared and sub-sampled for 500 $^{\circ}\text{C}$ heat (K) and glycerol (Mg) treatments. The relative abundances of clay minerals were estimated on the basis of peak intensity ratio by normalizing the relative proportions of clay minerals in the sample to 100 %. I determined the clay fraction CEC by dividing soil CEC by the proportion of clay in the < 2 mm soil fraction.

2.6 Geochemical mass balance to estimate extent of chemical weathering and major element losses

I used a mass balance approach to quantify the loss of rock forming elements and isolate climate driven patterns of chemical weathering on crests. Mass balance evaluates volumetric and chemical changes in a soil undergoing weathering from parent material (Brimhall and Dietrich, 1987). An immobile element's enrichment in soil relative to its concentration in parent material enables an estimate of soil's

volumetric strain and the degree of loss/ gain in mobile elements. Therefore, an immobile element and parent material were carefully selected to determine strain and mobile element gain/ loss (Brimhall and Dietrich, 1987). The most recalcitrant element was picked by evaluating the enrichment of known refractory elements relative to parent material concentrations, the most enriched element was then relatively immobile (Kurtz et al., 2000). An increase in immobile element concentration implies collapse of a horizon whereas a decrease indicates dilation (Brimhall et al., 1992). Volumetric strain was calculated as:

$$\varepsilon_{i,w} = \frac{V_w - V_p}{V_p} = \frac{V_w}{V_p} - 1 = \frac{\rho_p C_{i,p}}{\rho_w C_{i,w}} - 1 \quad (2)$$

where V is volume, w is soil, p is parent material, ρ is bulk density, C is concentration and i represents an immobile element. Losses and gains of mobile elements can be calculated relative to the enrichment of an immobile element in soil. The mass fraction of a mobile element j , added or lost from a soil relative to its mass in parent material was then calculated as:

$$\tau_{j,w} = \left(\frac{C_{j,w}}{C_{j,p}} \times \frac{C_{i,w}}{C_{i,p}} \right) - 1 \quad (3)$$

from which the loss of element j relative to its concentration in parent material on a mass per area basis can be calculated using horizon thickness, fraction of j in parent material and parent material bulk density ($= 2.65 \text{ g/ cm}^3$ for granite). The Sum of losses of j in each horizon results in total loss of j in the soil profile relative to parent material (Porder et al., 2007).

2.7 Kruger National Park geology, immobile element determination and model parent material

Kruger is underlain by Achaean basement granites of the Kaapval craton, the continental nucleus of South Africa (Barton et al., 1986). The Skukuza-Pretoriuskop area sits on the Nelspruit granite complex (± 3105 Ma) which forms a large batholith in the park's southern half (Schutte, 1986). The Nelspruit complex is derived from simple partial melting of more refined tonalites and trondhjemites or their sedimentary analogues (Barton et al., 1986). The southern granites are mostly quartz and K-feldspar with minor biotite and hornblende. The Nelspruit complex intrudes older tonalites and granodiorites (>3200 Ma) that underlie most of the Shingwedzi sites. The most abundant minerals in Shingwedzi are quartz, plagioclase, biotite and muscovite (Schutte, 1986). The Shingwedzi granites also contain greenstone inclusions that give them a more mafic character than rocks in Skukuza-Pretoriuskop (Venter, 1990). The ancient granitoids under Kruger are thus highly heterogeneous to begin with, and have also been intruded by mineralogically distinct rocks and metamorphosed to different extents in events following emplacement (Barton et al., 1986). This uncertainty in Kruger soil's genetic precursors complicates parent material assignment for mass balance calculations.

The set of index elements available for use in geochemical mass balance includes zirconium and titanium (Brimhall and Dietrich, 1987), although occasionally Al is used as well. Zirconium and Ti are used as index elements in most granitic settings because both are only mobilized in rainfall exceeding 1000 mm/yr (Riebe et al., 2004). Also, Zr is mobilized in soils containing high concentrations of organic ligands, an unlikely condition in Kruger given the low rainfall and high incidence of

fire. Table 2 shows the concentrations and enrichments of Zr, Ti and Al in the surface horizons of Pretoriuskop crests relative to rock concentrations. The most conserved of the three elements was Zr because it was the most enriched relative to rock concentrations in the wettest soils (Table 2 and Kurtz et al., 2000). Zirconium also displayed the largest enrichment in soil against losses of more mobile elements as rainfall increased from Shingwedzi to Pretoriuskop (Table 3). The concentration of mobile elements Al, Ca, Mg and Na decreased with increased rainfall while Si and Zr concentrations rose (Table 3). Therefore, I selected zirconium as the index element for mass balance calculations.

Once the immobile element has been chosen, the next item in geochemical mass balance is to select the parent material against which element losses/ gains are assessed. Rocks were collected below soils within a 100 m radius from crests to curtail compositional variation due to mafic contamination. Because of the bimodal composition of Kruger granites, two parent materials were used; one representing Shingwedzi and the other for the Skukuza-Pretoriuskop area. The model parent material in each case was the average element concentration for the two types of granite. Rocks sampled around Shingwedzi crests had a tonalitic to granodioritic composition according to Robb's (1977) K/ Na criterion. The rocks in the Skukuza-Pretoriuskop area had a granite *sensu stricto* composition (Table 4).

3. RESULTS

Sampled crests in each climate zone had average contributing areas of 26 ± 32 m² in Shingwedzi, 18 ± 6 m² in Skukuza and 46 ± 13 m² in Pretoriuskop. These averages were samples from a population with potential contributing areas in the

range 5 to 3786 m² for crest to toeslope positions on catenas. Cosmogenic ¹⁰Be concentrations in a representative crest per climate zone showed that crest soils in Kruger erode extremely slowly. Apparent erosion rates ranged from 1.1 ± 0.1 m/ Ma in Shingwedzi, 2.6 ± 0.2 m/ Ma in Skukuza and 0.7 ± <0.1 m/ Ma in Pretoriuskop (Table 5). The erosion rates translate to soil residence times of 0.48 Ma in Shingwedzi, 0.25 Ma in Skukuza and 2.74 Ma in Pretoriuskop using average soil depths given in Table 5. Crest antiquity in Pretoriuskop promotes much more intensely weathered and deep soils, while more youthful soils with shallow depths occur in the drier climates.

3.1 Soil morphology, exchange properties and clay mineralogy on crest soils across climate

Soil depths increased from 53 ± 4 cm in Shingwedzi, 64 ± 20 cm in Skukuza and to 192 ± 23 cm in Pretoriuskop with increasing effective rainfall (Table 5). Field textures were uniformly sandy by depth and over climate, with weak soil structures which in combination with the sandy textures pre-empt high saturated hydraulic conductivities that would facilitate efficient leaching (Table 6).

Exchangeable base cation concentrations dropped monotonically from Shingwedzi to Pretoriuskop indicating that rising water availability promoted leaching efficiency (Table 7). Average base cation concentrations followed the patterns

Shingwedzi	Ca>	Mg>	Na>	K
Skukuza	Ca>	Mg>	Na>	K
Pretoriuskop	K>	Ca>	Mg>	Na

from dry to wet crests. Base saturations (BS) decreased from 80 ± 8 % in Shingwedzi, to 48 ± 14 % in Skukuza and down to 35 ± 14 % in Pretoriuskop, also suggesting

accelerated leaching losses fueled by increased rainfall (Table 7). Oddly, the mean pH of crest soils was generally invariant across the three climate zones in spite of the rising loss of bases (Table 7). The pH range in Shingwedzi was 4.9 to 6.6, 5.1 to 5.9 in Skukuza and 5.2 to 5.6 in Pretoriuskop; and so, there was a decrease in maximum pH with higher rainfall. Like pH, mean CEC remained relatively unchanged with increased rainfall suggesting that organic carbon and clay mineralogy also remained even between the climate zones (Table 7). Indeed, organic carbon was low and uniform across the entire sample of crest soils (Table 7) pointing to scant organic contribution towards the CEC.

Mean depth-weighted average clay % in Shingwedzi was 9 ± 2 %, in Skukuza 7 ± 1 % and Pretoriuskop 11 ± 1 %. The mean maximum clay % in the crests ranged from 9 ± 2 % in Shingwedzi, to 8 ± 1 % in Skukuza and 13 ± 2 % in Pretoriuskop (Table 8). Total clay summed over whole pedons increased from 30 ± 16 kg/ m² in Shingwedzi, 42 ± 16 kg/ m² in Skukuza and 306 ± 135 kg/ m² in wet Pretoriuskop.

X-ray diffraction indicated that smectite dominated the clay fraction in Shingwedzi as commonly observed in dry soils containing biotite, and was consistent with the slightly higher CEC's recorded in Shingwedzi. Kaolinite was most prolific Pretoriuskop but was also present in lower concentrations in Shingwedzi and Skukuza (Table 8). Clay fraction CEC in Shingwedzi was 76 cmol (+)/ kg clay, 94 cmol (+)/ kg clay in Skukuza and 57 cmol (+)/ kg clay in Pretoriuskop. The clay fraction CEC's, together with clay mineralogy suggest soil clay in Kruger crests is a mixture of smectite, mica and kaolinite with decreasing contribution of smectite as rainfall increases. The decrease in clay-sized quartz and feldspar as rainfall increases is consistent with accelerated weathering (Table 8).

Appendix I gives the locations and morphological descriptions of all horizons sampled in the 13 crests; while Appendix II gives depth profiles of base cation concentration, CEC, BS, pH, organic C and clay %.

3.2 Fractional and total mass lost from crest soils along the climate gradient

Higher rainfall led to more elemental losses in soil horizons when indexed by proportion remaining relative to parent material abundances. These losses differ from element to element within and between climate zones (Table 9). Dry crests in Shingwedzi experienced greater Si, Al, Fe, Ca, Mg, Na and K losses in near-surface horizons suggesting more intense weathering conditions at the surface where water was likely more plentiful. Phosphorus, by contrast, had more loss at depth in dry soils suggesting active mining by plant roots from deep horizons towards the epipedon. While all other elements experienced losses in Shingwedzi, Titanium, in stark contrast, displayed gains relative to parent material concentrations in all horizons of the dry crests. Since crest soils lack upslope contributions of mass, added Ti most likely originated from exogenous dust inputs (see Chapter 4). In the crests of Skukuza under intermediate rainfall, most soils had maximum losses of Si, Ca, Na, K and P at depth. The sesquioxide forming elements (Al, Fe, Ti) and Mg experienced more losses in surface horizons and were probably translocated and re-deposited at depth following leaching down profiles (Table 9). In the wet soils of Pretoriuskop, Si, Fe and P experienced greater losses in deeper horizons, whereas Al, Mg, Na, and K had more surface losses. Calcium was almost 100 % lost in all horizons while Ti experienced maximum losses near the surface in half the sampled soils.

Elemental losses calculated on a mass per area basis integrated over whole

profiles indicated consistently increased leaching losses as rainfall intensified for all elements except Na, which experienced more loss in Shingwedzi than in Skukuza (Table 10).

4. DISCUSSION

Massive losses of major elements relative to their parent material concentrations attest to the relentless leaching of Kruger crest soils opportuned by their great antiquity and sluggish physical erosion. The low rates of erosion are a physiographic feature of the Lowveld imposed by low stream dissection and gentle slopes (Venter, 1990). The limited potential to erode is ultimately controlled by the Lebombo Mountains to the east of Kruger, which form a local base level below which rivers inside Kruger cannot cut. The low geomorphic energy in Kruger results in stable soils that last for millennia giving weathering agents ample time to work the soils. This is why the weathering extent of Kruger crests rivals that recorded under much wetter conditions (cf. Riebe et al., 2003).

I postulate that the loss of base cations and Si must occur by dissolution and toeslope-bound transport through the soils during periods when the water balance is positive. Framework elements, on the other hand, cannot dissolve and leach out under Kruger's pH and organic carbon regimes. Loss of Al and Fe can however occur efficiently by particulate and colloidal loss, but low erosion rates obviate significant particulate loss of Al and Fe. Therefore, the most parsimonious vehicle for the massive losses of Al and Fe appear to be significant colloidal loss during wet periods. Periods of intense material losses must occur, even if they are limited to the rare years

with unusually high rainfall, otherwise the soils would be spared systemic loss of most soil constituents.

Under the dry and low carbon conditions of Kruger – which retard colloid entrapment in water – colloidal loss by leaching can occur most efficiently in conjunction with ferrolysis (Paton et al., 1995). During wet conditions, reductive dissolution of Fe-sesquioxides releases easily leached Fe^{2+} into the soil solution. If Fe^{2+} concentration is sufficiently high, it overwhelms exchange sites replacing bases, which are then freely lost from the soil whilst Fe is retained. In the dry cycle, Fe is oxidized to ferric hydroxide with H ions as by-products, leading to acidic conditions conducive for clay attack thus releasing and leaching Si and Al (Chittleborough, 1992). The lower fractional loss of Fe relative to both Al and Si in Kruger crest soils would suggest that ferrolysis is likely.

4.1 Mass balance uncertainty due to dust addition

The addition of dust to soil is pervasive in most landscapes even in areas seemingly too far from a source (Simonson, 1995). Dust influx can offset elemental losses calculated by geochemical mass balance since the method assumes the parent material selected is soil's only precursor in a closed weathering system (Kurtz et al., 2001; Scribner et al., 2006). Thus any external dust inputs, often compositionally distinct, add uncertainty when elemental losses or gains are evaluated relative to the model parent material. Consequently, it remains vital to demonstrate or discount dust addition, and this can be done in several ways.

I begin with the silt to clay ratio: (1) figure 3 shows that there was more silt relative to clay in surface horizons of the crest soils; and (2) Kruger crest soils had

higher silt to clay ratios in surface than sub-surface horizons which suggests accretion of dust (Appendix I). Had chemical weathering been the only determinant of particle size distribution, surface horizons would have more clay than sub-surface horizons since they are normally the site of the most intense weathering (Simonson, 1995). Also, the sharp transitions in particle size by depth suggest dust has been added (Appendix I). Soils with inconsequential dust inputs exhibit gradual changes in particle size by depth (Birkeland, 1999). Thus evidence from the silt to clay ratios of the crest soils supports that dust has been added.

The addition of dust evident in the silt/ clay ratios was not re-enforced by depth profiles of major element taus because surface horizons were not less depleted than deeper horizons (Table 10). The dust influx is probably a periodic phenomenon whose legacy is obliterated by weathering over the long residence times of Kruger crest soils. Snapshot sampling such as the present campaign records dust augmentation anywhere between the onset of addition and long after. Since bioturbation has yet to sufficiently churn the soil to mask added silt in surface horizons, I can postulate a recent dust addition relative to the rate at which soil weathers and biota agitate horizons.

Ratios of elements housed in resistant minerals such as Zr in zircon and Ti in titanium oxides can also be used to discount dust addition by demonstrating uniformity in parent material (Ajmone Marsan et al., 1988). For example, a fairly constant Zr/Ti with depth points to uniform parent material (Mason and Jacobs, 1998). Applying Chittleborough et al. (1984)'s 25 % coefficient of variability criterion in the Zr/Ti, twelve of the thirteen crests sampled had uniform parent material (Table 11), hence dust addition was minor.

Altogether, dust accretion in Kruger is likely too recent to affect geochemical mass balance and the dust resembles granitic regolith too closely anyway to detect it using the Zr/Ti ratio.

5. CONCLUSIONS

The crests sampled in Kruger National Park span a narrow arid to semi-arid range in effective rainfall, 0.15 to 0.27. The gradient provides a test for how long-term weathering on a stable granitoid platform impacts soil properties and weathering induced losses of major elements. These conditions have held for thousands of years as evident in the tentative soil residence times of the crest soils. Since Kruger's climate is veritably bland in a global context, it is surprising that the extreme loss of major elements has even occurred. The leaching of soil in Kruger must therefore occur during hot moments (McClain et al., 2003) and "soil-forming intervals" (Chadwick and Davis, 1990) not captured in annual rainfall since soils under similar climate elsewhere are not nearly as depleted (cf Riebe et al., 2004). There is sufficient time for these un-documented hot moments to leach out the soils over their prolonged residence. The legacy of dry spells is not imprinted in the soils but whenever rapid pedogenesis occurs, a record remains in the soil. Thus despite being under the pervasive water deficit of an arid to semi-arid climate, cumulative wet conditions through millennia have resulted in highly leached crest soils over Kruger.

The depleted crest soils contribute dissolved and suspended material to downslope positions of the catenas. This material may either be completely lost from the catenas via rivers or may accumulate some distance away from crests. Since bases travel in the dissolved load of the downslope water vectors, they are likely transported

further away from crests than suspended Fe and Al. In Shingwedzi's drier climate, the downslope material flux may not be adequate to completely leach out catenas, therefore I would expect material to accumulate on the hillslopes. Where effective rainfall is high as in Pretoriuskop, it is more likely that catenas would be leached out completely. With intermediate rainfall like in Skukuza, material may not be leached out of the catena but would redeposit further downslope than in Shingwedzi. These questions are the subject of the next chapters which extend the crest analyses to whole catenas.

List of tables

Table 1. Parameters used to calculate effective rainfall in the three climate zones of Kruger National Park (temperature data courtesy of the South African Weather Service) (see text for abbreviations)

Table 2. Concentrations and enrichments relative to parent material (pm) of refractory elements Zr, Ti and Al in the surface horizons of the wettest crest soils in Kruger

Table 3. Mean and standard error of depth integrated major element and Zr concentrations in crest soils along the Kruger climate gradient

Table 4. Element concentrations of rocks used to calculate the model parent materials

Table 5. Site characteristic, erosion rates and soil residence times

Table 6. Selected field properties and bulk densities for a representative crest soil in each climate zone

Table 7. Depth integrated mean and standard errors of base cation concentration, cation exchange capacity, base saturation (BS), pH and % carbon (C) in crest soils across climate

Table 8. Semi-quantitative concentration of clay-sized minerals in B-horizons (0 = not detected, 5 = 100 % occurrence), depth integrated mean percent clay and standard error, mean maximum clay percent and standard error and clay fraction CEC

Table 9. Depth profiles of concentrations and fractional gains/ losses (τ) of major elements standardized by zirconium in crest soils along climate gradient

Table 10. Mean and standard error of model parent material calculated depth integrated mass gains and losses of Si, Al, Fe, base cations, Ti, P and total mass loss from crest soils across climate standardized by Zr concentration in soil and rock

Table 11. Mean, standard error and coefficient of variability in Zr/ Ti for crest horizons in Kruger to examine parent material uniformity

List of Figures

Figure 1. Kruger National Park showing mean annual rainfall of field sites and altitude across the climate gradient.

Figure 2. Daily and cumulative rainfall for the 2005/6 rainfall year in Shingwedzi, Skukuza and Pretoriuskop. Inserts show maximum daily, monthly and annual rainfalls between 1960 and 1990 in the three climate zones

Figure 3. Mean and standard error of silt to clay ratios of deep and surface horizons in crest soils across Kruger's climate gradient.

Appendices

Appendix I. Horizon field properties and soil profile locations of sampled crests

Appendix II. Horizon exchange properties and carbon content in sampled crest soils

Appendix III. Cosmogenic isotope method for determining erosion rates

Table 1. Parameters used to calculate effective rainfall in the three climate zones of Kruger National Park (temperature data courtesy of the South African Weather Service) (see text for abbreviations)

Parameter	Shingwedzi	Skukuza	Pretoriuskop
Altitude (m)	380	360	620
R _{ann} (°C)	12.1	9.6	9.0
R (°C)	24.0	22.5	21.7
Mean Temp (°C)	24.0	22.5	21.7
T-T _d	15.8	13.5	13.2
T _m	26.2	24.7	25.4
A (°)	23.1	25.0	25.1
E _o (mm)	8.5	7.5	7.5
Annual E _o (mm)	3096	2753	2721
Annual rainfall (mm)	468	550	734
Effective rainfall	0.15	0.20	0.27

Table 2. Concentrations and enrichments relative to parent material (pm) of refractory elements Zr, Ti and Al in the surface horizons of the wettest crest soils in Kruger

Soil	Max Zr (ppm)	Max Ti (%)	Max Al (%)	Max Zr/ pm Zr	Max Ti/ pm Ti	Max Al/ pm Al
pkop1a	523	0.4	8.3	5	4	1.0
pkop2c	905	0.5	6.1	9	5	0.8
pkop4h1	722	0.4	5.2	7	4	0.6
pkop4h2	568	0.4	5.7	5	4	0.7
mean	679	0.4	6.3	6.4	4.1	0.8
se	86	0.0	0.7	0.8	0.2	0.1
cv	25	11.7	22.0	25.4	11.7	22.0

Table 3. Mean and standard error of depth integrated major element and Zr concentrations in crest soils along the Kruger climate gradient

climate	Zr (ppm)	Si (%)	Al (%)	Fe (%)	Ca (%)	Mg (%)	Na (%)	K (%)	Ti (%)	LOI (%)
Shingwedzi	161.7 ± 14.3	33.8 ± 0.5	7.5 ± 0.1	1.5 ± 0.2	0.9 ± 0.1	0.20 ± 0.05	2.7 ± 0.2	1.7 ± 0.2	0.3 ± 0.04	3.0 ± 0.3
Skukuza	260.6 ± 25.8	35.5 ± 0.5	6.5 ± 0.4	1.1 ± 0.1	0.6 ± 0.1	0.07 ± 0.01	1.9 ± 0.3	2.7 ± 0.1	0.2 ± 0.03	2.3 ± 0.2
Pretoriuskop	541.9 ± 50.5	37.9 ± 0.2	4.6 ± 0.1	1.4 ± 0.04	0.2 ± 0.1	0.05 ± 0.02	0.6 ± 0.1	2.7 ± 0.3	0.3 ± 0.03	2.0 ± 0.2

Table 4. Element concentrations of rocks used to calculate the model parent materials

Site	Zr (ppm)	Si (%)	Al (%)	Fe (%)	Ca (%)	Mg (%)	Na (%)	K (%)	Ti (%)	P (%)	LOI (%)	K/ Na
ph6c ^s	23	35	8	0.5	1.4	0.012	4.2	0.8	0.01	0.004	0.5	0.2
ph5b ^s	19	35	8	0.4	0.9	0.003	4.2	0.8	0.01	0.009	0.7	0.2
ph5c ^s	52	35	7	0.7	1.0	0.283	2.0	1.4	0.03	0.004	2.5	0.7
ph6bc2 ^s	47	34	8	1.1	1.6	0.003	4.4	0.6	0.07	0.013	0.7	0.1
ph5bc2 ^s	34	34	8	1.1	0.3	0.006	2.8	4.1	0.06	0.013	1.0	1.5
mean ^s	35	35	8	0.7	1.0	0.062	3.5	1.5	0.04	0.009	1.1	0.4
sb2a ^{s-p}	211	34	7	1.5	0.5	0.127	1.4	3.3	0.20	0.009	2.8	2.3
sb3e ^{s-p}	14	33	8	0.5	0.1	0.003	1.1	8.1	0.03	0.009	0.8	7.6
sb3f ^{s-p}	8	31	10	0.2	0.1	0.003	2.0	9.3	0.01	0.002	0.5	4.6
sb4e ^{s-p}	89	32	7	3.0	4.8	0.042	0.1	2.7	0.08	0.013	1.9	33.2
sb5b ^{s-p}	19	35	8	0.4	0.9	0.003	4.2	0.8	0.01	0.009	0.8	0.2
pkop2b ^{s-p}	292	31	9	2.5	1.7	0.464	3.6	2.3	0.31	0.079	1.3	0.7
mean ^{s-p}	95	33	8	1.3	1.3	0.101	2.3	4.0	0.10	0.018	1.3	1.8

^sShingwedzi rock

^{s-p}Skukuza-Pretoriuskop rock

Table 5. Site characteristic, erosion rates and soil residence times

Site	Altitude range (m)	Latitude	Longitude	Effective rainfall	Contributing area of crests (m ²)*	Soil production rate (m/ Ma)	Soil depth (cm)	Soil residence time (Ma)
Shingwedzi	329-340	31° 18' E	23° 1' S	0.15	26 ± 32	1.1 ± 0.1	53 ± 4	0.48
Skukuza	248-362	31° 29' E	25° 2' S	0.20	18 ± 6	2.6 ± 0.2	64 ± 20	0.25
Pretoriuskop	510-577	31° 15' E	23° 2' S	0.27	46 ± 13	0.7 ± 0.0	192 ± 23	2.74

*the range in contributing area across an entire catena is between 5 and 3786 m²

Table 6. Selected field properties and bulk densities for a representative crest soil in each climate zone

Site	Horizon	Lower horizon depth (cm)	Moist colour	Structure	Gravel (%)	Field texture	Roots	Bulk density (g/ cm ³)
Shingwedzi	BA	1	7.5YR 2.5/2	0sg	10	ls	3vf	1.4
	Bw1	13	7.5YR 2.5/2	1vfsbk	17	ls	1vf,1f	1.5
	Bw2	22	2.5YR 5/8	2msbk	28	sl	2vf,2f	1.7
	Bw3	45	2.5YR 3/3	2fsbk	70	sl	2vf,2f	1.7
	C	50+	-	-	95	s	-	1.7
Skukuza	A	26	10YR 3/3	1csbk	< 5	ls	2vf,1f,1m,2co,1vc	1.6
	Bw1	43	10YR 2/2	1cabk	< 5	ls	3vf,2f1,m	1.7
	Bw2	63	5YR 4/4	1mabk	15	s	2vf,2f,1m	1.7
	Bw3	98	5YR 4/6	1fabk	55	s	2vf,1f	1.7
	BC	131+	7.5YR 4/6	0sg	65	s	1vf,1f	1.7
Pretoriuskop	BA	8	10YR 2/2	0sg,1vfsbk	0	ls	2vf,2f	1.5
	Bw1	17	7.5YR 3/3	1vfmsbk,0sg	2	s	3vf,3f,1co	1.7
	Bw2	39	7.5YR 4/4	0sg,1msbk,1csbk	5	s	2vf,2f,2m,2co	1.5
	Bw3	70	7.5YR 4/6	1mcsbk,0sg	5	s	3vf,3f,3m,2co	1.6
	Bw4	93	7.5YR 5/6	1msbk,1csbk	10	s	3vf,3f,1m,1co	1.8
	Bw5	115	5YR 5/4	1msbk,1csbk	80	s	2vf,2f,1m,1co	1.7
	Bw6	142	5YR 5/4	2msbk	65	s	2f,2m,1vc	1.7
	Bw7	164	5YR 4/4	1msbk,1csbk	65	ls	1f,1m	1.7
	Bw8	184	5YR 4/6	2msbk,2csbk	70	sl	1f,1m	1.7
	Bw9	205	5YR 4/6	1msbk,2csbk	65	sl	1m	1.7
	Bw10	230	7.5YR 4/6	1msbk,1csbk,0sg	35	sc	1f	1.7
Bw11	245+	7.5YR 5/6	0sg	45	s	-	1.7	

Table 7. Depth integrated mean and standard errors of base cation concentration, cation exchange capacity, base saturation (BS), pH and % carbon (C) in crest soils across climate

Climate	Na (cmol (+)/ kg)	Ca (cmol (+)/ kg)	K (cmol (+)/ kg)	Mg (cmol (+)/ kg)	CEC (cmol (+)/ kg)	BS (%)	pH	% C
Shingwedzi	0.75 ± 0.2	3.20 ± 0.8	0.43 ± 0.2	1.23 ± 0.3	6.9 ± 1.9	79.7 ± 7.9	5.4 ± 0.4	0.5 ± 0.083
Skukuza	0.44 ± 0.1	1.40 ± 0.2	0.35 ± 0.1	1.17 ± 0.2	6.6 ± 1.8	47.8 ± 13.7	5.3 ± 0.1	0.4 ± 0.035
Pretoriuskop	0.14 ± 0.1	0.74 ± 0.1	0.78 ± 0.0	0.20 ± 0.4	6.3 ± 1.4	34.7 ± 13.9	5.4 ± 0.2	0.2 ± 0.002

Table 8. Semi-quantitative concentration of clay-sized minerals in B-horizons (0 = not detected, 5 = 100 % occurrence), depth integrated mean percent clay and standard error, mean maximum clay percent and standard error and clay fraction CEC

Site	Smectite	Kaolinite	Mica	Quartz	Feldspar	Clay (%)	Max clay (%)	Total clay (kg/ m ²)	CEC _{clay} (cmol(+)/kg)
Shingwedzi	2	3	2	5	3	9 ± 2	9 ± 2	30 ± 16	~76
Skukuza	0	2	2	5	2	7 ± 1	8 ± 1	42 ± 16	~94
Pretoriuskop	0	5	1	1	0	11 ± 1	13 ± 2	306 ± 135	~57

Table 9. Depth profiles of concentrations and fractional gains/ losses (τ) of major elements standardized by zirconium in crest soils along climate gradient

Site/ lower horizon depth (cm)	Si (%)	τ Si	Al (%)	τ Al	Fe (%)	τ Fe	Ca (%)	τ Ca	Mg (%)	τ Mg	Na (%)	τ Na	K (%)	τ K	P (%)	τ P	Ti (%)	τ Ti	Zr (ppm)
Shingwedzi																			
ph1a																			
1	33.87	-0.86	6.95	-0.87	1.45	-0.72	1.03	-0.86	0.25	-0.43	2.40	-0.90	1.63	-0.85	0.04	-0.36	0.41	0.61	247
13	33.72	-0.86	7.16	-0.87	1.76	-0.67	0.99	-0.87	0.27	-0.37	2.33	-0.91	1.66	-0.85	0.03	-0.43	0.47	0.84	247
22	33.74	-0.85	7.27	-0.86	1.76	-0.64	0.92	-0.87	0.24	-0.40	2.29	-0.90	1.67	-0.84	0.03	-0.39	0.41	0.72	230
45	34.37	-0.80	7.25	-0.81	1.52	-0.58	0.80	-0.84	0.19	-0.36	2.41	-0.86	1.70	-0.78	0.03	-0.29	0.32	0.80	172
50+	33.22	-0.82	7.83	-0.81	1.64	-0.59	0.96	-0.83	0.21	-0.38	3.06	-0.84	1.25	-0.85	0.02	-0.53	0.22	0.12	188
ph3a																			
2	36.13	-0.72	6.37	-0.78	0.75	-0.73	0.54	-0.86	0.05	-0.77	2.03	-0.85	2.08	-0.64	0.03	-0.20	0.19	0.37	132
16	35.74	-0.74	6.66	-0.78	0.81	-0.72	0.55	-0.87	0.08	-0.68	2.06	-0.85	2.14	-0.65	0.03	-0.11	0.19	0.31	138
28	33.98	-0.76	8.06	-0.75	1.11	-0.64	0.82	-0.81	0.16	-0.38	2.76	-0.81	1.54	-0.76	0.02	-0.39	0.16	0.09	144
45																			
ph5c																			
23	32.59	-0.82	7.71	-0.81	1.74	-0.56	0.84	-0.85	0.23	-0.30	2.67	-0.86	2.29	-0.72	0.03	-0.25	0.35	0.85	186
45	32.72	-0.74	7.93	-0.72	2.09	-0.22	0.95	-0.75	0.33	0.50	2.50	-0.80	2.10	-0.62	0.02	-0.31	0.30	1.31	126
55																			
ph6c																			
12	33.53	-0.81	7.31	-0.82	1.88	-0.51	1.28	-0.76	0.22	-0.29	3.00	-0.83	1.21	-0.85	0.02	-0.51	0.24	0.30	179
29	33.65	-0.75	7.57	-0.74	1.87	-0.34	1.23	-0.69	0.15	-0.36	3.03	-0.77	1.09	-0.81	0.02	-0.47	0.20	0.45	133
53	33.58	-0.76	7.75	-0.75	1.55	-0.48	1.20	-0.71	0.20	-0.19	3.31	-0.76	1.02	-0.83	0.01	-0.75	0.25	0.71	140
63																			
Skukuza																			
sb1a																			
6	37.40	-0.23	5.20	-0.56	1.01	-0.50	0.35	-0.92	0.04	-0.69	1.17	-0.64	2.92	-0.53	0.01	-0.51	0.23	0.60	154
16	36.84	-0.34	5.64	-0.59	1.06	-0.54	0.38	-0.93	0.05	-0.65	1.21	-0.68	2.99	-0.58	0.01	-0.72	0.26	0.59	179
26	37.00	-0.30	5.47	-0.58	1.08	-0.51	0.32	-0.94	0.04	-0.76	1.10	-0.69	2.96	-0.56	0.01	-0.70	0.24	0.53	169
24																			
sb2a																			
26	35.38	-0.64	5.50	-0.78	1.06	-0.74	0.67	-0.82	0.08	-0.72	1.33	-0.80	2.89	-0.77	0.01	-0.76	0.18	-0.39	317
43	36.27	-0.63	5.53	-0.77	1.01	-0.75	0.53	-0.86	0.07	-0.76	1.25	-0.81	2.98	-0.77	0.01	-0.76	0.19	-0.36	316
63	36.41	-0.59	5.58	-0.74	1.06	-0.71	0.50	-0.85	0.06	-0.76	1.23	-0.79	2.95	-0.74	0.01	-0.82	0.19	-0.27	283
98	36.50	-0.47	5.54	-0.67	1.15	-0.59	0.46	-0.82	0.08	-0.59	1.14	-0.75	2.91	-0.67	0.01	-0.77	0.17	-0.14	218
131	36.43	-0.51	5.41	-0.70	1.17	-0.62	0.49	-0.83	0.09	-0.56	1.21	-0.76	2.72	-0.71	0.01	-0.79	0.19	-0.15	237
136																			
sb3f																			
3	34.94	-0.47	7.00	-0.57	1.33	-0.51	1.08	-0.57	0.05	-0.74	2.73	-0.38	1.80	-0.79	0.01	-0.64	0.25	0.30	209
11	34.00	-0.60	7.65	-0.63	1.33	-0.62	1.17	-0.63	0.09	-0.61	2.97	-0.47	1.76	-0.84	0.02	-0.63	0.34	0.38	268
30																			
sb4e																			
7	35.94	-0.58	6.64	-0.69	0.66	-0.81	0.48	-0.85	0.04	-0.82	2.07	-0.64	3.65	-0.67	<0.01	-0.91	0.15	-0.41	274
33	35.19	-0.64	6.82	-0.72	0.72	-0.82	0.45	-0.88	0.04	-0.86	2.04	-0.69	3.60	-0.71	<0.01	-1.00	0.18	-0.37	313
65	34.96	-0.61	7.32	-0.67	0.91	-0.75	0.46	-0.86	0.08	-0.68	2.00	-0.66	3.37	-0.70	<0.01	-0.97	0.18	-0.33	283
75																			
sb6c																			
10	35.61	-0.67	6.59	-0.75	0.91	-0.79	0.68	-0.83	0.04	-0.88	2.32	-0.68	2.59	-0.81	0.01	-0.78	0.14	-0.54	340
23	35.46	-0.69	6.80	-0.76	1.08	-0.77	0.65	-0.85	0.05	-0.83	2.23	-0.71	2.66	-0.82	<0.01	-0.93	0.20	-0.41	362
50	34.47	-0.63	7.11	-0.69	1.46	-0.62	0.57	-0.84	0.13	-0.51	2.31	-0.63	2.51	-0.79	0.01	-0.83	0.17	-0.37	297
60																			

Site/ depth (cm)	Si (%)	τ Si	Al (%)	τ Al	Fe (%)	τ Fe	Ca (%)	τ Ca	Mg (%)	τ Mg	Na (%)	τ Na	K (%)	τ K	P (%)	τ P	Ti (%)	τ Ti	Zr (ppm)
Pretoriuskop																			
pkop1a																			
8	39.31	-0.70	2.76	-0.91	0.83	-0.84	0.27	-0.94	0.02	-0.93	0.44	-0.95	1.87	-0.89	0.02	-0.70	0.21	-0.45	414
17	40.38	-0.71	2.72	-0.92	0.88	-0.85	0.18	-0.97	0.02	-0.95	0.44	-0.95	1.95	-0.89	0.01	-0.83	0.25	-0.39	443
39	39.82	-0.76	3.05	-0.92	1.13	-0.83	0.19	-0.97	0.01	-0.97	0.46	-0.96	2.13	-0.90	0.01	-0.90	0.29	-0.40	520
70	40.06	-0.75	3.06	-0.92	1.11	-0.83	0.18	-0.97	0.01	-0.97	0.51	-0.95	2.11	-0.90	<0.01	-0.95	0.26	-0.45	509
93	40.28	-0.73	2.94	-0.92	1.04	-0.83	0.16	-0.97	0.01	-0.97	0.70	-0.93	1.99	-0.90	0.01	-0.84	0.24	-0.45	475
115	38.28	-0.73	4.29	-0.88	1.24	-0.79	0.14	-0.97	0.03	-0.92	0.37	-0.96	2.27	-0.87	0.00	-0.94	0.25	-0.40	451
142	38.68	-0.73	4.11	-0.88	1.23	-0.79	0.16	-0.97	0.04	-0.91	0.45	-0.95	2.22	-0.88	0.01	-0.89	0.25	-0.41	450
164	37.86	-0.77	4.67	-0.88	1.33	-0.80	0.24	-0.96	0.05	-0.89	0.68	-0.94	2.16	-0.90	0.01	-0.85	0.28	-0.42	517
184	35.12	-0.79	6.33	-0.84	1.71	-0.75	0.29	-0.95	0.13	-0.72	1.11	-0.90	2.32	-0.89	0.01	-0.90	0.33	-0.32	523
205	33.75	-0.75	7.28	-0.78	1.95	-0.65	0.35	-0.93	0.16	-0.58	1.83	-0.80	2.16	-0.88	0.01	-0.88	0.33	-0.17	430
230	32.40	-0.60	7.85	-0.61	2.67	-0.21	0.91	-0.71	0.35	0.53	2.43	-0.56	1.38	-0.87	0.01	-0.71	0.35	0.46	261
245	31.78	-0.59	8.33	-0.56	2.71	-0.16	0.99	-0.66	0.41	0.89	2.72	-0.48	1.24	-0.88	0.01	-0.80	0.35	0.54	248
pkop2c																			
4	38.86	-0.80	3.09	-0.93	1.52	-0.81	0.26	-0.96	0.00	-0.99	0.50	-0.96	1.91	-0.92	0.01	-0.88	0.43	-0.25	610
0	40.73	-0.74	2.97	-0.92	1.41	-0.78	0.17	-0.97	0.00	-0.99	0.50	-0.95	1.83	-0.91	0.01	-0.90	0.40	-0.16	507
76	39.09	-0.79	3.76	-0.92	1.43	-0.81	0.15	-0.98	0.01	-0.98	0.42	-0.97	1.84	-0.92	0.01	-0.91	0.41	-0.24	587
105	37.52	-0.83	4.62	-0.91	1.65	-0.82	0.15	-0.98	0.02	-0.96	0.38	-0.97	1.92	-0.93	0.01	-0.93	0.43	-0.34	696
125	37.96	-0.84	4.57	-0.92	1.48	-0.85	0.14	-0.98	0.05	-0.92	0.42	-0.97	2.01	-0.93	0.01	-0.90	0.44	-0.36	749
146	38.45	-0.84	4.12	-0.93	1.38	-0.86	0.14	-0.98	0.01	-0.98	0.45	-0.97	2.06	-0.93	0.01	-0.94	0.45	-0.38	786
180	37.93	-0.87	4.49	-0.94	1.38	-0.88	0.14	-0.99	0.01	-0.98	0.48	-0.97	2.66	-0.93	0.01	-0.92	0.46	-0.45	905
212	36.05	-0.81	6.13	-0.87	1.43	-0.82	0.21	-0.97	0.08	-0.85	0.62	-0.95	3.10	-0.87	0.00	-0.96	0.39	-0.30	605
pkoph1																			
15	38.97	-0.73	3.89	-0.89	1.43	-0.76	0.07	-0.99	0.00	-0.99	0.41	-0.96	3.29	-0.82	0.01	-0.84	0.31	-0.27	459
31	38.53	-0.76	4.26	-0.89	1.39	-0.79	0.06	-0.99	0.02	-0.95	0.32	-0.97	3.20	-0.84	0.01	-0.85	0.32	-0.31	504
59	37.70	-0.77	4.66	-0.89	1.41	-0.80	0.06	-0.99	0.01	-0.97	0.36	-0.97	3.13	-0.85	0.01	-0.86	0.32	-0.34	532
87	38.01	-0.76	4.73	-0.88	1.33	-0.80	0.05	-0.99	0.03	-0.93	0.40	-0.96	3.02	-0.85	0.02	-0.80	0.32	-0.31	509
106	38.40	-0.77	4.36	-0.89	1.22	-0.82	0.05	-0.99	0.01	-0.97	0.39	-0.96	3.05	-0.85	0.01	-0.86	0.34	-0.31	522
131	37.86	-0.80	4.60	-0.90	1.22	-0.84	0.07	-0.99	0.02	-0.95	0.37	-0.97	3.34	-0.86	0.01	-0.92	0.37	-0.35	605
140	37.31	-0.84	5.16	-0.91	1.30	-0.86	0.06	-0.99	0.02	-0.96	0.40	-0.97	3.73	-0.87	0.01	-0.90	0.39	-0.42	722
pkoph2																			
10	37.60	-0.77	4.26	-0.90	1.42	-0.79	0.12	-0.98	0.02	-0.95	0.47	-0.96	3.42	-0.84	0.02	-0.76	0.34	-0.32	531
23	38.41	-0.77	4.26	-0.90	1.34	-0.81	0.11	-0.98	0.01	-0.97	0.47	-0.96	3.44	-0.84	0.01	-0.91	0.35	-0.30	540
49	38.20	-0.75	4.34	-0.89	1.41	-0.78	0.10	-0.98	0.02	-0.96	0.55	-0.95	3.49	-0.82	0.01	-0.85	0.37	-0.18	489
106	37.86	-0.73	4.40	-0.87	1.39	-0.76	0.08	-0.99	0.05	-0.86	0.31	-0.97	3.03	-0.83	0.02	-0.78	0.31	-0.26	454
135	38.09	-0.77	4.76	-0.88	1.46	-0.79	0.09	-0.99	0.05	-0.90	0.47	-0.96	3.17	-0.85	0.01	-0.86	0.35	-0.28	534
157	38.04	-0.79	4.77	-0.89	1.28	-0.83	0.09	-0.99	0.04	-0.93	0.45	-0.96	3.40	-0.85	0.02	-0.82	0.38	-0.28	568
170	36.73	-0.77	5.70	-0.85	1.37	-0.79	0.09	-0.98	0.04	-0.90	0.45	-0.96	3.62	-0.82	<0.01	-0.95	0.34	-0.27	507

Table 10. Mean and standard error of model parent material calculated depth integrated mass gains and losses of Si, Al, Fe, base cations, Ti, P and total mass loss from crest soils across climate standardized by Zr concentration in soil and rock

	Si	Al	Fe	Ca	Mg	Na	K	Ti	P	total
Kg/ m ²										
Shingwedzi	188 ± 59	42 ± 13	3 ± 1	6 ± 2	0.1 ± 0.05	20 ± 6	8 ± 3	-0.1 ± 0.05	0.03 ± 0.01	268 ± 83
Skukuza	201 ± 90	59 ± 28	10 ± 5	11 ± 5	0.7 ± 0.30	16 ± 9	32 ± 15	0.3 ± 0.15	0.15 ± 0.07	330 ± 151
Pretoriuskop	1126 ± 133	317 ± 34	48 ± 6	54 ± 5	3.6 ± 0.53	93 ± 10	164 ± 18	1.3 ± 0.15	0.71 ± 0.08	1806 ± 207

Table 11. Mean, standard error and coefficient of variability in Zr/ Ti for crest horizons in Kruger to examine parent material uniformity

Horizon	ph1a	ph3a	ph5c	ph6c	sb1a	sb2a	sb3f	sb4e	sb6c	pkop1a	pkop2c	pkop4h1	pkop4h2
1	0.61	0.71	0.53	0.75	0.68	1.76	0.83	1.84	2.36	1.97	1.43	1.47	1.58
2	0.53	0.74	0.42	0.67	0.68	1.70	0.78	1.71	1.83	1.76	1.28	1.56	1.55
3	0.56	0.89		0.57	0.70	1.48		1.61	1.71	1.81	1.42	1.64	1.31
4	0.54					1.25				1.98	1.63	1.57	1.46
5	0.87					1.28				1.98	1.69	1.55	1.51
6										1.79	1.75	1.65	1.50
7										1.83	1.96	1.85	1.48
8										1.88	1.55		
9										1.59			
10										1.30			
11										0.74			
12										0.70			
mean	0.62	0.78	0.47	0.66	0.69	1.49	0.81	1.72	1.97	1.61	1.59	1.62	1.49
se	0.06	0.06	0.05	0.05	0.01	0.11	0.02	0.07	0.20	0.13	0.08	0.05	0.03
cv (%)	22.87	12.24	15.77	13.40	2.32	15.72	4.01	6.95	17.71	28.37	13.54	7.50	5.79

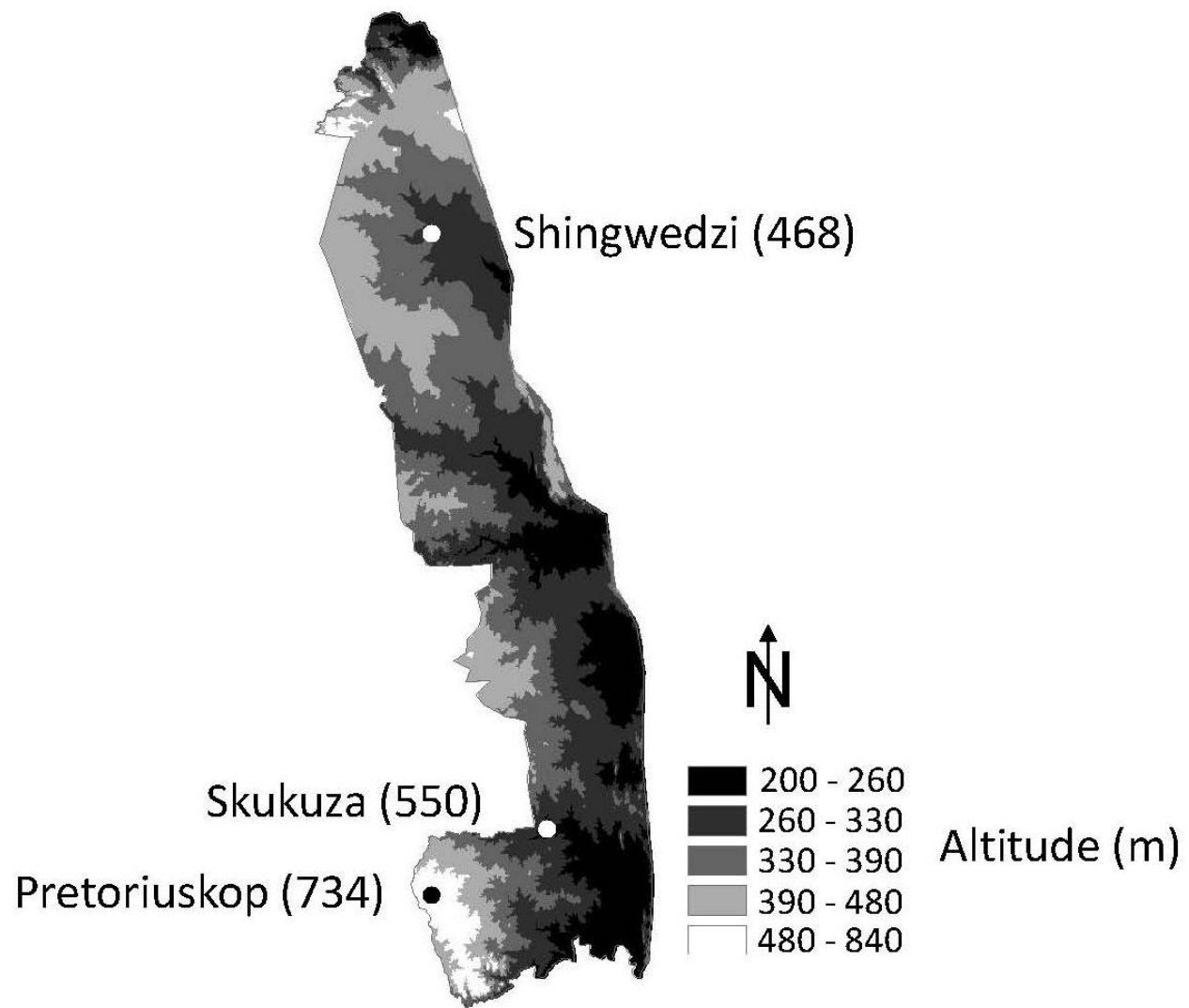


Figure 1. Kruger National Park showing mean annual rainfall of field sites and altitude across the climate gradient.

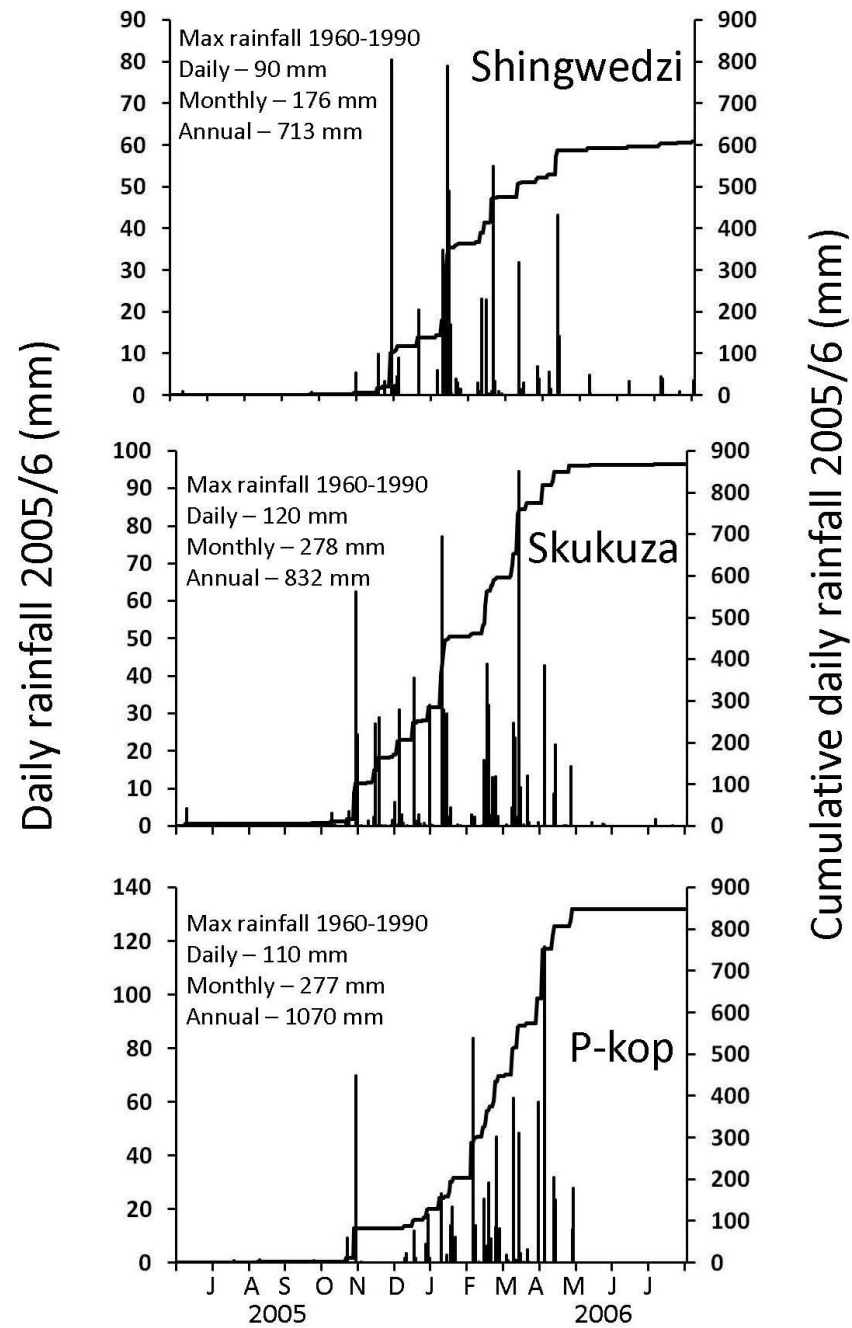


Figure 2. Daily and cumulative rainfall for the 2005/6 rainfall year in Shingwedzi, Skukuza and Pretoriuskop. Inserts show maximum daily, monthly and annual rainfalls between 1960 and 1990 in the three climate zones.

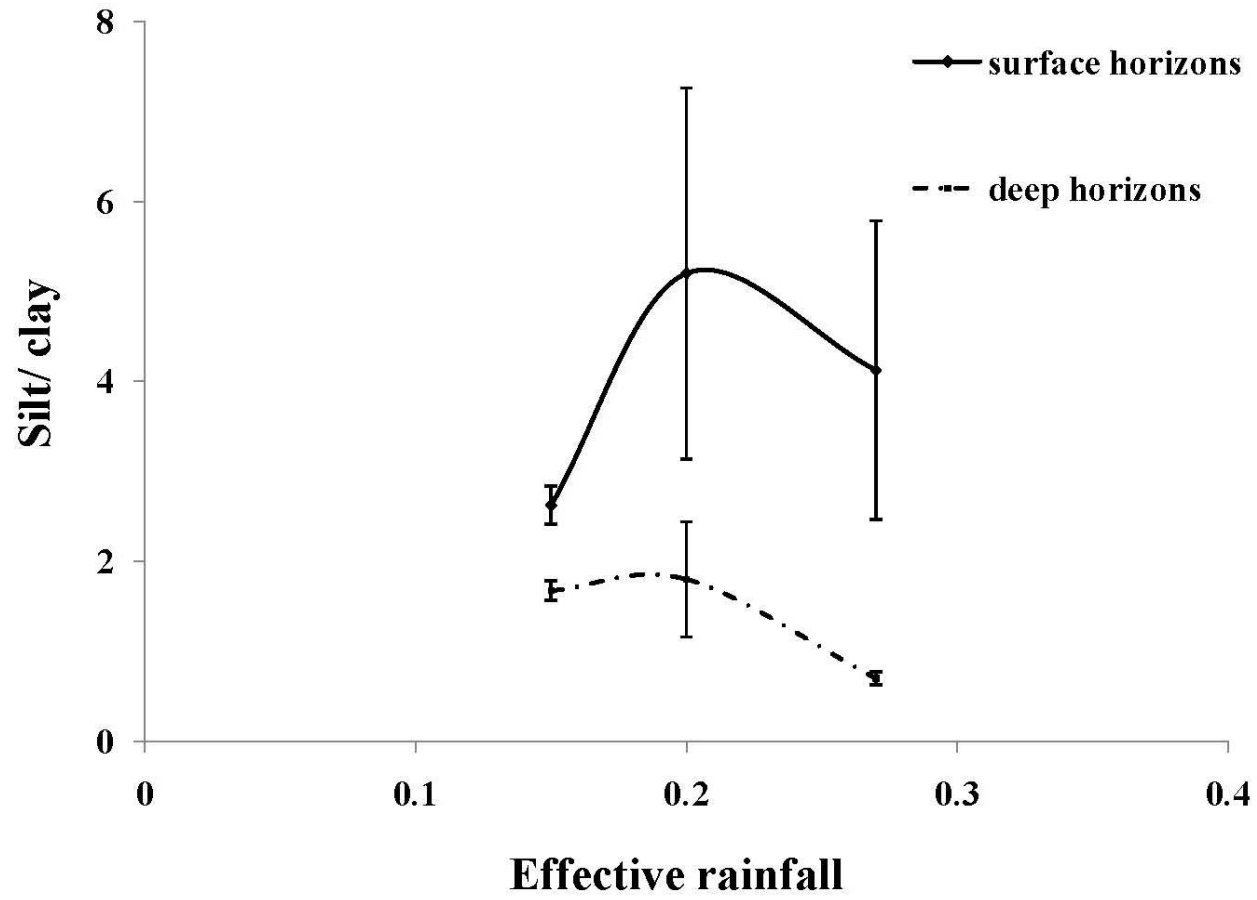


Figure 3. Mean and standard error of silt to clay ratios of deep and surface horizons in crest soils across Kruger's climate gradient.

Appendix I. Horizon field properties and soil profile locations of sampled crests

Effective rainfall/ site/ horizon	Latitude (m)	Longitude (m)	Lower horizon depth (cm)	Moist colour	Structure	Gravel (%)	Field texture	Silt/ clay	Roots
0.15 - Shingwedzi									
ph1a	322428	7451196							
BA			1	7.5YR 2.5/2	0sg	10	ls	2.7	3vf
Bw1			13	7.5YR 2.5/2	1vfsbk	17	ls	1.8	1vf,1f
Bw2			22	2.5YR 5/8	2msbk	28	sl	1.8	2vf,2f
Bw3			45	2.5YR 3/3	2fsbk	70	sl	1.5	2vf,2f
C			50+	-	-	95	s	1.8	-
ph3a									
A	316352	7453989	2	7.5yr 3/4	sg	10	ls	2.9	2vf
Bw1			16	7.5yr 3/4	2msbk	20	ls	1.6	2vf,2f,1m,c
2Bw2			28	7.5yr 3/4	1vfsbk	40	ls	2.2	2vf,2f,1vc
2C			45		m	70	ls		1vf
ph5c									
A	322713	7452153	2	7.5yr 3/4	sg	10	ls	2.9	1vf
Bw1			16	7.5yr 3/4	2msbk	20	ls	1.6	2vf,2f,1m,1c
2Bw2			28	7.5yr 3/4	1vfsbk	40	ls	2.2	2vf,2f,1vc
2C			45		m	70	ls		-
ph6c									
BA	318512	7449979	12	7.5YR 2.5/2	sg	70	sl	2.0	1vf,1f
BC			29	7.5YR 2.5/2	sg	85	ls	3.0	2vf,2f,1m
C			53	7.5YR 2.5/3	sg	90	ls	1.8	1vf,1f,1m
CR			63		m	95			
0.20 -Skukuza									
sb1a	377803	7247170							
A			26	10YR 3/3	1csbk	< 5	ls	2.6	2vf,1f,1m,2co,1vc
Bw1			43	10YR 2/2	1cabk	< 5	ls	2.3	3vf,2f1,m
Bw2			63	5YR 4/4	1mabk	15	s	1.7	2vf,2f,1m
Bw3			98	5YR 4/6	1fabk	55	s	2.0	2vf,1f
BC			131+	7.5YR 4/6	0sg	65	s		1vf,1f
sb2a									
A	348245	7232081	26	10YR 3/3	1csbk	0	ls	11.0	2vf,1f,1m,2c,1vc
				10YR 2/2 (.7), 7.5YR					
Bw1			43	2.5/3 (0.3)	1cabk	0	ls	1.6	3vf,2f,1m
Bw2			63	5YR 4/4	1mabk	15	s	0.9	2vf,2f,1m
Bw3			98	5YR 4/6	1fabk	55	s	1.0	2vf,1f
Bc			131	7.5YR 4/6	0sg	65	s	1.0	1vf,1f
CR			136			80			-
sb3									
A	363444	7235287	3	10YR 3/4	1f,mgr,1-2tnpl	35	ls	5.0	2vf
BC			11	10YR 3/6	1vf,f,sbk	50	sl	3.7	1vf,1f
CR			30		M	80			

Effective rainfall/ site/ horizon	Latitude (m)	Longitude (m)	Lower horizon depth (cm)	Moist colour	Structure	Gravel (%)	Field texture	Silt/ clay	Roots
sb4e	348286	7230808							
BA			7	10YR 3/3	1f,msbk,1fgr	5	ls	1.5	1vf,1f
Bw1			33	10YR 3/4	1f,msbk	10	ls	1.3	1vf,1f,1m,1co
CR/BC			65	10YR 4/4	sg,1fgr	70	ls-s	1.3	1f
RC			75		M	95			
sb6	346001	7227674							
BA			10	10YR 3/4	1vnpl,1f,msbk,1f,mgr	6	ls-sl	3.3	2vf,2f
Bw1			23	7.5YR 3/3	1f,msbk	11	ls	1.3	2vf,2f,2m
BC			50	7.5YR 3/4	sg,1fgr	43	ls	1.3	1vf,1f
CR			60		M	20			
ptk1a	326823	7211630							
BA			8	10YR 2/2	0sg,1vf,msbk	0	ls	7.0	2vf,2f
Bw1			17	7.5YR 3/3	1vf,msbk,0sg	2	s	6.0	3vf,3f,1co
Bw2			39	7.5YR 4/4	0sg,1msbk,1csbk	5	s	3.5	2vf,2f,2m,2co
Bw3			70	7.5YR 4/6	1mcsbk,0sg	5	s	5.0	3vf,3f,3m,2co
Bw4			93	7.5YR 5/6	1msbk,1csbk	10	s	3.5	3vf,3f,1m,1co
Bw5			115	5YR 5/4	1msbk,1csbk	80	s	1.4	2vf,2f,1m,1co
Bw6			142	5YR 5/4	2msbk	65	s	1.4	2f,2m,1vc
Bw7			164	5YR 4/4	1msbk,1csbk	65	ls	1.4	1f,1m
Bw8			184	5YR 4/6	2msbk,2csbk	70	sl	0.6	1f,1m
Bw9			205	5YR 4/6	1msbk,2csbk	65	sl	1.6	1m
Bw10			230	7.5YR 4/6	1msbk,1csbk,0sg	35	sc	2.0	1f
Bw11			245+	7.5YR 5/6	0sg	45	s	2.3	-
ptk2c	321217	7211736							
AB			4	10YR 2/1	1f,msbk,1fgr	0	sl	7.0	2vf,f
Bw1			30	10YR 3/4	2f,mabk	0	sl	1.0	2vf,2f,1m,1co
Bw2			76	5YR 4/4	2mabk	0	scl	0.9	1vf,1f
Bw3			105	5YR 4/4	2mabk	0	scl	1.2	1vf,1f,1m
Bw4			125	5YR 4/4	2mabk	0	scl	0.9	1vf,1f,1m
Bw5			146	5YR 4/4	2mabk	0	sl	1.0	1vf,1f,1m
2Bw6			180	5YR 4/4	sg,1f,msbk	0	sl	3.8	1vf,1f
C			212			5		1.0	
ptk4h2	323726	7211482							
Ba			10	10yr3/3	3m,coabk	<5	sl	1.4	3vf,3f,1m,1vc
Bw1			23	10yr3/4	3m,coabk	<5	sl	1.7	2vf,2f,1co,1vc,1m
Bw2			49	10yr3/6	2-3m,coabk	<5	sl-	1.2	1v,1f,1m,1co,1vc
Bw3			106	10yr4/6	2co,vc,skb	<5	sl	0.8	1vf,1f,1m,1vc
Bw4			135	5yr4/4	2f,msbk	15	scl	0.8	2vf,1f,1m
2Bw5			157	5yr4/4	m,1vf,fsbk,sg	50	scl	1.0	1vf,1f
3BC			170	5yr4/4	1vfabk,m,sg	72	scl	0.6	1vf
ptk4h1	323709	7211461							
Ba			15	7.5yr3/2	2m,coabk,1co,mgr	<5	sl	1.1	2vf,f
Bw1			31	5yr4/4	2m,coabk	<5	sl	0.9	2vf,f,m,co,vc
Bw2			59	5yr4/4	1-2f,abk	<5	sl	0.7	2vf,f,m,co
Bw3			87	5yr4/4	2m,coabk	<5	scl	0.6	2vf,f

Effective rainfall/ site/ horizon	Latitude (m)	Longitude (m)	Lower horizon depth (cm)	Moist colour	Structure	Gravel (%)	Field texture	Silt/ clay	Roots
Bw4			106	5yr4/4	1f,mabk	10	scl	0.9	1vf,f
Bbc1			131	5yr4/4	1-2m,coabk	20	scl	0.8	1vf,f,co,m
Bbc2			140	5yr4/4	sg,1co,mgr,m	85	scl	1.2	1vf

Appendix II. Horizon exchange properties and carbon content in sampled crest soils

Site/depth (cm)	Clay (%)	xK	xMg	xCa cmol(+)/kg	xNa	CEC	BS (%)	pH	% C
0.15									
ph1a									
0-1	11	0.74	1.22	5.00	1.20	5.10	100	6.7	1.1
1-13	14	0.30	1.23	4.57	1.21	6.02	100	6.6	0.6
13-22	15	0.19	1.16	3.77	1.15	5.18	100	6.8	0.4
22-45	14	0.22	1.39	4.18	1.37	5.71	100	6.6	0.4
45-50+	14	0.28	1.51	4.81	1.51	3.35	100	6.6	0.1
ph3a									
0-2	9	0.34	0.60	0.98	0.60	2.69	94	5.3	0.9
2-16	11	0.25	0.29	0.88	0.28	2.03	84	4.9	0.6
16-28	11	0.14	0.56	0.49	0.55	2.48	70	4.8	0.4
28-45									
ph5c									
0-23	6	0.36	1.20	5.04	0.98	10.40	73	6.1	0.7
23-45	5	0.30	1.06	3.53	0.82	11.63	49	5.9	0.8
45-55									
ph6c									
0-12	5	1.08	2.19	4.85	0.31	11.19	75	6.3	0.7
12-29	4	0.72	1.87	4.37	0.38	9.44	78	6.4	0.5
29-53	5	1.02	2.08	2.23	0.40	7.02	82	6.4	0.3
53-63									
0.20									
sb1a									
0-6	9	0.29	0.88	2.52	0.87	5.08	90	6.1	0.8
6-16	9	0.19	0.53	1.50	0.52	2.33	100	5.9	0.4
16-26	9	0.15	0.67	1.09	0.66	2.77	93	5.8	0.4
26-24	11	0.17	0.66	0.89	0.66	2.40	99	5.1	0.4
sb2a									
0-26	1	0.32	1.61	4.24	0.15	22.30	28	6.2	1.5
26-43	9	0.18	0.60	1.71	0.13	7.94	33	6.2	0.4
43-63	9	0.12	0.69	1.30	0.17	8.93	25	5.9	0.2
63-98	9	0.06	0.86	1.06	0.15	9.40	23	5.4	0.2
98-131	8	0.03	1.12	0.70	0.13	9.26	21	5.5	0.1
131-136									
sb3f									
0-3	3	0.48	0.85	1.17	0.49	6.79	44	5.6	0.5
3-11	4	0.24	0.84	0.77	0.56	5.32	45	5.2	0.3
11-30									
sb4e									
0-7	8	0.92	1.55	1.63	0.57	6.23	75	6.1	0.4
7-33	8	0.59	1.16	1.08	0.36	6.94	46	5.1	0.4
33-65	10	0.42	2.07	1.23	0.59	7.98	54	5.2	0.3
65-75									
sb6c									
0-10	4	0.60	1.28	1.89	0.32	6.67	61	5.8	0.6
10-23	10	0.55	1.19	1.47	0.35	7.66	47	5.4	0.4

Site/depth (cm)	Clay (%)	xK	xMg	xCa	xNa	CEC	BS (%)	pH	% C
				cmol(+)/kg					
23-50	8	0.62	2.07	1.61	0.34	10.00	46	4.8	0.3
50-60									
0.27									
pkop1a									
0-8	3	0.07	0.31	1.14	0.12	32.82	5	6.5	2.3
8-17	3	0.06	0.23	1.06	0.11	8.01	18	6.1	0.5
17-39	5	0.07	0.12	0.08	0.13	13.04	3	5.9	0.3
39-70	3	0.02	0.02	0.00	0.13	3.77	4	5.8	0.1
70-93	5	0.08	0.37	0.37	0.15	1.72	57	5.2	0.1
93-115	10	0.06	0.41	0.54	0.17	11.51	10	5.1	0.1
115-142	11	0.06	0.38	0.61	0.20	8.60	14	5.4	0.1
142-164	11	0.09	0.57	0.91	0.25	11.18	16	5.7	0.1
164-184	15	0.12	0.83	1.33	0.35	11.05	24	5.9	0.1
184-205	13	0.16	0.95	1.50	0.23	13.83	21	5.7	0.1
205-230	13	0.18	0.96	1.38	0.24	14.56	19	6.2	0.0
230-245	8	0.11	0.62	1.85	0.15	14.42	19	6.2	0.0
pkop2c									
0-4	3	0.56	2.55	3.62	0.53	7.98	91	6.2	1.0
4-30	8	0.39	1.85	1.01	0.47	3.10	100	5.5	0.2
30-76	13	0.30	1.83	0.87	0.52	4.72	75	5.0	0.2
76-105	15	0.22	1.76	0.74	0.54	5.16	63	4.9	0.2
105-125	18	0.22	1.52	0.66	0.48	5.32	54	5.2	0.2
125-146	16	0.27	1.61	0.84	0.61	4.17	80	5.3	0.1
146-180	6	0.23	1.59	0.88	0.63	4.29	78	5.5	0.1
180-212	18	0.24	2.26	1.30	0.62	5.63	79	6.0	0.1
pkoph1									
0-15	6	0.19	0.33	0.69	0.01	4.08	30	5.8	
15-31	8	0.07	0.23	0.36	0.01	5.04	13	5.6	
31-59	11	0.06	0.30	0.41	0.02	5.25	15	5.2	
59-87	12	0.08	0.38	0.80	0.04	4.88	27	5.4	
87-106	10	0.08	0.30	0.83	0.04	5.06	25	5.5	
106-131	10	0.10	0.34	1.10	0.07	4.79	34	5.8	
131-140	10	0.12	0.38	0.75	0.07	4.89	27	5.9	
pkoph2									
0-10	5	0.12	0.45	1.41	0.02	5.61	36	5.8	
10-23	5	0.08	0.27	0.69	0.01	4.53	23	5.7	
23-49	7	0.04	0.26	0.33	0.02	4.45	15	5.7	
49-106	9	0.06	0.34	0.63	0.02	5.38	19	5.5	
106-135	10	0.09	0.30	0.56	0.04	5.19	19	5.6	
135-157	8	0.12	0.29	0.55	0.06	4.88	21	5.7	
157-170	10	0.17	0.47	0.82	0.07	5.25	29	5.9	

Appendix III. Cosmogenic isotope method for determining erosion rates

The concentration of cosmogenic ^{10}Be provides an estimate of the long-term erosion rate from which a soil residence time (age) can be inferred. Erosion rates are estimated under the assumption of uniform soil production rate, bulk density and soil depth through time. The erosion rate at the interface between mobile soil undergoing bioturbation and immobile saprolite is

$$\varepsilon = -\frac{\partial e}{\partial t} = \frac{\Lambda}{\rho r} \left(\frac{P(h, \theta)}{C - \lambda} \right) \quad (1)$$

where $\Lambda \sim 165 \text{ g/cm}^2$ is the mean attenuation length of cosmic rays into soil, ρr is the rock bulk density in g/cm^3 , $P(h, \theta)$ is the rate of ^{10}Be production in quartz at the soil/saprolite boundary under h cm of soil on a θ° inclined slope, C is the number of ^{10}Be atoms in a gram of quartz and λ is the decay constant of ^{10}Be ($= 4.6 \times 10^5 \text{ y}^{-1}$). Under steady state conditions, soil production = soil erosion = the rate at which the soil/saprolite interface descend into bedrock. The production rate of cosmogenic isotopes varies with latitude, elevation and topographic shielding for which standard corrections are made (Nishiizumi et al., 1991).

^{10}Be concentration in quartz reflects the sample's exposure age, its rate of production at that depth and the soil's erosion rate at that point in the landscape. We collected one kilogram of saprolite at the boundary with soil to a depth of 1 – 10 cm to ensure retrieval from regolith's immobile zone. The boundary was marked by C-horizon properties such as an increase in particle size variability and loss of coherent soil structure. The rock/soil sample was crushed, sieved through a 1 mm mesh and purified according to Kohl and Nishiizumi (1992). Forty kilograms of quartz (10 g is the

Accelerator Mass Spectrometer (AMS) detection limit) are required from the entire sample of soil/ rock collected in the field after crushing to monomineralic grains and chemical treatment. Quartz is the target mineral for these analyses because of its crustal abundance and the relative ease with which it separates from other minerals. The interlocking mineral structure and exclusive Si-O composition minimizes contamination by meteoric ^{10}Be (garden variety, not *in situ* produced but atmosphere derived) and enables simple theoretical predictions of ^{10}Be production rates. Four 10-h ultrasonic leaches heated to 95°C were used to remove meteoric ^{10}Be to measure only the *in situ* produced isotope (Heimsath et al., 1999). We used a Be carrier calibrated by Nishiizumi's et al. (1989) whose Be atomic absorption standard and ours differ by less than 2 %. Be was then extracted from the dissolved quartz using ion exchange chromatography. ^{10}Be concentration was measured at the Lawrence Livermore National Laboratory AMS facility and the $^{12}\text{Be}/^{10}\text{Be}$ was normalized to the ICN ^{10}Be standard. An erosion rate was then determined from (1) and a soil residence time estimates as the product of erosion rate's inverse and measured soil depth. Erosion rates were only measured in three soils, one in each climate zone, thus these rates are hardly conclusive.

CHAPTER 3. CLAY AND BASE CATION DISTRIBUTION ALONG CATENAS IN DIFFERENT CLIMO-TOPOGRAPHIC SETTINGS OF KRUGER NATIONAL PARK

1. INTRODUCTION

Rock minerals weather in soils to produce clay minerals, which in turn provide fundamental controls over water retention and nutrient storage making soils clay factories and clay a master soil property. Clay is the sole weathering product as palpable as the rock from which it formed amongst other, less sturdy rock-derived soil constituents. The singular importance of clay derives from two properties: a much larger surface area to volume ratio relative to other soil particles and a negative charge. Clay exerts its control on soil by modulating the concentrations of positively charged soil constituents adsorbed onto its enormous surface of negative charge. Since many essential plant nutrients are positively charged base cations, their sorption onto clay surfaces is one of the most important biogeochemical processes for ecosystem productivity. The formation and translocation of clay in different parts of a catena result in patches of soil that differ in clay content. These patches form the template upon which plants find suitable habitats for establishment, growth and persistence. Therefore, the amount and mineralogy of clay – and its distribution down soil profiles and across catenas – are some of the most critical soil properties that can be quantified in a landscape.

Since clay is a product of weathering and soil formation; its distribution in natural landscapes depends on soil forming factors (Jenny, 1941). Remarkably, very few studies

have in fact addressed the question of how clay is distributed across catenas in factorial space with an integrated and rigorous approach. Some have investigated the effect of climate on clay (Dahlgren et al., 1997), others have tackled how clay is distributed across a catena, seldom catenas in the plural sense (as Gunn, 1974 did on basalt), and yet others have looked at the effect of time on clay amount (Botha and Porat, 2007). Arguably, the most well documented relationship between a soil forming factor and clay amount remains the topography-clay pattern between crests and toeslopes on catenas as originally described by Milne (1935) and extended by many others (Burt and Park, 1999; Chappel, 1992; Nye, 1955a; Scholes and Walker, 1993; Watson, 1964). Of all these studies, none have examined how coupled climate, relief and hillslope position interact to yield patterns in clay abundance or type along catenas. Results from the crest-to-toeslope studies have been broadly consistent; soils near crests are clay poor whereas soils in the toeslopes are clay rich. In southern Africa and Australia, the contrast between crest and toeslope soils has been found to be so striking that the term duplex soil was coined. Duplex soils are the lowland, clay-rich soils (Chittleborough, 1992) with a strong texture contrast between the surface and subsurface horizons, and are essentially accentuated argillic or Bt horizons (Birkeland, 1999). However, none of the many studies have considered how the classic catena pattern of leached crests and clay-rich toeslope soils responds to variation in soil-forming factors, specifically climate and relief.

So, the driving question for the present study is how does climate and relief modify clay distribution along catenas? Climate or more directly water availability, being the chief agent of weathering and soil formation (Chadwick et al., 2003), can hardly be expected to fuel catena differentiation uniformly. There are likely to be some key

thresholds across climate gradients wherein too little or too much water fails to yield the classic distribution of clay along catenas. Evidently, between the two end-members of too much and too little water, clay distribution on catenas will correspond to the amount of water shunting material through the landscape. Similarly, the dimensions of a catena; relief, length and area will also impinge on how wet the catena is, and consequently whether there will be clay and where that clay occurs.

Now, nutrients, specifically the base cations magnesium, potassium and calcium are also influenced by the same soil forming factors that control clay distribution. However, in addition to factorial control, nutrient bases are much more mobile than clay when in soil solution. Again, many studies have investigated the distribution of bases on catenas (Burt and Park, 1999), but not in complex factorial space. The consensus amongst most of these studies is overwhelmingly that bases accumulate in the toeslopes of catenas (Scholes and Walker, 1993). Such remarkable agreement might have hindered any work to identify how this general pattern is altered by varying strengths of water-induced retraslocation of bases. Obviously, there could be some situations under which bases are completely lost from the system and yet others where bases are not even released from primary minerals, but this seemingly straightforward investigation remains unexplored.

Herein, I examine clay distribution and associated base cation concentrations in various settings of climate and topography on catenas in Kruger National Park's granitic landscape. Specifically, I target clay amounts in pedons and catenas, the contrast in percent clay in pedons and catenas, clay mineralogy along catenas and base cation concentrations on those catenas in relation to clay and soil forming factors.

2. STUDY SITES AND METHODS

Kruger National Park is located in the Limpopo and Mpumalanga provinces on the far east of South Africa along the Mozambique border (Fig. 1). The climate is arid to semi-arid with alternating warm/dry and hot/wet seasons each lasting for about 5-7 months. There is high inter-annual variability in rainfall in part associated with the El Nino-Southern Oscillation. The range in rainfall across the 250 km span of my field sites is between 400 and 700 mm annually with temperatures ranging between 25 and 30 °C (Scholes et al., 2003). The area is underlain by granitoid rocks in excess of 3 Ga and consists of relatively low gradient terrain abutted by the Lebombo Mountains to the east and the Great Escarpment to the west (Fig. 1). Vegetation in Kruger is generally bush savanna, with broad- and fine-leaved vegetation in clay-poor and clay-rich soil respectively. This vegetation-clay pattern is observed under any climate in granitic soil throughout Kruger (Gertenbach, 1983). However, the intricacies of how the pattern changes across gradients of climate and relief have yet to be detailed.

I explored clay and base cation distribution on nine catenas spread across gradients of climate, relief and distance from crest. Climate zones were designated by calculating an aridity index using daily temperature data and mean annual rainfall (Linacre, 1977). The calculation is essentially a simplified version of the FAO Penman-Monteith equation that only uses daily temperatures to estimate potential evapotranspiration (PET). The index is the ratio of mean annual precipitation (MAP) and PET or effective precipitation (EP). UNESCO guidelines define arid as less than 0.20 in EP and semi-arid as more than 0.20 but less than 0.50 (Tilahun, 2006).

I characterized catenas in three climate zones: arid catenas near Shingwedzi (0.15 in EP, D: dry) in the north of Kruger, arid to semi-arid catenas in Skukuza (0.20 in EP, I: intermediate) and semi-arid catenas in Pretoriuskop (0.27 in EP, W: wet). In each climate zone, three catenas were selected for characterization: a high relief catena (H: high) in the upper reaches of a river catchment, a middle relief catena (M: middle) and a low relief catena (L: low) adjacent to a fourth or fifth order stream. Thus, nine catenas were investigated across a nested matrix of climate and relief: DH, DM, DL, IH, IM, IL, WH, WM, and WL.

Terrain attributes for each catena were extracted from DEM's generated from various altimetry sources, but primarily 1:50 000 topographic maps and Shuttle Radar Topography Mission (SRTM) data. The terrain attributes recorded were elevation range from the crest to the toeslope of each catena, catena length between hillcrest and toeslope, slope steepness, relief, curvature, aspect and solar irradiance. Slope steepness is the angle from the horizontal to the catena surface. Relief is the elevation difference between either ends of a catena standardized by catena length. Both slope steepness and relief index the potential for material transfer on a catena. High values of each imply rapid transportation rates through the catena, other things being equal. Curvature is the change in slope per unit hillslope length. Positive curvature is associated with convex landforms, negative curvature is associated with concave landforms, and planar hillslope have zero curvature. Curvature can be measured in profile – a two-dimensional representation of a hillslope – or plan – a map-based view intended to represent changes in slope along contours – view (Parsons, 1977). I calculated curvature based on the average outcome of the profile and plan curvatures. Solar irradiance is a measure of the insulation received from the Sun and

accounts for variations in elevation, slope, aspect, shadows cast by topographic features and geographic location. Insulation influences soil moisture by altering air temperature and evapotranspiration at points along hillslopes (ESRI, 2005).

Within each catena, soils were described and sampled by standard means between crests and toeslopes (Schoeneberger et al., 2002). Sample location was determined by apparent changes in vegetation, surface soil colour switches, slope breaks on the ground and soil morphological observations in test pits across catenas. Soils were sampled in horizons along pit-faces to the depth of saprolite or bedrock. In total, I sampled 362 horizons from 64 pedons in 9 catenas across the whole park.

Soil bulk density was estimated using the saran coated clod method and measured volumetrically by Archimedes' principle. Total clay % of the fine earth fraction (< 2 mm) in each horizon was measured by the hydrometer method (Carter, 1993). The total clay in a soil profile was then calculated by summing the clay in each horizon on a mass basis by incorporating horizon bulk density, horizon thickness and the proportion of gravel (> 2 mm) in the horizon. I calculated a clay contrast index at three scales; for each pedon, each hillslope and within a climate zone. The index takes the form

$$I_t = \frac{clay_{upper}}{clay_{max}} \text{ (Young, 1976), where } clay_{upper} \text{ represents clay in the topmost}$$

horizon and $clay_{max}$ represents the maximum clay for all horizons in the pedon. At the scale of the hillslope, $clay_{upper}$ was taken as the depth-weighted average clay in the crest soil and $clay_{max}$ was the highest depth-weighted average clay for all pedons on the hillslope. Within each climate zone $clay_{upper}$ represented the mean depth-weighted average clay content of all pedons on the steepest catena (as an analog of a top-most

horizon or crest) while clay_{max} was the highest mean depth-weighted average clay content in the three hillslopes of each climate zone. High I_t values indicate low textural contrast or little difference in texture; and a low I_t indicates high clay contrast or highly distinct textures, whether at the pedon, catena or climate-zone scale.

Clay minerals were separated from bulk soil in B-horizon samples from selected pedons spanning the observed diversity in soil morphology in the field. Samples were treated with 30 % hydrogen peroxide to remove organic matter and disaggregated with sodium metahexaphosphate (Soil Survey Staff, 1996). Repeated purification by centrifuge and vigorous stirring followed the chemical treatments after which smear mounts of the clay were made onto glass slides prepared for X-ray diffraction (XRD). Peak intensity ratios of the resultant XRD scans were used to derive semi-quantitative abundances of clay minerals.

Exchangeable base cations (Ca, Mg, Na and K) and cation exchange capacity (CEC), buffered at pH 7, were extracted with NH_4Oac and 1 N KCl, respectively, and measured with atomic absorption spectrometry (bases) and a Lachat autoanalyser (CEC) (Sauve and Hendershot, 1995). Soil electrical conductivity (EC), an indirect estimate of the amount of dissolved salts in the soil, and pH, were measured in a 1:1 soil-water mixture after ten 30-minute intervals of shaking and settling. Sodium saturation of the exchange complex was estimated by the ratio of exchangeable Na concentration and the CEC or Exchangeable Sodium Percentage (ESP) ($\text{ESP} = [\text{exchangeable Na}]/\text{CEC} \times 100$) (Brady and Weil, 2002).

3. RESULTS

Table 1 gives the physiographic setting for each of the nine catenas investigated. Shown are ranges in elevation, catena length, slope steepness, relief, curvature between crests and toeslopes, aspect and solar irradiance. Catenas furthest north in the dry climate occurred between 300 and 365 m above mean sea level (amsl), and the highest-lying catenas were in wet Pretoriuskop at a range of 511-578 m amsl. In Skukuza, catena elevations were lowest at 248-351 m amsl, probably because the low relief catena in Skukuza was adjacent to a sixth order stream, whereas in the other climate zones, sampled catenas were next to smaller rivers. Catenas were marginally longer in the wet climate, ranging between 900 and 1376 m, while in the dry zone, the lengths ranged between 320 and 970 m. Longer catenas were generally associated with gentler slope angles, for example, Skukuza's IL with maximum length at 1600 m, also had the gentlest relief amongst all catenas. The curvatures, aspects and solar irradiances of the study catenas did not exhibit any dominant trends, and so may be discounted in explaining clay and base cation distribution across catenas. With curvatures however, there was some suggestion of increased concavity with reduced relief, particularly in Skukuza and Pretoriuskop (Table 1). In the end, the resolution of SRTM data were too coarse to extract meaningful terrain attributes for sampled pedons.

3.1 Soil morphology and field properties in the relief-climate matrix

Soil location, horizon designation, gravel content, field texture, structure, colour and roots (size and abundance) by horizon are given in Appendix I. In general, two modes of soil morphology were evident across Kruger's relief-climate matrix. The dichotomy was neither controlled by relief nor climate, but was expressed across each catena with subtle topo-climatic modification. Soils near crests were deep and had loamy sand and sandy loam textures whereas soils further downslope were shallower to rock with less rock fragments and finer textures.

Soil depths for the 62 pedons ranged between 19 and 245 cm, with minimum depths in dry Shingwedzi and maximum depths in wet Pretoriuskop. Mean soil depth increased from 64 ± 8 cm in Shingwedzi, 82 ± 7 cm in Skukuza and 148 ± 9 cm in Pretoriuskop. Thus on the whole, higher rainfall led to deeper soils when depths were averaged for all pedons in each climate zone (Table 2). Variation in depth by relief class within climate zones suggests reduced relief resulted in deeper soils; however, the distinction in depth between relief classes was not as pronounced as depth disparities between climate zones (Fig. 2). Shingwedzi soils became deeper with reduced relief. In Skukuza, soil depths were shallowest in the high relief catena, and slightly deeper in the middle and low relief catenas. Pretoriuskop catenas, on the other hand, had invariant depths across relief classes, but those depths were not to rock but saprolite because the soils were generally far too deep to be hand-dug (up to 5 m to rock in one soil), unlike in the drier sites.

3.2 Impact of climate and relief on clay accumulation and redistribution

The minimum clay percent in all sampled soils, 1 %, occurred 225 m from a crest on a middle relief catena in the intermediate climate zone. The maximum, 65 % clay, occurred at the toeslope of a high relief catena in the wet climate. The location of these clay-extremes in non-extreme locations of climate and relief shows that the relationship between clay and climate-relief was not straightforward. Average clay in catenas near Shingwedzi was 12 ± 2 %, in those near Skukuza – 14 ± 2 % and those near Pretoriuskop – 14 ± 3 %. Thus pooled clay amounts in all pedons for each climate zone were invariant across the 0.15 to 0.27 range in effective rainfall (Fig. 3).

Likewise, variation in relief from catena to catena within climate had little bearing on clay amounts. Changes in clay % from high to low relief Shingwedzi catenas were 11 ± 1 %, 13 ± 3 % and 10 ± 3 %. In Skukuza the pattern was 15 ± 5 %, 17 ± 4 % and 12 ± 3 %; and in Pretoriuskop clay % across decreasing relief was 18 ± 9 %, 12 ± 3 % and 15 ± 4 %. Clay amount as a function of relief within climate was thus largely uniform. Even contrasting the gentlest (IL – 1.1°) and steepest (WH – 2.9°) catenas sampled, overlapping clay contents were recorded (IL = 12 ± 3 % and WH = 18 ± 9 %), despite those hillslopes being in different climate zones (Fig. 4). The low clay contrasts for all catenas within climate zones ($I_t > 0.8$) also shows that relief did not significantly alter clay amounts (Table 3).

3.3 Clay distribution along catenas

Clay contrast indices for all but one catena indicated high contrasts in clay between crests and toeslopes. The “no contrast” catena (DH) had a clay contrast index of 0.8. All other catenas sampled had contrasts of 0.3 and less (Table 3). Table 3 also presents the clay contrast index at sample pedons and Appendix I gives clay % by depth. Two modes in the depth profile of clay were evident across Kruger’s relief-climate matrix. The first: soils lacking texture contrast with depth occurring in any relief or climate but always near crests. The clay contrast for these soils generally exceeded 0.5 and they were skeletal and non-clayey by depth (Table 3). The second group of soils had high clay contrasts (<0.5), and occurred in any climate or relief but in distal sections of catenas. These duplex soils invariably occurred near the toeslopes under any relief or climatic context.

Figure 5 shows, for sampled pedons on catenas: (1) total clay on a mass per area basis; (2) maximum clay and (3) soil depths for the nine catenas sampled. In Shingwedzi, soils with a high clay-contrast occurred only in the middle (DM) and low (DL) relief catenas (Table 3). On DM, the clay-rich zone was in the distal 40 % of the catena, while in DL, the clay-rich zone occurred further downslope, in 30 % of the hillslope. With increased rainfall, Skukuza’s high relief catena (IH), unlike DH in Shingwedzi, had a clay-rich zone, in 19 % of the catena. With lowered relief, the clay-rich zone increased to 53 % in IM while IL had a clay-rich zone in 39 % of the catena. Thus, in Skukuza, the clay-rich zone was most extensive in the middle relief catena, and least extensive in the high relief catena.

Patterns observed in Skukuza also held in the wetter catenas of Pretoriuskop. The clay-rich zone occurred in the most distal soil of WH occupying 1 % of the catena, in 18 % of WM and 12 % of WL (Figure 5). Therefore, peak extent of the clay-rich zone in Pretoriuskop's catenas also occurred in the middle relief catena as in the drier climates, but clay rich zones in Pretoriuskop were thinnest relative to those in both Shingwedzi and Skukuza. Moreover, the clay-poor/ clay-rich contact along catenas occurred furthest downslope in Pretoriuskop.

3.4 Clay mineralogy and CEC along catenas

Kaolinite occurred in all sampled horizons while smectite appeared in about half (Table 4). Smectite occurred most frequently in the dry soils of catenas near Shingwedzi. Of the nine samples analysed by XRD in Shingwedzi, smectite was recorded in four; and of the four, two had a higher abundance of smectite than kaolinite (Table 4). In Skukuza, six of ten samples contained smectite, and of these, only one had higher smectite relative to kaolinite. There was even less smectite in Pretoriuskop, just three incidents in eight samples of which none were higher than the abundance of kaolinite (Table 4). Therefore, increased rainfall resulted in a greater proportion of kaolinite relative to smectite suggesting desilication and loss of base cations as soils got wetter. The increase in the amount of clay-sized quartz also suggests greater intensity of weathering and desilication as soils became wetter (Table 4).

On a catena-by-catena basis, Shingwedzi's DH and DL had smectite only on the crest and kaolinite throughout, but both minerals were in low abundances (< 20 %, Table 4). In middle relief DM, smectite was absent from the crest and throughout the clay-poor zone, but was in very high abundance in the distal, clay-rich zone (> 80 % in DM4 and DM6, Table 4).

In Skukuza, kaolinite had an abundance of 10 % in every sample except that from IL10, where the abundance was between 40 and 60 % (Table 4). Unlike in Shingwedzi, smectite was absent in the crest and near-crest samples, it only occurred in the distal soils of the three catenas. The abundance of smectite in Skukuza soils was lower than in Shingwedzi, not reaching the 80 to 100 % observed in DM.

Finally, Pretoriuskop had the highest kaolinite in sampled horizons. There, even a distal soil (WH6) had over 80 % kaolinite (Table 4). Where smectite occurred, it was less abundant compared to the drier soils. There was therefore a distinct switch from smectite to kaolinite with increased rainfall.

Clay fraction CEC's did not, however, substantiate observed clay mineral shifts. The clay fraction CEC's presented in Table 4 were anomalously high in 60 % of the samples (Table 4). This conclusion was based on samples whose CEC to clay-percent ratios were near 1 or greater. The discrepancy was not due to high organic carbon because where organic C data were available; they were not high enough to account for much of the soil CEC (Table 4). The error was then surely analytical: incomplete soil dispersion which led to aggregation of clay minerals to silt-size. These silt-size clay aggregates were subsequently unaccounted for when clay % was measured, but they

contributed to soil CEC. The clay fraction CEC's were hence unreliable indicators of clay mineralogy and could not be used to support XRD results.

The CEC's of the fine earth fraction of soil (< 2 mm), unlike those estimated for the clay fraction (< 2 μm), reflected clay mineralogy with high activity clays (smectite) co-occurring with high CEC's. DH in Shingwedzi, with low clay percent and low clay mineral abundances had CEC's under 7 cmol (+)/ kg throughout. In the two lower relief catenas, DM and DL, CEC's in the clay-rich zones exceeded those in clay-poor soils near the crests. The CEC's in toeslope locations of DM and DL approached and exceeded 20 cmol (+)/ kg. Increasing CEC downslope on both catenas was consistent with higher clay percent and validated the switch from low-CEC kaolinite in near-crest positions to high-CEC smectite in the toeslopes (Fig. 6).

Similar to what was seen in Shingwedzi, Skukuza's three catenas had low CEC's in the skeletal soils of clay-poor zones (below 10 cmol (+)/ kg). Beyond the clay poor zones, CEC's on IH peaked at 28.0 cmol (+)/ kg, on IM the peak was 28.1 cmol (+)/ kg and on IL 24.9 cmol (+)/ kg. In Pretoriuskop, CEC trends along catenas were not unlike those in the drier climates; however, CEC's were lower in magnitude due to lower clay % and the drop-off in smectite and increase in kaolinite abundance (Fig. 6).

3.5 Exchangeable sodium and the potential for clay dispersion

Soil dispersion is caused by exchangeable sodium in much higher concentration than calcium and magnesium. When an overburden of sodium on exchange sites causes clay to disperse, the soil's mechanical integrity is compromised and soil loss by erosion

may ensue. In addition, a very high concentration of Na may result in pH's > 9, and when combined with low electrical conductivity, sodic conditions unfavorable for normal plant growth occur. In general, the depth integrated pH's in most sampled soils sampled in this study were not high enough (pH > 9) to adversely affect plant growth (Fig. 7). A few horizons, however, did have pH's above 9, notably three in IM8 (Appendix II).

On a soil by soil basis, ESP's in DH near Shingwedzi were approximately 20 % and above, thus high enough to induce clay dispersion leading to unstable soil structure (Fig. 7). But, the low concentration of smectite on DH may curtail adverse effects of high ESP because smectite is more easily dispersed (Table 4). The lower relief catenas in Shingwedzi displayed low ESP near crests and higher ESP in toeslopes, thus had stable mechanical conditions upslope and potential instability downslope in the clay-rich zone. DM was especially likely to develop dispersion due to the high abundance of smectite therein (Table 4) in conjunction with high ESP and high pH (Fig. 7).

Sodium saturation in Skukuza was below 10 % in 19 of the 22 soils sampled. The most potentially sodic soil was IM8 at the distal tip of IM, with a 45 % ESP. High sodium, plus high pH (Fig. 7) and low electrical conductivity (Appendix II) in this soil means it is highly susceptible to mechanical instability.

Catenas in Pretoriuskop were not highly saturated with sodium, and had low pH's and EC's. Therefore, soils in Pretoriuskop were less likely to develop sodic conditions due to greater leaching efficiency as a result of higher rainfall. In the drier climates, higher evapotranspirative demands could concentrate salts following redistribution from upslope. Under these conditions, sodic soils can develop.

3.6 Nutritional base cation concentrations

Figure 8 shows depth weighted average concentrations of K, Ca and Mg in each soil sampled on catenas across climate and relief. Potassium concentration in high relief catenas across climate was consistently below 1 cmol (+)/ kg. On middle relief catenas, K accumulated solely in the clay-rich zone of DM in Shingwedzi; and neither accumulated in IM from Skukuza nor in Pretoriuskop's WM. Average K in the clay-poor soils of DM was under 1 cmol (+)/ kg from the crest to DM5, and concentrations increased to a 9.6 cmol (+)/ kg peak in the most distal soil, DM6. In Skukuza and Pretoriuskop, K was under 1 cmol (+)/ kg throughout IM and WM (Fig. 8).

In low relief catenas, K concentration peaked at 22.9 cmol (+)/ kg in DL7, with low concentrations between the crest and DL5, and high concentrations throughout the clay-rich zone towards the toeslope. A similar pattern of low K in near-crest soils and high K in distal soils was also observed on IL in Skukuza. By contrast, the low relief catena in Pretoriuskop had less than 1 cmol (+)/ kg K in all its soils with slightly more K accumulating in toeslope positions (Fig. 8). Therefore in summary: (1) K did not accumulate in all high relief catenas, (2) for middle relief catenas, K accumulated only in Shingwedzi and (3) in low relief catenas, K accumulated in Shingwedzi and Skukuza.

The divalent cations, magnesium and calcium, showed no accumulation in all three DH soils where both ranged between 0.4 and 2.0 cmol (+)/ kg (Fig. 8). The two cations did however accumulate in the clay-rich sections of the wetter, high relief catenas, IH and WH. On IH, Mg was up to ~5 cmol (+)/ kg in IH4 while Ca reached 13 cmol (+)/ kg in IH5, the last soil on the catena. In Pretoriuskop's high relief catena, WH,

Mg and Ca were leached furthest downslope and had peak concentrations in the last soil, in line with clay.

On middle relief catenas, Mg- and Ca-rich zones spread wider than in high relief hillslopes consistent with the wider extents of clay-rich zones. In Shingwedzi's DM, Mg and Ca peaks were 6.8 and 18.2 cmol (+)/ kg respectively, with the Mg peak further upslope than the Ca peak (Fig. 8). In Skukuza's IM, Mg and Ca peaks were 7.0 and 18.2 cmol (+)/ kg respectively, with the Mg peak in the last soil and the Ca peak 500 m (56 %) from the crest (Fig 8). The narrowest accumulation zones for Mg and Ca occurred in Pretoriuskop where peaks in Mg and Ca concentration in WM were 3.6 and 4.1 cmol (+)/ kg in WM10 (88 %) and WM11 (99 %) respectively (Fig. 8).

For low relief catenas, the high-Mg zone diminished progressively with increased rainfall whereas high-Ca soils were most extensive in Skukuza. Magnesium and Ca concentrations had coincident peaks of 6.6 and 14.5 cmol (+)/ kg in DL6 of Shingwedzi. In Skukuza as well, peak Mg and Ca co-occurred in IL9 with magnitudes of 7.5 and 19.2 cmol (+)/ kg respectively. Low relief Pretoriuskop had a 6.6 cmol (+)/ kg Mg peak and a 5.2 Ca cmol (+)/ kg peak in the most distal soil.

4. DISCUSSION

The field sites investigated here traversed an arid to semiarid transition in climate that contrasts with broader climatic gradients examined in some recent studies (Chadwick et al., 2003; Dahlgren et al., 1997; Porder et al., 2007). Similar to a study of changes in soil properties across the narrow hyperarid to arid climate published by Ewing (2006),

my study revealed patterns in clay and base cation distribution across arid to semi-arid climate, and what those patterns imply for the soils as media for plant growth. The arid to semi-arid barrier in climate is breached across many locations on Earth, and what holds true for Kruger National Park, should apply elsewhere, especially in other African savannas.

A number of pedogenic transitions (Chadwick and Chorover, 2001) can be highlighted from the effective rainfall gradient in Kruger. In the dry, high relief catena (DH), low rainfall and miniscule catchment area precluded clay production resulting in clay-poor, skeletal soils throughout. Lower down in the Shingwedzi catchment, a dry (DH) to wet (DM) transition was breached and initiated clay production and accumulation. Even more water availability associated with greater catchment size in DL led to the expansion and downslope shift in the clay-rich zone. The relief-induced transition was also evident in both Skukuza and Pretoriuskop but was modified by increased rainfall with clay-rich zones occurring even in high relief catenas. However, in the wetter climates, the monotonic increase in the width of the clay-rich zone was absent, rather, peak clay extent in Skukuza and Pretoriuskop occurred in the middle relief catenas. Thus, increased rainfall resulted in an additional transition wherein high water availability in low relief catenas led to clay loss and narrower clay-rich zones.

4.1 Clay and base cation distribution

The distribution of clay in Kruger's diverse landscapes depended on the spatial scale at which patterns were viewed. At the resolution encompassing all sampled soils,

there were no disparities in clay amounts across climate. Likewise, pooled data from pedons in different relief classes across each climate yielded invariant clay amounts. However, when clay distribution was assessed for each catena, a clear pattern was evident. Two populations of clay distribution emerged at the catena scale; clay-poor skeletal soils near crests and clay-rich soils with Bt horizons towards the toeslopes. This pattern was consistently repeated in each relief class and climate zone with added climate/ relief-induced subtleties. Maximum clay retention occurred in catenas with intermediate rainfall. This suggests that the downslope redistribution of clay from Skukuza crests was more intense than in Shingwedzi and less powerful than in Pretoriuskop, resulting in maximum clay retention. In a similar, arid to semi-arid rainfall transition study, Bravo et al. (2007) recorded clay % in 30 epipedons (not on catenas) with rainfall between 280 and 540 mm. Like clay retention in this study, maximum clay occurred in soils with intermediate rainfall. Therefore, Skukuza's IM with intermediate climate and relief was the optimal catena for maximizing clay retention. Unlike a catena in an excessively dry climate, IM was wet enough to produce clay in the first place; and unlike an overly steep or wet catena, IM retained the clay following production. Thus the physiographic context of IM along climo-topographic gradients led to ideal conditions for clay production and retention. These conditions might also be ideal for nutrient distribution and consequent plant establishment, other things being equal.

Base cation distribution in Kruger did indeed mimic the bimodal pattern of clay occurrence along catenas in the various climo-topographic contexts. Where clay amounts were low *i.e.* in skeletal soils near crests, base cation concentrations were also low. But

since bases move easier and further downslope than clay, they did not mirror clay distribution with perfect fidelity.

4.2 Clay mineralogy

The consensus in southern Africa is that smectite is formed in toeslopes while kaolinite occurs on crests (Scholes, 1986; Scholes, 1987). Scholes's work took place in the Lowveld just to the west of Kruger and is corroborated by Chapel (1992) working broadly in the same area. These conclusions are supported by the general principle that in semi-arid areas of Africa, smectite accumulates at the bottoms of profiles and downslope on catenas whereas the dominant clay mineral in more porous upslope soils is kaolinite (Buhmann and Kirsten, 1991; Tardy et al., 1973). My data showed that the distribution of clay minerals on hillslopes is quite complex when viewed along various catenas spanning relief and climatic gradients. While it is true that smectite did occur on toeslopes, it was also present in crests and there was unexpectedly little in the toeslopes of wet catenas.

The occurrence of smectite in near-crest positions of dry catenas may compensate for limited water availability because smectite has a high capacity for binding nutrients, as evident in the higher concentrations of base cations in the dry skeletal soils relative to wet skeletal soils. The interplay between clay mineralogy and base cation concentration was clearly exemplified in DM6, a soil with the highest smectite and K concentrations. Continuing with K for illustration, wet catenas failed to retain much of it because of high leaching power. Potassium retention may also be a supply problem in wet soils, where the input of K from highly insoluble K-feldspar was much slower than the leaching flux of

liberated K down catenas. In addition, wet catenas have a reduced capacity to retain K because of the prevalence of kaolinite over smectite. Thus wet catenas have limited capacity for high nutrient status in many ways including: the slow weathering of some primary minerals like K-feldspar, low clay, limiting clay mineralogy and high leaching intensity.

List of tables

Table 1. Physiographic setting of study catenas in Kruger National Park, D = dry, I = intermediate, W = wet, H = high relief, M = middle, L = low

Table 2. Variation in the depth of sampled soils across climate and relief

Table 3. Position of study pedons relative to reference crests and in proportion to hillslope length, clay amount and clay contrast indices

Table 4. Clay fraction smectite, kaolinite and quartz abundances in select horizons analysed by X-ray diffraction. Abundances represent peak intensity ratios with 0 = not detected, 1 = <20 %, 2 = 20- 40 %, 3 = 40- 60 %, 4 = 60- 80 % and 5 = 80- 100 %. Also shown are clay %, soil CEC, organic C and clay fraction CEC for the reference horizons

List of figures

Figure 1. Study site showing Kruger National Park, Shingwedzi in the dry north, Skukuza with intermediate rainfall and wet Pretoriuskop, lines indicate transect location.

Figure 2. Mean depths and standard errors of sampled pedons across climate and relief class in Kruger.

Figure 3. Mean clay % and standard error at the three points across the effective rainfall gradient in Kruger.

Figure 4. Mean clay % and standard error across relief ($\times 100$) in the three climate zones of Kruger.

Figure 5. Clay inventories and soil depth across climate, relief and catena position in Kruger. Vertical line demarcates the clay poor and clay rich zones on catenas, number to the left of line represents percentage of catena occupied by the clay poor zone and the number on the right is the percent extent of the clay rich zone.

Figure 6. Depth-weighted average soil CEC across climate, relief and catena position in Kruger.

Figure 7. Depth-weighted average sodium saturation (ESP) of the exchange complex and soil solution pH across climate, relief and catena position in Kruger.

Figure 8. Depth-weighted average distribution of plant required base cations across climate, relief and catena position in Kruger.

Appendices

I – Selected field properties of study pedons

II – Exchange properties of study pedons

III – Elemental composition of soil horizons in sampled pedons

Table 1. Physiographic setting of study catenas in Kruger National Park, D = dry, I = intermediate, W = wet, H = high relief, M = middle, L = low

Site/ hillslope	Elevation range (m)	Catena length (m)	Effective rainfall	Slope steepness (°)	Relief	Curvature	Aspect	Solar irradiance (GW/hr)
Shingwedzi			0.15 arid					
DH	345-365	320		1.6	0.028	0.022	S	1.63
DM	320-329	350		1.5	0.026	-0.008	N	1.64
DL	300-320	970		1.2	0.021	0.011	E	1.56
Skukuza			0.20 arid to semi arid					
IH	324-341	410		2.4	0.041	0.015	NE	1.55
IM	324-351	700		1.4	0.024	0.020	SE	1.55
IL	248-279	1600		1.1	0.019	0.007	N	1.68
Pretoriuskop			0.27 semi-arid					
WH	519-565	900		2.9	0.051	0.059	SE	1.61
WM	511-578	1376		2.7	0.047	0.043	SW	1.61
WL	528-576	1210		2.2	0.039	0.025	SE	1.62

Table 2. Variation in the depth of sampled soils across climate and relief

	Mean	Min	Max
		m	
All pedons, n = 63	102 ± 7	19	245
Shingwedzi, n = 16	64 ± 8	19	120
DH, n = 3	23 ± 3	19	28
DM, n = 6	66 ± 6	50	87
DL, n = 7	79 ± 13	42	120
Skukuza, n = 22	82 ± 7	26	175
IH, n = 5	66 ± 7	47	83
IM, n = 7	85 ± 15	26	175
IL, n = 10	87 ± 10	30	130
Pretoriuskop, n = 23	148 ± 9	60	245
WH, n = 6	146 ± 14	116	212
WM, n = 11	149 ± 12	80	210
WL, n = 6	150 ± 17	60	245

Table 3. Position of study pedons relative to reference crests and in proportion to hillslope length, clay amount and clay contrast indices

Climate zone catena/ pedon	Distance form crest (m)	Distance (%)	Clay %	Texture class	Pedon clay contrast index	Hillslope clay contrast index	Climate zone clay contrast index
DH1	15	5	11	sl	0.8	0.8	0.8
DH2	130	39	14	sl	0.6		
DH3	320	97	9	sl	1		
DM1	15	4	5	s	1	0.2	
DM2	180	49	6	s	0.7		
DM3	220	60	24	scl	0.4		
DM4	275	75	19	scl	0.2		
DM5	295	81	15	ls	0.4		
DM6	350	96	11	ls	0.1		
DL1	15	1	6	s	1	0.2	
DL2	150	12	5	s	0.7		
DL3	270	22	8	s	0.5		
DL4	380	31	4	s	0.4		
DL5	500	41	8	s	0.2		
DL6	850	70	17	sl	0.4		
DL7	970	79	24	scl	0.5		
IH1	15	4	7	s	0.4	0.3	0.9
IH2	170	40	6	s	0.6		
IH3	270	64	5	s	0.3		
IH4	340	81	25	scl	0.2		
IH5	410	98	32	scl	0.8		
IM1	15	2	9	s	0.8	0.1	
IM3	225	25	1	s	0.5		
IM4	330	37	7	s	0.7		
IM5	425	47	20	scl	0.3		
IM6	500	56	30	scl	0.3		
IM7	610	68	21	scl	0.8		
IM8	700	78	28	scl	0.1		
IL1	15	1	3	s	0.7	0.2	
IL2	400	22	5	s	0.7		
IL3	755	41	4	s	1		
IL4	895	48	3	s	0.9		
IL5	977	53	3	s	0.9		
IL6	1123	61	17	sl	0.3		
IL7	1275	69	26	scl	0.5		
IL8	1385	75	17	scl	0.5		

Climate zone catena/ pedon	Distance form crest (m)	Distance (%)	Clay %	Texture class	Pedon clay contrast index	Hillslope clay contrast index	Climate zone clay contrast index
IL9	1550	84	21	scl	0.2		
IL10	1600	86	23	scl	0.4		
WH1	15	2	13	s	0.1	0.2	1.1
WH2	300	33	6	s	0.6		
WH3	544	60	7	s	0.7		
WH4	820	90	4	s	0.3		
WH5	860	95	11	ls	0.8		
WH6	900	99	65	c	0.2		
WM1	15	1	8	s	0.5	0.2	
WM2	20	5	10	s	0.5		
WM3	225	16	10	s	0.3		
WM4	397	29	8	s	0.2		
WM5	513	37	4	s	0.9		
WM6	640	46	4	s	0.4		
WM7	777	56	5	s	0.3		
WM8	1048	75	6	s	0.4		
WM9	1133	82	35	scl	0.2		
WM10	1223	88	26	scl	0.4		
WM11	1376	99	17	sl	0.2		
WL1	15	1	9	s	0.2	0.3	
WL2	546	45	4	s	0.4		
WL3	1000	82	9	s	0.1		
WL4	1060	87	20	scl	0.2		
WL5	1185	97	17	scl	0.1		
WL6	1210	99	30	scl	0.1		

Table 4. Clay fraction smectite, kaolinite and quartz abundances in select horizons analysed by X-ray diffraction. Abundances represent peak intensity ratios with 0 = not detected, 1 = <20 %, 2 = 20- 40 %, 3 = 40- 60 %, 4 = 60- 80 % and 5 = 80- 100 %. Also shown are clay %, soil CEC, organic C and clay fraction CEC for the reference horizons

Site	Position on catena (%)	Depth	Smectite	Kaolinite	Quartz	Clay %	CEC (cmol(+)/kg)	Organic C (%)	Clay fraction CEC (cmol(+)/kg)
DH1	5	13-22	1	1	1	15	5	0.4	34
DH2	39	14-23	0	1	1	14	3	0.4	24
DH3	97	0-1	0	1	1	11	5	0.7	46
DM1	4	12-29	0	1	1	4	9	0.5	252
DM4	75	51-63	5	1	2	18	26		147
DM6	96	76-87	5	1	1	20	22		108
DL1	1	23-45	1	2	2	5	12	0.8	233
DL3	22	2-19	0	1	1	3	12		484
DL7	79	11-40	0	1	1	25	27		107
IH1	4	0-10	1	1	1	4	7	0.6	178
IH3	64	26-40	1	1	2	5	4		81
IH5	98	31-49	3	1	2	33	30		91
IM5	47	25-62	0	1	1	34	30		89
IM7	68	25-46	1	1	1	30	34		113
IL1	1	3-11	0	1	2	4	5	0.3	142
IL6	61	1-24	0	1	1	5	6		126
IL7	69	1-16	0	1	1	11	15		134
IL9	84	35-57	1	1	2	25	25		98
IL10	86	34-60	3	3	3	28	24		87
WH4	90	24-47	0	2	2	5	4		86
WH6	99	29-50	0	5	5	58	44		77
WL1	1	93-115	0	3	3	10	12	0.1	115
WL2	45	71-94	0	1	5	1	4		318
WL3	82	45-60	2	4	3	5	6		122
WL4	87	0-9	0	1	3	5	9		175
WL5	97	0-11	1	1	3	4	11		288
WL6	99	40-63	2	3	2	30	22		75
D-Basalt			>>5	0	0				
D-Gabbro			>>5	1	1				

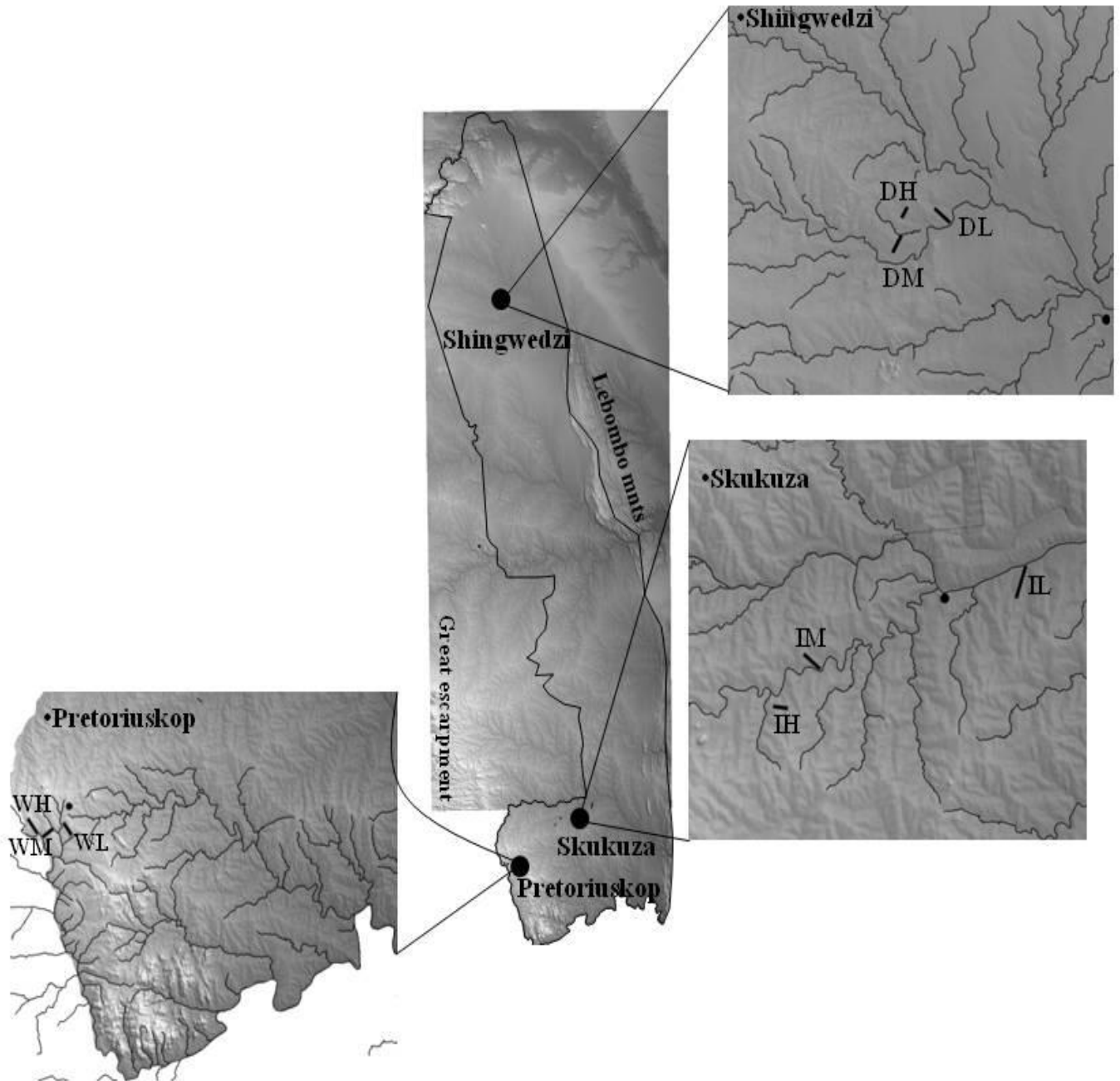


Figure 1. Study site showing Kruger National Park, Shingwedzi in the dry north, Skukuza with intermediate rainfall and wet Pretoriuskop, lines indicate transect location.

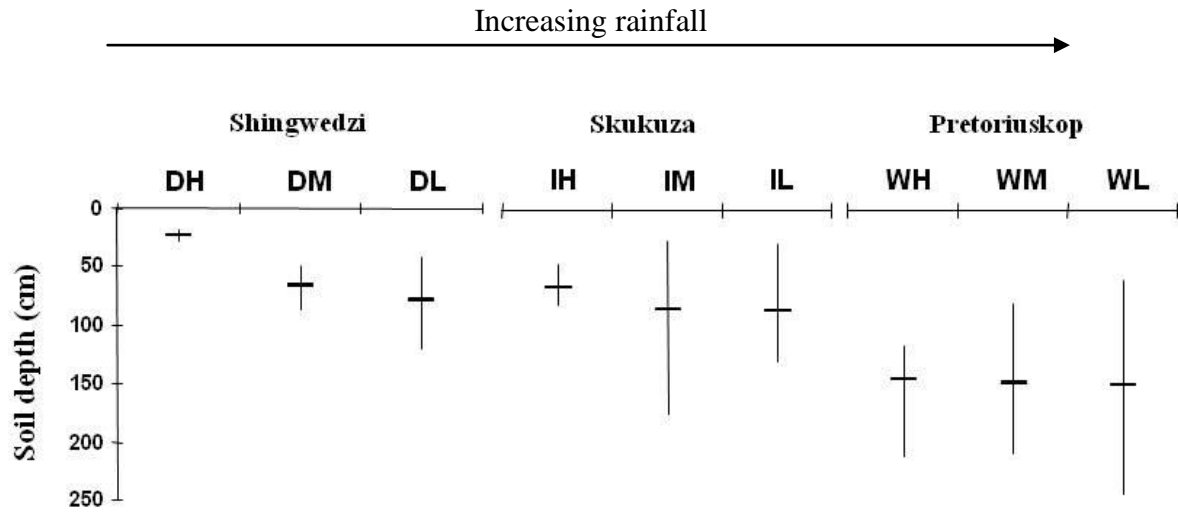


Figure 2. Mean depths and standard errors of sampled pedons across climate and relief class in Kruger.

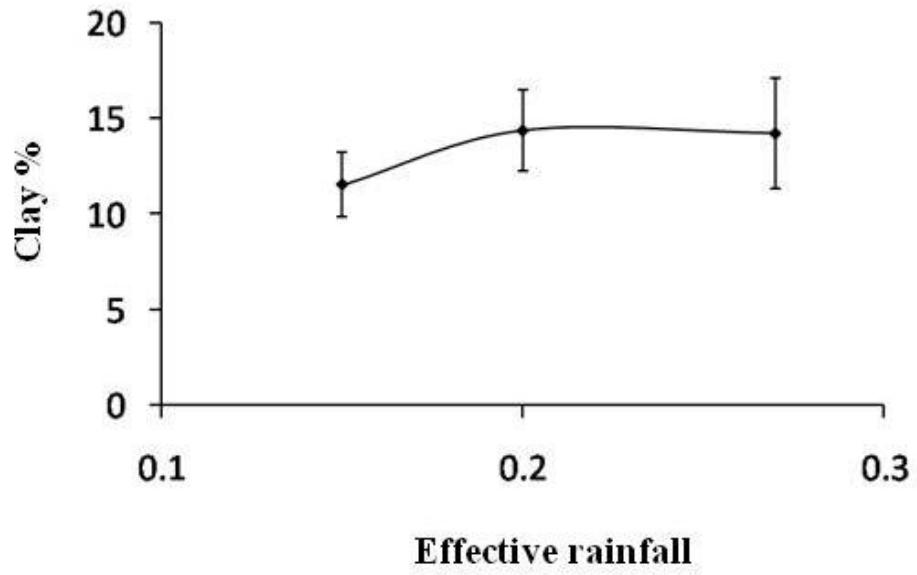


Figure 3. Mean clay % and standard error at the three points across the effective rainfall gradient in Kruger.

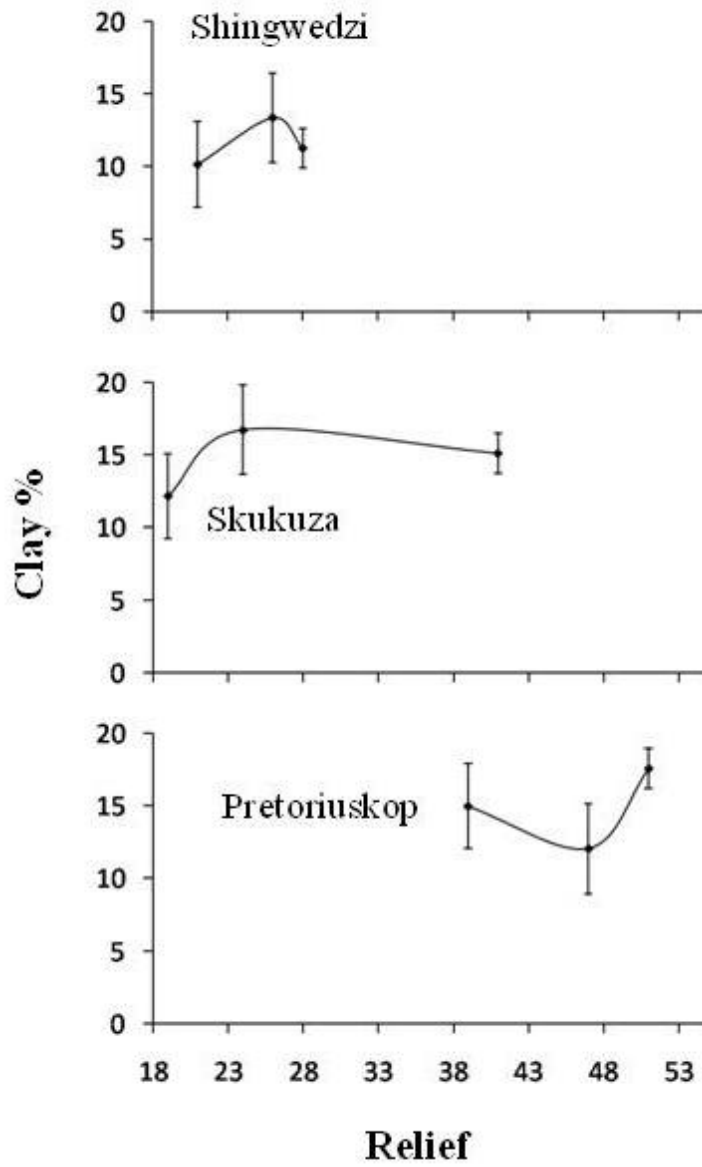


Figure 4. Mean clay % and standard error across relief ($\times 100$) in the three climate zones of Kruger.

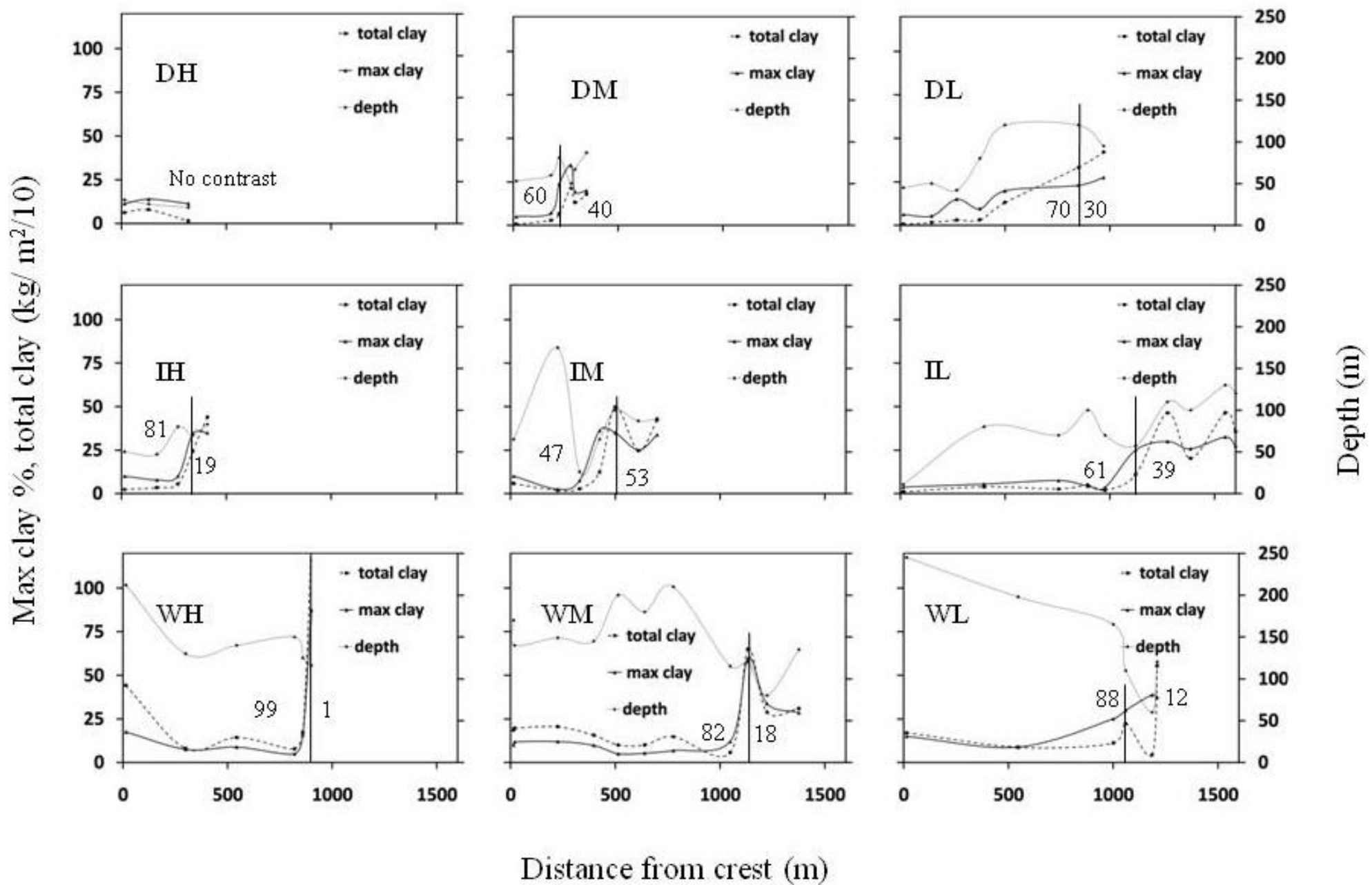


Figure 5. Clay inventories and soil depth across climate, relief and catena position in Kruger. Vertical line demarcates the clay poor and clay rich zones on catenas, number to the left of line represents percentage of catena occupied by the clay poor zone and the number on the right is the percent extent of the clay rich zone.

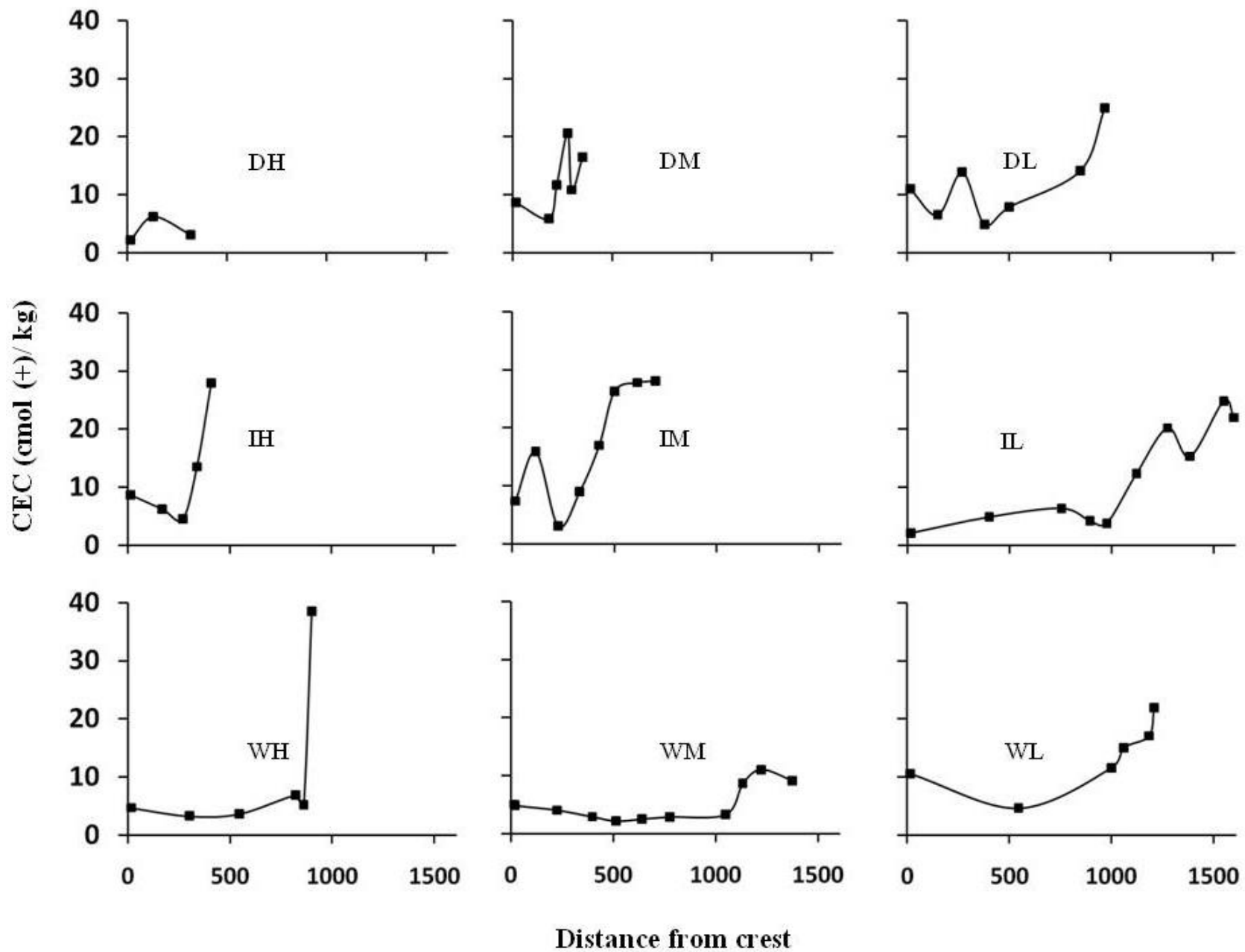


Figure 6. Depth-weighted average soil CEC across climate, relief and catena position in Kruger.

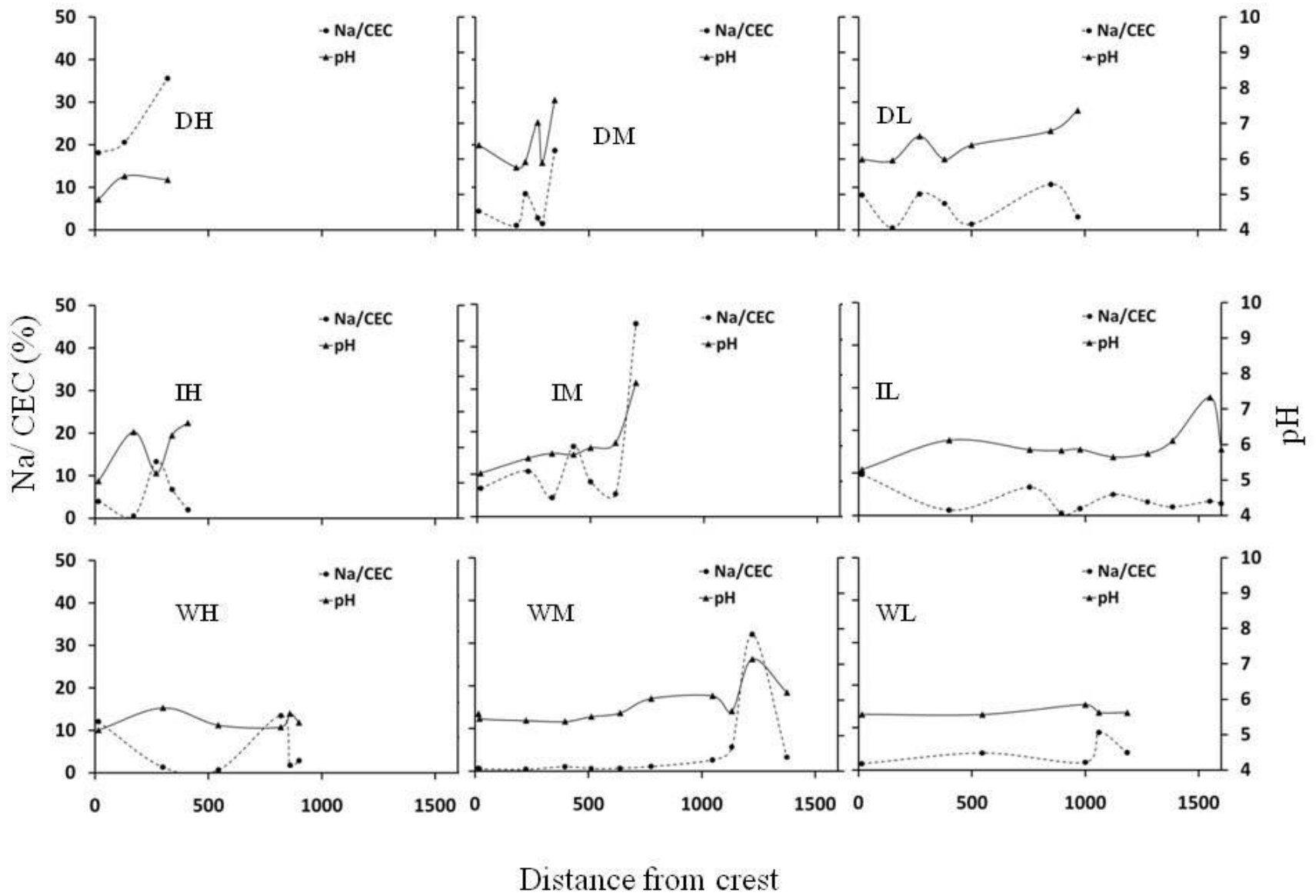


Figure 7. Depth-weighted average sodium saturation (ESP) of the exchange complex and soil solution pH across climate, relief and catena position in Kruger.

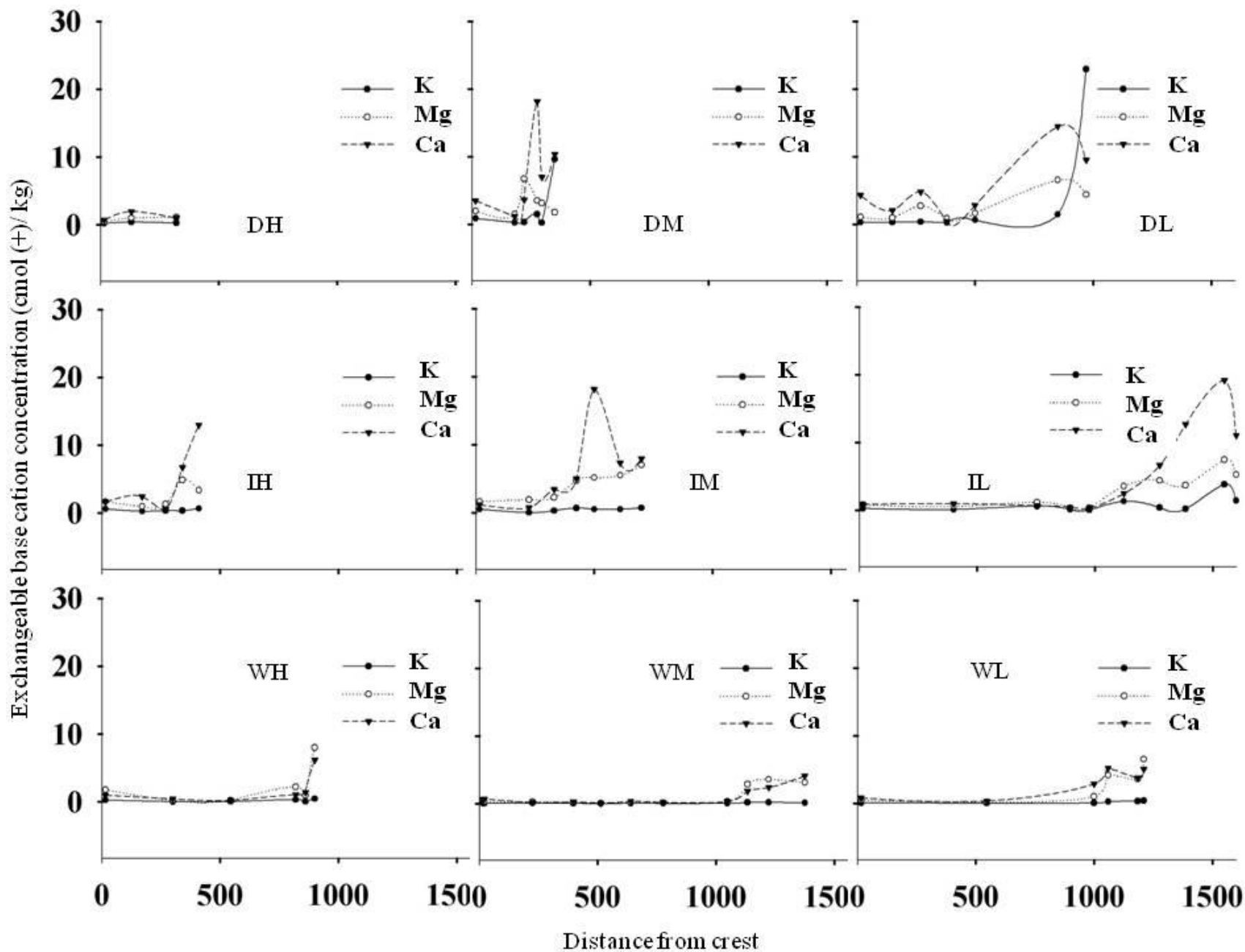


Figure 8. Depth-weighted average distribution of plant required base cations across climate, relief and catena position in Kruger.

Appendix I. Selected field properties of study pedons

Depth	Horizon	Longitude (m)	Latitude (m)	Distance from crest (m)	% gravel	Texture	Structure	Moist colour	Roots
Shingwedzi									
DH1		316352	7453989	0					
0-2	A				10	ls	sg	7.5YR3/4	-
2-16	Bw1				20	ls	2msbk	7.5YR3/4	1m, 2vf, f, 1c
16-28	2Bw2				40	ls	1vfsbk	7.5YR3/4	2vf, f, 1vc
28-45	2C				70	-	m		-
DH2		316137	7453951	130					
0-1	A				20	s	sg	10YR3/4	-
1-14	Bw1				20	ls	1fsbk	7.5YR3/3	1vf,f
14-23	2Bw2				70	ls	avfsbk	7.5YR3/4	1vf,f,c
23-43	2C				80	-	m		1vf,f
DH3		315951	7453896	320					
0-1	A				15	ls	sg	10YR3/2	1vf
1-19	Bw1				70	s	sg,m	10YR3/3	1vf,2f,1c
DM1		318626	7450293	0					
0-12	BA				70	s	sg	7.5YR2.5/2	1vf,f
12-29	BC				85	s	sg	7.5YR2.5/2	2vf,f,1m
29-53	C				90	s	sg	7.5YR2.5/3	1vf,f,m
53-63	CR				95	-	m		
DM2		318583	7450145	180					
0-1	A				5	s	sg,1fpl	5YR3/2	1vf,v
1-13	Bw1				5	s	1vf,fsbk	5YR3/2	2vf,f,m
13-32	2Bc1				55	s	sg,m	5YR3/3	1m,2vf,f,3co,vc
32-46	2Bc2				70	s	sg,m	10YR3/4	1vf,f
46-60	2Bc3				80	s	sg,m	10YR4/3	1vf,f,2m
DM3		318598	7450180	220					
0-1	A				10	s	sg,1mgr	10YR3/1	1vf
1-4	Bw1				80	s	1f,msbk	10YR3/1	2vf,f
4-20	2Bc1				55	s	sg	10YR3/2	3vf,f,m
20-39	3Bct2				65	scl	m,3mabk	10YR4/1	1vf,f
39-50	3Bc3				80	scl	m,3mcoabk	10YR4/1	1vf
DM4		318603	7450226	275					
0-2	A				0	ls	1mpl,vf,f,sbk,sg	10YR3/3	1vf
2-18	Bw1				0	sl	2f,msbk	7.5YR3/3	2vf,f
18-51	2Bt1				0	sl	3coabk,2msbk	7.5YR3/3	1vf,2f
51-63	2Bt2				10	sl	2mabk,sbk	7.5YR3/3	1m,2vf,f
63-81	3BC				45	scl	1msbk	7.5YR3/4	1m2vf,f
81-91	C				60	-			
DM5		318616	7450241	295					
0-4	Ba				5	s	2msbk	2.5YR2.5/1	1vf,f
4-19	Bw1				10	ls	2-3m,coabk	2.5YR3/1	1vf,f
19-35	Bw2				10	ls	2f,mabk,sbk	2.5YR3/2	1vf,f,m,co
35-52	2Bc1				20	sl	2vf,fsbk	2.5YR2.5/2	1vf,f,m,co,vc
52-67	2Bc2				40	sl	1-2vf,f,msbk	2.5YR3/2	1vf
DM6		318626	7450293	350					
0-4	A				18	ls	1vfsg	10YR3/4	1vf,f
4-10	AB				10	s	1vfsg,msbk	10YR3/4	2vf,f

Depth	Horizon	Longitude (m)	Latitude (m)	Distance from crest (m)	% gravel	Texture	Structure	Moist colour	Roots
10-31	Btk1				2	ls	3mabk,coabk	10YR4/3	1vf,f
31-52	2Bw1				0	ls	2mabk,coabk	10YR4/4	1vf,f
52-76	Btk2				5	ls	2msbk,cosbk	10YR4/6	1vf
76-87	3Bw3				8	sl	2fsbk	7.5YR4/4	1vf
87-97	C				60	-	m		
DL1		322713	7452153	0					
0-23	BA				80	s	sg	7.5YR2.5/2	2f,vf,1m
23-45	BC				90	s	sg	7.5YR3/4	1f,m,2vf
45-55	C				100	-			
DL2		322803	7452043	150					
0-6	Ba				10	s	1fsbk	10YR3/3	1vf,f
6-22	Bw1				50	s	sg	7.5YR3/3	1vf,f
22-35	2Bc1				80	s	sg,m	7.5YR2.5/3	2vf,f
35-50	2Bc2				70	s	sg,m	7.5YR3/4	1-2vf,f
DL3		322890	7451948	270					
0-2	A				8	s	1f,vf,gr,vfsbk	10YR2/1	1vf,f
2-19	Bw1				0	s	1msbk	10YR2/1	2vf,f,m
19-34	Bw2				10	ls	2msbk	10YR3/2	1vf,f,m
34-42	BC				90	ls	m,sg		
42-52	C				95				
DL4		322929	7451841	380					
0-1	Ab				5	s	1mpl,sg	10YR3/2	2vf
1-9	Bw1				5	s	sg	10YR3/2	2vf,f,1m,co
9-24	Bw2				5	s	1fabk,sg	10YR3/2	1vf,f,m
24-40	Bw3				10	s	1f,msbk,sg	10YR3/2	1vf,f
40-55	Bw4				20	s	m,sg,1fsbk	10YR4/2	1vf
55-67	2Bc1				85	s	m,sg	10YR4/1	1vf
67-75	2Bc2				90	s	m,sg,1f,sbk	10YR4/1	1vf
DL5		323039	7451776	500					
0-4	Ab				<5	s	1f,msbk	10YR2/2	1vf
4-13	Bw1				<5	s	1f,msbk	10YR2/2	1vf,f,m
13-30	Bw2				<5	s	2f,msbk	7.5YR2.5/1	1vf,f,m,co,vc
30-51	Bw3				<5	s	2f,msbk,abk	2.5YR2.5/1	1vf,f,m
51-76	Bw4				5	s	2f,msbk,abk	10YR3/3	1vf,f,m
76-112	2Bw5				15	s	2mabk	10YR3/3	1vf
112-120	2Bw6				45	sl	sg,2f,mabk,sbk	10YR3/3	1vf
DL6		323285	7451537	850					
0-1	Ab				5	ls	sg	7.5YR3/2	1vf
1-4	Bw1				5	ls	1msbk	7.5YR3/2	1vf,fm
4-20	2Bt2				5	sl	3vcabk,m	5YR3/1	2vf,1f,m,co
20-59	2Bt3				5	scl	3vcabk,m	5YR3/2	1vf,f,m,co,vc
59-95	2Bt4				5	sl	3vcabk,m	5YR3/3	1vf,f,m,co,vc
95-110	3Bw5				10	sl	2m,cosbk	5YR3/3	1vf,f
110-120	3Bw6				10	sl	2m,cosbk	5YR3/3	1vf
DL7		323478	7451179	970					
0-1	BA				40	ls	1vfgr,sg	7.5YR3/3	no roots
1-11	Btk1				5	scl	1f,vfsbk	7.5YR3/3	2vf
11-40	Btk2				0	scl	2f,msbk	7.5YR3/4	2vf,f,1m
40-68	2Bw1				0	scl	3f,m,coabk	7.5YR3/4	1vf,f,m

Depth	Horizon	Longitude (m)	Latitude (m)	Distance from crest (m)	% gravel	Texture	Structure	Moist colour	Roots
68-95	2Bw2				0	scl	3co,coabk	7.5YR3/4	1vf
Skukuza									
IH1		346001	7227674	0					
0-10	BA				30	s	1vnpl,1f,msbk,1f,mgr	10YR3/4	2vf,f
10-23	Bw1				45	ls	1f,msbk	7.5YR3/3	2vf,f,m
23-50	BC				80	s	sg,1fgr	7.5YR3/4	1vf,f
50-60	CR				100		M	-	-
IH2		345994	7227900	170					
0-10	BA				5	s	1-2f,msbk	2.5YR2.5/1	1vf,f
10-20	Bw1				5	s	2msbk	2.5YR2.5/2	1vf
20-30	Bw2				5	s	2msbk	2.5YR2.5/2	1vf,f,co,vc
30-47	Bc				70	s	1vfgr,sg	2.5YR3/3	1vf,f
IH3		346085	7227885	270					
0-7	AB				1	s	1vf,f,msbk	10YR3/1	1vf,f,3m
7-26	Bw1				5	s	2f,mabk,sbk	10YR3/2	1vf,f,vc
26-40	Bw2				5	s	1f,msbk	10YR5/2	1vf,f,m,co,vc
40-60	Bw3				8	s	1vf,fsbk,sg	10YR5/2	1vf,f,m,co
60-80	BC				50	ls	sg,M		
80-90					75				
IH4		346146	7227881	340					
0-9	AB				5	s	2mgr,1f,msbk	10yr2/2	3vf,f
9-20	BA				5	s	1f,msbk	10yr2/2	2vf,f
20-50	Bt1				2	scl	m,3vcabk	10yr2/2	1vf,f
50-62	Bt2				30	scl	m,3co,vcabk	10yr3/1	1vf,f
62-70	2BC				80	scl	1fgr,sg,m	10yr3/1	1vf
IH5		346208	7227883	410					
0-10	BA				0	scl	sg,3f,mabk	10YR2/2	
10-31	Bt1				0	scl	3mabk	7.5YR2.5/0	
31-49	Bt2				5	scl	3mabk	5YR2.5/4	
49-83	Bt3				5	scl	2msbk,sg	5YR2.5/1	
83-93	BCR				50		M		
IM1		348286	7230808	0					
0-7	BA				5	s	1f,msbk,1fgr	10YR3/3	1vf,f
7-33	Bw1				10	s	1f,msbk	10YR3/4	1vf,f,fm,co
33-65	CR/BC				70	ls	sg,1fgr	10YR4/4	1f
65-75	RC				95		M	-	-
IM2		348365	7230725	115					
0-5	A				5	s	1f,msbk	10YR3/2	
5-17	Bw1				10	ls	1msbk	10YR2/1	
17-42	Bw2				40	sl	2,3mabk	7.5YR3/3	
42-56	Bw3				60	sc	2mabk,sbk	7.5YR3/3	
56-70	2CB				80	s	m		
70-80	Rc				95				
IM3		348438	7230644	225					
0-16	AB				2	s	0fmsbk	10YR3/2	
16-42	Bw1				2	s	1f,msbk	10YR4/3	
42-70	Bw2				15	s	1f,msbk	7.5YR5/4	
70-120	2BC1				60	s	M	10YR5/3	
120-151	2BC2				40	s	M,sg	10YR6/3	
151-175	2BC3				30	s	M,sg	10YR6/3	
IM4		348502	7230557	330					
0-7	BA				0	s	2f,msbk	10YR2/2	
7-26	Bw/Bt				5	s	2mabk	10YR3/2	

Depth	Horizon	Longitude (m)	Latitude (m)	Distance from crest (m)	% gravel	Texture	Structure	Moist colour	Roots
26-30	C				95		m		
IM5		348602	7230527	425					
0-13	BA				1	ls	1m,cosbk,sg,1vfgr	10YR 2/1	1vf,f,m
13-25	Bt1				20	scl	3mabk	10YR 2/1	1vf
25-40	BtC				60	scl	2mabk,M,sg	10YR 4/1	1vf
40-65	CR				80	ls	M,sg	-	-
65-75	R				100	-	-	-	-
IM6		348664	7230485	500					
0-9	BA				2	ls	1vf,fgr,sg,1f,msbk	10YR 2/2	1vf,f
9-25	Bt1				2	scl	2f,msbk,3f,mabk	10YR 3/1	1vf,f,m,co
25-62	Bt2				2	scl	3m,coabk,3fgr	10YR 3/1	1f,co
62-90	2Bt3				2	scl	2f,mabk,abk	10YR 4/1 - 10YR3/1	1f,m
90-100	CR				10	scl	sg,M	-	-
100-110	R				80	-	-	-	-
IM7		348741	7230400	610					
0-4	A				2	s	2fsbk	10yr2/1	
4-10	BA1				2	scl	2msbk	10yr2/1	
10-22	BA2				2	s	1msbk	10yr2/1	
22-40	2Bw1				10	s	2mabk	10yr3/1	
40-63	2Bw2				15	sl	3mabk	10yr3/1	
63-70	2Bw3				20	scl			
70-77	2Bw4				30	scl			
77-87	2Bw5				40	scl			
IM8		348775	7230314	700					
0-7	BA				0	s	2f,msbk,1fgr,sg	10YR 2/2	1vf,f,m
7-25	Bt1				0	scl	3f,mabk,cl	10YR 3/1	1vf,f,m,co
25-46	Bt2				0	scl	2f,mabk	10YR 3/1	1vf,f
46-62	Bt3				0	scl	2f,mabk	10YR 3/2	1vf
62-90	BC				0	scl	2vf,fabk,sbk,1fgr,sg	10YR 4/2	-
IL1		363444	7235287	0					
1-3	A				35	s	1f,mgr,1-2tnpl	10YR3/4	2vf
3-11	BC				50	s	1vf,f,sbk	10YR3/6	1vf,f
11-30	CR				80		M		
IL2		363607	7235646	400					
0-10	BA				5	s	sg,1mgr	7.5YR4/6	3vf,f,1m
10-39	Bw1				10	s	2msbk	7.5YR3/3	1vf,f,m
39-60	2Bw2, e				50	s	1msbk,sg	7.5YR3/3	1vf,f,m
60-80	2Bc				75	s	sg	5YR3/3	1vf,f
IL3		363626	7235987	755					
0-2	A				10	s	1vfgr,1vtpl	10YR3/4	1vf
2-25	Bw1				5	s	1vf,fsbk	10YR3/4	1vf,f,m,co
25-47	Bw2				25	s	1vf,fsbk,1fgr	10YR3/4	1vf,f,co,vc
47-70	BC				80	s	1vfgr,M	7.5YR4/6	1vf
IL4		363699	7236150	895					
0-12	BA				5	s	1msbk,1f,mgr	10YR3/3	1vf,f,m
12-48	Bw1				5	s	1msbk	10YR3/3	1vf,f,m,vc
48-70	Bw2				20	s	1m,cosbk	10YR3/4	1vf,f,m,co
70-85	Bw3				30	s	sg,1vf,fgr	10YR4/4	1vf
85-100	CB				85	s	m,sg	10YR4/3	1vf
IL5		363710	7236182	977					
0-11	BA				5	s	2f,mabk	10YR3/2	1vf,f,co
27-53	2Bc				60	s	sg	10YR5/1	1vf,f

Depth	Horizon	Longitude (m)	Latitude (m)	Distance from crest (m)	% gravel	Texture	Structure	Moist colour	Roots
53-70	2Cr				85	s	sg	10YR6/2	1vf
IL6		363769	7236324	1123					
0-1	A				5	s	sg,1vfgr	10YR3/1	2vf,1f
1-24	Bw1				2	s	2m,coabk,sbk	10YR3/2	1vf,f,m,co,vc
24-57	BC				40	scl	2-3m,coabk	10YR3/1-2	1f,vf,m
57-67	C				80	-	-	-	-
IL7		363840	7236470	1275					
0-1	A				1	ls	sg,1vfgr	7.5YR2.5/3	1vf,f
1-16	Bw1				0	ls	2f,msbkabk	5YR3/2	1vf,f,2,m,co,vc
16-30	Bw2				0	scl	2f,mabk	5YR3/3	1f,m
30-63	Bw3				5	scl	3vcabk,M	2.5YR2.5/3	1vf,f,m
63-110	BC				10	scl	sg,2fabk	2.5YR3/3	1vf,f,co
110-120	CR				40		M,sg	-	-
IL8		363894	7236547	1385					
0-13	BA				10	s	2mabk	10YR3/2	1vf,f,m
13-53	Bt1				20	scl	3vcabk,m	10YR3/2	1vf,f,m,co
53-70	Bt2				40	sl	3vcabk	10YR3/2	1vf,f
70-85	2Bw3				65	s	1-2f,mabk,sg	10YR4/2	1vf,f
85-100	2Bc				80	s	1fabk,sbk,sg	10YR4/3	1vf
IL9		363874	7236749	1550					
0-3	BA				0	s	1vf,fsbk,1fgr,1vnpl	10YR3/3	-
3-17	Bt1				0	ls	3m,coabk	10YR3/3- 10YR3/4	1vf
17-35	2Bt2				0	scl	2m,coabk,3m,co,vcabk	10YR3/2	1vf,f,m,co
35-57	3Btk3				0	scl	3m,co,cvabk	10YR4/3	1vf
57-80	3Btk4				0	scl	1-2m,cosbk	10YR4/3	1vf
80-110	3Btk5				2	sl	1m,cosbk	10YR4/4	-
110-130	BC				2	s	-	-	-
IL10		363892	7236772	1600					
0-7	AB				0	sil	1f,msbk	10YR3/3	1vf,f
7-34	Bt1				1	sl	2m,coabk	7.5YR2.5/2	1vf,f,m
34-60	2Bt2				30	scl	3mcoabk	5YR3/2	1vf,f
60-85	3Bt3				5	scl	3f,m,coabk	10YR3/2	-
85-111	3Bt4				60	scl	2f,mabk	10YR3/3	1vf
111-120	4BC				80	sl	-	-	-
Pretoriuskop									
WH1		321217	7211736	0					
0-4	AB				0	s	1f,msbk,1fgr	10YR2/1	2vf,f
4-30	Bw1				0	s	2f,mabk	10YR3/4	2vf,f,1m,co
30-76	Bw2				0	ls	2mabk	5YR4/4	1vf,f
76-105	Bw3				0	ls	2mabk	5YR4/4	1vf,f,m
105-125	Bw4				0	sl	2mabk	5YR4/4	1vf,f,m
125-146	Bw5				0	sl	2mabk	5YR4/4	1vf,f,m
146-180	2Bw6				0	s	sg,1f,msbk	5YR4/4	1vf,f
180-212	C				5	sl	-	-	-
WH2		321373	7211499	300					
0-13	Ba				5	s	1f,msbk	10YR3/2	2vf,f,m
13-29	Bw1				5	s	1vf,fsbk	10YR4/2	2vf,f
29-49	Bw2				15	s	1vf,fsbk	10YR5/2	1vf,f
49-87	Bw3				20	s	1f,msbk	10YR5/2	1vf,f
87-124	Bw4				80	s	2m,coabk	5y6/2	1vf,f
124-130	BC				90	s	m,gr,sg	-	1f
WH3		321534	7211347	544					

Depth	Horizon	Longitude (m)	Latitude (m)	Distance from crest (m)	% gravel	Texture	Structure	Moist colour	Roots
0-17	AB				4	s	1-2f,msbk	10YR3/4	2vf,f
17-58	Bw1				4	s	1,f,msbk	10YR4/4	3vc,1vf,f,m
58-88	Bw2				4	s	sg,1fsbk	10YR4/4	1vf,f,co
88-112	Bw3				10	s	1,2fsbk,sg	10YR5/4	1vf,f
112-128	Bw4				20	s	1,fsb	10YR4/3	1vf,f
128-140	2BC				80	s	m,sg	10YR4/4	1vf
WH4		321645	7211072	820					
0-5	AB				1	s	1f,msbk,1vf,fg	10YR3/2	2vf,f,1m
5-24	Bw1				5	s	2f,msbk	10YR3/4	2vf,f,1m,co
24-47	Bw2				5	s	1f,msbk	10YR3/6	2vf,f,1m,co
47-67	Bw3				5	s	2f,msbk	10YR3/6	1vf,f
67-89	2Bw4				20	s	2f,msbk,abk	10YR4/6	1vf,f
89-115	3Bw5				60	s	2f,mabk,M	10YR 5/8(.6), 10YR4/4(.4)	1vf,f,m
115-150	3Bw6				45	s	2f,mabk	10YR4/4	1vf,f
150-160	R				80		M	-	-
WH5		321645	7211037	860					
0-13	Ab				2	ls	1-2m,cosbk	10YR3/2	1vf,f,m,co
13-28	Bw1				2	s	1f,msbk	10YR3/1	2vf.f,m,vo
28-42	Bw2				5	s	1vf,fsbk	10YR4/1	1f,m,co
42-55	Bw3				5	s	1vf,fsbk	10YR5/2	1f,m,co
55-76	Bw4				10	s	1vf,fsbk	10YR5/2	1m,co
76-94	Bw5				10	sl	1vfsbk	10YR5/3	1f,m
94-115	2BC				80	ls	m,sg,	2-5YR5/4	1f
115-125	2BCR				90	ls	m	1gley6/5gy	1vf
WH6		321655	7210984	900					
0-10	BA				0	scl	1fgr,1,2f,msbk	10YR2/1	3f,m
10-29	Bt1				0	c	3co,vcabk	10YR4/3	2f,m
29-50	Bt2				1	c	3co,vcabk	10YR3/2	2vf,f
50-80	Bt3				5	c	3m,co,vcabk	10YR4/2	1vf
80-106	2Bt4				10	c	2-3m,coabk	10YR4/2	1vf
106-116	2BtC				25	c	-	-	-
WM1		323726	7211482	0					
0-10	BA				5	s	3m,coabk	10YR3/3	3vf,f,1m,vc
10-23	Bw1				5	s	3m,coabk	10YR3/4	2vf,f,1co,vc,m
23-49	Bw2				5	s	2-3m,coabk	10YR3/6	1v,f,m,co,vc
49-106	Bw3				5	s	2co,vc,sbk	10YR4/6	1vf,f,m,vc
106-135	2Bw4				15	s	2f,msbk	5YR4/4	2vf,f,m
135-157	2Bw5				50	s	m,1vf,fsbk,sg	5YR4/4	1vf,f
157-170	3BC				72	s	1vfabk,m,sg	5YR4/4	1vf
WM2		323709	7211461	20					
0-15	BA				5	s	2m,coabk,1co,mgr	7.5YR3/2	2vf,f
15-30	Bw1				5	s	2m,coabk	5YR4/4	2vf,f,m,co,vc
30-59	Bw2				5	s	1-2f,abk	5YR4/4	2vf,f,m,co
59-87	Bw3				5	ls	2m,coabk	5YR4/4	2vf,f
87-106	Bw4				10	s	1f,mabk	5YR4/4	1vf,f
106-131	Bw5				20	s	1-2m,coabk	5YR4/4	1vf,f,co,m
131-140	BC				85	s	sg,1co,mgr,m	5YR4/4	1vf
WM3		323361	7211530	225					
0-17	BA				5	s	sg,2fsbk	5YR3/3	2vf,1f,m,co
17-36	Bw1				5	s	2f,msbk	5YR4/4	1vf,f,m,co
36-71	Bw2				10	ls	2f,msbk	5YR4/4	1vf,f,m,co,vc
71-86	Bw3				10	ls	2f,msbk	5YR4/4	1vf.,m

Depth	Horizon	Longitude (m)	Latitude (m)	Distance from crest		Texture	Structure	Moist colour	Roots
				(m)	(m)				
86-115	Bw4					ls	2f,msbk	5YR4/4	1vf,f,m
115-141	2Bc1					ls	m,sg	7.5YR4/6	1vf,f
141-149	2BC2					ls	m,sg	7.5YR4/6	1vf
WM4		323342	7211307	397					
0-10	BA					s	sg,1fsbk	7.5YR2.5/2	2vf,f
10-31	Bw1					s	2m,coabk	7.5YR4/4	1vf,f,m,co,vc
31-57	Bw2					s	1f,msbk	7.5YR4/6	1vf,f,m,co,vc
57-93	Bw3					s	1-2f,m,cosbk	7.5YR4/6	1vf,f,m,co,vc
93-131	Bw4					s	2f,msbk	7.5YR4/4-4/6	1f,m,co
131-145	2BC					s	sg,m	7.5YR4/4	1vf
WM5		323259	7211228	513					
0-12	BA					s	sg,1fgr	10YR3/4	3vf,f,1m,co
12-50	Bw1					s	1fsbk,sg	10YR4/4	2vf,f,1m,co,vc
50-96	Bw2					s	sg,1fsbk	10YR5/6	1vf,f,m,co
96-128	Bw3					s	sg	10YR5/4	1vf,f,m
128-152	Bw4					s	sg	10YR5/3	1vf
152-185	2BC1					s	m,sg	10YR5/4	1vf
185-200	2BC2					s	m,sg	10YR5/3	1vf
WM6		323144	7211160	640					
0-10	BA					s	1cogr,sg	10YR3/2	2vf,f
0-23	Bw1					s	1msbk	10YR3/3	2vf,f,1co,cv
23-53	Bw2					s	sg,1fsbk	10YR4/4	2,1vf,f,1m,co,vc
53-90	Bw3					s	sg,1f,msbk	10YR4/4	1-2vf, f, m, 1co, cv
90-129	Bw4					s	sg,1msbk	10YR4/6	1vf,fco,vc
129-164	2BC1					s	sg,m	10YR4/4	1vf,f
164-180	2BC2					s	m	10YR5/6	1vf
WM7		323050	7211060	777					
0-11	BA					s	1cogr,sg	10YR2/1	3vf,f
11-29	Bw1					s	sg,1mgr	10YR3/4	3vf,f
29-61	Bw2					s	sg	10YR4/6	2vf,f,1m,co,vc
61-107	Bw3					s	sg,1f,msbk	10YR4/6	1vf,f,co
107-152	Bw4					s	sg,1f,sbk	10YR4/6	1vf,f,m,co
152-165	2BC1					s	m	-	1vf,f,m
165-190	2BC2					s	sg	10YR5/6	1vf,f
190-210	2BC3					s	sg,m	10YR5/6	1vf
WM8		322874	7210854	1048					
0-9	BA					s	2f,msbk,2mgr	10YR2/2	2vf,f
9-22	Bw1					s	1-2f,msbk	10YR3/2	1vf,f,vc,co,m
22-48	Bw2					s	sg,1f,mgr	10YR4/2	1vf,f,m
48-62	2Bw3					s	sg	10YR4/3	1co
62-82	3Bw4					s	sg	10YR4/4	1vf
82-105	3BC1					s	sg,2f,msbk,abk	10YR4/1	1vf
105-115	3BC2					ls	sg,1fsbk,abk	-	-
WM9		322797	7210814	1133					
0-8	BA					ls	2m,cosbk	10YR2/1	2vf,f
8-20	Bw1					ls	2m,cosbk,abk	10YR2/2	2vf,f,vc,m
20-40	2Bw2, e					s	sg, loose sand	10YR4/6	2m,co
40-80	3Bt1					c	m,2-3c,vcabk	10YR4/3	1vf,f,m
80-101	3Bt2					sc	m,2c,vcabk	10YR5/6	1vf
101-113	4BC1					scl	2c,vcabk,sbk	-	1vf
113-120	4BC2					sl	sg,m	-	-
WM10		322707	7210785	1223					

Depth	Horizon	Longitude (m)	Latitude (m)	Distance from crest (m)	% gravel	Texture	Structure	Moist colour	Roots
0-9	BA				5	sl	3m,co,abk	7.5YR3/2	2vf,f
0-33	Bt1				5	scl	3m,co,abk	7.5YR3/1	1vf,f
33-68	Bt2				20	scl	m,3m,co,vcabk	7.5YR5/1	1vf
68-80	2BC				70	sl	sg,m	7.5YR4/1	-
WM11		322442	7210894	1367					
0-10	AB				5	s	1vf,f,skb,1mgr	10YR2/2	3vf,f
10-40	Bw1				5	s	2f,mabk	10YR4/3	2vf,f,vc
40-70	Bw2				10	s	1-2f,msbk/abk	10YR4/4	1-2vf,f
70-95	2Bt1				10	scl	m	10YR4/1	1vf
95-120	2Bt2				15	scl	m	10YR3/1	1vf
120-135	3BC				70	scl	m,sg,	-	-
WL1		0326823	7211630	0					
0-8	AB				0	s	0sg/1vfsbk	10YR2/2	2vff
8-17	Bw1				2	s	1vfmsbk/0sg	7.5YR3/3	3vff1c
17-39	Bw2				5	s	0sg/1mcsbk	7.5YR4/4	2vffmc
39-70	Bw3				5	s	1mcsbk/0sg	7.5YR4/6	3vffmc
70-93	Bw4				10	s	1mcsbk	7.5YR5/6	3vff1mc
93-115	2Bw5				80	s	1mcsbk	5YR5/4	2vff1mc
115-142	2Bw6				65	ls	2msbk	5YR5/4	2fm1vc
142-164	2Bw7				65	ls	1cmsbk	5YR4/4	1fm
164-184	3BC1				70	sl	2cmsbk	5YR4/6	0.5fm
184-205	3BC2				65	ls	1msbk/2csbk	5YR4/6	0.5m
205-230	3BC3				35	ls	1mcsbk/0sg	7.5YR4/6	0.5f
230-245	3BC4				45	s	0ma	7.5YR5/6	-
WL2		0327082	7211163	546					
0-12	AB				5	s	1msbk/0sg	10YR3/2	3vff1m
12-24	Bw1				40	s	2mcsbk/0sg	10YR4/4	3vf1c
24-39	Bw2				35	s	1mcsbk/0sg	7.5YR4/4	2vf1fmc
39-71	Bw3				30	s	1mcsbk/0sg	7.5YR4/4	1vffmc
71-94	Bw4				10	s	1mcsbk/0sg	7.5YR5/4	0.5vff
94-119	Bw5				75	s	1mcsbk/0sg	7.5YR5/4	1vffm
94-150	Bw6				45	s	2mcsbk	10YR4/4	-
150-172	Bw7				30	s	0sg/0ma	5YR5/8 (.7), 7.5YR6/4 (0.3) 10YR6/3 (.7), 7.5YR 5/6 (0.3)	-
172-198	3BC				40	s	0ma		-
WL3		0327299	7210743	1000					
0-5	A				5	s	1mgr/1fsbk	10YR3/3	3fmc
5-17	Bw1				5	s	1mgr/1fsbk	10YR4/4	3fmc
17-26	Bw2				10	s	1vffsbk	10YR4/6	3vff2c
26-45	Bw3				10	s	2fsbk	10YR4/6 (.7), 7.5YR 5/8 (.3) 10YR6/4 (.7), 10YR 5/8 (.3)	2fmc
45-60	Bw4				10	s	2fsbk		2fmc
60-77	2BC1				100	ls	1msbk	10YR6/4	2f1m
77-98	2BC2				50	scl	1msbk	10YR5/4	1f
98-132	2Cr1				60	sl	0ma	10YR5/6	0.5vf
132-155	2Cr2				65	s	0ma	10YR5/6	-
155-165	2Cr3				65	s	0ma	10YR6/6	-
WL4		0327218	7210661	1060					
0-9	BA				0	s	1vfgr,1fsbk	10YR3/1	1f,m,2f
9-24	Bw1				5	s	2f,msbk	10YR4/1	1vf,f,m,co
24-41	2Bw2				60	s	2msbk,abk,sg	10YR4/1	2vf,f

Depth	Horizon	Longitude (m)	Latitude (m)	Distance from crest (m)	% gravel	Texture	Structure	Moist colour	Roots
41-75	3Bt1				40	scl	3mabk,M	10YR4/3	1vf
75-110	3Bt2				65	scl	3mabk,M	10YR4/1	1vf
110-120	CR				80		M	-	-
WL5		0327309	7210551	1185					
0-14	BA				30	s	2msbk,1vfgr,vnpl	10YR2/2	2vf,f
14-40	BC1				70	s	M,1vfsbk,1vfgr,sg	7.5YR2.5/2	2vf,f
40-60	BC2				80	sc	3f,mabk	10YR3/1 (.4)	1vf
60-70	R				100				
WL6		0327296	7210546	1210					
0-11	BA				20	s	sg,1f,msbk,1fgr	7.5YR2.5/1	3vf,f
11-40	Bt1				20	sc	3m,coabk	10YR3/2	1vf,f,co
40-63	Bt2				30	scl	3co,vcabk	Gley 1 6/10y	1vf,f
63-84	Bt3				30	sc	3co,vcabk	Gley 1 7/10y	1vf,f
84-120	2Bt4				15	scl	3m,coabk	Gley 1 5/10y	1vf,f

Appendix II. Exchange properties of study pedons

Depth (cm)	Horizon	Clay %	xK	xMg	xCa cmol(+)/kg	xNa	CEC	BS (%)	pH	EC mS
DH1										
0-2	A	8	0.34	0.60	0.98	0.60	2.69	94	5.3	0.0
2-16	Bw1	11	0.25	0.29	0.88	0.28	2.03	84	4.9	0.0
16-28	2Bw2	11	0.14	0.56	0.49	0.55	2.48	70	4.8	0.0
28-45	2C	-	-	-	-	-	-	-	-	-
DH2										
0-1	A	8	0.34	1.18	2.52	1.17	5.23	99	5.7	0.0
1-14	Bw1	13	0.37	0.87	1.89	0.86	8.32	48	5.5	0.0
14-23	2Bw2	13	0.50	1.20	2.01	1.19	3.38	147	5.5	0.0
23-43	2C	-	-	-	-	-	-	-	-	-
DH3										
0-1	A	11	0.42	1.06	2.68	1.05	5.24	99	5.8	-
1-19	Bw1	8	0.28	1.10	0.94	1.09	3.00	114	5.4	-
DM1										
0-12	BA	5	1.08	2.19	4.85	0.31	11.19	75	6.3	0.0
12-29	BC	3	0.72	1.87	4.37	0.38	9.44	78	6.4	0.0
29-53	C	5	1.02	2.08	2.23	0.40	7.02	82	6.4	0.0
53-63	CR	-	-	-	-	-	-	-	-	-
DM2										
0-1	A	5	0.33	1.14	1.93	0.04	5.79	59	6.0	0.1
1-13	Bw1	5	0.32	0.92	1.95	0.03	5.49	59	5.8	0.1
13-32	2Bc1	6	0.29	1.23	1.42	0.05	5.82	51	5.7	0.0
32-46	2Bc2	7	0.29	1.88	0.94	0.08	6.70	48	5.7	0.0
46-60	2Bc3	5	0.23	2.15	0.40	0.10	5.58	52	5.9	0.0
DM3										
0-1	A	6	0.32	1.55	1.45	0.45	7.05	54	5.3	0.2
1-4	Bw1	9	0.40	2.75	5.54	0.33	9.83	92	6.5	0.2
4-20	2Bc1	9	0.34	2.27	2.85	0.26	7.34	78	6.0	0.1
20-39	3Bct2	34	0.47	9.40	4.00	1.42	13.26	115	5.9	0.1
39-50	3Bc3	34	0.26	10.29	3.83	2.18	16.18	102	5.9	0.1
DM4										
0-2	A	10	0.73	2.57	3.74	0.33	10.04	73	6.6	0.0
2-18	Bw1	17	2.55	3.64	6.56	0.44	19.37	68	6.8	0.1
18-51	2Bt1	18	1.68	3.39	8.94	0.59	19.44	75	7.0	0.0
51-63	2Bt2	17	0.69	3.76	33.26	0.73	25.75	150	7.4	0.1
63-81	3BC	23	0.89	3.69	36.87	0.67	21.71	195	7.4	0.1
81-91	C	-	-	-	-	-	-	-	-	-
DM5										
0-4	Ba	6	0.44	1.76	3.83	0.05	8.49	72	6.1	0.1
4-19	Bw1	11	0.38	2.85	6.27	0.10	10.77	89	5.7	0.1
19-35	Bw2	12	0.22	2.83	6.11	0.13	10.38	89	5.8	0.1
35-52	2Bc1	17	0.22	3.61	7.56	0.20	11.65	99	6.0	0.1
52-67	2Bc2	19	0.21	3.79	8.85	0.28	11.25	116	6.2	0.1
DM6										
0-4	A	2	0.51	1.40	4.64	1.05	12.00	63	7.3	0.0
4-10	AB	2	1.43	0.90	4.25	0.72	13.65	53	7.5	0.3
10-31	Btk1	12	11.61	1.49	4.78	1.05	21.67	87	7.7	2.0

Depth (cm)	Horizon	Clay %	xK	xMg	xCa cmol(+)/kg	xNa	CEC	BS (%)	pH	EC mS
31-52	2Bw1	11	12.12	1.61	9.62	0.91	16.15	150	7.7	2.7
52-76	Btk2	10	13.20	2.18	19.81	0.56	11.51	311	7.7	2.7
76-87	3Bw3	20	1.11	2.69	7.01	23.96	21.59	161	7.7	3.5
87-97	C	-	-	-	-	-	-	-	-	-
DL1										
0-23	BA	6	0.36	1.20	5.04	0.98	10.40	73	6.1	0.0
23-45	BC	5	0.30	1.06	3.53	0.82	11.63	49	5.9	0.0
45-55	C	-	-	-	-	-	-	-	-	-
DL2										
0-6	Ba	3	0.50	1.03	2.95	0.03	7.15	63	6.6	0.1
6-22	Bw1	4	0.28	0.75	2.05	0.03	6.39	49	6.1	0.1
22-35	2Bc1	5	0.31	0.93	2.18	0.03	6.52	53	5.9	0.1
35-50	2Bc2	5	0.36	1.26	1.71	0.04	6.45	52	5.8	0.1
DL3										
0-2	A	7	0.37	2.56	4.81	1.14	12.74	70	6.5	0.0
2-19	Bw1	2	0.29	1.87	5.00	0.96	12.10	67	6.5	0.0
19-34	Bw2	10	0.50	3.07	4.53	1.24	14.40	65	6.7	0.0
34-42	BC	15	0.43	4.01	5.10	1.53	16.98	65	6.9	
42-52	C									
DL4										
0-1	Ab	4	0.56	0.60	1.46	0.36	5.61	53	6.5	0.1
1-9	Bw1	4	0.45	0.67	1.45	0.73	6.16	54	5.6	0.3
9-24	Bw2	4	0.50	0.74	0.79	0.40	6.20	39	5.9	0.1
24-40	Bw3	2	0.23	0.59	0.29	0.25	4.63	29	6.0	0.1
40-55	Bw4	2	0.15	0.76	0.15	0.16	4.32	28	6.2	0.1
55-67	2Bc1	1	0.11	0.85	0.11	0.14	3.24	37	6.2	0.1
67-75	2Bc2	9	0.25	2.67	0.33	0.71	6.31	63	6.2	0.1
DL5										
0-4	Ab	3	0.63	1.39	3.73	0.06	7.45	78	6.7	0.2
4-13	Bw1	3	0.68	1.43	2.14	0.06	7.06	61	6.5	0.1
13-30	Bw2	6	0.79	1.30	2.45	0.06	8.08	57	6.4	0.1
30-51	Bw3	6	0.91	1.66	2.59	0.06	7.57	69	6.6	0.1
51-76	Bw4	7	0.67	1.70	2.74	0.07	6.52	79	6.3	0.1
76-112	2Bw5	7	0.46	1.52	2.26	0.16	7.80	56	6.3	0.1
112-120	2Bw6	19	0.75	3.10	7.24	0.41	14.39	80	6.5	0.2
DL6										
0-1	Ab	10	0.75	2.27	5.06	0.15	8.80	94	6.5	0.1
1-4	Bw1	12	1.25	2.24	6.27	0.08	11.03	89	6.5	0.1
4-20	2Bt2	20	1.28	2.97	8.15	0.22	11.34	111	6.6	0.1
20-59	2Bt3	23	1.54	5.33	10.19	0.54	13.39	131	6.5	0.3
59-95	2Bt4	11	1.64	8.29	21.02	1.88	15.69	209	7.4	0.4
95-110	3Bw5	20	1.42	9.38	19.03	3.79	15.79	212	7.9	0.4
110-120	3Bw6	12	1.25	8.53	14.42	4.69	15.23	189	7.9	0.7
DL7										
0-1	BA	12	9.77	1.94	4.22	0.53	18.21	90	6.7	1.8
1-11	Btk1	22	22.63	5.85	18.26	0.78	25.99	183	7.7	9.4
11-40	Btk2	25	23.48	5.69	12.99	0.77	26.63	161	7.3	11.1
40-68	2Bw1	27	24.34	3.93	8.39	0.63	23.29	160	7.4	6.3

Depth (cm)	Horizon	Clay %	xK	xMg	xCa cmol(+)/kg	xNa	CEC	BS (%)	pH	EC mS
68-95	2Bw2	21	21.01	3.07	3.56	0.91	24.52	116	7.4	6.3
IH1										
0-10	BA	3	0.60	1.28	1.89	0.32	6.67	61	5.8	0.0
10-23	Bw1	10	0.55	1.19	1.47	0.35	7.66	47	5.4	0.0
23-50	BC	7	0.62	2.07	1.61	0.34	10.00	46	4.8	0.0
50-60	CR									
IH2										
0-10	BA	4	0.41	1.06	3.03	0.04	6.68	68	6.6	0.1
10-20	Bw1	5	0.28	0.70	2.17	0.03	5.88	54	6.4	0.0
20-30	Bw2	7	0.22	0.84	2.15	0.03	6.08	53	6.4	0.1
30-47	Bc	7	0.18	1.14	2.35	0.04	6.40	58	6.4	0.0
IH3										
0-7	AB	2	0.52	1.02	1.16	0.29	5.08	59	5.5	0.1
7-26	Bw1	5	0.51	1.08	0.77	0.39	6.47	43	5.0	0.0
26-40	Bw2	5	0.33	1.10	0.44	0.47	4.05	58	5.3	0.0
40-60	Bw3	2	0.23	1.24	0.34	0.52	3.29	71	5.2	0.0
60-80	BC	10	0.25	1.81	0.48	0.95	4.37	80	6.1	0.1
80-90										
IH4										
0-9	AB	6	0.43	1.50	3.49	0.10	8.42	65	6.2	0.1
9-20	BA	7	0.36	1.52	2.54	0.11	7.70	59	6.3	0.1
20-50	Bt1	34	0.32	6.35	8.07	1.21	16.27	98	6.3	0.1
50-62	Bt2	29	0.31	6.23	8.51	1.61	14.98	111	6.5	0.3
62-70	2BC	27	0.38	5.91	8.61	1.89	15.27	109	6.6	0.3
IH5										
0-10	BA	26	1.03	3.72	8.37	0.72	22.22	62	6.2	0.0
10-31	Bt1	27	0.53	3.02	10.80	0.68	26.03	58	6.5	0.0
31-49	Bt2	32	0.84	3.57	15.08	0.67	29.52	68	6.9	0.1
49-83	Bt3	35	0.55	3.39	14.54	0.35	30.04	63	7.3	0.2
83-93	BCR									
IM1										
0-7	BA	7	0.92	1.55	1.63	0.57	6.23	75	6.1	0.0
7-33	Bw1	7	0.59	1.16	1.08	0.36	6.94	46	5.1	0.0
33-65	CR/BC	10	0.42	2.07	1.23	0.59	7.98	54	5.2	0.0
65-75	RC									
IM2										
0-5	A	3	0.36	2.91	9.13	0.50	14.64	88	6.7	0.0
5-17	Bw1	12	0.10	3.20	7.86	0.40	15.35	75	6.1	0.0
17-42	Bw2	17	0.20	3.34	10.30	0.50	18.28	78	6.0	0.0
42-56	Bw3	45	0.24	3.02	16.17	0.47	17.88	111	6.7	0.1
56-70	2CB	7	0.02	2.51	26.32	0.26	10.50	277	7.9	0.1
70-80	Rc									
IM3										
0-16	AB	1	0.00	0.23	0.59	0.05	3.66	24	6.1	0.0
16-42	Bw1	1	0.14	1.27	1.18	0.13	3.92	69	5.4	0.0
42-70	Bw2	2	0.05	1.40	0.65	0.16	2.77	81	5.1	0.0
70-120	2BC1	0	0.01	1.71	0.49	0.21	2.13	113	6.1	0.0
120-151	2BC2	0	0.09	3.66	0.96	0.77	3.59	152	6.5	0.0

Depth (cm)	Horizon	Clay %	xK	xMg	xCa cmol(+)/kg	xNa	CEC	BS (%)	pH	EC mS
151-175	2BC3	0	0.00	2.58	0.85	0.60	3.30	122	6.5	0.0
IM4										
0-7	BA	5	0.48	2.12	3.60	0.42	7.96	83	6.1	0.0
7-26	Bw/Bt	7	0.28	2.35	3.36	0.39	9.38	68	5.7	0.0
26-30	C									
IM5										
0-13	BA	12	0.76	1.85	2.67	0.68	7.62	78	5.1	0.4
13-25	Bt1	30	0.92	5.03	4.28	1.96	22.98	53	6.0	0.2
25-40	BtC	36	0.86	7.83	6.48	4.66	27.74	72	7.7	0.5
40-65	CR	10	0.50	4.28	5.72	3.01	12.42	108	9.0	0.3
65-75	R									
IM6										
0-9	BA	10	0.58	2.68	4.33	0.68	13.21	63	5.5	0.0
9-25	Bt1	25	0.46	3.85	6.36	0.96	24.13	48	5.3	0.0
25-62	Bt2	33	0.53	5.37	11.40	1.76	29.88	64	6.8	0.1
62-90	2Bt3	31	0.55	6.01	31.69	3.33	25.95	160	8.1	0.6
90-100	CR	35	0.65	6.62	36.56	3.90	29.17	163	8.1	0.8
100-110	R									
IM7										
0-4	A	20	0.74	2.86	3.59	0.56	16.31	47	5.9	0.0
4-10	BA1	20	0.74	2.86	3.72	0.48	13.81	56	5.7	0.0
10-22	BA2	20	0.81	3.56	4.34	0.59	20.24	45	5.6	0.0
22-40	2Bw1	20	0.36	3.72	4.06	0.70	21.03	42	5.9	0.0
40-63	2Bw2	20	0.34	6.47	7.48	1.93	35.56	45	7.1	0.2
63-70	2Bw3	22	0.53	6.85	7.43	2.35	32.86	52	7.8	0.3
70-77	2Bw4	25	0.50	7.79	8.36	2.84	35.16	55	7.9	0.4
77-87	2Bw5	25	0.74	9.01	19.67	3.62	35.16	93	8.2	0.6
IM8										
0-7	BA	2	0.83	1.52	2.94	1.12	9.40	68	6.7	0.1
7-25	Bt1	25	0.80	6.55	3.78	9.84	26.94	78	8.6	1.5
25-46	Bt2	30	0.72	8.87	7.48	16.25	34.05	98	9.1	2.6
46-62	Bt3	33	0.68	7.19	6.29	14.69	28.73	100	9.1	2.6
62-90	BC	30	0.70	7.26	13.21	15.59	28.57	128	9.1	2.9
IL1										
1-3	A	2	0.48	0.85	1.17	0.49	6.79	44	5.6	0.0
3-11	BC	3	0.24	0.84	0.77	0.56	5.32	45	5.2	0.0
11-30	CR									
IL2										
0-10	BA	3	0.22	0.54	1.38	0.02	5.48	40	6.0	0.1
10-39	Bw1	4	0.11	0.60	1.32	0.06	4.63	45	6.1	0.1
	2Bw2,									
39-60	e	4	0.14	0.59	0.67	0.07	4.89	30	6.1	0.1
60-80	2Bc	5	0.13	0.61	0.67	0.07	4.93	30	6.3	0.1
IL3										
0-2	A	7	0.79	1.23	0.90	0.33	5.24	62	6.9	0.0
2-25	Bw1	1	0.58	1.13	0.68	0.26	5.71	46	5.9	0.0
25-47	Bw2	5	0.78	1.26	0.62	0.43	6.39	48	6.0	0.0
47-70	BC	5	0.61	1.23	0.73	0.63	7.10	45	5.7	0.0

Depth (cm)	Horizon	Clay %	xK	xMg	xCa cmol(+)/kg	xNa	CEC	BS (%)	pH	EC mS
IL4										
0-12	BA	4	0.36	0.54	1.00	0.03	5.24	37	6.2	0.2
12-48	Bw1	4	0.14	0.36	0.54	0.02	4.02	26	5.8	0.0
48-70	Bw2	4	0.07	0.37	0.34	0.02	4.05	20	5.9	0.0
70-85	Bw3	1	0.06	0.41	0.24	0.03	4.28	17	5.8	0.0
85-100	CB	2	0.05	0.37	0.25	0.03	3.99	17	5.7	0.0
IL5										
0-11	BA	3	0.14	0.29	0.57	0.03	4.49	23	5.4	0.1
11-27	Bw1	3	0.08	0.35	0.44	0.06	4.13	22	5.9	0.0
27-53	2Bc	2	0.06	0.41	0.28	0.07	3.62	23	6.1	0.1
53-70	2Cr	1	0.04	0.48	0.16	0.08	3.35	23	6.2	0.0
IL6										
0-1	A	7	0.89	1.40	1.81	0.34	6.03	74	5.6	0.0
1-24	Bw1	5	0.64	1.45	1.63	0.38	6.31	65	5.4	0.0
24-57	BC	25	1.84	5.14	3.09	0.71	16.83	64	6.0	0.0
57-67	C									
IL7										
0-1	A	13	0.51	2.34	5.71	1.24	14.92	66	6.2	0.1
1-16	Bw1	11	0.48	2.70	5.80	1.06	15.04	67	6.2	0.0
16-30	Bw2	21	0.54	3.67	5.73	0.52	18.73	56	5.8	0.0
30-63	Bw3	30	0.40	5.17	5.81	0.47	21.27	56	5.5	0.0
63-110	BC	28	0.39	4.72	7.78	0.60	21.71	62	5.9	0.0
110-120	CR									
IL8										
0-13	BA	12	0.26	1.80	4.06	0.05	10.09	61	5.6	0.1
13-53	Bt1	25	0.16	3.37	8.67	0.29	15.11	83	6.0	0.1
53-70	Bt2	15	0.28	4.22	14.30	0.42	15.52	123	6.8	0.2
70-85	2Bw3	7	0.24	4.39	21.40	0.48	17.56	150	7.3	0.2
85-100	2Bc	6	0.26	4.90	20.49	0.45	17.86	146	7.3	0.2
IL9										
0-3	BA	6	0.51	1.99	4.66	0.62	9.96	78	6.7	0.1
3-17	Bt1	12	0.74	2.74	5.70	1.06	13.85	74	6.5	0.1
17-35	2Bt2	32	1.42	6.95	10.63	1.03	26.55	75	7.4	0.2
35-57	3Btk3	25	1.68	7.50	20.74	0.81	24.56	125	8.4	0.3
57-80	3Btk4	30	3.31	8.38	21.02	0.69	24.96	133	8.7	0.3
80-110	3Btk5	17	6.33	8.93	23.09	0.65	28.53	136	8.6	0.8
110-130	BC	10	8.10	8.70	28.89	0.55	28.10	164	8.6	1.5
IL10										
0-7	AB	10	1.0	5.1	9.30	0.39	18.49	85	7.0	0.2
7-34	Bt1	17	0.5	3.0	5.17	0.72	16.03	58	5.4	0.1
34-60	2Bt2	27	1.1	5.0	6.44	0.56	23.89	55	5.7	0.1
60-85	3Bt3	27	1.6	5.7	8.78	0.60	20.20	83	7.6	0.1
85-111	3Bt4	27	2.4	7.1	21.61	0.61	28.13	112	8.3	0.5
111-120	4BC	17	2.6	6.8	19.24	0.43	24.56	118	8.6	0.4
WH1										
0-4	AB	2	0.56	2.55	3.62	0.53	7.98	91	6.2	0.0
4-30	Bw1	7	0.39	1.85	1.01	0.47	3.10	119	5.5	0.0
30-76	Bw2	12	0.30	1.83	0.87	0.52	4.72	75	5.0	0.0

Depth (cm)	Horizon	Clay %	xK	xMg	xCa cmol(+)/kg	xNa	CEC	BS (%)	pH	EC mS
76-105	Bw3	15	0.22	1.76	0.74	0.54	5.16	63	4.9	0.0
105-125	Bw4	17	0.22	1.52	0.66	0.48	5.32	54	5.2	0.0
125-146	Bw5	16	0.27	1.61	0.84	0.61	4.17	80	5.3	0.0
146-180	2Bw6	6	0.23	1.59	0.88	0.63	4.29	78	5.5	0.0
180-212	C	17	0.24	2.26	1.30	0.62	5.63	79	6.0	0.0
WH2										
0-13	Ba	4	0.06	0.19	0.37	0.01	3.62	17	5.7	0.0
13-29	Bw1	4	0.03	0.08	0.17	0.02	3.13	9	5.7	0.0
29-49	Bw2	5	0.03	0.15	0.38	0.05	3.48	18	6.2	0.0
49-87	Bw3	6	0.02	0.15	0.32	0.04	3.36	16	5.7	0.0
87-124	Bw4	7	0.03	0.28	0.60	0.06	3.03	32	6.0	0.1
124-130	BC	7	0.03	0.53	1.01	0.09	3.56	46	6.1	0.1
WH3										
0-17	AB	6	0.09	0.03	0.35	0.01	4.06	17	6.5	0.1
17-58	Bw1	8	0.03	0.09	0.18	0.01	4.08	13	5.3	0.1
58-88	Bw2	6	0.04	0.05	0.07	0.03	3.92	9	5.0	0.1
88-112	Bw3	6	0.03	0.04	0.27	0.03	3.09	19	5.5	0.1
112-128	Bw4	5	0.02	0.03	0.26	0.03	2.89	19	5.8	0.1
128-140	2BC	2	0.02	0.03	0.35	0.04	3.28	23	6.0	0.0
WH4										
0-5	AB	1	0.46	1.25	1.48	0.43	4.80	75	6.0	0.0
5-24	Bw1	4	0.70	0.84	0.82	0.53	22.54	13	5.3	0.0
24-47	Bw2	5	0.46	2.09	0.85	0.57	4.29	93	4.9	0.0
47-67	Bw3	3	0.28	2.32	0.75	0.56	3.52	111	5.0	0.0
67-89	2Bw4	5	0.20	2.42	0.72	0.51	8.89	43	5.5	0.0
89-115	3Bw5	4	0.24	2.52	0.99	0.68	3.36	131	5.7	0.0
115-150	3Bw6	5	0.23	2.81	1.70	0.70	3.68	147	5.9	0.0
150-160	R						4.17		6.1	0.0
WH5										
0-13	Ab	13	0.56	2.55	3.62	0.53	7.98	26	5.9	0.1
13-28	Bw1	9	0.39	1.85	1.01	0.47	3.10	27	5.4	0.1
28-42	Bw2	8	0.30	1.83	0.87	0.52	4.72	27	5.5	0.1
42-55	Bw3	7	0.22	1.76	0.74	0.54	5.16	30	5.8	0.1
55-76	Bw4	9	0.22	1.52	0.66	0.48	5.32	43	6.4	0.1
76-94	Bw5	16	0.27	1.61	0.84	0.61	4.17	70	5.7	0.1
94-115	2BC	14	0.23	1.59	0.88	0.63	4.29	62	5.6	0.1
115-125	2BCR	12	0.24	2.26	1.30	0.62	5.63	66	5.6	0.1
WH6										
0-10	BA	21	0.50	2.76	2.60	0.62	19.01	34	4.8	0.1
10-29	Bt1	85	0.52	6.80	5.40	1.00	39.60	35	5.0	0.1
29-50	Bt2	58	0.56	8.61	6.70	1.12	44.44	38	5.6	0.0
50-80	Bt3	88	0.39	10.07	7.73	1.22	43.65	44	6.2	0.0
80-106	2Bt4	55	0.51	8.80	6.59	1.19	39.68	43	6.3	0.1
106-116	2BtC	40	0.26	6.07	4.74	1.01	25.99	47	6.6	0.0
WM1										
0-10	BA	5	0.12	0.45	1.41	0.02	5.61	36	5.8	0.1
10-23	Bw1	5	0.08	0.27	0.69	0.01	4.53	23	5.7	0.1
23-49	Bw2	7	0.04	0.26	0.33	0.02	4.45	15	5.7	0.1

Depth (cm)	Horizon	Clay %	xK	xMg	xCa cmol(+)/kg	xNa	CEC	BS (%)	pH	EC mS
49-106	Bw3	9	0.06	0.34	0.63	0.02	5.38	19	5.5	0.0
106-135	2Bw4	10	0.09	0.30	0.56	0.04	5.19	19	5.6	0.0
135-157	2Bw5	8	0.12	0.29	0.55	0.06	4.88	21	5.7	0.1
157-170	3BC	10	0.17	0.47	0.82	0.07	5.25	29	5.9	0.0
WM2										
0-15	BA	6	0.19	0.33	0.69	0.01	4.08	30	5.8	0.1
15-30	Bw1	8	0.07	0.23	0.36	0.01	5.04	13	5.6	0.1
30-59	Bw2	11	0.06	0.30	0.41	0.02	5.25	15	5.2	0.1
59-87	Bw3	12	0.08	0.38	0.80	0.04	4.88	27	5.4	0.1
87-106	Bw4	10	0.08	0.30	0.83	0.04	5.06	25	5.5	0.0
106-131	Bw5	10	0.10	0.34	1.10	0.07	4.79	34	5.8	0.1
131-140	BC	10	0.12	0.38	0.75	0.07	4.89	27	5.9	0.0
WM3										
0-17	BA	3	0.19	0.34	0.56	0.01	4.22	26	5.8	0.1
17-36	Bw1	8	0.11	0.15	0.09	0.01	3.75	10	5.6	0.0
36-71	Bw2	11	0.10	0.25	0.05	0.02	4.38	9	5.2	0.0
71-86	Bw3	12	0.12	0.26	0.05	0.02	4.20	11	5.4	0.0
86-115	Bw4	11	0.12	0.23	0.10	0.02	3.48	13	5.4	0.0
115-141	2Bc1	12	0.13	0.38	0.36	0.03	4.28	21	5.6	0.0
141-149	2BC2	12	0.10	0.47	0.54	0.06	4.84	24	5.6	0.0
WM4										
0-10	BA	2	0.12	0.25	0.96	0.02	2.86	47	5.8	0.1
10-31	Bw1	5	0.07	0.11	0.27	0.02	2.43	19	5.5	0.1
31-57	Bw2	8	0.06	0.17	0.08	0.01	3.39	10	5.3	0.0
57-93	Bw3	9	0.07	0.18	0.06	0.02	2.82	12	5.1	0.1
93-131	Bw4	10	0.05	0.18	0.34	0.04	2.95	21	5.8	0.0
131-145	2BC	6	0.14	0.43	0.50	0.11	3.37	35	5.9	0.0
WM5										
0-12	BA	4	0.07	0.16	0.50	0.01	2.77	27	6.0	0.1
12-50	Bw1	4	0.04	0.06	0.06	0.01	2.53	7	5.4	0.0
50-96	Bw2	5	0.04	0.11	0.03	0.01	2.19	8	5.6	0.0
96-128	Bw3	3	0.03	0.05	0.02	0.02	2.22	6	5.5	0.0
128-152	Bw4	2	0.04	0.05	0.11	0.01	1.97	11	5.7	0.1
152-185	2BC1	3	0.05	0.12	0.15	0.02	1.97	17	5.5	0.1
185-200	2BC2	3	0.06	0.19	0.24	0.03	2.11	25	5.5	0.1
WM6										
0-10	BA	2	0.18	0.67	2.52	0.04	4.57	75	6.0	0.1
0-23	Bw1	4	0.12	0.24	0.74	0.02	2.80	40	5.9	0.1
23-53	Bw2	5	0.07	0.15	0.28	0.02	2.49	21	5.7	0.0
53-90	Bw3	5	0.03	0.11	0.08	0.01	2.67	8	5.5	0.0
90-129	Bw4	4	0.05	0.12	0.09	0.01	2.41	11	5.5	0.1
129-164	2BC1	4	0.04	0.22	0.17	0.02	2.08	22	5.7	0.0
164-180	2BC2	5	0.09	0.41	0.34	0.03	2.52	35	6.0	0.0
WM7										
0-11	BA	2	0.09	0.22	0.68	0.02	3.11	32	5.8	0.1
11-29	Bw1	6	0.08	0.18	0.34	0.02	2.77	22	5.9	0.0
29-61	Bw2	7	0.03	0.15	0.10	0.01	2.81	10	6.2	0.0
61-107	Bw3	7	0.05	0.14	0.05	0.03	3.03	9	6.3	0.0

Depth (cm)	Horizon	Clay %	xK	xMg	xCa cmol(+)/kg	xNa	CEC	BS (%)	pH	EC mS
107-152	Bw4	5	0.05	0.11	0.05	0.04	2.99	8	6.1	0.0
152-165	2BC1	6	0.05	0.15	0.19	0.05	2.46	18	6.0	0.0
165-190	2BC2	5	0.06	0.30	0.43	0.05	2.90	29	6.6	0.1
190-210	2BC3	5	0.07	0.39	0.57	0.07	3.20	34	5.6	0.0
WM8										
0-9	BA	5	0.25	0.39	0.52	0.08	4.18	30	6.1	0.1
9-22	Bw1	4	0.09	0.15	0.22	0.04	2.96	17	6.2	0.1
22-48	Bw2	5	0.05	0.10	0.17	0.07	2.85	14	6.1	0.1
48-62	2Bw3	5	0.06	0.14	0.19	0.08	3.00	16	6.2	0.1
62-82	3Bw4	3	0.04	0.14	0.16	0.05	2.63	15	6.2	0.1
82-105	3BC1	10	0.07	0.67	0.50	0.14	3.82	36	6.0	0.1
105-115	3BC2	12	0.12	1.44	1.05	0.32	5.48	53	6.2	0.1
WM9										
0-8	BA	13	0.28	1.04	1.25	0.28	5.84	49	6.6	0.1
8-20	Bw1	15	0.17	0.79	0.77	0.11	5.64	33	5.9	0.1
	2Bw2,									
20-40	e	5	0.06	0.32	0.31	0.05	3.29	23	5.5	0.1
40-80	3Bt1	60	0.30	4.79	2.95	0.85	12.36	72	5.5	0.1
80-101	3Bt2	40	0.18	3.51	2.23	0.75	9.70	69	5.9	0.1
101-113	4BC1	35	0.19	3.53	2.23	0.80	10.03	67	6.3	0.1
113-120	4BC2	17	0.10	2.32	1.42	0.54	7.07	62	6.3	0.1
WM10										
0-9	BA	15	0.30	2.12	1.79	1.19	7.10	76	6.3	0.1
0-33	Bt1	25	0.23	3.53	2.31	3.14	11.48	80	7.4	0.2
33-68	Bt2	34	0.23	4.20	2.44	4.64	12.74	90	8.8	0.6
68-80	2BC	17	0.14	3.10	2.87	3.45	8.53	112	8.8	0.5
WM11										
0-10	AB	6	0.24	1.01	1.88	0.06	5.90	54	5.5	0.1
10-40	Bw1	8	0.09	1.19	1.56	0.06	5.78	50	6.3	0.0
40-70	Bw2	8	0.06	1.15	1.37	0.09	5.49	49	6.4	0.0
70-95	2Bt1	29	0.25	5.37	6.63	0.65	14.11	91	6.3	0.1
95-120	2Bt2	27	0.19	5.50	7.32	0.74	11.71	117	6.7	0.1
120-135	3BC	24	0.23	5.37	7.01	0.77	13.60	98	6.4	0.1
WL1										
0-8	AB	3	0.07	0.31	1.14	0.12	32.82	5	6.4	0.11
8-17	Bw1	3	0.06	0.23	1.06	0.11	8.01	18	6.0	0.01
17-39	Bw2	5	0.07	0.12	0.08	0.13	13.04	3	5.9	0.00
39-70	Bw3	3	0.02	0.02	0.00	0.13	3.77	4	5.7	0.00
70-93	Bw4	5	0.08	0.37	0.37	0.15	1.72	56	5.1	0.00
93-115	2Bw5	10	0.06	0.41	0.54	0.17	11.51	10	5.1	0.00
115-142	2Bw6	11	0.06	0.38	0.61	0.20	8.60	14	5.4	0.00
142-164	2Bw7	11	0.09	0.57	0.91	0.25	11.18	16	5.6	0.00
164-184	3BC1	15	0.12	0.83	1.33	0.35	11.05	23	5.8	0.00
184-205	3BC2	13	0.16	0.95	1.50	0.23	13.83	20	5.7	0.00
205-230	3BC3	13	0.18	0.96	1.38	0.24	14.56	18	6.1	0.00
230-245	3BC4	8	0.11	0.62	1.85	0.15	14.42	18	6.1	0.00
WL2										
0-12	AB	4	0.07	0.14	0.20	0.13	13.70	3	5.9	0.00

Depth (cm)	Horizon	Clay %	xK	xMg	xCa cmol(+)/kg	xNa	CEC	BS (%)	pH	EC mS
12-24	Bw1	4	0.05	0.06	0.09	0.11	3.11	9	5.6	0.00
24-39	Bw2	4	0.01	0.04	0.00	0.14	5.76	3	5.3	0.00
39-71	Bw3	5	0.01	0.01	0.00	0.11	2.91	4	5.2	0.00
71-94	Bw4	1	0.09	0.40	0.11	0.32	3.97	23	5.2	0.00
94-119	Bw5	1	0.04	0.20	0.25	0.12	5.36	11	5.5	0.00
94-150	Bw6	6	0.02	0.33	0.27	0.18	2.71	29	6.0	0.00
150-172	Bw7	9	0.02	0.54	0.44	0.18	3.97	29	6.0	0.00
172-198	3BC	1	0.07	0.33	1.79	0.11	5.69	40	6.0	0.00
WL3										
0-5	A	1	0.09	0.25	0.66	0.11	14.36	7	5.9	0.04
5-17	Bw1	1	0.03	0.25	0.49	0.11	6.15	14	5.9	0.00
17-26	Bw2	1	0.01	0.28	0.37	0.14	8.87	9	5.8	0.00
26-45	Bw3	1	0.01	0.27	0.34	0.12	5.16	14	5.8	0.00
45-60	Bw4	5	0.01	0.31	0.47	0.11	6.09	14	5.3	0.00
60-77	2BC1	11	0.01	0.39	0.87	0.20	11.05	13	5.5	0.00
77-98	2BC2	25	0.00	1.23	2.76	0.23	6.02	69	5.9	0.00
98-132	2Cr1	19	0.03	1.70	3.56	0.24	17.34	31	6.3	0.00
132-155	2Cr2	1	0.02	1.98	3.70	0.23	19.98	29	6.2	0.00
155-165	2Cr3	1	1.04	2.20	17.49	0.17	13.83	151	6.3	0.00
WL4										
0-9	BA	5	0.42	1.57	1.91	0.34	8.77	48	5.4	0.00
9-24	Bw1	8	0.22	1.33	1.20	0.39	6.63	47	5.1	0.00
24-41	2Bw2	1	0.19	1.16	0.81	0.48	3.37	78	5.4	0.01
41-75	3Bt1	30	0.34	5.06	3.98	1.38	19.40	55	6.0	0.09
75-110	3Bt2	30	0.25	6.69	11.16	2.33	21.83	93	7.6	0.37
110-120	CR									
WL5										
0-14	BA	3	0.43	1.98	2.67	0.48	9.84	56	6.0	0.03
14-40	BC1	9	0.32	2.45	2.85	0.48	11.47	53	5.4	0.01
40-60	BC2	39	0.37	6.21	5.82	1.07	29.56	45	5.9	0.05
60-70	R									
WL6										
0-11	BA	4	0.48	2.22	2.57	0.52	10.79	53	5.6	0.04
11-40	Bt1	38	0.38	4.89	3.88	1.56	20.36	52	6.2	0.12
40-63	Bt2	30	0.53	7.32	6.71	3.34	22.46	79	8.2	0.54
63-84	Bt3	35	0.41	7.27	5.77	4.39	21.19	84	8.5	0.70
84-120	2Bt4	30	0.36	8.34	5.39	5.76	26.90	73	8.4	0.89

Appendix III. Elemental composition of soil horizons in sampled pedons

Depth/ site	Horizon	Si	Al	Fe	Ca	Mg	Na	K	Ti	Mn	P	Zr (ppm)
		%										
DH1												
0-2	A	36.1	6.4	0.75	0.54	0.05	2.03	2.08	0.19	<0.01	0.03	132
2-16	Bw1	35.7	6.7	0.81	0.55	0.08	2.06	2.14	0.19	0.01	0.03	138
16-28	2Bw2	34.0	8.1	1.11	0.82	0.16	2.76	1.54	0.16	<0.01	0.02	144
28-45	2C											
DH2												
0-1	A	35.5	6.4	0.80	0.74	0.07	2.46	1.67	0.24	0.01	0.03	158
1-14	Bw1	34.1	7.2	1.62	0.70	0.11	2.32	1.89	0.37	0.02	0.03	191
14-23	2Bw2	34.0	7.4	1.61	0.69	0.13	2.35	1.91	0.35	0.02	0.03	178
23-43	2C											
DH3												
0-1	A	33.7	7.0	1.75	0.74	0.14	2.44	1.88	0.46	0.02	0.03	230
1-19	Bw1	35.7	6.8	0.94	0.70	0.05	2.44	1.79	0.23	0.01	0.01	144
DM1												
0-12	BA	33.5	7.3	1.88	1.28	0.22	3.00	1.21	0.24	0.03	0.02	179
12-29	BC	33.6	7.6	1.87	1.23	0.15	3.03	1.09	0.20	0.05	0.02	133
29-53	C	33.6	7.7	1.55	1.20	0.20	3.31	1.02	0.25	0.02	0.01	140
53-63	CR											
DM2												
0-1	a	34.5	7.3	1.34	1.14	0.19	3.03	1.20	0.26	0.03	0.02	191
1-13	bw1	34.2	7.2	1.41	1.09	0.19	3.14	1.20	0.27	0.03	0.02	182
13-32	2bc1	34.6	7.2	1.40	1.07	0.18	3.03	1.17	0.24	0.02	0.02	165
32-46	2bc2	34.5	7.2	1.40	1.04	0.17	2.97	1.02	0.22	0.02	0.02	137
46-60	2bc3	34.6	7.3	1.25	1.17	0.14	3.33	0.95	0.23	0.02	0.02	133
DM3												
0-1	a	34.4	6.9	1.27	1.09	0.19	3.20	1.10	0.17	0.02	0.02	114
1-4	bw1	33.0	7.1	1.63	1.14	0.22	2.97	1.10	0.23	0.02	0.02	147
4-20	2bc1	34.1	7.2	1.48	1.05	0.19	3.15	1.16	0.20	0.02	0.02	125
20-39	3bct2	28.8	8.6	3.63	0.62	0.47	1.70	1.02	0.34	0.02	0.02	77
39-50	3bc3	29.8	9.0	2.94	0.79	0.42	2.43	0.94	0.31	0.01	0.01	75
DM4												
0-2	A	32.7	7.2	2.62	1.36	0.39	2.98	1.16	0.57	0.05	0.02	304
2-18	Bw1	31.6	7.5	3.18	1.19	0.42	2.59	1.20	0.44	0.05	0.02	211
18-51	2Bt1	31.2	7.6	3.27	1.22	0.46	2.46	1.18	0.46	0.05	0.02	183
51-63	2Bt2	30.1	7.6	3.54	1.62	0.51	2.28	1.08	0.52	0.06	0.02	175
63-81	3BC	30.0	7.5	3.39	1.97	0.49	2.26	1.06	0.43	0.06	0.02	158
81-91	C											
DM5												

Depth/ site	Horizon	Si	Al	Fe	Ca	Mg	Na	K	Ti	Mn	P	Zr (ppm)
%												
0-4	ba	33.2	7.1	2.48	1.35	0.39	3.03	1.16	0.49	0.05	0.02	227
4-19	bw1	31.9	7.3	2.94	1.27	0.48	2.83	1.20	0.53	0.06	0.02	197
19-35	bw2	31.7	7.5	3.00	1.22	0.43	2.84	1.15	0.46	0.05	0.02	181
35-52	2bc1	31.8	7.6	3.13	1.13	0.43	2.60	1.10	0.48	0.05	0.01	170
52-67	2bc2	31.0	7.8	3.43	1.17	0.49	2.48	1.10	0.44	0.06	0.02	159
DM6												
0-4	A	34.6	6.5	1.99	1.20	0.36	2.76	1.20	0.44	0.03	0.02	245
4-10	AB	35.8	6.1	1.50	1.17	0.24	2.90	1.05	0.41	0.02	0.01	306
10-31	Btk1	33.8	6.6	2.10	1.30	0.38	2.89	1.15	0.31	0.02	0.01	133
31-52	2Bw1	33.6	6.6	2.33	1.05	0.38	2.76	1.14	0.34	0.02	0.01	165
52-76	Btk2	33.7	6.3	2.26	1.61	0.43	2.78	1.11	0.37	0.03	0.01	200
76-87	3Bw3	32.2	6.7	2.89	1.15	0.61	2.65	1.13	0.46	0.05	0.01	157
87-97	C											
DL1												
0-23	BA	32.6	7.7	1.74	0.84	0.23	2.67	2.29	0.35	0.03	0.03	186
23-45	BC	32.7	7.9	2.09	0.95	0.33	2.50	2.10	0.30	0.02	0.02	126
45-55	C											
DL2												
0-6	ba	33.5	7.1	1.35	0.99	0.27	2.90	1.63	0.34	0.04	0.04	156
6-22	bw1	34.2	7.2	1.38	1.03	0.25	2.88	1.51	0.29	0.03	0.03	141
22-35	2bc1	34.5	7.3	1.31	0.97	0.24	2.96	1.53	0.27	0.02	0.03	146
35-50	2bc2	34.2	7.3	1.27	0.92	0.24	2.93	1.53	0.27	0.02	0.03	135
DL3												
0-2	A	33.0	6.8	2.76	1.19	0.40	2.61	1.42	0.55	0.04	0.03	225
2-19	Bw1	33.3	6.7	2.62	1.23	0.39	2.61	1.36	0.59	0.04	0.04	276
19-34	Bw2	33.1	6.9	2.77	1.12	0.39	2.68	1.44	0.56	0.03	0.02	204
34-42	BC	32.4	7.3	2.94	0.99	0.43	2.45	1.44	0.44	0.02	0.03	190
42-52	C	35.5	7.7	0.44	0.94	0.00	4.19	0.82	0.01	<0.01	0.01	19
DL4												
0-1	ab	36.1	5.8	1.20	1.03	0.34	2.79	1.05	0.24	0.02	0.02	139
1-9	bw1	36.3	5.8	1.07	0.94	0.30	2.73	1.00	0.17	0.02	0.02	95
9-24	bw2	36.1	6.0	1.14	0.96	0.31	2.64	1.14	0.27	0.02	0.01	131
21-40	bw3	36.5	5.8	1.02	1.00	0.34	2.83	1.11	0.29	0.02	0.02	161
40-55	bw4	36.5	6.1	0.97	1.05	0.39	2.89	1.20	0.32	0.02	0.01	158
55-67	2bc1	36.3	6.1	0.97	0.99	0.31	2.89	1.20	0.32	0.02	0.01	167
67-75	2bc2	35.0	6.7	1.31	0.77	0.30	2.79	1.51	0.38	0.02	0.02	141
DL5												
0-4	ab	35.8	5.5	1.76	1.01	0.33	2.33	0.95	0.43	0.04	0.03	160
4-13	bw1	35.6	5.6	1.86	1.01	0.34	2.38	1.00	0.49	0.05	0.03	182
13-30	bw2	35.7	5.5	1.90	0.97	0.31	2.32	1.01	0.49	0.05	0.03	173

Depth/ site	Horizon	Si	Al	Fe	Ca	Mg	Na	K	Ti	Mn	P	Zr
												(ppm)
30-51	bw3	35.5	5.7	2.07	0.98	0.36	2.28	1.06	0.55	0.05	0.03	189
51-76	bw4	35.7	5.8	2.10	0.97	0.36	2.34	1.06	0.53	0.05	0.03	202
76-112	2bw5	35.4	5.9	2.13	0.94	0.36	2.35	1.06	0.55	0.04	0.02	184
112-120	2bw6	32.9	6.5	3.01	0.84	0.47	1.85	1.09	0.44	0.04	0.02	143
DL6												
0-1	ab	32.9	6.6	2.83	1.34	0.52	2.61	1.03	0.59	0.07	0.05	179
1-4	bw1	32.2	6.8	3.11	1.29	0.54	2.43	1.08	0.58	0.08	0.06	174
4-20	2bt2	30.9	7.1	3.77	1.26	0.57	2.21	1.11	0.61	0.09	0.07	186
20-59	2bt3	28.1	8.1	5.17	1.07	0.77	1.73	1.19	0.65	0.09	0.04	165
59-95	2bt4	26.8	8.1	5.42	1.71	0.87	1.70	1.16	0.70	0.11	0.04	182
95-110	3bw5	26.1	8.0	5.42	2.03	0.95	1.67	1.14	0.73	0.11	0.03	183
110-120	3bw6	26.4	8.1	5.44	1.90	0.94	1.66	1.10	0.71	0.11	0.04	189
DL7												
0-0.1	BA	31.6	6.9	3.68	1.24	0.58	2.41	0.95	0.73	0.06	0.03	288
0.1-11	Btk1	29.0	7.2	4.05	1.66	0.69	2.54	0.96	0.55	0.06	0.03	173
11-40	Btk2	28.9	7.4	4.47	1.42	0.76	2.54	0.98	0.58	0.07	0.03	175
40-68	2Bw1	29.6	7.5	4.48	1.32	0.70	2.49	0.98	0.61	0.07	0.02	192
68-95	2Bw2	30.2	7.4	4.31	1.13	0.64	2.60	0.94	0.61	0.07	0.02	190
sb6c												
0-10	BA	35.6	6.6	0.91	0.68	0.04	2.32	2.59	0.14	0.02	0.01	340
10-23	Bw1	35.5	6.8	1.08	0.65	0.05	2.23	2.66	0.20	0.01	<0.01	362
23-50	BC	34.5	7.1	1.46	0.57	0.13	2.31	2.51	0.17	0.01	0.01	297
50-60	CR											
sb6bc												
0-10	BA	34.9	6.6	1.04	0.59	0.11	2.05	3.13	0.14	0.02	0.02	206
10-20	Bw1	34.7	6.8	1.11	0.59	0.17	2.13	3.25	0.17	0.02	0.01	233
20-30	Bw2	34.7	6.9	1.13	0.56	0.17	2.09	3.11	0.17	0.02	0.02	229
30-47	Bc	34.7	7.0	1.15	0.51	0.14	2.00	3.35	0.20	0.02	0.01	215
sb6b												
0-7	AB	36.4	6.0	0.70	0.39	0.01	2.05	3.18	0.11	<0.01	<0.01	209
7-26	Bw1	36.6	6.2	0.62	0.40	0.01	2.07	3.20	0.10	<0.01	0.01	227
26-40	Bw2	36.3	6.1	0.66	0.40	0.04	2.13	3.09	0.10	<0.01	<0.01	250
40-60	Bw3	36.7	6.3	0.55	0.41	0.02	2.31	3.27	0.11	<0.01	<0.01	268
60-80	BC	36.0	6.5	0.96	0.45	0.04	2.20	3.11	0.18	0.02	<0.01	275
80-90												
sb6ab												
0-9	AB	34.1	6.8	1.20	0.65	0.17	2.31	2.95	0.19	0.02	0.02	307
9-20	BA	34.6	6.6	1.24	0.59	0.14	2.14	2.95	0.17	0.02	0.01	264
20-50	Bt1	29.2	8.7	2.69	0.47	0.33	1.30	2.16	0.28	0.02	0.02	174
50-62	Bt2	30.4	8.2	2.46	0.55	0.37	1.61	2.32	0.24	0.02	0.01	191

Depth/ site	Horizon	Si	Al	Fe	Ca	Mg	Na	K	Ti	Mn	P	Zr (ppm)
62-70 sb6a	2BC	30.4	8.2	2.90	0.62	0.34	1.28	2.55	0.23	0.02	0.02	150
0-10	BA	30.8	7.8	2.46	0.97	0.46	1.89	2.57	0.25	0.05	0.02	332
10-31	Bt1	30.6	7.7	2.50	0.94	0.39	1.65	2.41	0.24	0.05	0.02	248
31-49	Bt2	30.6	7.9	2.79	0.95	0.48	1.65	2.33	0.26	0.05	0.02	221
49-83	Bt3	29.6	8.2	2.90	1.03	0.49	1.62	2.27	0.28	0.05	0.02	222
83-93 sb4e	BCR											
0-7	BA	35.9	6.6	0.66	0.48	0.04	2.07	3.65	0.15	0.02	<0.01	274
7-33	Bw1	35.2	6.8	0.72	0.45	0.04	2.04	3.60	0.18	0.02	<0.01	313
33-65 65-75 sb4ed1	CR/BC RC	35.0	7.3	0.91	0.46	0.08	2.00	3.37	0.18	0.01	<0.01	283
0-5	A	34.2	7.1	2.25	0.34	0.42	0.82	2.17	0.28	0.04	0.01	257
5-17		31.7	7.8	2.63	0.99	0.53	0.83	2.01	0.30	0.06	0.02	277
17-42		33.8	7.2	1.46	0.85	0.23	2.12	2.66	0.29	0.04	0.02	512
42-56		33.6	7.4	1.60	0.74	0.24	1.96	2.59	0.27	0.04	0.01	428
56-70 70-80 sb4ed2		31.7	7.9	2.03	0.75	0.32	1.97	2.42	0.31	0.05	0.01	447
0-16	AB	33.1	8.1	2.01	0.85	0.36	2.00	2.63	0.31	0.05	0.01	391
16-42	Bw1	33.2	7.1	1.19	0.57	0.25	1.87	4.10	0.14	0.03	0.01	128
42-70	Bw2	36.7	5.9	0.55	0.59	0.07	1.87	2.73	0.14	0.02	0.01	221
70-120	2BC1	38.3	6.0	0.55	0.53	0.07	1.83	2.95	0.14	0.01	0.01	430
120-151	2BC2	37.3	5.7	0.50	0.52	0.07	1.83	2.79	0.13	0.01	0.01	189
151-175 sb4ed3	2BC3	38.0	5.9	0.52	0.59	0.08	2.00	2.87	0.13	0.01	0.01	252
0-7	BA	35.4	6.7	1.20	0.79	0.29	2.65	2.62	0.17	0.02	<0.01	196
7-26	Bw/Bt	36.2	6.6	0.95	0.90	0.21	2.55	2.31	0.18	0.01	0.01	207
26-30 sb4d	C											
0-13	BA	37.2	1.1	0.65	0.42	0.06	1.82	2.64	0.15	0.01	0.01	235
13-25	Bt1	34.3	1.3	1.83	0.29	0.22	1.30	2.14	0.20	0.01	0.01	162
25-40	BtC	31.6	1.8	2.46	0.43	0.33	1.32	2.13	0.28	0.02	0.01	143
40-65 65-75 sb4c	CR	32.5	2.9	1.90	0.85	0.39	2.55	2.61	0.21	0.01	0.00	114
0-9	BA	35.9	5.6	1.52	0.49	0.11	1.51	2.22	0.20	0.02	0.01	321
9-25	Bt1	33.9	7.1	1.89	0.41	0.22	1.30	2.13	0.23	0.01	0.01	251
25-62	Bt2	31.9	7.5	2.33	0.54	0.27	1.22	1.84	0.25	0.02	0.01	189

Depth/ site	Horizon	Si	Al	Fe	Ca	Mg	Na	K	Ti	Mn	P	Zr
												(ppm)
62-90	2Bt3	32.7	7.2	2.11	1.47	0.39	1.31	2.08	0.27	0.04	0.01	257
90-100	CR	30.5	7.3	2.20	1.65	0.41	1.23	1.95	0.27	0.05	0.01	264
100-110	R											
sb4bc												
0-4	A	34.6	6.8	1.09	0.76	0.15	2.00	2.48	0.23	0.02	0.01	342
4-10	BA1	35.4	6.6	0.93	0.83	0.12	2.13	2.64	0.23	0.03	0.01	365
10-22	BA2	37.0	4.6	1.08	0.27	0.12	0.92	2.31	0.25	0.04	0.01	368
22-40	2Bw1	37.4	4.8	1.21	0.26	0.14	0.92	2.35	0.26	0.05	0.01	342
40-63	2Bw2	35.1	5.7	1.56	0.30	0.18	0.93	2.40	0.30	0.04	0.02	355
63-70	2Bw3	35.5	5.3	1.41	0.23	0.17	0.89	2.23	0.24	0.03	0.01	426
70-77	2Bw4	33.9	6.7	2.08	0.31	0.33	0.86	2.15	0.27	0.04	0.01	267
77-87	2Bw5	33.1	6.5	2.00	0.30	0.35	0.82	2.06	0.26	0.04	0.01	281
sb4b												
0-7	BA	37.2	5.1	0.77	0.48	0.09	1.60	2.51	0.20	0.03	0.02	322
7-25	Bt1	34.8	6.2	1.54	0.34	0.34	1.42	2.22	0.22	0.03	0.01	238
25-46	Bt2	32.9	7.1	1.98	0.40	0.50	1.36	2.03	0.23	0.03	0.01	222
46-62	Bt3	33.0	7.0	1.94	0.42	0.51	1.39	1.99	0.25	0.04	<0.01	264
62-90	BC	32.8	6.8	1.91	0.78	0.55	1.43	2.09	0.25	0.04	0.01	283
sb3f												
1-3	A	34.9	7.0	1.33	1.08	0.05	2.73	1.80	0.25	0.02	0.01	209
3-11	BC	34.0	7.7	1.33	1.17	0.09	2.97	1.76	0.34	0.02	0.02	268
11-30	CR											
sb3fe												
0-10	BA	35.0	6.8	1.08	0.99	0.07	2.58	2.01	0.23	0.02	0.01	231
10-39	Bw1	35.5	6.7	1.06	0.97	0.08	2.48	2.03	0.25	0.02	0.01	228
39-60	2Bw2, e	36.0	6.4	0.95	0.85	0.06	2.27	2.07	0.17	0.02	0.01	198
60-80	2Bc	35.1	6.9	1.36	0.84	0.06	2.28	1.97	0.20	0.02	0.01	191
sb3e												
0-2	A	34.8	7.2	1.33	1.09	0.07	2.74	1.91	0.24	0.02	0.01	225
2-25	Bw1	34.5	7.4	1.11	1.12	0.06	2.93	1.94	0.24	0.02	0.00	218
25-47	Bw2	34.6	7.3	1.40	1.08	0.08	2.78	1.91	0.33	0.02	0.01	241
47-70	BC	33.9	7.6	1.34	1.02	0.13	2.56	1.89	0.26	0.01	0.01	194
sb3de												
0-12	BA	36.0	6.4	0.83	0.92	0.07	2.51	1.99	0.25	0.02	<0.01	165
12-48	Bw1	36.1	6.2	0.80	0.87	0.07	2.43	1.91	0.22	0.01	0.01	149
48-70	Bw2	36.2	6.3	1.28	0.89	0.04	2.48	1.93	0.21	0.01	0.01	146
70-85	Bw3	36.3	6.4	0.76	0.93	0.07	2.52	2.03	0.20	0.02	0.01	153
85-100	CB	36.9	6.2	0.73	0.92	0.03	2.54	1.94	0.22	0.02	0.01	160
sb3de1												

Depth/ site	Horizon	Si	Al	Fe	Ca	Mg	Na	K	Ti	Mn	P	Zr
												(ppm)
0-11	BA	35.5	6.9	0.71	1.09	0.05	2.92	1.95	0.25	0.02	0.01	227
11-27	Bw1	35.6	7.0	0.71	1.07	0.05	2.85	2.02	0.26	0.02	0.01	247
27-53	2Bc	35.8	6.9	0.56	1.08	0.05	2.96	2.09	0.22	0.01	0.01	198
53-70	2Cr	36.2	6.8	0.54	1.02	0.03	3.04	2.13	0.15	0.02	<0.01	142
sb3d												
0-1	A	35.5	6.4	1.03	1.00	0.10	2.44	1.83	0.28	0.01	0.01	186
1-24	Bw1	35.5	6.5	1.37	0.98	0.08	2.46	1.89	0.23	0.01	0.01	180
24-57	BC	32.0	7.4	2.28	0.75	0.30	1.68	1.78	0.28	0.01	0.01	124
57-67	C											
sb3c												
0-1	A	33.1	6.5	2.25	0.96	0.15	2.17	1.61	0.53	0.05	0.02	251
1-16	Bw1	32.4	7.0	2.97	0.95	0.20	2.05	1.64	0.73	0.05	0.02	286
16-30	Bw2	31.9	7.2	3.04	0.87	0.23	2.00	1.59	0.71	0.05	0.02	259
30-63	Bw3	31.4	7.8	3.41	0.78	0.27	1.77	1.53	0.66	0.05	0.02	229
63-110	BC	30.0	8.2	3.88	0.84	0.34	1.67	1.56	0.68	0.05	0.02	236
110-120	CR											
sb3cb												
0-13	BA	33.9	6.7	1.97	0.71	0.11	2.05	1.86	0.59	0.04	0.02	306
13-53	Bt1	31.7	7.8	2.74	0.66	0.22	1.60	1.67	0.56	0.03	0.01	240
53-70	Bt2	30.0	8.0	3.11	0.81	0.29	1.53	1.64	0.63	0.05	0.02	265
70-85	2Bw3	30.2	7.9	3.11	1.01	0.34	1.60	1.57	0.62	0.05	0.02	256
85-100	2Bc	29.0	8.6	3.44	0.90	0.33	1.43	1.68	0.55	0.07	0.02	191
sb3b												
0-3	BA	35.0	5.8	1.70	0.73	0.12	1.84	1.93	0.32	0.03	0.03	330
3-17	Bt1	34.6	6.4	2.08	0.69	0.16	1.87	1.93	0.38	0.03	0.02	320
17-35	2Bt2	31.1	7.7	3.00	0.70	0.37	1.39	1.73	0.46	0.03	0.02	278
35-57	3Btk1	31.6	7.3	2.85	1.08	0.39	1.54	1.78	0.44	0.04	0.01	299
57-80	3Btk2	30.4	7.3	2.78	1.15	0.46	1.57	1.65	0.46	0.05	0.02	319
80-110	3Btk3	29.8	7.7	3.25	1.54	0.52	1.60	1.64	0.52	0.07	0.02	325
110-130	BC	29.6	7.4	2.94	2.33	0.52	1.62	1.66	0.49	0.06	0.01	295
sb3a												
0-7	AB	29.6	7.5	3.95	0.95	0.52	1.47	2.10	0.50	0.10	0.03	678
7-34	Bt1	33.8	6.9	2.04	0.67	0.21	1.66	2.11	0.47	0.03	0.01	607
34-60	2Bt2	32.4	7.3	2.64	0.60	0.28	1.43	1.87	0.41	0.02	0.02	448
60-85	3Bt3	32.5	7.0	2.59	0.72	0.35	1.54	1.90	0.46	0.04	0.01	513
85-111	3Bt4	31.0	7.2	2.70	1.28	0.52	1.50	1.88	0.51	0.05	0.02	496
111-120	4BC	31.5	7.2	2.79	1.12	0.47	1.56	2.03	0.47	0.05	0.02	462
pkop2c												
0-4	AB	38.9	3.1	1.52	0.26	0.00	0.50	1.91	0.43	0.05	0.01	610
4-30	Bw1	40.7	3.0	1.41	0.17	0.00	0.50	1.83	0.40	0.04	0.01	507

Depth/ site	Horizon	Si	Al	Fe	Ca	Mg	Na	K	Ti	Mn	P	Zr
												(ppm)
30-76	Bw2	39.1	3.8	1.43	0.15	0.01	0.42	1.84	0.41	0.03	0.01	587
76-105	Bw3	37.5	4.6	1.65	0.15	0.02	0.38	1.92	0.43	0.03	0.01	696
105-125	Bw4	38.0	4.6	1.48	0.14	0.05	0.42	2.01	0.44	0.03	0.01	749
125-146	Bw5	38.5	4.1	1.38	0.14	0.01	0.45	2.06	0.45	0.04	0.01	786
146-180	2Bw6	37.9	4.5	1.38	0.14	0.01	0.48	2.66	0.46	0.05	0.01	905
180-212	C	36.1	6.1	1.43	0.21	0.08	0.62	3.10	0.39	0.04	<0.01	605
pkop2bc2												
0-13	Ba	40.8	3.1	0.71	0.30	0.01	0.82	1.74	0.40	0.03	0.01	439
13-29	Bw1	40.9	3.1	0.64	0.29	0.01	0.84	1.74	0.34	0.02	0.01	399
29-49	Bw2	40.0	3.7	0.80	0.34	0.00	1.08	2.13	0.40	0.03	0.01	583
49-87	Bw3	40.0	3.6	0.75	0.31	0.01	0.88	2.10	0.41	0.02	<0.01	628
87-124	Bw4	39.9	3.6	0.86	0.30	0.02	0.82	2.09	0.40	0.02	<0.01	620
124-130	BC	38.4	3.8	1.99	0.27	0.00	0.76	2.15	0.45	0.22	<0.01	617
pkop2bc1												
0-17	AB	39.7	3.6	1.11	0.35	0.02	0.94	1.78	0.41	0.05	0.01	482
17-58	Bw1	39.6	3.7	1.07	0.30	0.01	0.91	1.79	0.43	0.05	0.01	485
58-88	Bw2	39.7	3.9	1.13	0.31	0.03	0.91	1.88	0.40	0.04	0.01	532
88-112	Bw3	39.2	3.9	1.05	0.31	0.01	0.88	1.88	0.40	0.04	0.00	609
112-128	Bw4	39.7	3.9	1.01	0.33	0.01	1.04	1.98	0.41	0.03	0.01	645
128-140	2BC	39.3	4.1	1.20	0.32	0.02	0.98	2.03	0.41	0.07	0.01	712
pkop2b												
0-5	AB	36.5	5.3	0.87	0.85	0.02	1.67	2.24	0.37	0.03	0.01	517
5-24	Bw1	36.4	6.0	1.11	0.74	0.04	1.74	2.50	0.52	0.03	0.01	702
24-47	Bw2	36.3	6.1	1.03	0.76	0.04	1.81	2.44	0.55	0.03	<0.01	697
47-67	Bw3	35.6	6.7	1.22	0.87	0.04	2.08	2.41	0.61	0.04	<0.01	894
67-89	2Bw4	36.1	6.3	1.06	0.86	0.04	1.98	2.27	0.58	0.03	0.01	778
89-115	3Bw5	35.3	6.7	1.64	1.02	0.14	2.28	1.95	0.50	0.03	0.01	757
115-150	3Bw6	33.1	7.5	2.60	1.28	0.34	2.67	1.80	0.52	0.04	0.02	665
150-160	R	30.7	9.4	2.54	1.71	0.46	3.57	2.34	0.31	0.04	0.08	292
pkop2ab												
0-13	Ab	35.7	6.3	0.93	0.83	0.04	2.11	2.02	0.35	0.02	0.01	406
13-28	Bw1	36.1	6.4	0.76	0.87	0.05	2.14	2.09	0.35	0.02	0.01	485
28-42	Bw2	35.6	6.8	0.78	0.99	0.06	2.35	1.99	0.37	0.02	0.01	438
42-55	Bw3	35.2	7.0	0.84	1.04	0.04	2.58	1.96	0.40	0.03	0.01	455
55-76	Bw4	35.3	6.9	1.15	0.99	0.08	2.34	1.93	0.44	0.03	0.01	508
76-94	Bw5	31.0	8.6	3.60	1.32	0.29	3.16	1.48	0.37	0.02	0.02	292
94-115	2BC	30.3	8.9	3.46	1.37	0.46	3.48	1.39	0.40	0.03	0.02	284
115-125	2BCR	31.3	8.8	2.86	1.37	0.44	3.38	1.42	0.36	0.03	0.02	253
pkop2a												
0-10	BA	31.9	7.5	2.24	0.74	0.10	1.57	1.60	0.58	0.02	0.01	534

Depth/ site	Horizon	Si	Al	Fe	Ca	Mg	Na	K	Ti	Mn	P	Zr
												(ppm)
10-29	Bt1	22.9	11.9	5.97	0.43	0.28	0.60	0.86	0.57	0.02	0.01	182
29-50	Bt2	23.2	12.2	5.62	0.43	0.34	0.54	0.80	0.53	0.02	0.01	163
50-80	Bt3	23.7	10.8	6.71	0.61	0.37	0.70	0.87	0.67	0.06	0.01	201
80-106	2Bt4	23.4	12.1	5.63	0.59	0.37	0.91	0.79	0.54	0.02	0.01	195
106-116	2BtC	25.7	11.4	4.23	0.99	0.27	2.10	0.81	0.40	0.02	0.01	234
pkop4h2												
0-10	BA	37.6	4.3	1.42	0.12	0.02	0.47	3.42	0.34	0.04	0.02	531
10-23	Bw1	38.4	4.3	1.34	0.11	0.01	0.47	3.44	0.35	0.04	0.01	540
23-49	Bw2	38.2	4.3	1.41	0.10	0.02	0.55	3.49	0.37	0.04	0.01	489
49-106	Bw3	37.9	4.4	1.39	0.08	0.05	0.31	3.03	0.31	0.03	0.02	454
106-135	2Bw4	38.1	4.8	1.46	0.09	0.05	0.47	3.17	0.35	0.03	0.01	534
135-157	2Bw5	38.0	4.8	1.28	0.09	0.04	0.45	3.40	0.38	0.03	0.02	568
157-170	3BC	36.7	5.7	1.37	0.09	0.04	0.45	3.62	0.34	0.03	<0.01	507
pkop4h1												
0-15	BA	39.0	3.9	1.43	0.07	0.00	0.41	3.29	0.31	0.04	0.01	459
15-30	Bw1	38.5	4.3	1.39	0.06	0.02	0.32	3.20	0.32	0.03	0.01	504
30-59	Bw2	37.7	4.7	1.41	0.06	0.01	0.36	3.13	0.32	0.03	0.01	532
59-87	Bw3	38.0	4.7	1.33	0.05	0.03	0.40	3.02	0.32	0.03	0.02	509
87-106	Bw4	38.4	4.4	1.22	0.05	0.01	0.39	3.05	0.34	0.03	0.01	522
106-131	Bw5	37.9	4.6	1.22	0.07	0.02	0.37	3.34	0.37	0.04	0.01	605
131-140	BC	37.3	5.2	1.30	0.06	0.02	0.40	3.73	0.39	0.04	0.01	722
pkop4gh2												
0-17	BA	39.2	3.6	1.67	0.09	0.01	0.38	3.07	0.31	0.03	0.01	358
17-36	Bw1	37.6	4.1	2.85	0.07	0.01	0.33	3.16	0.47	0.04	0.01	455
36-71	Bw2	38.2	4.6	1.48	0.06	0.01	0.29	2.95	0.28	0.02	0.01	420
71-86	Bw3	38.0	4.8	1.38	0.04	0.01	0.39	3.02	0.29	0.03	0.01	430
86-115	Bw4	38.4	4.6	1.27	0.06	0.02	0.39	3.09	0.30	0.02	0.01	485
115-141	2Bc1	36.7	5.5	1.31	0.05	0.02	0.31	3.52	0.30	0.03	0.01	443
141-149	2BC2	36.4	6.1	1.20	0.06	0.05	0.40	4.01	0.25	0.03	0.01	358
pkop4gh1												
0-10	BA	40.6	3.0	0.94	0.11	0.01	0.33	2.30	0.31	0.05	0.01	438
10-31	Bw1	39.9	3.2	1.00	0.10	0.02	0.35	2.42	0.34	0.03	0.01	463
31-57	Bw2	40.1	3.4	0.99	0.08	0.00	0.31	2.03	0.29	0.03	0.02	428
57-93	Bw3	39.7	3.7	1.07	0.09	0.02	0.32	2.08	0.29	0.03	0.01	440
93-131	Bw4	40.1	3.5	0.91	0.09	0.01	0.39	2.18	0.35	0.03	0.01	522
131-145	2BC	38.0	4.8	1.22	0.08	0.04	0.31	2.81	0.38	0.04	0.02	585
pkop4g												
0-12	BA	41.7	2.3	0.56	0.08	0.00	0.47	1.81	0.20	0.02	0.01	272
12-50	Bw1	41.7	2.6	0.59	0.08	0.00	0.44	1.91	0.23	0.02	0.01	327
50-96	Bw2	41.7	2.6	0.61	0.06	0.01	0.46	1.91	0.23	0.02	0.01	366

Depth/ site	Horizon	Si	Al	Fe	Ca	Mg	Na	K	Ti	Mn	P	Zr
												(ppm)
96-128	Bw3	42.3	2.4	0.58	0.06	0.00	0.37	1.83	0.21	0.02	<0.01	379
128-152	Bw4	42.3	2.2	0.49	0.06	0.00	0.36	1.76	0.23	0.02	0.01	376
152-185	2BC1	41.8	2.5	0.59	0.06	0.00	0.41	1.92	0.22	0.02	<0.01	449
185-200	2BC2	41.2	2.8	0.77	0.06	0.01	0.36	2.15	0.28	0.04	<0.01	527
pkop4f												
0-10	BA	37.8	5.7	0.64	0.21	0.00	0.54	1.77	0.24	0.03	0.02	326
10-23	Bw1	40.7	2.9	0.72	0.18	0.02	0.57	2.00	0.26	0.03	0.01	322
23-53	Bw2	41.0	2.9	0.73	0.17	0.00	0.62	1.96	0.26	0.02	0.01	342
53-90	Bw3	41.2	2.9	0.69	0.15	0.00	0.49	1.90	0.24	0.02	0.01	372
90-129	Bw4	41.4	2.7	0.62	0.14	0.00	0.56	1.92	0.25	0.02	<0.01	436
129-164	2BC1	40.9	3.0	0.68	0.12	0.00	0.46	2.23	0.23	0.02	0.01	396
164-180	2BC2	39.9	3.8	0.82	0.12	0.00	0.51	2.69	0.30	0.02	0.01	593
pkop4e												
0-11	BA	41.0	2.9	0.62	0.19	0.00	0.56	1.96	0.24	0.02	<0.01	306
11-29	Bw1	40.9	3.1	0.69	0.18	0.01	0.64	2.04	0.27	0.02	0.01	326
29-61	Bw2	40.2	3.4	0.70	0.20	0.00	0.62	2.14	0.29	0.02	0.01	401
61-107	Bw3	40.0	3.6	0.81	0.20	0.00	0.59	2.19	0.31	0.02	<0.01	462
107-152	Bw4	40.2	3.7	0.77	0.21	0.01	0.64	2.21	0.36	0.02	0.01	538
152-165	2BC1	40.7	3.3	0.74	0.18	0.01	0.63	2.11	0.28	0.02	0.01	505
165-190	2BC2	39.4	4.2	0.85	0.19	0.03	0.57	2.57	0.32	0.02	0.02	574
190-210	2BC3	38.2	4.8	1.06	0.21	0.07	0.68	2.96	0.30	0.02	0.01	507
pkop4d												
0-9	BA	39.3	3.9	0.66	0.27	0.01	0.93	2.50	0.31	0.02	0.01	443
9-22	Bw1	40.0	3.7	0.59	0.26	0.00	0.91	2.36	0.28	0.02	0.01	431
22-48	Bw2	39.8	4.1	0.61	0.26	0.00	1.02	2.65	0.30	0.02	<0.01	564
48-62	2Bw3	39.6	4.1	0.60	0.23	0.00	0.98	2.71	0.28	0.02	<0.01	510
62-82	3Bw4	39.6	3.9	0.81	0.19	0.00	0.84	2.93	0.25	0.02	0.01	446
82-105	3BC1	37.9	5.0	1.34	0.17	0.04	0.80	3.23	0.29	0.02	0.01	432
105-115	3BC2	35.6	6.6	1.49	0.19	0.07	1.14	3.27	0.36	0.05	0.01	548
pkop4c												
0-8	BA	36.5	5.1	1.56	0.25	0.04	0.92	2.70	0.35	0.02	0.01	591
8-20	Bw1	36.9	5.4	1.50	0.33	0.08	0.90	2.20	0.26	0.02	0.02	327
20-40	2Bw2, e	41.2	2.5	1.06	0.11	0.00	0.39	1.43	0.13	0.02	0.01	122
40-80	3Bt1	26.3	12.2	3.65	0.16	0.21	0.42	1.63	0.34	0.01	0.02	138
80-101	3Bt2	28.6	10.6	3.30	0.22	0.15	0.91	2.79	0.29	0.01	0.01	103
101-113	4BC1	30.0	9.7	3.32	0.28	0.19	1.05	2.33	0.28	0.01	<0.01	119
113-120	4BC2	31.8	9.2	1.88	0.45	0.10	2.15	3.04	0.16	0.01	0.01	70
pkop4b												
0-9	BA	35.3	6.1	1.68	0.59	0.09	1.49	1.70	0.37	0.02	0.01	463

Depth/ site	Horizon	Si	Al	Fe	Ca	Mg	Na	K	Ti	Mn	P	Zr (ppm)
9-33	Bt1	32.0	8.0	2.36	0.53	0.17	1.45	1.46	0.35	0.03	0.02	369
33-68	Bt2	32.5	8.0	2.22	0.57	0.25	1.45	1.36	0.34	0.02	0.01	334
68-80	2BC	29.9	9.3	3.25	1.63	0.48	2.97	1.22	0.38	0.05	0.07	271
pkop4a												
0-10	AB	34.2	7.1	1.25	0.99	0.06	2.80	1.98	0.40	0.04	0.01	482
10-40	Bw1	34.0	7.4	1.36	0.97	0.07	2.80	1.98	0.38	0.03	0.01	541
40-70	Bw2	34.2	7.6	1.41	0.99	0.05	2.82	2.13	0.44	0.03	0.01	654
70-95	2Bt1	30.0	8.9	2.93	0.80	0.32	1.94	1.79	0.44	0.03	0.01	479
95-120	2Bt2	30.4	8.7	2.82	0.85	0.32	2.14	1.86	0.48	0.04	0.02	534
120-135	3BC	29.2	8.8	3.52	0.77	0.37	1.96	2.27	0.42	0.46	0.02	429
pkop1a												
0-8		39.3	2.8	0.8	0.3	0.02	0.4	1.9	0.21	0.02	0.02	414
8-17		40.4	2.7	0.9	0.2	0.02	0.4	2	0.25	0.02	0.01	443
17-39		39.8	3.1	1.1	0.2	0.01	0.5	2.1	0.29	0.02	0.01	520
39-70		40.1	3.1	1.1	0.2	0.01	0.5	2.1	0.26	0.01	<0.01	509
70-93		40.3	2.9	1.0	0.2	0.01	0.7	2	0.24	0.01	0.01	475
93-115		38.3	4.3	1.2	0.1	0.03	0.4	2.3	0.25	0.01	<0.01	451
115-142		38.7	4.1	1.2	0.2	0.04	0.5	2.2	0.25	0.01	0.01	450
142-164		37.9	4.7	1.3	0.2	0.05	0.7	2.2	0.28	0.02	0.01	517
164-184		35.1	6.3	1.7	0.3	0.13	1.1	2.3	0.33	0.02	0.01	523
184-205		33.8	7.3	2.0	0.4	0.16	1.8	2.2	0.33	0.02	0.01	430
205-230		32.4	7.9	2.7	0.9	0.35	2.4	1.4	0.35	0.02	0.01	261
230-245		31.8	8.3	2.7	1	0.41	2.7	1.2	0.35	0.02	0.01	248
pkop1b												
0-12		40.7	2.4	0.6	0.1	0.01	0.3	1.9	0.17	0.02	0.01	288
12-24		40.8	2.6	0.5	0.1	0.01	0.4	2.1	0.18	0.01	0.01	318
24-39		41.7	2.2	0.5	0.1	<0.01	0.3	1.8	0.16	<0.01	0.01	304
39-71		40.9	2.7	0.6	0.1	0.01	0.4	2.2	0.2	<0.01	0.01	373
71-94		41.2	2.6	0.5	0.1	<0.01	0.5	2.1	0.2	<0.01	0.01	387
94-119		41.2	2.7	0.6	0.1	<0.01	0.3	2.1	0.2	<0.01	<0.01	387
94-150		40.0	3.3	0.6	0.1	0.03	0.4	2.5	0.28	<0.01	<0.01	557
150-172		38.9	3.9	0.8	0.1	<0.01	0.5	3.0	0.37	0.01	<0.01	749
172-198		38.2	4.8	0.7	0.1	<0.01	0.6	3.2	0.35	<0.01	<0.01	758
pkop1c												
0-5	A	38.1	4.6	0.7	0.3	0.01	0.9	3.1	0.2	0.02	0.01	447
5-17	Bw1	38.6	4.5	0.6	0.2	0.01	0.8	3	0.19	0.01	<0.01	413
17-26	Bw2	38.6	4.7	0.5	0.2	<0.01	0.8	3	0.17	0.01	0.01	439
26-45	Bw3	38.9	4.1	0.8	0.2	0.02	0.9	2.9	0.22	<0.01	0.01	433
45-60	Bw4	38.1	4.4	0.8	0.2	0.01	0.9	3	0.22	0.01	0.01	482
60-77	2BC1	38.1	4.5	0.7	0.2	0.02	0.8	3.2	0.19	<0.01	<0.01	415

Depth/ site	Horizon	Si	Al	Fe	Ca	Mg	Na	K	Ti	Mn	P	Zr (ppm)
						%						
77-98	2BC2	37.7	5.0	0.9	0.2	0.02	0.9	3.3	0.17	<0.01	<0.01	362
98-132	2Cr1	34.0	7.3	1.6	0.6	0.15	1.9	2.3	0.23	<0.01	<0.01	217
132-155	2Cr2	33.3	7.5	1.7	0.7	0.18	1.9	2.2	0.25	0.01	<0.01	205
155-165	2Cr3	33.9	7.7	1.5	0.6	0.13	2.0	2.4	0.22	0.01	0.01	151
pkop1d												
0-9	BA	36.0	5.4	0.9	0.3	0.02	1.9	2.4	0.22	0.02	0.01	524
9-24	Bw1	37.2	5.4	0.8	0.3	0.02	1.9	2.4	0.23	0.01	0.01	486
24-41	2Bw2	38.6	4.4	0.8	0.2	<0.01	1.5	2.3	0.16	<0.01	<0.01	301
41-75	3Bt1	33.1	7.3	2.0	0.3	0.16	1.3	2.1	0.23	<0.01	0.01	292
75-110	3Bt2	31.1	8.7	2.2	0.5	0.28	1.9	2.3	0.28	0.02	0.01	243
110-120	CR	23.9	5.5	0.6	11	0.47	1.8	2.4	0.08	<0.01	<0.01	68
pkople												
0-14	BA	36.3	5.3	1.3	0.3	0.06	1.7	2.2	0.31	0.02	<0.01	562
14-40	BC1	35.9	5.8	1.4	0.4	0.11	1.8	2.3	0.31	0.02	0.01	531
40-60	BC2	28.9	9.6	2.9	0.3	0.31	1.7	2.5	0.28	0.02	0.01	221
60-70	R	34.6	7.3	0.5	0.1	0.04	1.6	6.5	0.05	0.02	<0.01	14
pkop1f												
0-11	BA	37.5	4.0	1.4	0.3	0.08	1	1.7	0.32	0.02	0.01	488
11-40	Bt1	35.0	5.7	2.1	0.3	0.22	0.8	1.5	0.25	0.02	<0.01	284
40-63	Bt2	34.1	6.1	2.4	0.4	0.29	0.9	1.5	0.25	0.02	0.01	266
63-84	Bt3	34.5	5.9	2.3	0.4	0.28	0.8	1.5	0.24	0.01	<0.01	248
84-120	2Bt4	34.6	6.1	2.4	0.3	0.34	0.9	1.4	0.25	0.02	0.01	227

CHAPTER 4: CHEMICAL MASS BALANCE ON GEOLOGICALLY COMPLEX CATENAS ALONG GRADIENTS OF RELIEF AND CLIMATE I: PARENT MATERIAL AND INDEX ELEMENT CHOICE

1. INTRODUCTION

As early as the late 19th century, geochemists were already grappling with tracing the quantitative conversion of rock into soil during chemical weathering (Merrill, 1897). Rudimentary mass balance approaches were evident and underwent gradual improvements over the last century culminating in the formal presentation of the method by Brimhall and Dietrich (1987). More recently, geochemical mass balance has been refined to incorporate the complexities implied by Jenny's (1941) factors of soil formation and the dynamic nature of landscapes (see review in Brantley et al., 2007). Efforts include the integration of mass balance with sediment flux across catenas (Green et al., 2006), quantifying the impact of climate on chemical weathering rates (Riebe et al., 2004), the impact of dust (Porder et al., 2007) and determination of how landform age influences weathering extent (Yoo et al., 2007). Curiously, the two basic assumptions of mass balance have not been rigorously tested consistently whenever the method is applied. Of the two, the choice of immobile element has received the greatest attention in field (Nesbitt and Markovics, 1997) and lab settings (Hodson, 2002). However, most studies yield site-specific results under which generalisations are difficult to make, and so the issue of immobile element choice remains contentious. The second assumption; that of choice of model parent material and demonstrating that the soil is uniformly derived

from it, has largely been neglected, even though it is especially important in geologically heterogeneous landscapes. These two issues are the general backdrop for this study within the broader scheme of analyzing chemical weathering on catenas in different climatic and topographic contexts of semi-arid Kruger National Park, South Africa.

The efficacy of titanium and zirconium as index elements in mass balance, particularly that of Zr, is long-standing and founded on theoretical and experimental grounds (Brimhall and Dietrich, 1987; Merrill, 1897). Some recent studies, however, have questioned their indiscriminant use without the actual test of immobility, more so titanium since it can form secondary phases in soil that are part of soil's mobile colloidal fraction (Cornu et al., 1999; Neaman et al., 2006; Taboada et al., 2006). Most workers are in agreement that Zr and Ti only move under specific conditions of high organic ligand content, high rainfall or a combination. Therefore any mass balance study must inspect the recalcitrance of the two elements as they have been shown to be mobile under many laboratory and field settings. The important thing however, is to demonstrate relative immobility and realize that no element can be absolutely immobile in the soil environment at all scales.

Most mass balance studies arrive at a model parent material for the soil by averaging rocks collected during the soil survey, whether from beneath regolith or in exposed tors and river-beds. Some studies only use rock below soil. While rock-below-soil may be fine for mass balance where the rock is uniform at the scale of the pedon, in cases where fine-scale variations in lithology are transmitted to soil horizons, rock-below-soil may be an inadequate representative of the soil's parent material. Where exogenous inputs of dust and mass movement of pre-weathered colluvium on the

hillslope are suspected but not quantified, an average parent material may be the best option. Worse still is the case where variation in lithology, dust and colluvium concomitantly limit the use of both rock-below-soil and averaged rock composition. In such cases, the heterogeneity in soil parent material warrants the creation of a reconstituted parent material that integrates the range of all possibilities in parent material.

In this chapter, I investigate two crucial prerequisites for a successful geochemical mass balance in soil *viz.* the choice of index element and choice of parent material against which losses and gains of rock-derived elements are calculated. First, I present a direct comparison of the recalcitrance of Zr and Ti relative to each other in soils spanning a topo-climatic matrix. Secondly, I demonstrate subtleties in parent material choice that will, if overlooked as often happens in physiographically heterogeneous landscapes, result in erroneous results difficult to interpret across wide spans of soil landscapes.

2. METHODS

I established transects from crest to toeslope on nine catenas, each characterized by a specific topo-climatic context. Three catenas were studied in the dry climate of mean annual precipitation (MAP) 468 mm (Shingwedzi), three in Skukuza with an MAP of 550 mm and a further three catenas in the wettest climate with an MAP of 734 mm (Pretoriuskop). The three catenas in each rainfall zone were distinguished by difference in relief and length to yield continua of increasing contributing area inside each climate zones. The cross sections of study catenas are shown in figure 1 with positions of

sampled pedons indicated along hillslopes. All subsequent soil profile data presentations follow the nine-box sampling template displayed in the figure. The descriptions of the catenas and their soils are provided in chapter 3 and herein I maintain the same coding as was used in that chapter.

Soils were sampled by horizon to rock/ saprolite and analyzed for major element and zirconium concentrations by XRF at ALSChemex in Sparks, Nevada. All data are presented on an air-dried and < 2 mm sieved basis. Bulk density was measured through the saran-coated clod method or in a cylinder of known volume.

The losses and gains of major elements were estimated using the open-chemical-system transport function (Kurtz et al., 2001) by which the fraction of an element added to or lost from soil during weathering is:

$$\bar{\eta}_{j,w} = \left(\frac{C_{j,w}}{C_{j,p}} \times \frac{C_{i,w}}{C_{i,p}} \right) - 1, \text{ where } C_j \text{ is the element under scrutiny and } C_i \text{ is the}$$

relatively immobile index element, w and p refer to a soil horizon and parent material respectively. The strain of a soil horizon, on the other hand, is computed by:

$$\varepsilon_{i,w} = \frac{V_w - V_p}{V_p} = \frac{V_w}{V_p} - 1 = \frac{\rho_p C_{i,p}}{\rho_w C_{i,w}} - 1, \text{ where } \rho \text{ is bulk density. A positive strain}$$

implies dilation of the horizon by material addition whereas a negative strain designates a horizon where losses have occurred or soil collapse.

2.1 Study-site geology

The Nelspruit granite suite underlying the Skukuza-Pretoriuskop area contains an assortment of granitic rocks which range in composition/ texture from gneiss/ migmatite

to porphyritic granite. The rock is pink-grayish with quartz, plagioclase, biotite and K-feldspar. The Nelspruit granite exhibits considerable heterogeneity in composition as indicated by large variations in K_2O and Na_2O , which range between <1-6 % and 2-4 % respectively (Robb, 1977). Also occurring sporadically throughout the batholith are gneisses with granodioritic to tonelitic composition, which commonly form valleys in the area due to greater susceptibility to weathering. The Nelspruit granite shows little Sr isotopic variation in its exposed areas (Robb, 1977) which suggests that any rock variability occurring between Skukuza and Pretoriuskop can be attributed to internal heterogeneity within the rock suite, and not to a provincial change in the geology. Mafic xenoliths in the batholith may reach up to 20 m × 2 m, consisting mainly of amphibolite derived from invaded greenstone fragments. When the xenoliths are intensely infiltrated by granitic material with diffuse boundaries and high assimilation, the granitic country rock becomes basified by mafic biotite and hornblende (Minnitt, 1975).

The Shingwedzi area, on the other hand, is underlain by the Goudplaats gneiss, an older variety of similarly heterogeneous granitoid gneisses (Vorster, 1979). The gneiss in Shingwedzi is light to dark grey and composed of varying proportions of plagioclase, quartz, K-feldspar, biotite and hornblende. Importantly, mafic tendency in the rocks underlying the catenas sampled for this study is highest in Shingwedzi due to greater preponderance of migmatization, a result that is not necessarily evident from my rock sampling for that area as described below. The migmatites of Shingwedzi form flatter terrain than the south of Kruger with notoriously poor exposures (Venter, 1990). Poor exposures in the north of Kruger are possibly due to close proximity to the Lebombo monocline which results in damming and alluviation of the landscape. Rivers in the south

of the Park, specifically in Skukuza around the Sabie River, are bedrock controlled, thus exposures are plentiful (Rountree et al., 2000).

3. RESULTS

Before presenting results on elemental mass balance across catenas in the next chapter, I investigated parent material uniformity in soils generally and specifically examined an unanticipated fractionation in soil geochemistry during weathering of the migmatite underlying Shingwedzi soils. Evaluation of parent material uniformity is required prior to mass balance interpretation. My analysis of migmatite fractionation shows that even at centimeter scales, parent material issues can confound geochemical mass balance. Secondly, I selected the better index element, by inspecting mobilities of zirconium and titanium in sampled soils and catenas. Finally, I derive a method for estimating the composition of soil parent material in heterogeneous landscapes impacted by lithological diversity, mass movement, dust inputs, etc. Following these preliminaries, soil strain and mass balance of major elements along catenas in Kruger are quantified in the next chapter.

3.1 Parent material assignment to sampled soils

The lack of suitably unaltered rock outcrops in Shingwedzi presented a problem; only rock underneath soils could be sampled to create the model parent material. The average elemental composition of rocks collected under Shingwedzi soils is given in

Table 1. When compared to composition of rocks sampled from outcrops (Table 2), the composition of rocks under soils was low in Fe, Mg, Ti, P and Zr. In particular, the rocks under soils concentrations of Ti and Zr were respectively 0.02 ± 0.01 % and 32 ± 6 ppm (Table 1). By contrast, the Ti and Zr concentrations reported in the literature were 0.17 ± 0.03 % and 135 ± 19 ppm, respectively (Table 2). Continuing with Ti and Zr for illustration, their concentrations in the leucosome (felsic) part of the migmatite more closely resembled that for rocks under soils (0.07 % and 60 ppm, respectively, Table 1). The melanosome (mafic) component, on the other hand, had higher concentrations of both Ti and Zr (0.98 % and 143 ppm respectively, Table 1), unlike those recorded in the rocks under soils. Therefore, my sampling of Shingwedzi rocks was inadequate and the composition of migmatite fractions in table 1 suggests why this was more than merely a sampling error, but a product of how migmatite weathers. As a result of migmatite fractionation in Shingwedzi during weathering, my subsequent mass balance calculations uses parent material obtained from outcrop rocks published in the literature, which retain the geochemical composition of unfractionated migmatite (Table 2).

The composition of twenty rocks collected in the Skukuza-Pretoriuskop, where outcrops were plenty, is also shown in Table 2. Their average Ti and Zr concentrations were 0.18 ± 0.04 % and 125 ± 20 %, respectively. Rocks in the Skukuza-Pretoriuskop area were hence not subject to the fractionation evident in the Shingwedzi; and this was due to less widespread occurrences of migmatite in the lithology and the availability of fresh outcrops for sampling.

3.2 Mobility of Zirconium and Titanium during weathering in Kruger soils

3.2.1 Evidence from crest soils

That Zr and Ti were the least mobile elements in Kruger's crest soils was supported by chapter 2 results showing: (1) their strong residual enrichment in the surface horizons of the wettest crest soils relative to concentrations in rock; and (2) that they experienced the largest enrichment in crest soils with increased rainfall between Shingwedzi and Pretoriuskop. Of the two, Zr was the most demonstrably less mobile. Therefore in crest positions, which present the least ambiguous situation concerning mass loss and gain; Zr and Ti were the least mobile elements and moreover, Zr was less mobile than Ti.

3.2.2 Evidence from catenas in Pretoriuskop-Skukuza

To evaluate which of the two index element candidates was least mobile along catenas, I inspected each one's mobility against the other, in alternative hypotheses starting with Ti as the index element. For the Pretoriuskop-Skukuza soils, Zr loss/gain standardized by Ti was positive (implying Zr gains) in most pedons, except in some toeslope soils of IL, WH and WM (Fig. 2). The most parsimonious scenario for Zr gain is addition of zirconium-rich dust. So then the question is: was Zr-rich dust addition evident in the surface soils of Pretoriuskop-Skukuza? Higher Zr/Ti in soil compared to the ratio in the Pretoriuskop-Skukuza parent material (0.9 ± 0.1 , Table 2) suggests addition of dust

rich in Zr (Appendix I). However, Zr enrichment in soil relative to rock concentration was not generally higher in surface horizons across catenas, suggesting that dust was not added (Appendix I). Finally, the tendency for tau Zr curves to switch to net losses or approach zero fractional loss/gain in the distal positions of Pretoriuskop-Skukuza catenas begs the interpretation that there was preferential loss of Zr over Ti, highly unlikely turn. Evidence across Skukuza-Pretoriuskop catenas hence suggests that Ti was not immobile and its mobility when regarded as an index element violated principles of how Zr behaves in soil.

The alternative scenario, premising Zr immobility in Pretoriuskop-Skukuza soils, gave results indicating Ti loss, more so in near-crest positions of the catenas (Fig 2.). In toeslope positions, Ti was lost less or exhibited an overall gain relative to its parent material concentrations. The accumulation or reduced loss of Ti in distal sections of the catenas (Fig. 2) was likely due to accumulation of clay charged with substituted Ti. But was there evidence that Ti moved with colloids? The mimicry of the clay-associated tau Al depth profiles by tau Ti depth profiles suggests so (Fig. 3). Paired clay-poor and clay-rich pedons in the Pretoriuskop-Skukuza area, IH3 and IH4, IM4 and IM5, IL5 and IL6, WH5 and WH6, WM8 and WM9 and WL5 and WL6; show that Ti and Al experienced less loss or were gained in the clay-rich horizons of toeslopes suggesting both moved in colloidal form (Fig. 3a and 3b). Magnitudes of Ti and Al loss/gain in clay-poor soils of Pretoriuskop and Skukuza were as low as -0.63 and -0.88 respectively, whereas in the clay-rich soils, both elements showed less loss or gains to more than double rock concentrations, in conjunction with clay accumulation in Bt horizons.

3.2.3 Evidence from catenas in Shingwedzi

In Shingwedzi, tau Zr indexed by Ti was negative in all pedons across the three catenas, indicating Zr losses exceeding 50 % in each soil sampled (Fig. 2). Loss of Zr under the low leaching and low organic ligand conditions of Shingwedzi, up to 80 % loss relative to parent material concentrations, is highly unlikely. By contrast, zirconium as the index element resulted in apparent addition of Ti in excess to the Ti/Zr ratio in the model parent material, a result that can be explained by dust addition (see below). In the end, the most compelling evidence from both Shingwedzi and Skukuza-Pretoriuskop is for Zr immobility over Ti. In subsequent mass balance calculations in the next chapter, I shall thus use Zr as the index element.

4. DISCUSSION

4.1 The role of dust

The switch from dust-influenced catenas in Shingwedzi seen above, to weathering- and leaching-controlled catenas in Skukuza-Pretoriuskop was apparent in raw Zr versus Ti plots as well (Fig. 4). The slope of the Zr-Ti plot for Shingwedzi soils was relatively flat suggesting greater change in Ti against change in Zr. This implies that either Ti was being residually enriched and Zr lost, or Ti was being added to a greater extent than Zr, and it is more reasonable that material with a lower Zr/Ti ratio than the rock was added. Along Skukuza catenas, the slopes of the Zr-Ti plots were steeper, even

steeper still in Pretoriuskop, suggesting a process shift away from an aeolian input system to a weathering/leaching system (Fig. 4). The shift, however, does not mean lack of dust in the wetter soils, but that weathering and leaching were removing much of the aeolian signal that persisted in the drier soils. The plots for Skukuza-Pretoriuskop had two populations of points with different slopes. The lower slope population may represent greater Ti input from aeolian sources or alternately, soils with a different parent material.

4.2 Titanium v/s Zirconium in mass balance

When the averaged parent material compositions in Table 2 were used to calculate fractional gains and losses of Zr and Ti, tau Zr (using Ti as the index element) and tau Ti (using Zr as the index element) displayed losses and gains inconsistent with both being refractory (Fig. 2). Titanium was most likely the mobile of the two because it is housed in minerals that are less resistant to weathering, rutile and ilmenite, than those that host zirconium, principally zircons (Taboada et al., 2006). In addition, Ti has secondary phases in soil (anatase) that can substitute for Al in clay minerals making colloidal movement a probable vector for Ti mobility.

Both Ti and Zr are used widely as index elements in mass balance due to their relative recalcitrance in soils (Brimhall et al., 1988). Titanium was favored over Zr due to its greater abundance in soil which made it less prone to analytic errors in concentration estimates relative to Zr (Cox, 1995; Stiles et al., 2003). White (1995), working in very wet soils of Puerto Rico, with rainfall up to 4000 mm, reported unambiguous Ti mobility. Others have discounted Ti recalcitrance in the field (Mongelli et al., 1998) and in

experiments (Hodson, 2002; Neaman et al., 2006), but it is still used as a viable refractory element in mass balance (e.g. Schaetzl and Anderson, 2005). I found field-based evidence that titanium was mobile even under semi-arid conditions within the 400 mm to 750 mm range in annual rainfall, based on evidence in soil profiles and across catenas.

4.3 Uncertainty in parent material and soil provenance

Due to poor rock exposure in the Shingwedzi area, suitably unweathered rock samples could not be obtained. My model parent material using rocks sampled from excavated soils was thus unrepresentative of what actually weathered into the soils. The fractionation was due to the fabric of migmatite itself; the rock consists of a mafic (melanosome) and felsic (leucosome) component which weather at different rates (Robb, 1977). The mafic part is much more susceptible to weathering and so dwindles relative to the persistent felsic part as weathering proceeds. However, the products of melanosome weathering, more especially refractory elements such as Zr, remain in the soil. There was therefore a disjunct between the Zr in the rock that persists under soils and the Zr in the soils. The soils also bore the signature of higher Zr from the mafic component of their migmatite parent material. However, what lay below the soils was the Zr-starved felsic remnant of the migmatite. Table 1 shows the heterogeneous composition of migmatite constituents illustrated in Figure 5. The felsic and mafic end-members are the leucosome and the melanosome respectively. The melanosome has much higher concentrations of elements (Fe, Mg and Ti) hosted by mafic minerals such as hornblende.

It is not only migmatite fractionation at the pedon scale that can confound mass balance. Mass movement on catenas and dust inputs are additional sources of discontinuity in provenance between soil and the underlying rock. Thus, for a soil at any point in the landscape, the parent material is not merely the rock underneath it, but includes a canvas of heterogeneous lithologies from below soil, upslope-derived material and airborne dust inputs. Below I develop a method designed to curb uncertainty in soil parent material for improved mass balance estimates in heterogeneous terrain, based on the Zr to Titanium ratio in soil.

The Zr/Ti ratio in soil can be used to index the span in parent materials that a soil inherits. When the coefficient of variability (cv) in Zr/Ti in a soil is very high, it can be reasonably supposed that the soil has multiple parent materials. Following Chittleborough and Oades (1980), a 20 % threshold in cv marks whether a soil has uniform parent material, cv's exceeding 20 % indicate soils with various parent materials. There were soils sampled in this study whose Zr/Ti cv's were much higher than 20 % (Table 3), throwing strong doubt for uniformity in their parent material. Table 3 also shows the two rocks whose Zr/Ti ratio enveloped soil Zr/Ti. The rocks were mostly granitic but also included mafic dykes, basalt and gabbro, as probable contributors to soil parent material. Therefore any attempt to estimate soil parent material by averaging a set of granitic rocks will always be limited in a soil landscape consisting of varied rocks, mass transport and dust inputs. The average dampens the signals from all contributing parent materials to the soil, leading to erroneous estimates of weathering extent derived from mass balance.

A more rewarding approach to proxy parent material composition and overcome uncertainty in soil provenance is to create a synthetic parent material from available rocks

in the landscape. This is a novel method for estimating parent material composition not unlike those employed in isotope biogeochemistry to trace nutrient sources amongst various contributors (Bern et al., 2007), in remote sensing to un-mix multiple signals in a pixel (Rosin, 2001) and in quantitative mineralogy to deconvolve XRD spectral outputs to provide estimates of mineral quantities (Guilfoyle et al., 2001). Here, using a similar principle, I formulate an alternative method for deriving a parent material for each soil horizon.

4.4 A synthetic parent material for mass balance

First, the geochemical provenance for each soil horizon was established from the Zr/Ti ratios, presented in Table 3. Where the two elements are relatively immobile, the ratio is reasonably conserved between parent material and soil. Secondly, two rocks that sandwiched the Zr/Ti of the horizons in the soil were selected from a suite of samples; and from these rocks, the proportional contribution of the elect parent materials was calculated from a simple two-component mixing model. Thus the fractional input of rock A in a system involving contributions from rocks A and B is calculated by:

proportional contribution of A in horizon = $(Zr/Ti_{soil} - Zr/Ti_A) / (Zr/Ti_B - Zr/Ti_A) = p$,

modified from Still et al. (2003). And finally, it follows that the concentration of element X in the precursor of the horizon becomes:

$[X] = (p \times [X]_A) + \{(1-p) \times [X]_B\}$. Contrasting the tau Ti and tau Zr curves in figure 2

(average parent material) and figure 6 (synthetic parent material) shows that the synthetic parent material yields a product not too different in overall trends from the loss/gain

calculated straightforwardly, more especially in the Skukuza-Pretoriuskop catenas. In Shingwedzi, the synthetic parent material indicated Zr gains when Ti was considered immobile (Fig. 6), in contrast to the more precarious Zr loss found with the averaged parent material. Across all sites, the dominant difference was that the synthetic tau curves had smaller amplitudes as a result of using the Zr/Ti as the basis for fixing the parent material. More than this, not much can be said without an independent assessment of the efficacy of the two approaches to estimating parent material composition.

The synthetic parent material approach can be improved in three other ways: first, using a more stringently conserved ratio than the Zr/Ti since my own data shows that Ti is mobile in Kruger; secondly, using isotope data to isolate soil provenance, like strontium, which is diagnostic amongst soil material sources such as dust and rock; and lastly, using a multiple- instead of two-member mixing model to reconstitute the parent material would result in less erratic trends in the mass balance calculations.

List of tables

Table 1. Composition whole migmatite, its two components and average composition of Shingwedzi rocks collected in this study.

Table 2. Composition of the two model parent material applied to mass balance in Kruger.

Table 3. Zirconium to Titanium ratio statistics in sampled soil pedons. Rocks A and B are id's of the two rocks that enveloped a pedon's Zr/Ti .

List of figures

Figure 1. Cross sections of the nine sampled hillslopes in Kruger's relief climate matrix with sampled pedons indicated.

Figure 2. Depth weighted average net losses and gains of Zr and Ti in soil profile along catenas in Kruger's relief-climate matrix using parent materials given in Table 2.

Figure 3a. Depth profiles of net losses and gains in Ti and Al in paired clay-poor and clay-rich pedons of three catenas in Skukuza.

Figure 3b. Depth profiles of net losses and gains in Ti and Al in paired clay-poor and clay-rich pedons of three catenas in Pretoriuskop.

Figure 4. Soil Zr and Ti relationships in the three climate zones.

Figure 5. Diagram illustrating the compositional heterogeneity of the migmatite underlying the Shingwedzi area in Kruger, modified from Robb (1983).

Figure 6. Depth weighted net losses and gains of Zr and Ti in soil profiles in the Kruger's relief-climate matrix using a parent material synthesized using two lithologic end members.

Appendix I. Depth profiles of the silt: clay and Zr: Ti ratios, fractional losses/gains of major elements, strain and the Zr enrichment factor

Table 1. Composition whole migmatite, its two components and average composition of Shingwedzi rocks collected in this study

Migmatite fraction	Si	Al	Fe	Ca	Mg	Na	K	Ti	P	Zr
	%									ppm
Leucosome ¹	33.4	7.9	0.6	0.7	<0.00	1.9	2.2	0.07	<0.00	60
Melanosome ¹	23.3	6.1	7.1	1.6	3.60	1.1	2.6	0.98	0.43	147
Whole rock ¹	28.5	7.0	3.0	1.9	1.67	2.2	1.1	0.36	0.25	107
Shingwedzi rock under soils (n = 5)	35.4 ± 0.4	7.5 ± 0.3	0.5 ± 0.1	1.0 ± 0.1	0.06 ± 0.1	3.6 ± 0.4	1.3 ± 0.4	0.02 ± 0.01	0.006 ± <0.01	32 ± 6

¹From Robb (1977)

Table 2. Composition of the two model parent material applied to mass balance in Kruger

Site	No. of samples	Si	Al	Fe	Ca	Mg	Na	K	Ti	P	Zr	Zr/ Ti × 10 ⁻³
		%									ppm	
Shingwedzi ¹	6	33.0 ± 0.4	8.3 ± 0.2	1.3 ± 0.2	1.5 ± 0.1	0.3 ± 0.1	4.1 ± 0.2	1.6 ± 0.2	0.17 ± 0.03	0.06 ± 0.01	135 ± 19	0.83 ± 0.1
Skukuza-Pretoriuskop	20	32.0 ± 0.7	7.8 ± 0.2	2.1 ± 0.4	2.2 ± 0.5	0.47 ± 0.3	1.8 ± 0.3	4.2 ± 0.6	0.18 ± 0.04	0.021 ± <0.01	125 ± 20	0.91 ± 0.1

¹From Vorster (1979)

Table 3. Zirconium to Titanium ratio statistics in sampled soil pedons. Rocks A and B are id's of the two rocks that enveloped a pedon's Zr/Ti

Climate/ relief/ soil pit	# horizons	Min Zr/ Ti	Max Zr/ Ti	Average Zr/ Ti	CV Zr/ Ti	Rock A	Rock B
Shingwedzi							
DH1	3	0.7	0.9	0.8	12	72	111
DH2	3	0.5	0.6	0.6	15	14	72
DH3	2	0.5	0.6	0.6	17	71	72
DM1	3	0.6	0.7	0.7	13	81	85
DM2	5	0.6	0.7	0.7	8	81	82
DM3	5	0.2	0.7	0.5	46	17	72
DM4	5	0.3	0.5	0.4	19	73	80
DM5	5	0.4	0.5	0.4	11	73	71
DM6	6	0.3	0.7	0.5	26	73	82
DL1	2	0.4	0.5	0.5	16	73	80
DL2	4	0.5	0.5	0.5	7	73	80
DL3	4	0.4	0.5	0.4	10	73	71
DL4	7	0.4	0.6	0.5	13	73	80
DL5	7	0.3	0.4	0.4	6	84	8
DL6	7	0.3	0.3	0.3	9	73	102
DL7	5	0.3	0.4	0.3	12	110	8
Skukuza							
IH1	3	1.7	2.3	2.0	18	5	70
IH2	4	1.1	1.4	1.3	12	68	5
IH3	5	1.5	2.4	2.1	18	76	70
IH4	5	0.6	1.6	1.1	48	80	6
IH5	4	0.7	0.8	1.0	24	72	5
IM1	3	1.6	1.8	1.7	7	68	7
IM2	5	0.9	1.8	0.2	30	77	7
IM3	6	0.9	1.9	1.7	45	77	4
IM4	3	0.9	1.2	1.1	14	77	5
IM5	4	0.5	1.6	0.9	59	71	6
IM6	5	0.8	1.6	1.1	28	5	70
IM7	8	0.9	1.6	1.4	20	111	7
IM8	5	1	1.6	1.2	20	68	5
IL 1	2	0.8	0.8	0.8	4	72	83
IL 2	4	0.9	1.1	1.0	9	77	5
IL 3	4	0.7	0.9	0.8	13	72	68
IL 4	5	0.7	0.8	0.7	5	80	82
IL 5	3	0.9	1.0	0.9	3	72	68
IL 6	5	0.4	0.8	0.6	26	73	82
IL 7	5	0.3	0.5	0.4	13	73	4
IL 8	5	0.4	0.5	0.4	14	73	80
IL 9	7	0.6	1.0	0.7	21	81	74
IL 10	6	1.0	1.4	1.1	14	111	5
Pretoriuskop							
WH1	8	1.3	2.0	1.6	13	76	7
WH2	6	1.1	1.6	1.4	14	76	6
WH3	6	1.1	1.7	1.4	17	76	6
WH4	8	0.9	1.5	1.3	13	111	5

Climate/ relief/ soil pit	# horizons	Min Zr/ Ti	Max Zr/ Ti	Average Zr/ Ti	CV Zr/ Ti	Rock A	Rock B
WH5	8	0.7	1.4	1.0	25	72	5
WH6	6	0.3	0.9	0.5	53	110	111
WM1	7	1.3	1.6	1.5	6	76	5
WM2	7	1.5	1.9	1.6	8	76	7
WM3	7	1.0	1.6	1.4	17	111	6
WM4	6	1.4	1.5	1.5	4	76	5
WM5	7	1.4	2.0	1.7	14	76	70
WM6	7	1.2	2.0	1.6	17	76	70
WM7	8	1.2	1.8	1.5	15	76	7
WM8	7	1.4	1.9	1.7	12	76	7
WM9	7	0.4	1.7	0.8	66	73	6
WM10	4	0.7	1.3	1.0	22	72	5
WM11	6	1.0	1.5	1.2	16	68	5
WL1	12	0.7	2.0	1.2	42	72	70
WL2	9	0.5	1.9	2.0	7	5	70
WL3	10	0.6	2.5	1.8	38	72	70
WL4	6	0.8	2.4	1.6	42	83	70
WL5	3	0.8	1.8	1.4	38	72	7
WL6	5	0.9	1.5	1.0	9	77	5

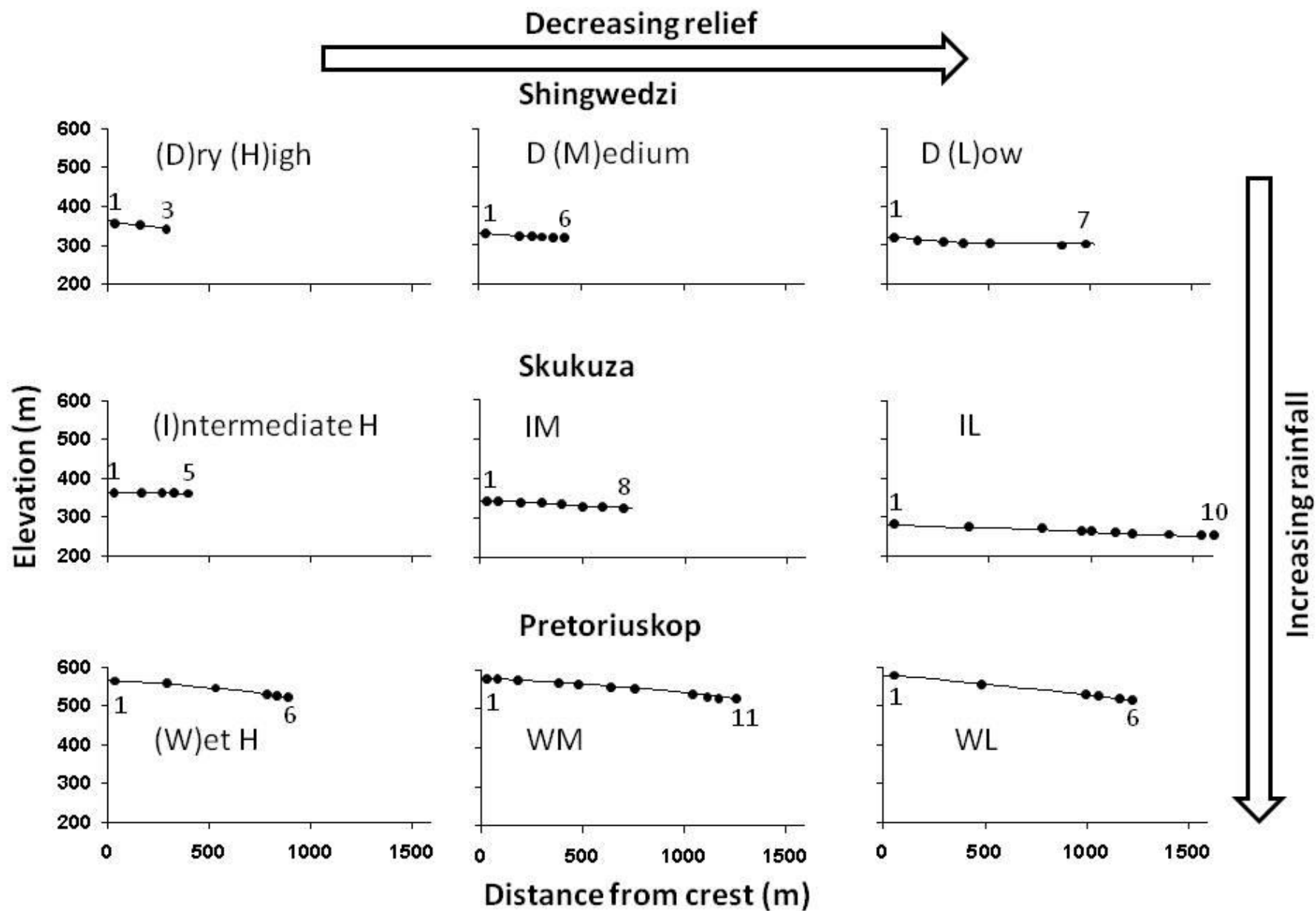


Figure 1. Cross sections of the nine sampled hillslopes in Kruger's relief climate matrix with sampled pedons indicated.

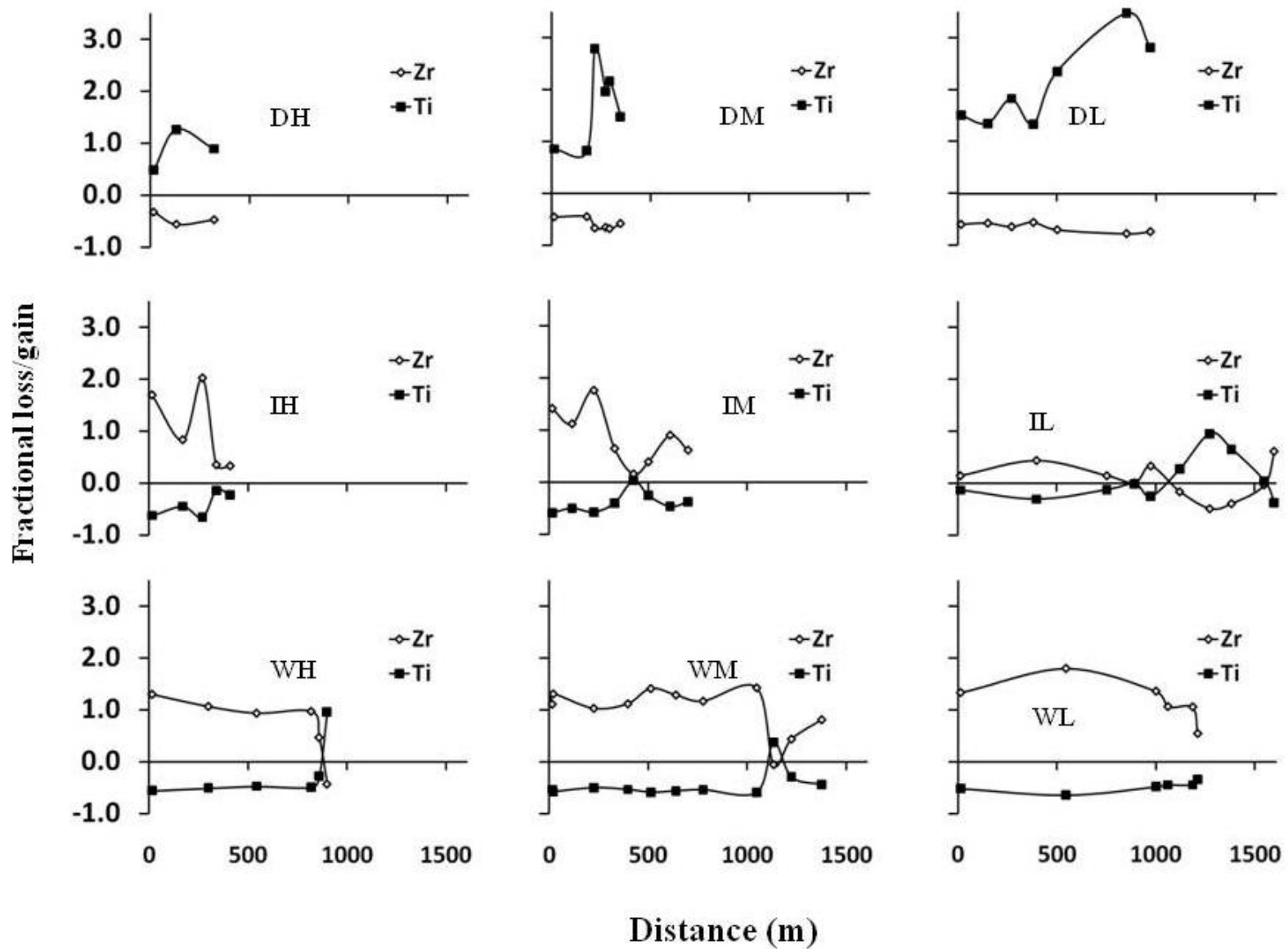


Figure 2. Depth weighted average net losses and gains of Zr and Ti in soil profile along catenas in Kruger's relief-climate matrix using parent materials given in Table 2.

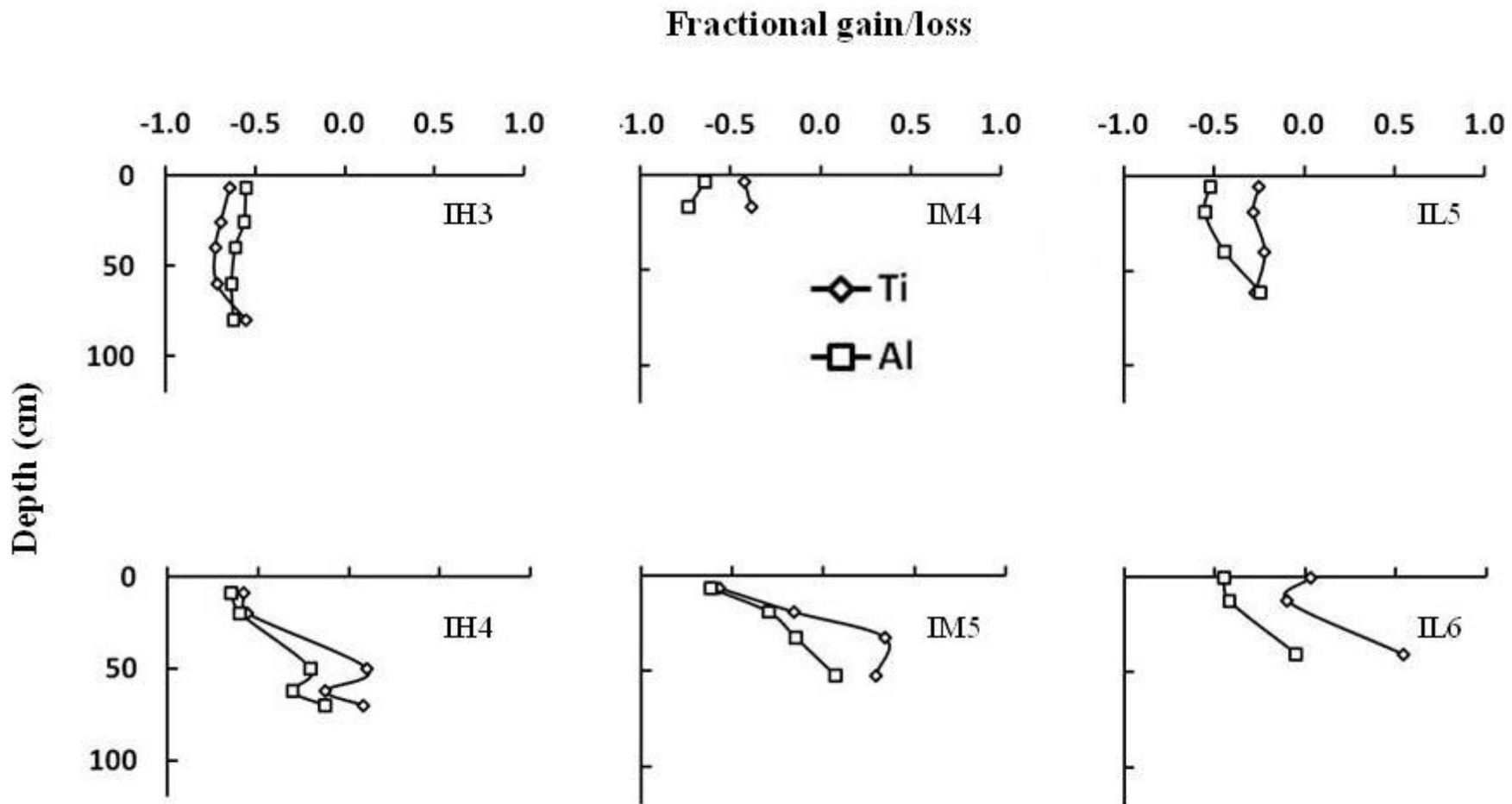


Figure 3a. Depth profiles of net losses and gains in Ti and Al in paired clay-poor and clay-rich pedons of three catenas in Skukuza.

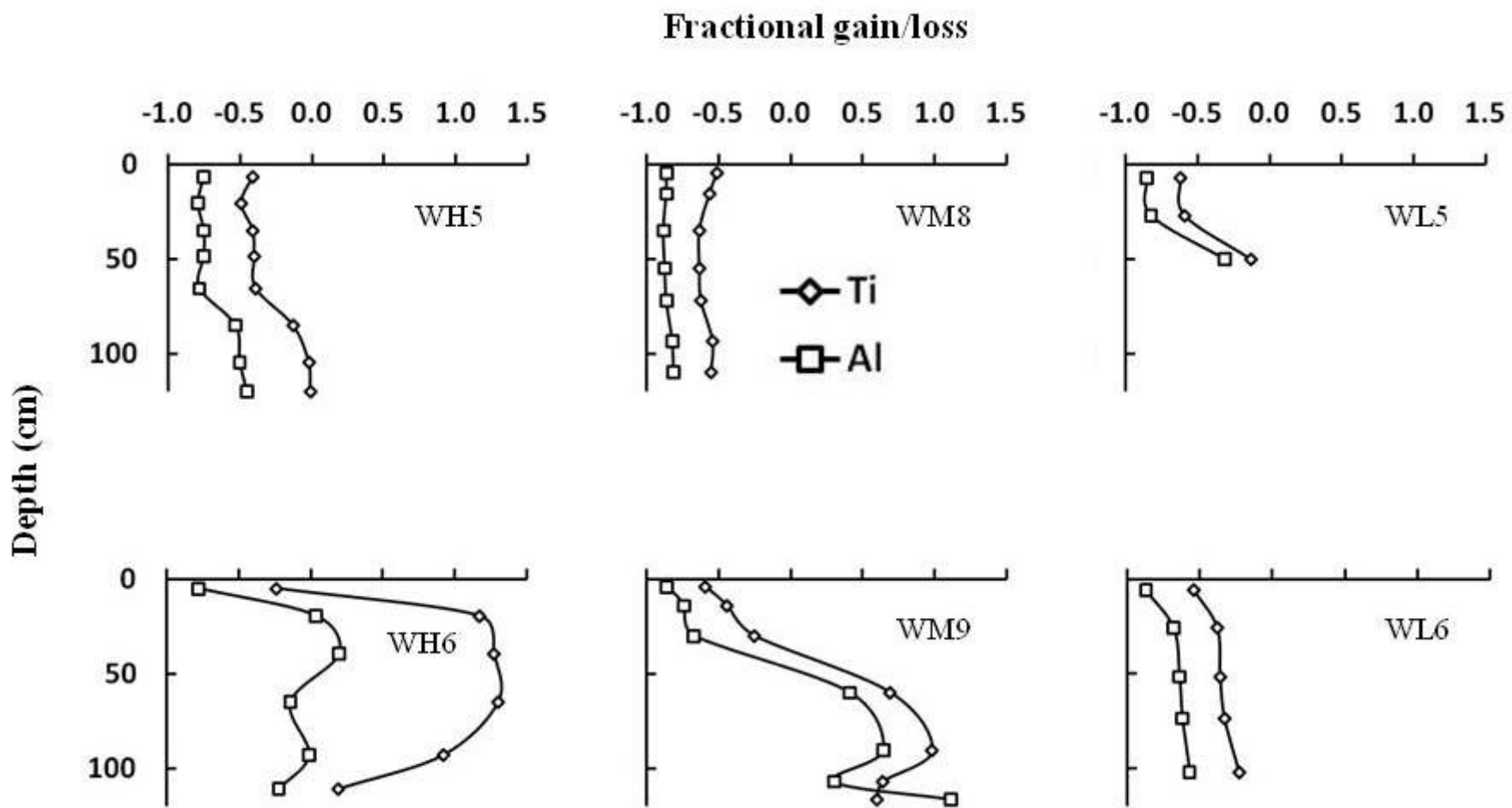


Figure 3b. Depth profiles of net losses and gains in Ti and Al in paired clay-poor and clay-rich pedons of three catenas in Pretoriuskop.

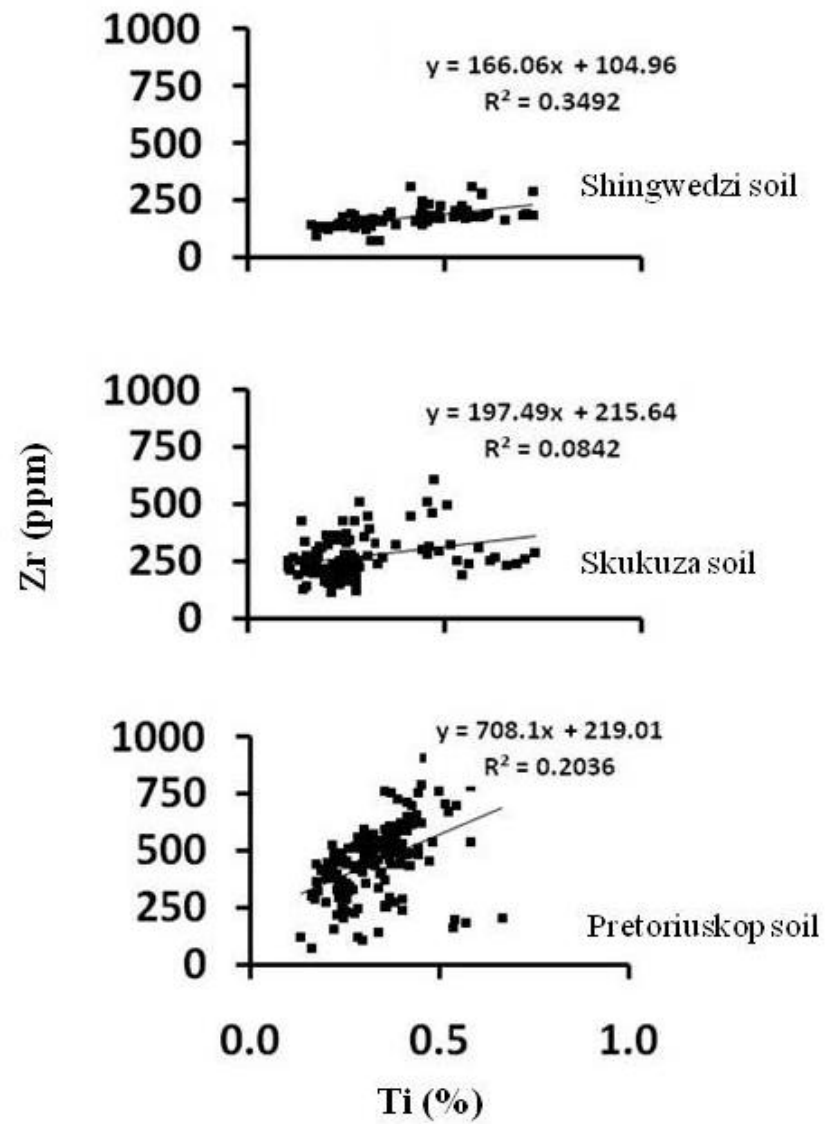


Fig 4. Soil Zr and Ti relationships in the three climate zones.

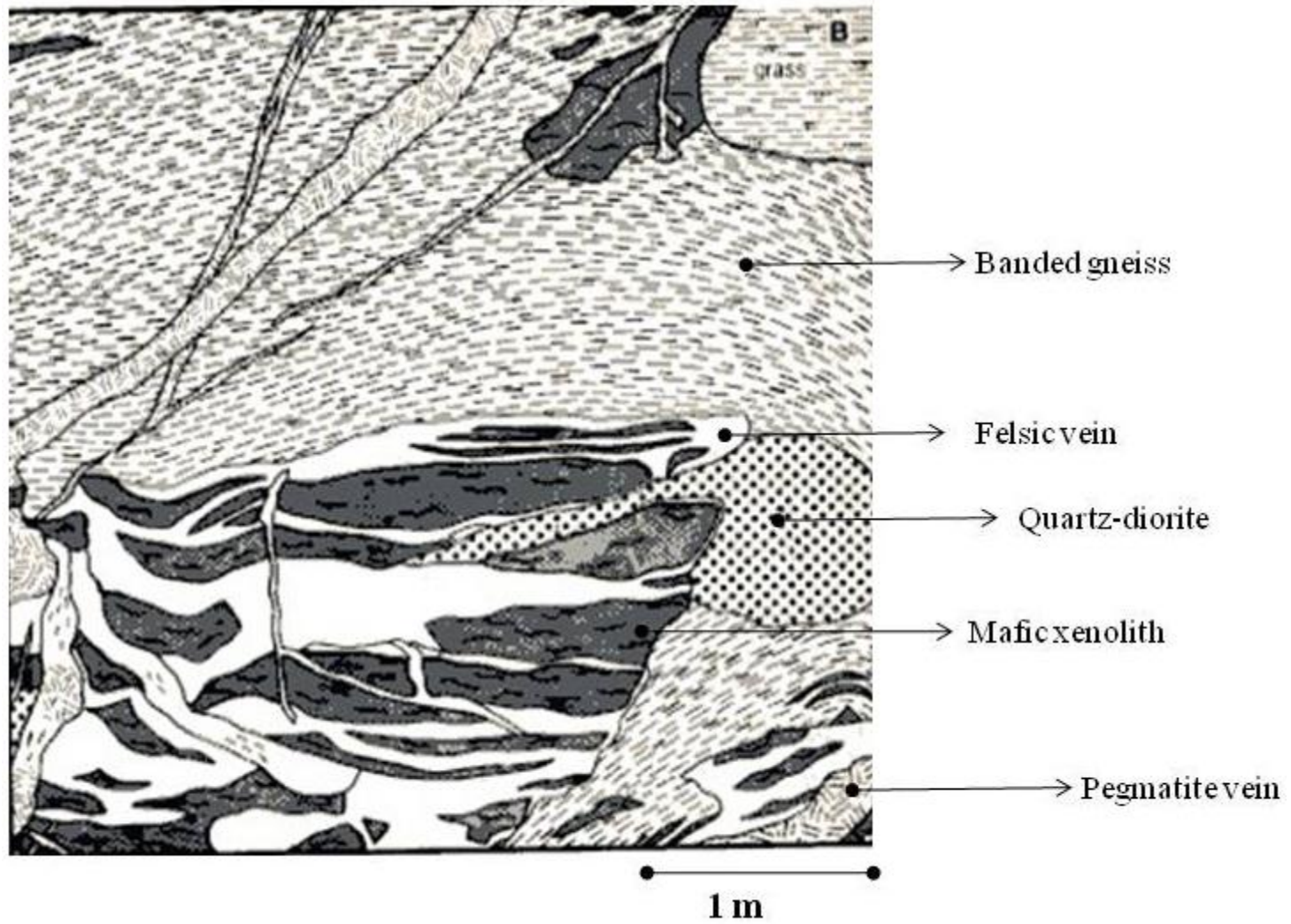


Figure 5. Diagram illustrating the compositional heterogeneity of the migmatite underlying the Shingwedzi area in Kruger, modified from Robb (1983).

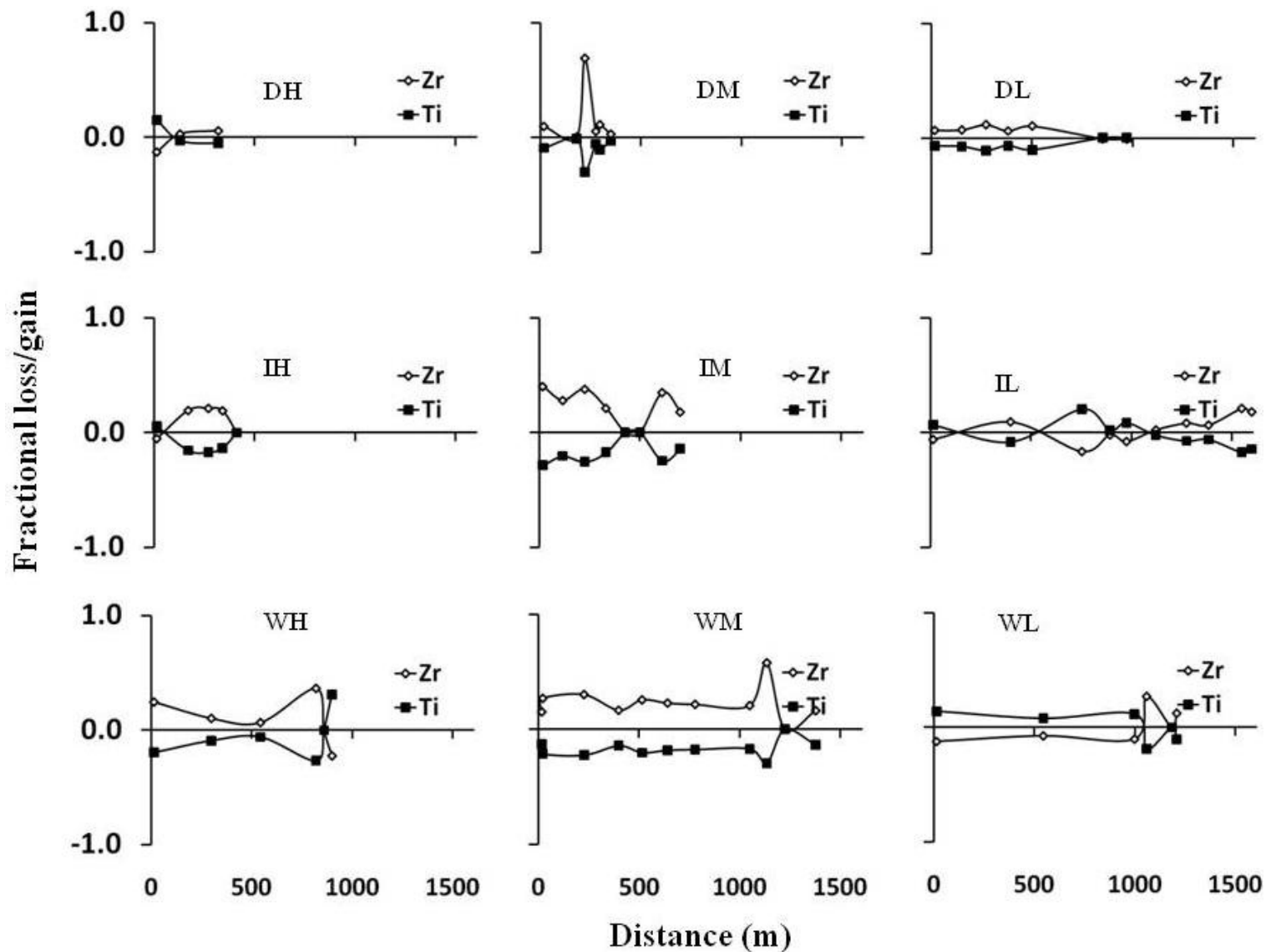


Figure 6. Depth weighted net losses and gains of Zr and Ti in soil profiles in the Kruger's relief-climate matrix using a parent material synthesized using two lithologic end members.

Appendix I. Depth profiles of the silt: clay and Zr: Ti ratios, fractional losses/gains of major elements, strain and the

Zr enrichment factor

Site /depth	Silt clay	Zr/ Ti $\times 10^{-3}$	τ Si	τ Al	τ Fe	τ Ca	τ Mg	τ Na	τ K	τ Ti	τ P	Strain	τ Zr (Ti)	$\frac{Zr_{soil}}{Zr_{rock}}$
0-2	2.9	0.71	-0.76	-0.80	-0.62	-0.87	-0.79	-0.87	-0.61	0.86	0.03	-0.55	-0.46	4.2
2-16	1.6	0.74	-0.77	-0.80	-0.61	-0.87	-0.71	-0.87	-0.62	0.77	0.14	-0.60	-0.44	4.4
16-28	2.2	0.89	-0.79	-0.77	-0.49	-0.82	-0.44	-0.83	-0.74	0.48	-0.22	-0.66	-0.32	4.6
28-45														
DH2														
0-1	1.7	0.66	-0.80	-0.83	-0.66	-0.85	-0.76	-0.86	-0.74	1.00	-0.14	-0.63	-0.50	5.0
1-14	1.6	0.52	-0.84	-0.84	-0.44	-0.88	-0.71	-0.89	-0.76	1.52	-0.05	-0.71	-0.60	6.0
14-23	1.3	0.50	-0.83	-0.83	-0.40	-0.87	-0.63	-0.88	-0.74	1.62	-0.11	-0.73	-0.62	5.6
23-43														
DH3														
0-1	1.8	0.50	-0.87	-0.87	-0.49	-0.90	-0.68	-0.91	-0.80	1.64	-0.21	-0.74	-0.62	7.3
1-19	0.9	0.63	-0.78	-0.80	-0.57	-0.84	-0.83	-0.85	-0.69	1.08	-0.53	-0.64	-0.52	4.6
DM1														
0-12	2.0	0.75	-0.83	-0.83	-0.30	-0.77	-0.36	-0.85	-0.83	0.77	-0.37	-0.67	-0.43	5.7
12-29	3.0	0.67	-0.77	-0.76	-0.07	-0.70	-0.42	-0.80	-0.80	0.96	-0.32	-0.59	-0.49	4.2
29-53	1.8	0.57	-0.79	-0.77	-0.27	-0.72	-0.27	-0.79	-0.82	1.31	-0.68	-0.61	-0.57	4.4
53-63														
DM2														
0-1	0.8	0.72	-0.84	-0.85	-0.54	-0.81	-0.50	-0.86	-0.85	0.82	-0.41	-0.75	-0.45	6.0
1-13	0.7	0.67	-0.83	-0.83	-0.49	-0.81	-0.46	-0.85	-0.84	0.95	-0.38	-0.73	-0.49	5.8
13-32	0.7	0.69	-0.81	-0.82	-0.44	-0.79	-0.44	-0.84	-0.83	0.92	-0.32	-0.71	-0.48	5.2
32-46	0.7	0.63	-0.78	-0.81	-0.32	-0.75	-0.34	-0.81	-0.82	1.08	-0.18	-0.65	-0.52	4.3
46-60	0.9	0.58	-0.77	-0.73	-0.37	-0.72	-0.46	-0.78	-0.83	1.26	-0.32	-0.64	-0.56	4.2
DM3														
0-1	0.5	0.66	-0.73	-0.74	-0.26	-0.69	-0.13	-0.75	-0.76	1.01	-0.21	-0.58	-0.50	3.6
1-4	0.4	0.63	-0.80	-0.80	-0.26	-0.75	-0.22	-0.82	-0.82	1.10	-0.23	-0.67	-0.52	4.7
4-20	0.4	0.61	-0.76	-0.76	-0.22	-0.73	-0.23	-0.78	-0.77	1.15	-0.28	-0.61	-0.53	4.0
20-39	0.1	0.23	-0.67	-0.53	2.13	-0.74	2.14	-0.81	-0.67	4.75	0.17	-0.37	-0.83	2.4
39-50	0.1	0.24	-0.65	-0.50	1.60	-0.66	1.85	-0.72	-0.69	4.48	-0.10	-0.36	-0.82	2.4
DM4														
0-2	1.5	0.53	-0.90	-0.90	-0.43	-0.86	-0.35	-0.91	-0.91	1.47	-0.63	-0.81	-0.59	9.6
2-18	0.6	0.48	-0.87	-0.85	0.00	-0.82	0.03	-0.89	-0.86	1.77	-0.47	-0.74	-0.64	6.7
18-51	0.6	0.40	-0.85	-0.83	0.19	-0.78	0.29	-0.88	-0.84	2.28	-0.51	-0.72	-0.70	5.8
51-63	1.0	0.34	-0.85	-0.82	0.34	-0.70	0.50	-0.89	-0.85	2.93	-0.36	-0.71	-0.75	5.5
63-81	0.6	0.37	-0.83	-0.80	0.42	-0.60	0.61	-0.87	-0.84	2.55	-0.43	-0.69	-0.72	5.0
81-91														
DM5														
0-4	0.7	0.46	-0.87	-0.87	-0.27	-0.81	-0.13	-0.88	-0.87	1.85	-0.50	-0.79	-0.65	7.2

Site /depth	Silt clay	Zr/ Ti $\times 10^{-3}$	τ Si	τ Al	τ Fe	τ Ca	τ Mg	τ Na	τ K	τ Ti	τ P	Strain	τ Zr (Ti)	$\frac{Zr_{soil}}{Zr_{rock}}$
4-19	0.8	0.37	-0.86	-0.84	-0.01	-0.79	0.24	-0.87	-0.85	2.57	-0.43	-0.75	-0.72	6.2
19-35	0.7	0.39	-0.84	-0.83	0.10	-0.78	0.23	-0.86	-0.84	2.36	-0.38	-0.73	-0.70	5.7
35-52	0.4	0.35	-0.83	-0.81	0.22	-0.79	0.29	-0.87	-0.84	2.72	-0.60	-0.72	-0.73	5.4
52-67	0.3	0.36	-0.83	-0.79	0.44	-0.76	0.60	-0.86	-0.83	2.68	-0.29	-0.70	-0.73	5.0
DM6														
0-4	5.0	0.55	-0.87	-0.89	-0.46	-0.84	-0.24	-0.90	-0.88	1.39	-0.63	-0.76	-0.58	7.8
4-10	1.0	0.74	-0.90	-0.92	-0.68	-0.88	-0.61	-0.92	-0.92	0.78	-0.78	-0.83	-0.44	9.7
10-31	1.0	0.43	-0.77	-0.79	0.05	-0.68	0.47	-0.81	-0.79	2.09	-0.66	-0.65	-0.68	4.2
31-52	0.6	0.49	-0.82	-0.83	-0.06	-0.79	0.18	-0.85	-0.83	1.68	-0.59	-0.72	-0.63	5.2
52-76	0.6	0.55	-0.85	-0.87	-0.25	-0.74	0.12	-0.88	-0.86	1.41	-0.66	-0.78	-0.58	6.3
76-87	0.4	0.34	-0.82	-0.82	0.22	-0.76	0.99	-0.85	-0.82	2.82	-0.57	-0.72	-0.74	5.0
87-97														
DL1														
0-23	2.6	0.53	-0.84	-0.83	-0.38	-0.85	-0.37	-0.87	-0.70	1.51	-0.03	-0.68	-0.60	5.9
23-45	2.5	0.42	-0.77	-0.74	0.10	-0.76	0.35	-0.83	-0.59	2.13	-0.10	-0.57	-0.68	4.0
45-55		1.74												
DL2														
0-6	2.1	0.46	-0.81	-0.81	-0.43	-0.80	-0.11	-0.84	-0.74	1.89	0.30	-0.69	-0.65	4.9
6-22	1.3	0.49	-0.78	-0.79	-0.35	-0.76	-0.08	-0.82	-0.74	1.69	0.28	-0.66	-0.63	4.5
22-35	0.9	0.54	-0.79	-0.79	-0.40	-0.79	-0.15	-0.82	-0.74	1.43	0.24	-0.67	-0.59	4.6
35-50	1.1	0.50	-0.77	-0.77	-0.37	-0.78	-0.08	-0.81	-0.72	1.63	0.00	-0.64	-0.62	4.3
DL3														
0-2	1.7	0.41	-0.87	-0.87	-0.18	-0.83	-0.09	-0.90	-0.85	2.20	-0.30	-0.74	-0.69	7.1
2-19	5.5	0.47	-0.89	-0.90	-0.37	-0.86	-0.28	-0.92	-0.88	1.83	-0.26	-0.80	-0.65	8.7
19-34	1.4	0.37	-0.86	-0.86	-0.10	-0.82	-0.03	-0.88	-0.83	2.60	-0.45	-0.73	-0.72	6.5
34-42	0.3	0.43	-0.85	-0.84	0.03	-0.83	0.16	-0.89	-0.81	2.04	-0.29	-0.73	-0.67	6.0
42-52														
DL4														
0-1	0.9	0.58	-0.77	-0.82	-0.42	-0.76	0.27	-0.82	-0.81	1.27	-0.35	-0.65	-0.56	4.4
1-9	0.6	0.55	-0.66	-0.74	-0.25	-0.68	0.63	-0.75	-0.74	1.41	-0.05	-0.49	-0.59	3.0
9-24	0.8	0.49	-0.75	-0.81	-0.42	-0.76	0.23	-0.82	-0.79	1.71	-0.48	-0.63	-0.63	4.1
21-40	1.3	0.55	-0.80	-0.85	-0.58	-0.80	0.08	-0.85	-0.83	1.40	-0.30	-0.70	-0.58	5.1
40-55	1.2	0.49	-0.79	-0.84	-0.59	-0.79	0.25	-0.84	-0.81	1.70	-0.71	-0.69	-0.63	5.0
55-67	1.8	0.53	-0.81	-0.85	-0.62	-0.81	-0.05	-0.85	-0.82	1.51	-0.59	-0.71	-0.60	5.3
67-75	0.4	0.37	-0.78	-0.80	-0.38	-0.82	0.08	-0.83	-0.74	2.53	-0.36	-0.66	-0.72	4.5
DL5														
0-4	1.5	0.38	-0.80	-0.86	-0.27	-0.80	0.06	-0.87	-0.85	2.51	0.13	-0.70	-0.71	5.1
4-13	1.7	0.37	-0.83	-0.87	-0.32	-0.82	-0.03	-0.89	-0.86	2.52	-0.01	-0.73	-0.72	5.8
13-30	1.1	0.35	-0.82	-0.87	-0.27	-0.82	-0.07	-0.88	-0.86	2.74	-0.22	-0.72	-0.73	5.5
30-51	0.9	0.34	-0.83	-0.87	-0.27	-0.83	-0.02	-0.89	-0.86	2.85	-0.28	-0.74	-0.74	6.0
51-76	0.8	0.38	-0.84	-0.88	-0.31	-0.84	-0.10	-0.90	-0.87	2.44	-0.33	-0.76	-0.71	6.4

Site /depth	Silt clay	Zr/ Ti $\times 10^{-3}$	τ Si	τ Al	τ Fe	τ Ca	τ Mg	τ Na	τ K	τ Ti	τ P	Strain	τ Zr (Ti)	$\frac{Zr_{soil}}{Zr_{rock}}$
76-112	0.8	0.34	-0.83	-0.87	-0.23	-0.84	-0.01	-0.89	-0.86	2.91	-0.39	-0.74	-0.74	5.8
112-120	0.4	0.32	-0.79	-0.81	0.40	-0.81	0.69	-0.89	-0.81	3.09	-0.21	-0.66	-0.76	4.5
DL6														
0-1	1.0	0.30	-0.84	-0.85	0.05	-0.76	0.49	-0.87	-0.86	3.37	0.39	-0.73	-0.77	5.7
1-4	1.0	0.30	-0.83	-0.84	0.19	-0.76	0.60	-0.88	-0.85	3.36	0.82	-0.72	-0.77	5.5
4-20	0.7	0.31	-0.85	-0.84	0.35	-0.78	0.57	-0.90	-0.85	3.29	0.82	-0.74	-0.77	5.9
20-59	0.8	0.25	-0.85	-0.80	1.08	-0.79	1.38	-0.91	-0.82	4.22	0.37	-0.71	-0.81	5.2
59-95	2.5	0.26	-0.87	-0.81	0.98	-0.70	1.45	-0.92	-0.84	4.08	0.24	-0.73	-0.80	5.8
95-110	1.4	0.25	-0.87	-0.82	0.97	-0.64	1.66	-0.92	-0.85	4.22	-0.01	-0.74	-0.81	5.8
110-120	2.4	0.27	-0.88	-0.82	0.91	-0.67	1.56	-0.92	-0.86	3.93	0.19	-0.74	-0.80	6.0
DL7														
0-0.1	1.3	0.40	-0.90	-0.90	-0.15	-0.86	0.03	-0.93	-0.92	2.32	-0.45	-0.80	-0.70	9.1
0.1-11	1.1	0.31	-0.85	-0.83	0.56	-0.69	1.04	-0.87	-0.86	3.20	-0.22	-0.72	-0.76	5.5
11-40	0.6	0.30	-0.85	-0.82	0.70	-0.74	1.23	-0.87	-0.86	3.38	-0.10	-0.72	-0.77	5.5
40-68	0.5	0.31	-0.86	-0.84	0.55	-0.78	0.87	-0.89	-0.87	3.20	-0.41	-0.77	-0.76	6.1
68-95	0.8	0.31	-0.86	-0.84	0.51	-0.81	0.73	-0.88	-0.88	3.24	-0.41	-0.78	-0.76	6.0
Skukuza														
IH1														
0-10	3.3	2.36	-0.59	-0.69	-0.84	-0.89	-0.97	-0.54	-0.77	-0.71	-0.77	-0.36	2.41	2.7
10-23	1.3	1.83	-0.62	-0.70	-0.82	-0.90	-0.96	-0.58	-0.78	-0.62	-0.93	-0.47	1.64	2.9
23-50	1.3	1.71	-0.55	-0.62	-0.71	-0.89	-0.89	-0.47	-0.75	-0.59	-0.83	-0.39	1.46	2.4
50-60														
IH2														
0-10	0.8	1.43	-0.34	-0.49	-0.70	-0.83	-0.85	-0.33	-0.55	-0.52	-0.50	-0.07	1.06	1.6
10-20	1.0	1.39	-0.42	-0.53	-0.72	-0.85	-0.81	-0.38	-0.59	-0.50	-0.67	-0.18	1.00	1.9
20-30	0.5	1.32	-0.41	-0.52	-0.71	-0.86	-0.81	-0.38	-0.60	-0.47	-0.55	-0.17	0.90	1.8
30-47	0.6	1.09	-0.37	-0.48	-0.68	-0.86	-0.82	-0.37	-0.54	-0.36	-0.64	-0.11	0.57	1.7
IH3														
0-7	6.0	1.94	-0.32	-0.55	-0.80	-0.89	-0.99	-0.33	-0.55	-0.64	-0.94	0.04	1.79	1.7
7-26	1.3	2.23	-0.37	-0.56	-0.84	-0.90	-0.99	-0.38	-0.58	-0.69	-0.77	-0.16	2.21	1.8
26-40	3.3	2.45	-0.43	-0.61	-0.84	-0.91	-0.96	-0.42	-0.63	-0.72	-0.90	-0.24	2.54	2.0
40-60	4.0	2.35	-0.47	-0.63	-0.88	-0.91	-0.98	-0.42	-0.64	-0.71	-0.95	-0.33	2.39	2.1
60-80	1.8	1.53	-0.49	-0.62	-0.79	-0.91	-0.96	-0.46	-0.67	-0.55	-0.91	-0.34	1.20	2.2
80-90														
IH4														
0-9	1.2	1.65	-0.57	-0.65	-0.77	-0.88	-0.86	-0.49	-0.72	-0.58	-0.58	-0.38	1.38	2.5
9-20	0.9	1.57	-0.49	-0.60	-0.72	-0.87	-0.86	-0.45	-0.67	-0.56	-0.71	-0.28	1.27	2.1
20-50	0.2	0.63	-0.35	-0.21	-0.09	-0.84	-0.50	-0.50	-0.63	0.10	-0.41	0.10	-0.09	1.4
50-62	0.3	0.80	-0.38	-0.31	-0.24	-0.83	-0.49	-0.43	-0.64	-0.13	-0.59	0.00	0.15	1.5
62-70	0.2	0.64	-0.21	-0.13	0.14	-0.76	-0.40	-0.42	-0.50	0.08	-0.31	0.27	-0.08	1.2
IH5														

Site /depth	Silt clay	Zr/ Ti $\times 10^{-3}$	τ Si	τ Al	τ Fe	τ Ca	τ Mg	τ Na	τ K	τ Ti	τ P	Strain	τ Zr (Ti)	$\frac{Zr_{soil}}{Zr_{rock}}$
0-10	0.9	1.32	-0.64	-0.62	-0.56	-0.83	-0.63	-0.61	-0.77	-0.47	-0.69	-0.47	0.90	2.7
10-31	0.4	1.03	-0.52	-0.50	-0.40	-0.78	-0.58	-0.55	-0.71	-0.33	-0.58	-0.29	0.49	2.0
31-49	0.5	0.84	-0.46	-0.43	-0.25	-0.75	-0.43	-0.50	-0.69	-0.17	-0.53	-0.19	0.21	1.8
49-83	0.3	0.79	-0.48	-0.41	-0.23	-0.73	-0.41	-0.51	-0.70	-0.12	-0.42	-0.11	0.14	1.8
83-93		1.13												
IM1														
0-7	1.5	1.85	-0.49	-0.61	-0.86	-0.90	-0.96	-0.49	-0.61	-0.62	-0.90	-0.32	1.66	2.2
7-33	1.3	1.71	-0.56	-0.65	-0.86	-0.92	-0.97	-0.56	-0.66	-0.59	-1.00	-0.43	1.46	2.5
33-65	1.3	1.61	-0.52	-0.59	-0.81	-0.91	-0.93	-0.52	-0.65	-0.57	-0.97	-0.36	1.32	2.3
65-75		1.06												
IM2														
0-5	6.0	1.27	-0.48	-0.56	-0.48	-0.92	-0.57	-0.78	-0.75	-0.24	-0.72	-0.21	0.32	2.1
5-17	1.7	0.90	-0.55	-0.55	-0.44	-0.79	-0.50	-0.80	-0.79	-0.24	-0.61	-0.27	0.31	2.2
17-42	1.0	1.54	-0.74	-0.78	-0.83	-0.91	-0.88	-0.72	-0.85	-0.61	-0.81	-0.60	1.58	4.1
42-56	0.5	3.12	-0.69	-0.72	-0.78	-0.90	-0.85	-0.69	-0.82	-0.56	-0.84	-0.53	1.29	3.4
56-70	0.5	1.50	-0.72	-0.72	-0.73	-0.90	-0.81	-0.70	-0.84	-0.52	-0.81	-0.55	1.10	3.6
70-80		1.90												
IM3														
0-16	7.0	1.27	-0.67	-0.67	-0.70	-0.87	-0.76	-0.65	-0.80	-0.45	-0.81	-0.48	0.83	3.1
16-42	7.0	0.90	0.01	-0.11	-0.45	-0.74	-0.48	-0.01	-0.05	-0.23	-0.68	0.59	0.30	1.0
42-70	2.0	1.54	-0.35	-0.58	-0.85	-0.85	-0.92	-0.43	-0.64	-0.55	-0.70	-0.08	1.22	1.8
70-120	0.3	3.12	-0.65	-0.78	-0.93	-0.93	-0.96	-0.71	-0.80	-0.78	-0.89	-0.53	3.50	3.4
120-151	0.3	1.50	-0.23	-0.52	-0.84	-0.84	-0.91	-0.35	-0.56	-0.54	-0.84	0.07	1.17	1.5
151-175	0.4	1.90	-0.41	-0.62	-0.88	-0.87	-0.91	-0.46	-0.66	-0.64	-0.88	-0.19	1.74	2.0
IM4														
0-7	2.8	1.19	-0.30	-0.46	-0.64	-0.77	-0.61	-0.09	-0.61	-0.42	-0.90	0.03	0.71	1.6
7-26	1.5	1.12	-0.32	-0.49	-0.73	-0.75	-0.74	-0.16	-0.67	-0.38	-0.81	-0.02	0.62	1.7
26-30		0.90												
IM5														
0-13	1.2	1.62	-0.38	-0.62	-0.84	-0.90	-0.94	-0.47	-0.67	-0.57	-0.82	-0.19	1.33	1.9
13-25	0.3	0.83	-0.17	-0.30	-0.33	-0.90	-0.64	-0.46	-0.61	-0.16	-0.75	0.07	0.19	1.3
25-40	0.3	0.52	-0.14	-0.15	0.01	-0.83	-0.39	-0.38	-0.56	0.34	-0.64	0.42	-0.25	1.1
40-65	0.5	0.54	0.11	0.07	-0.02	-0.57	-0.11	0.51	-0.32	0.29	-0.83	0.78	-0.22	0.9
65-75														
IM6														
0-9	1.4	1.58	-0.56	-0.72	-0.72	-0.91	-0.77	-0.68	-0.80	-0.56	-0.76	-0.24	1.27	2.6
9-25	0.4	1.07	-0.47	-0.55	-0.56	-0.91	-0.62	-0.65	-0.75	-0.35	-0.72	-0.08	0.55	2.0
25-62	0.3	0.77	-0.34	-0.36	-0.27	-0.84	-0.60	-0.56	-0.71	-0.10	-0.73	-0.21	0.11	1.5
62-90	0.4	0.96	-0.50	-0.55	-0.52	-0.67	-0.59	-0.66	-0.76	-0.27	-0.78	-0.23	0.38	2.1
90-100	0.4	0.98	-0.55	-0.56	-0.51	-0.64	-0.95	-0.69	-0.78	-0.29	-0.89	-0.32	0.41	2.1
100-110		0.33												

Site /depth	Silt clay	Zr/ Ti $\times 10^{-3}$	τ_{Si}	τ_{Al}	τ_{Fe}	τ_{Ca}	τ_{Mg}	τ_{Na}	τ_{K}	τ_{Ti}	τ_{P}	Strain	τ_{Zr} (Ti)	$\frac{Zr_{soil}}{Zr_{rock}}$
IM7														
0-4	0.0	1.51	-0.61	-0.68	-0.81	-0.87	-0.89	-0.60	-0.79	-0.54	-0.81	-0.41	1.18	2.7
4-10	0.3	1.61	-0.62	-0.71	-0.85	-0.87	-0.91	-0.60	-0.79	-0.57	-0.80	-0.44	1.32	2.9
10-22	0.4	1.48	-0.61	-0.80	-0.83	-0.96	-0.91	-0.83	-0.81	-0.53	-0.83	-0.45	1.13	2.9
22-40	0.3	1.32	-0.57	-0.77	-0.79	-0.96	-0.89	-0.82	-0.80	-0.48	-0.76	-0.41	0.91	2.7
40-63	0.9	1.20	-0.61	-0.75	-0.74	-0.95	-0.86	-0.82	-0.80	-0.42	-0.74	-0.43	0.73	2.8
63-70	0.8	1.76	-0.67	-0.80	-0.80	-0.97	-0.90	-0.86	-0.85	-0.61	-0.81	-0.52	1.54	3.4
70-77	0.8	0.98	-0.50	-0.60	-0.54	-0.93	-0.67	-0.78	-0.76	-0.29	-0.70	-0.24	0.41	2.1
77-87	0.9	1.07	-0.54	-0.63	-0.58	-0.94	-0.67	-0.80	-0.78	-0.35	-0.70	-0.28	0.54	2.3
IM8														
0-7	6.0	1.58	-0.55	-0.74	-0.86	-0.91	-0.92	-0.66	-0.77	-0.56	-0.71	-0.38	1.27	2.6
7-25	0.3	1.10	-0.43	-0.58	-0.62	-0.92	-0.63	-0.60	-0.72	-0.37	-0.74	-0.24	0.58	1.9
25-46	0.4	0.98	-0.42	-0.49	-0.47	-0.90	-0.41	-0.59	-0.73	-0.29	-0.77	-0.12	0.41	1.8
46-62	0.3	1.08	-0.51	-0.58	-0.57	-0.91	-0.49	-0.64	-0.78	-0.36	-0.90	-0.28	0.55	2.1
62-90	0.3	1.15	-0.55	-0.61	-0.60	-0.84	-0.49	-0.66	-0.78	-0.40	-0.86	-0.32	0.66	2.3
IL1														
1-3	5.0	0.83	-0.35	-0.47	-0.63	-0.70	-0.94	-0.12	-0.75	-0.16	-0.63	0.04	0.20	1.7
3-11	3.7	0.78	-0.51	-0.54	-0.71	-0.75	-0.91	-0.25	-0.81	-0.12	-0.62	-0.29	0.13	2.1
11-30		0.67												
IL2														
0-10	1.4	0.99	-0.41	-0.53	-0.73	-0.76	-0.92	-0.24	-0.74	-0.30	-0.67	-0.17	0.42	1.9
10-39	1.0	0.93	-0.39	-0.53	-0.73	-0.76	-0.91	-0.27	-0.74	-0.25	-0.77	-0.16	0.34	1.8
39-60	0.8	1.14	-0.29	-0.49	-0.72	-0.75	-0.92	-0.22	-0.69	-0.39	-0.61	-0.04	0.64	1.6
60-80	0.6	0.97	-0.28	-0.43	-0.58	-0.75	-0.92	-0.19	-0.70	-0.28	-0.73	0.00	0.39	1.5
IL3														
0-2	0.8	0.94	-0.40	-0.49	-0.65	-0.72	-0.92	-0.18	-0.75	-0.26	-0.77	-0.04	0.35	1.8
2-25	11.0	0.91	-0.38	-0.46	-0.70	-0.71	-0.93	-0.09	-0.74	-0.24	-0.88	-0.17	0.31	1.7
25-47	2.0	0.73	-0.44	-0.52	-0.66	-0.74	-0.91	-0.22	-0.77	-0.05	-0.79	-0.25	0.05	1.9
47-70	2.0	0.74	-0.32	-0.37	-0.59	-0.70	-0.83	-0.11	-0.71	-0.06	-0.60	-0.06	0.06	1.6
IL4														
0-12	0.8	0.66	-0.15	-0.38	-0.70	-0.68	-0.89	0.03	-0.64	0.06	-0.84	0.16	-0.06	1.3
12-48	0.9	0.69	-0.05	-0.34	-0.68	-0.67	-0.87	0.11	-0.62	0.01	-0.48	0.28	-0.01	1.2
48-70	0.5	0.70	-0.03	-0.31	-0.48	-0.65	-0.92	0.15	-0.61	0.00	-0.47	0.31	0.00	1.2
70-85	3.3	0.75	-0.07	-0.33	-0.71	-0.65	-0.89	0.12	-0.61	-0.08	-0.49	0.25	0.08	1.2
85-100	2.2	0.72	-0.10	-0.38	-0.73	-0.67	-0.95	0.08	-0.64	-0.04	-0.68	0.19	0.04	1.3
IL5														
0-11	1.3	0.92	-0.39	-0.52	-0.82	-0.73	-0.94	-0.13	-0.75	-0.25	-0.66	-0.16	0.33	1.8
11-27	1.4	0.96	-0.44	-0.55	-0.83	-0.75	-0.94	-0.22	-0.76	-0.28	-0.79	-0.23	0.38	2.0
27-53	1.3	0.89	-0.30	-0.44	-0.83	-0.69	-0.94	0.01	-0.69	-0.22	-0.61	-0.04	0.29	1.6
53-70	1.9	0.95	-0.01	-0.24	-0.78	-0.59	-0.94	0.45	-0.56	-0.27	-0.91	0.34	0.37	1.1
IL6														

Site /depth	Silt clay	Zr/ Ti $\times 10^{-3}$	τ Si	τ Al	τ Fe	τ Ca	τ Mg	τ Na	τ K	τ Ti	τ P	Strain	τ Zr (Ti)	$\frac{Zr_{soil}}{Zr_{rock}}$
0-1	0.7	0.67	-0.26	-0.45	-0.67	-0.69	-0.86	-0.11	-0.71	0.03	-0.58	0.16	-0.03	1.5
1-24	2.5	0.77	-0.23	-0.42	-0.55	-0.69	-0.89	-0.08	-0.69	-0.10	-0.57	0.12	0.11	1.4
24-57	0.4	0.45	0.01	-0.05	0.09	-0.65	-0.36	-0.08	-0.58	0.54	-0.38	0.45	-0.35	1.0
57-67		2.54												
IL7														
0-1	1.0	0.47	-0.49	-0.59	-0.47	-0.78	-0.84	-0.42	-0.81	0.48	-0.49	-0.14	-0.32	2.0
1-16	1.7	0.39	-0.56	-0.61	-0.39	-0.81	-0.82	-0.51	-0.83	0.77	-0.55	-0.32	-0.44	2.3
16-30	0.5	0.37	-0.52	-0.56	-0.31	-0.81	-0.77	-0.48	-0.82	0.90	-0.50	-0.25	-0.47	2.1
30-63	0.3	0.35	-0.47	-0.46	-0.12	-0.81	-0.69	-0.48	-0.80	1.00	-0.55	-0.19	-0.50	1.8
63-110	0.6	0.35	-0.50	-0.45	-0.03	-0.80	-0.62	-0.52	-0.81	1.01	-0.56	-0.24	-0.50	1.9
110-120		0.27												
IL8														
0-13	0.9	0.52	-0.57	-0.65	-0.62	-0.87	-0.91	-0.55	-0.82	0.33	-0.58	-0.38	-0.25	2.5
13-53	0.5	0.43	-0.49	-0.48	-0.33	-0.84	-0.76	-0.55	-0.80	0.63	-0.68	-0.20	-0.39	1.9
53-70	1.4	0.42	-0.56	-0.52	-0.31	-0.83	-0.71	-0.61	-0.82	0.65	-0.51	-0.28	-0.39	2.1
70-85	2.5	0.41	-0.54	-0.51	-0.28	-0.77	-0.65	-0.58	-0.82	0.67	-0.60	-0.25	-0.40	2.1
85-100	2.5	0.35	-0.41	-0.28	0.06	-0.73	-0.54	-0.49	-0.74	0.98	-0.32	0.00	-0.50	1.5
IL9														
0-3	3.2	1.02	-0.59	-0.72	-0.70	-0.87	-0.90	-0.62	-0.83	-0.32	-0.45	-0.45	0.47	2.6
3-17	1.0	0.85	-0.58	-0.68	-0.62	-0.88	-0.87	-0.61	-0.82	-0.18	-0.68	-0.42	0.22	2.6
17-35	0.2	0.61	-0.56	-0.56	-0.36	-0.86	-0.65	-0.66	-0.82	0.14	-0.54	-0.37	-0.12	2.2
35-57	0.5	0.67	-0.59	-0.61	-0.44	-0.79	-0.66	-0.65	-0.82	0.03	-0.74	-0.41	-0.03	2.4
57-80	0.5	0.69	-0.63	-0.64	-0.49	-0.79	-0.62	-0.67	-0.85	0.00	-0.68	-0.37	0.00	2.6
80-110	1.7	0.63	-0.64	-0.62	-0.41	-0.73	-0.58	-0.67	-0.85	0.10	-0.68	-0.33	-0.09	2.6
110-130	2.8	0.61	-0.61	-0.60	-0.41	-0.55	-0.53	-0.63	-0.83	0.14	-0.74	-0.31	-0.12	2.4
IL10														
0-7	4.3	1.36	-0.83	-0.82	-0.66	-0.92	-0.80	-0.85	-0.91	-0.49	-0.70	-0.61	0.96	5.4
7-34	0.7	1.28	-0.78	-0.82	-0.80	-0.94	-0.91	-0.82	-0.90	-0.46	-0.87	-0.68	0.85	4.9
34-60	0.4	1.08	-0.72	-0.74	-0.65	-0.92	-0.83	-0.78	-0.88	-0.36	-0.71	-0.61	0.56	3.6
60-85	1.1	1.13	-0.75	-0.78	-0.70	-0.92	-0.82	-0.80	-0.89	-0.38	-0.85	-0.65	0.62	4.1
85-111	0.5	0.97	-0.76	-0.77	-0.68	-0.85	-0.72	-0.80	-0.89	-0.29	-0.79	-0.64	0.40	4.0
111-120	0.6	0.99	-0.74	-0.75	-0.64	-0.86	-0.73	-0.77	-0.87	-0.30	-0.78	-0.61	0.42	3.7
Pretoriuskop														
WH1														
0-4	7.0	1.43	-0.75	-0.92	-0.85	-0.98	-1.00	-0.94	-0.91	-0.52	-0.87	-0.65	1.07	4.9
4-30	1.0	1.28	-0.69	-0.91	-0.84	-0.98	-1.00	-0.93	-0.89	-0.46	-0.90	-0.62	0.85	4.1
30-76	0.9	1.42	-0.74	-0.90	-0.86	-0.99	-0.99	-0.95	-0.91	-0.51	-0.91	-0.64	1.05	4.7
76-105	1.2	1.64	-0.79	-0.89	-0.86	-0.99	-0.99	-0.96	-0.92	-0.58	-0.93	-0.71	1.36	5.6
105-125	0.9	1.69	-0.80	-0.90	-0.88	-0.99	-0.98	-0.96	-0.92	-0.59	-0.90	-0.76	1.43	6.0
125-146	1.0	1.75	-0.81	-0.92	-0.90	-0.99	-1.00	-0.96	-0.92	-0.60	-0.93	-0.76	1.52	6.3
146-180	3.8	1.96	-0.84	-0.92	-0.91	-0.99	-1.00	-0.96	-0.91	-0.65	-0.91	-0.79	1.83	7.2

Site /depth	Silt clay	Zr/ Ti $\times 10^{-3}$	τ_{Si}	τ_{Al}	τ_{Fe}	τ_{Ca}	τ_{Mg}	τ_{Na}	τ_{K}	τ_{Ti}	τ_{P}	Strain	τ_{Zr} (Ti)	$\frac{Zr_{soil}}{Zr_{rock}}$
180-212	1.0	1.55	-0.77	-0.84	-0.86	-0.98	-0.97	-0.93	-0.85	-0.55	-0.96	-0.68	1.24	4.8
WH2														
0-13	1.1	1.11	-0.64	-0.89	-0.91	-0.96	-0.99	-0.87	-0.88	-0.37	-0.88	-0.57	0.60	3.5
13-29	1.2	1.17	-0.60	-0.87	-0.90	-0.96	-0.99	-0.86	-0.87	-0.41	-0.87	-0.52	0.68	3.2
29-49	1.6	1.47	-0.73	-0.90	-0.92	-0.97	-1.00	-0.87	-0.89	-0.53	-0.91	-0.67	1.12	4.7
49-87	1.1	1.52	-0.75	-0.91	-0.93	-0.97	-1.00	-0.91	-0.90	-0.54	-0.96	-0.70	1.19	5.0
87-124	1.0	1.57	-0.75	-0.91	-0.92	-0.97	-0.99	-0.91	-0.90	-0.56	-0.96	-0.69	1.26	5.0
124-130	1.1	1.37	-0.76	-0.90	-0.81	-0.97	-1.00	-0.92	-0.90	-0.49	-0.98	-0.69	0.98	4.9
WH3														
0-17	0.5	1.17	-0.68	-0.88	-0.86	-0.96	-0.99	-0.87	-0.89	-0.40	-0.89	-0.60	0.68	3.9
17-58	0.3	1.14	-0.68	-0.88	-0.87	-0.96	-0.99	-0.87	-0.89	-0.39	-0.89	-0.61	0.64	3.9
58-88	0.9	1.32	-0.71	-0.88	-0.87	-0.97	-0.99	-0.88	-0.90	-0.48	-0.85	-0.64	0.91	4.3
88-112	1.5	1.52	-0.75	-0.90	-0.90	-0.97	-1.00	-0.90	-0.91	-0.54	-0.98	-0.69	1.19	4.9
112-128	1.5	1.56	-0.76	-0.90	-0.91	-0.97	-1.00	-0.89	-0.91	-0.56	-0.92	-0.70	1.25	5.2
128-140	4.3	1.72	-0.78	-0.91	-0.90	-0.97	-0.99	-0.91	-0.92	-0.60	-0.93	-0.73	1.48	5.7
WH4														
0-5	11.0	1.39	-0.72	-0.84	-0.90	-0.91	-0.99	-0.78	-0.87	-0.50	-0.85	-0.65	1.00	4.1
5-24	8.3	1.36	-0.80	-0.86	-0.91	-0.94	-0.99	-0.83	-0.89	-0.49	-0.93	-0.72	0.96	5.6
24-47	3.0	1.28	-0.80	-0.86	-0.91	-0.94	-0.98	-0.82	-0.90	-0.46	-0.96	-0.70	0.84	5.6
47-67	14.0	1.48	-0.84	-0.88	-0.92	-0.94	-0.99	-0.84	-0.92	-0.53	-0.97	-0.78	1.13	7.2
67-89	1.5	1.34	-0.82	-0.87	-0.92	-0.94	-0.99	-0.83	-0.91	-0.48	-0.93	-0.77	0.93	6.2
89-115	2.7	1.52	-0.82	-0.86	-0.87	-0.92	-0.95	-0.80	-0.92	-0.54	-0.93	-0.75	1.19	6.1
115-150	4.3	1.28	-0.81	-0.82	-0.77	-0.89	-0.87	-0.73	-0.92	-0.46	-0.84	-0.73	0.84	5.3
150-160		0.94												
WH5														
0-13	0.7	1.17	-0.66	-0.75	-0.86	-0.88	-0.97	-0.65	-0.85	-0.41	-0.87	-0.53	0.68	3.3
13-28	0.3	1.37	-0.71	-0.79	-0.91	-0.90	-0.97	-0.70	-0.87	-0.49	-0.89	-0.61	0.98	3.9
28-42	0.4	1.18	-0.68	-0.75	-0.89	-0.87	-0.96	-0.64	-0.87	-0.41	-0.88	-0.56	0.70	3.5
42-55	0.5	1.15	-0.70	-0.75	-0.89	-0.87	-0.98	-0.62	-0.87	-0.40	-0.83	-0.58	0.66	3.6
55-76	0.4	1.15	-0.73	-0.78	-0.87	-0.89	-0.96	-0.69	-0.89	-0.39	-0.85	-0.62	0.65	4.1
76-94	0.3	0.80	-0.59	-0.53	-0.27	-0.74	-0.74	-0.27	-0.85	-0.13	-0.65	-0.35	0.15	2.3
94-115	0.1	0.71	-0.58	-0.50	-0.28	-0.72	-0.57	-0.17	-0.85	-0.02	-0.55	-0.33	0.02	2.3
115-125	0.4	0.70	-0.52	-0.45	-0.33	-0.69	-0.54	-0.10	-0.83	-0.01	-0.49	-0.25	0.01	2.0
WH6														
0-10	0.9	0.92	-0.77	-0.78	-0.75	-0.92	-0.95	-0.80	-0.91	-0.24	-0.86	-0.52	0.32	4.3
10-29	0.0	0.32	-0.51	0.04	0.93	-0.86	-0.59	-0.78	-0.86	1.17	-0.57	0.20	-0.54	1.5
29-50	0.2	0.31	-0.45	0.20	1.03	-0.85	-0.45	-0.78	-0.86	1.27	-0.53	0.21	-0.56	1.3
50-80	0.0	0.30	-0.54	-0.14	0.97	-0.83	-0.52	-0.76	-0.87	1.30	-0.61	-0.10	-0.56	1.6
80-106	0.1	0.36	-0.53	-0.01	0.70	-0.83	-0.50	-0.69	-0.88	0.92	-0.74	-0.09	-0.48	1.6
106-116	0.2	0.58	-0.57	-0.22	0.07	-0.76	-0.70	-0.39	-0.90	0.19	-0.78	-0.22	-0.16	1.9
WM1														

Site /depth	Silt clay	Zr/ Ti $\times 10^{-3}$	τ_{Si}	τ_{Al}	τ_{Fe}	τ_{Ca}	τ_{Mg}	τ_{Na}	τ_{K}	τ_{Ti}	τ_{P}	Strain	τ_{Zr} (Ti)	$\frac{Zr_{soil}}{Zr_{rock}}$
0-10	1.4	1.58	-0.72	-0.87	-0.84	-0.99	-0.99	-0.94	-0.81	-0.56	-0.76	-0.59	1.28	4.3
10-23	1.7	1.55	-0.72	-0.87	-0.85	-0.99	-1.00	-0.94	-0.81	-0.55	-0.90	-0.65	1.24	4.3
23-49	1.2	1.32	-0.70	-0.86	-0.83	-0.99	-0.99	-0.92	-0.79	-0.47	-0.84	-0.57	0.90	3.9
49-106	0.8	1.46	-0.67	-0.85	-0.82	-0.99	-0.98	-0.95	-0.80	-0.52	-0.77	-0.56	1.10	3.6
106-135	0.8	1.51	-0.72	-0.86	-0.84	-0.99	-0.99	-0.94	-0.82	-0.54	-0.86	-0.66	1.18	4.3
135-157	1.0	1.50	-0.74	-0.87	-0.87	-0.99	-0.99	-0.95	-0.82	-0.54	-0.82	-0.67	1.17	4.5
157-170	0.6	1.48	-0.72	-0.82	-0.84	-0.99	-0.99	-0.94	-0.79	-0.53	-0.95	-0.63	1.14	4.1
WM2														
0-15	1.1	1.47	-0.67	-0.86	-0.82	-0.99	-1.00	-0.94	-0.79	-0.53	-0.83	-0.53	1.12	3.7
15-30	0.9	1.56	-0.70	-0.87	-0.84	-0.99	-0.99	-0.96	-0.81	-0.55	-0.85	-0.62	1.24	4.0
30-59	0.7	1.64	-0.72	-0.86	-0.84	-0.99	-1.00	-0.95	-0.83	-0.58	-0.85	-0.60	1.37	4.3
59-87	0.6	1.57	-0.71	-0.85	-0.85	-0.99	-0.99	-0.95	-0.82	-0.56	-0.80	-0.60	1.27	4.1
87-106	0.9	1.56	-0.71	-0.87	-0.86	-0.99	-1.00	-0.95	-0.83	-0.55	-0.85	-0.65	1.24	4.2
106-131	0.8	1.65	-0.76	-0.88	-0.88	-0.99	-0.99	-0.96	-0.84	-0.58	-0.91	-0.69	1.38	4.8
131-140	1.2	1.85	-0.80	-0.89	-0.89	-0.99	-0.99	-0.96	-0.85	-0.63	-0.89	-0.74	1.67	5.8
WM3														
0-17	1.5	1.17	-0.57	-0.84	-0.72	-0.99	-0.99	-0.93	-0.75	-0.41	-0.86	-0.47	0.69	2.9
17-36	0.3	0.96	-0.68	-0.85	-0.63	-0.99	-1.00	-0.95	-0.79	-0.28	-0.83	-0.58	0.38	3.6
36-71	0.6	1.52	-0.65	-0.82	-0.79	-0.99	-1.00	-0.95	-0.79	-0.54	-0.88	-0.55	1.20	3.4
71-86	0.5	1.46	-0.66	-0.82	-0.81	-0.99	-1.00	-0.94	-0.79	-0.53	-0.82	-0.56	1.11	3.4
86-115	0.6	1.62	-0.69	-0.85	-0.85	-0.99	-0.99	-0.95	-0.81	-0.57	-0.84	-0.61	1.33	3.9
115-141	0.6	1.48	-0.68	-0.80	-0.83	-0.99	-0.99	-0.95	-0.77	-0.53	-0.88	-0.57	1.13	3.5
141-149	0.6	1.42	-0.60	-0.73	-0.80	-0.99	-0.98	-0.92	-0.67	-0.51	-0.86	-0.47	1.05	2.9
WM4														
0-10	2.9	1.41	-0.64	-0.89	-0.87	-0.99	-1.00	-0.95	-0.84	-0.51	-0.88	-0.56	1.02	3.5
10-31	0.8	1.38	-0.66	-0.89	-0.87	-0.99	-0.99	-0.95	-0.85	-0.50	-0.89	-0.59	0.99	3.7
31-57	0.9	1.49	-0.64	-0.87	-0.86	-0.99	-1.00	-0.95	-0.86	-0.53	-0.76	-0.55	1.14	3.4
57-93	0.7	1.50	-0.65	-0.87	-0.86	-0.99	-0.99	-0.95	-0.86	-0.54	-0.82	-0.57	1.16	3.5
93-131	0.7	1.48	-0.70	-0.89	-0.90	-0.99	-1.00	-0.95	-0.88	-0.53	-0.90	-0.63	1.13	4.2
131-145	2.0	1.55	-0.75	-0.87	-0.88	-0.99	-0.99	-0.96	-0.86	-0.55	-0.82	-0.67	1.23	4.7
WM5														
0-12	0.5	1.38	-0.40	-0.86	-0.88	-0.98	-1.00	-0.88	-0.80	-0.50	-0.81	-0.30	0.98	2.2
12-50	1.1	1.44	-0.50	-0.87	-0.89	-0.99	-1.00	-0.91	-0.83	-0.52	-0.84	-0.42	1.07	2.6
50-96	1.0	1.57	-0.56	-0.89	-0.90	-0.99	-1.00	-0.91	-0.85	-0.56	-0.86	-0.48	1.26	2.9
96-128	1.3	1.81	-0.56	-0.90	-0.91	-0.99	-1.00	-0.93	-0.86	-0.62	-0.93	-0.50	1.60	3.0
128-152	1.7	1.65	-0.56	-0.91	-0.92	-0.99	-1.00	-0.93	-0.86	-0.58	-0.79	-0.49	1.38	3.0
152-185	0.9	2.02	-0.64	-0.91	-0.92	-0.99	-1.00	-0.94	-0.87	-0.66	-0.94	-0.58	1.92	3.6
185-200	2.7	1.87	-0.70	-0.92	-0.91	-0.99	-1.00	-0.95	-0.88	-0.63	-0.95	-0.64	1.70	4.2
WM6														
0-10	2.2	1.36	-0.55	-0.72	-0.88	-0.96	-1.00	-0.89	-0.84	-0.49	-0.68	-0.42	0.96	2.6
10-23	0.6	1.25	-0.51	-0.85	-0.87	-0.97	-0.99	-0.88	-0.82	-0.45	-0.76	-0.41	0.80	2.6

Site /depth	Silt clay	Zr/ Ti $\times 10^{-3}$	τ Si	τ Al	τ Fe	τ Ca	τ Mg	τ Na	τ K	τ Ti	τ P	Strain	τ Zr (Ti)	$\frac{Zr_{soil}}{Zr_{rock}}$
23-53	0.7	1.30	-0.53	-0.86	-0.87	-0.97	-1.00	-0.88	-0.83	-0.47	-0.77	-0.44	0.87	2.7
53-90	0.8	1.55	-0.57	-0.88	-0.89	-0.98	-1.00	-0.91	-0.85	-0.55	-0.79	-0.49	1.24	3.0
90-129	1.2	1.73	-0.63	-0.90	-0.92	-0.98	-1.00	-0.91	-0.87	-0.60	-0.94	-0.56	1.50	3.5
129-164	0.9	1.74	-0.60	-0.88	-0.90	-0.98	-1.00	-0.92	-0.83	-0.60	-0.87	-0.52	1.51	3.2
164-180	1.0	1.98	-0.74	-0.90	-0.92	-0.99	-1.00	-0.94	-0.87	-0.65	-0.87	-0.68	1.85	4.7
WM7														
0-11	2.0	1.28	-0.48	-0.85	-0.88	-0.97	-1.00	-0.88	-0.81	-0.46	-0.92	-0.38	0.84	2.5
11-29	0.5	1.21	-0.51	-0.85	-0.88	-0.97	-1.00	-0.87	-0.82	-0.43	-0.84	-0.42	0.74	2.6
29-61	0.4	1.37	-0.61	-0.87	-0.90	-0.97	-1.00	-0.90	-0.84	-0.49	-0.81	-0.52	0.97	3.2
61-107	0.4	1.48	-0.66	-0.88	-0.90	-0.98	-1.00	-0.91	-0.86	-0.53	-0.97	-0.59	1.14	3.7
107-152	1.1	1.50	-0.71	-0.89	-0.92	-0.98	-1.00	-0.92	-0.88	-0.54	-0.90	-0.65	1.16	4.3
152-165	0.8	1.79	-0.69	-0.89	-0.91	-0.98	-1.00	-0.92	-0.88	-0.61	-0.90	-0.62	1.58	4.0
165-190	1.5	1.77	-0.73	-0.88	-0.91	-0.98	-0.99	-0.93	-0.87	-0.61	-0.82	-0.67	1.56	4.6
190-210	1.1	1.69	-0.71	-0.85	-0.88	-0.98	-0.98	-0.91	-0.83	-0.59	-0.90	-0.62	1.44	4.1
WM8														
0-9	0.6	1.42	-0.65	-0.86	-0.91	-0.97	-1.00	-0.86	-0.83	-0.51	-0.88	-0.57	1.05	3.5
9-22	0.7	1.56	-0.64	-0.86	-0.92	-0.97	-1.00	-0.86	-0.84	-0.56	-0.88	-0.56	1.25	3.5
22-48	1.3	1.88	-0.73	-0.88	-0.94	-0.97	-1.00	-0.88	-0.86	-0.63	-0.98	-0.66	1.71	4.5
48-62	1.6	1.85	-0.70	-0.87	-0.93	-0.97	-1.00	-0.87	-0.84	-0.63	-0.95	-0.63	1.67	4.1
62-82	1.6	1.81	-0.65	-0.86	-0.89	-0.98	-1.00	-0.87	-0.81	-0.62	-0.88	-0.57	1.62	3.6
82-105	0.7	1.50	-0.66	-0.82	-0.82	-0.98	-0.98	-0.88	-0.78	-0.54	-0.88	-0.56	1.16	3.5
105-115	1.1	1.52	-0.75	-0.81	-0.84	-0.98	-0.98	-0.86	-0.82	-0.55	-0.91	-0.65	1.20	4.4
WM9														
0-8	0.5	1.67	-0.76	-0.86	-0.84	-0.98	-0.99	-0.90	-0.87	-0.59	-0.87	-0.68	1.41	4.7
8-20	0.4	1.24	-0.56	-0.74	-0.73	-0.94	-0.96	-0.81	-0.80	-0.44	-0.61	-0.42	0.79	2.6
20-40	0.1	0.93	0.32	-0.67	-0.49	-0.95	-1.00	-0.79	-0.65	-0.25	-0.37	0.56	0.33	1.0
40-80	0.1	0.41	-0.26	0.41	0.56	-0.93	-0.75	-0.80	-0.65	0.69	-0.25	0.38	-0.41	1.1
80-101	0.2	0.35	0.08	0.64	0.89	-0.88	-0.76	-0.40	-0.20	0.98	-0.25	0.85	-0.50	0.8
101-113	0.2	0.42	-0.02	0.30	0.65	-0.87	-0.74	-0.41	-0.42	0.64	-0.78	0.60	-0.39	1.0
113-120	0.3	0.43	0.77	1.11	0.59	-0.63	-0.78	1.08	0.28	0.60	-0.26	1.72	-0.38	0.6
WM10														
0-9	0.7	1.27	-0.70	-0.79	-0.79	-0.93	-0.97	-0.78	-0.89	-0.45	-0.89	-0.59	0.83	3.7
9-33	0.0	1.04	-0.66	-0.65	-0.62	-0.92	-0.92	-0.74	-0.88	-0.34	-0.72	-0.48	0.50	3.0
33-68	0.1	1.00	-0.62	-0.62	-0.61	-0.90	-0.88	-0.71	-0.88	-0.30	-0.77	-0.43	0.43	2.7
68-80	0.1	0.72	-0.57	-0.45	-0.29	-0.66	-0.72	-0.26	-0.87	-0.03	0.43	-0.30	0.03	2.2
WM11														
0-10	0.9	1.22	-0.72	-0.77	-0.85	-0.88	-0.98	-0.61	-0.88	-0.43	-0.84	-0.60	0.76	3.9
10-40	0.5	1.41	-0.76	-0.78	-0.85	-0.90	-0.98	-0.65	-0.89	-0.51	-0.86	-0.65	1.03	4.3
40-70	0.8	1.49	-0.80	-0.82	-0.87	-0.91	-0.99	-0.71	-0.90	-0.54	-0.88	-0.71	1.15	5.2
70-95	0.3	1.08	-0.76	-0.71	-0.64	-0.90	-0.89	-0.73	-0.89	-0.36	-0.84	-0.60	0.56	3.8
95-120	0.3	1.11	-0.78	-0.74	-0.69	-0.91	-0.90	-0.73	-0.90	-0.38	-0.81	-0.64	0.61	4.3

Site /depth	Silt clay	Zr/ Ti $\times 10^{-3}$	τ_{Si}	τ_{Al}	τ_{Fe}	τ_{Ca}	τ_{Mg}	τ_{Na}	τ_{K}	τ_{Ti}	τ_{P}	Strain	τ_{Zr} (Ti)	$\frac{Zr_{soil}}{Zr_{rock}}$
120-135	0.3	1.02	-0.74	-0.67	-0.52	-0.90	-0.86	-0.69	-0.84	-0.32	-0.76	-0.56	0.47	3.4
WL1														
0-8	7.0	2.0	-0.63	-0.89	-0.88	-0.96	-0.99	-0.93	-0.87	-0.65	-0.69	-0.48	1.84	3.3
8-17	6.0	1.8	-0.64	-0.90	-0.88	-0.98	-0.99	-0.93	-0.87	-0.61	-0.83	-0.57	1.54	3.5
17-39	3.5	1.8	-0.70	-0.91	-0.87	-0.98	-1.00	-0.94	-0.88	-0.62	-0.90	-0.60	1.60	4.2
39-70	5.0	2.0	-0.69	-0.90	-0.87	-0.98	-1.00	-0.93	-0.88	-0.65	-0.95	-0.60	1.85	4.1
70-93	3.5	2.0	-0.67	-0.90	-0.87	-0.98	-1.00	-0.90	-0.88	-0.65	-0.84	-0.62	1.85	3.8
93-115	1.4	1.8	-0.67	-0.85	-0.84	-0.98	-0.99	-0.94	-0.85	-0.61	-0.94	-0.58	1.58	3.6
115-142	1.4	1.8	-0.66	-0.85	-0.84	-0.98	-0.99	-0.93	-0.85	-0.62	-0.89	-0.58	1.64	3.6
142-164	1.4	1.9	-0.71	-0.86	-0.85	-0.97	-0.98	-0.91	-0.88	-0.63	-0.85	-0.63	1.70	4.1
164-184	0.6	1.6	-0.74	-0.81	-0.81	-0.97	-0.96	-0.86	-0.87	-0.56	-0.90	-0.64	1.29	4.2
184-205	1.6	1.3	-0.69	-0.73	-0.73	-0.95	-0.94	-0.71	-0.85	-0.47	-0.88	-0.56	0.88	3.4
205-230	2.0	0.7	-0.52	-0.52	-0.40	-0.80	-0.78	-0.37	-0.84	-0.06	-0.70	-0.27	0.06	2.1
230-245	2.3	0.7	-0.50	-0.46	-0.36	-0.77	-0.73	-0.26	-0.85	-0.01	-0.79	-0.24	0.01	2.0
WL2														
0-12	3.3	1.7	-0.45	-0.87	-0.87	-0.98	-0.99	-0.92	-0.81	-0.60	-0.82	-0.33	1.47	2.3
12-24	2.3	1.8	-0.50	-0.87	-0.90	-0.99	-1.00	-0.92	-0.80	-0.61	-0.84	-0.40	1.55	2.5
24-39	3.3	1.9	-0.46	-0.88	-0.90	-0.99	-1.00	-0.93	-0.82	-0.63	-0.83	-0.37	1.71	2.4
39-71	1.8	1.9	-0.57	-0.88	-0.91	-0.99	-0.99	-0.94	-0.83	-0.63	-0.86	-0.49	1.72	3.0
71-94	9.0	1.9	-0.58	-0.89	-0.92	-0.99	-1.00	-0.91	-0.84	-0.63	-0.87	-0.51	1.74	3.1
94-119	8.0	2.0	-0.58	-0.89	-0.90	-0.99	-1.00	-0.94	-0.84	-0.65	-0.93	-0.51	1.82	3.1
94-150	3.0	2.0	-0.72	-0.90	-0.94	-0.99	-0.99	-0.95	-0.87	-0.65	-0.95	-0.66	1.85	4.5
150-172	3.4	2.0	-0.80	-0.92	-0.94	-1.00	-1.00	-0.96	-0.88	-0.66	-0.97	-0.75	1.90	6.0
172-198	24.0	2.1	-0.80	-0.90	-0.94	-1.00	-1.00	-0.94	-0.87	-0.68	-0.98	-0.75	2.09	6.1
WL3														
0-5	7.0	2.2	-0.67	-0.84	-0.91	-0.97	-1.00	-0.87	-0.79	-0.68	-0.88	-0.57	2.16	3.6
5-17	10.0	2.2	-0.64	-0.83	-0.91	-0.97	-1.00	-0.87	-0.79	-0.69	-0.94	-0.54	2.20	3.3
17-26	11.0	2.5	-0.66	-0.83	-0.93	-0.97	-1.00	-0.88	-0.80	-0.73	-0.88	-0.57	2.64	3.5
26-45	11.0	2.0	-0.65	-0.85	-0.90	-0.97	-0.99	-0.87	-0.80	-0.65	-0.88	-0.56	1.89	3.5
45-60	3.0	2.2	-0.69	-0.85	-0.90	-0.97	-1.00	-0.88	-0.82	-0.68	-0.89	-0.60	2.13	3.9
60-77	1.2	2.2	-0.64	-0.83	-0.90	-0.97	-0.99	-0.87	-0.77	-0.68	-0.94	-0.54	2.12	3.3
77-98	0.6	2.1	-0.59	-0.78	-0.85	-0.96	-0.99	-0.83	-0.73	-0.67	-0.93	-0.47	2.00	2.9
98-132	1.1	1.0	-0.39	-0.46	-0.57	-0.84	-0.89	-0.40	-0.69	-0.27	-0.94	-0.12	0.37	1.7
132-155	15.0	0.8	-0.37	-0.41	-0.50	-0.81	-0.86	-0.37	-0.68	-0.17	-0.87	-0.07	0.20	1.6
155-165	12.0	0.7	-0.12	-0.18	-0.41	-0.76	-0.86	-0.11	-0.52	0.02	-0.66	0.26	-0.02	1.2
WL4														
0-9	5.5	2.4	-0.73	-0.84	-0.89	-0.96	-0.99	-0.76	-0.87	-0.71	-0.90	-0.58	2.50	4.2
9-24	2.3	2.1	-0.70	-0.82	-0.90	-0.96	-0.99	-0.74	-0.86	-0.67	-0.89	-0.58	2.00	3.9
24-41	14.0	1.9	-0.50	-0.77	-0.84	-0.96	-1.00	-0.66	-0.77	-0.63	-0.91	-0.33	1.68	2.4
41-75	0.4	1.2	-0.56	-0.60	-0.60	-0.94	-0.91	-0.70	-0.79	-0.44	-0.82	-0.45	0.80	2.3
75-110	0.5	0.9	-0.50	-0.43	-0.47	-0.88	-0.81	-0.46	-0.72	-0.20	-0.68	-0.33	0.24	1.9

Site /depth	Silt clay	Zr/ Ti $\times 10^{-3}$	τ_{Si}	τ_{Al}	τ_{Fe}	τ_{Ca}	τ_{Mg}	τ_{Na}	τ_{K}	τ_{Ti}	τ_{P}	Strain	τ_{Zr} (Ti)	$\frac{Zr_{soil}}{Zr_{rock}}$
110-120		0.9												
WL5														
0-14	8.0	1.8	-0.75	-0.85	-0.86	-0.97	-0.98	-0.79	-0.88	-0.62	-0.95	-0.63	1.60	4.5
14-40	1.6	1.7	-0.74	-0.82	-0.84	-0.96	-0.97	-0.77	-0.87	-0.59	-0.85	-0.62	1.45	4.3
40-60	0.0	0.8	-0.49	-0.31	-0.23	-0.91	-0.77	-0.49	-0.67	-0.13	-0.77	-0.22	0.15	1.8
60-70		0.3												
WL6														
0-11	5.0	1.5	-0.70	-0.87	-0.83	-0.97	-0.97	-0.86	-0.90	-0.54	-0.89	-0.57	1.17	3.9
11-40	0.3	1.1	-0.52	-0.68	-0.56	-0.95	-0.87	-0.81	-0.84	-0.38	-0.91	-0.41	0.63	2.3
40-63	0.3	1.1	-0.50	-0.64	-0.46	-0.92	-0.82	-0.78	-0.83	-0.36	-0.81	-0.36	0.56	2.1
63-84	0.1	1.0	-0.46	-0.62	-0.45	-0.92	-0.81	-0.78	-0.82	-0.33	-0.90	-0.36	0.49	2.0
84-120	0.3	0.9	-0.41	-0.57	-0.39	-0.93	-0.75	-0.75	-0.82	-0.23	-0.77	-0.28	0.30	1.8

CHAPTER 5: CHEMICAL MASS BALANCE ON GEOLOGICALLY COMPLEX CATENAS ALONG GRADIENTS OF RELIEF AND CLIMATE II: STRAIN AND MAJOR ELEMENT LOSS/GAIN

1. INTRODUCTION

Kruger national park is a valuable setting akin to the model ecosystem of Hawaii (Vitousek, 2004) to investigate the coupled impacts of soil-forming factors (Jenny, 1941) on weathering of rock to soil. The conversion of rock to soil entails a number of interacting processes whose magnitudes depend on climate, hillslope length and hillslope position, among other things (Birkeland, 1999). These processes include mineral transformations and elemental translocations whose net effect is loss or gain of a specific element at some point in the landscape (Sommer and Schlichting, 1997). Since the original elemental budgets in soils come from rock, it is against concentration in rock that losses and gains are assessed using geochemical mass balance (Brimhall and Dietrich, 1987).

The fate of major elements released by weathering of primary minerals that form the rocks underlying catenas is subject to: (1) interaction of an element with the soil environment (Birkeland, 1999; Schaetzl and Anderson, 2005) entailing whether the element is taken up by plants or not, whether it is soluble in water, participation of the element in clay formation, etc; (2) the topographic setting *i.e.* how steep the catena is relative to its length – a short, steep catena will more likely be completely leached of an element compared to a longer, gentler catena, other things being equal; and (3) climate,

through its control on effective soil moisture, is the ultimate driver of elemental translocations (Chadwick et al., 2003; White and Blum, 1995) so that wetter catenas will be more leached of mobile elements. The very few mass balance-based studies investigating elemental exchanges across catenas have only done so on single catenas (Sommer et al., 2000; Yoo et al., 2007) but see Tardy et al. (1973) and Birkeland et al. (1991) for mineralogical and morphological analogues using idealized catenas.

The aim of this study was to interpret the geochemical trajectories of major rock forming elements during soil formation on catenas sampled along gradients of topography and climate. Soil profiles were sampled to rock extensively across nine catenas and I show how a narrow precipitation gradient between 400 and 750 mm impacts chemical weathering and soil development along the catenas.

2. MATERIALS AND METHODS

Most of the methods and study site descriptions have been discussed in the previous chapters. But briefly, soils were sampled in the 9-box relief by climate matrix to evaluate weathering extent by geochemical mass balance. Samples were analysed for major element and zirconium concentrations and data were presented on depth-weighted average basis. I focused on two aspects of mass balance: the calculation of volumetric strain along sampled pedons and the examination of the fate of major elements along catenas.

3. RESULTS

3.1 Zirconium-based soil expansion/collapse

After selecting Zr as the index element in the previous chapter, soil strain was calculated by the equation

$$\text{strain} = \frac{\rho_{\text{granite}} [\text{Zr}]_{\text{model parent material}}}{\rho_{\text{soil}} [\text{Zr}]_{\text{soil}}}$$

to determine the volumetric expansion/collapse of soils along catenas in the relief-climate matrix.

Shingwedzi soils experienced positive strain in most pedons regardless of relief and catena position. Depth-weighted strains ranged between a collapse of 10 % in DL3 and an almost two-fold expansion relative to rock volume in DM3. On the shortest catena, DH, high expansion occurred at the crest (40 %) and in the toeslope pedon (30 %), with a 5 % minimum expansion in the central soil (Fig. 1). In the middle relief hillslope, DM, similar patterns to DH were observed but occurred over a longer distance. There was relatively high expansion on the crest (42 %), lowered expansion in the next pedon, DM2 (17 %) and a 97 % maximum expansion in DM3. The rest of the catena spanning DM4 to DM5 was characterized by comparatively unchanged volume relative to rock (< 5 % expansion throughout) (Fig. 1). The longest Shingwedzi catena, DL, was the only one with some collapse in its soils, but it also experienced expansion in most sampled locations. The crest underwent maximum expansion to 38 % of the original volume of rock, proceeded by a reduced expansion in DL2 (26 %) down to a net collapse of 11 % in DL3. Strain reverted to expansion in DL4 with a 25 % volumetric increase;

and, similar to DM, soils in the distal portion of DL hovered around the zero strain mark from 2 % collapse in DL5, 1 % expansion in DL6 and lastly, 9 % expansion in DL7 (Fig. 1).

In Skukuza, soils were generally more collapsed than in Shingwedzi with less pronounced expansions. The overall strain in Skukuza ranged between a 64 % collapse to an expansion of 37 %. In the short catena, IH, all soils experienced negative strains. The crest was the most collapsed with a 41 % volumetric reduction and the minimum collapse occurred in IH4 at just 2 % less volume than the rock, while the most distal soil, IH5 was 22 % collapsed (Fig 1). On the whole, the general trend on IH was maximum collapse in near-crest positions and less soil shrinkage at and near the toeslope. IM, on the other hand, had 50 % maximum collapse in IM2 and 37 % maximum expansion in IM5 (Fig. 1). The general trend in IM too was collapse in near-crest positions and reduced collapse towards the toeslope. The longest catena in Skukuza, IL, had strains in the range 64 % collapse in the most distal soil (IL10) and 31 % dilation in IL6. Most of the soils had negative strains except IL6 and IL4 (25 %). The zone straddling the crest and IL4 had collapses not exceeding 20 % while the downslope zone from IL6 experienced a monotonic increase in collapse culminating in 64 % in IL10 (Fig. 1).

Pretoriuskop catenas were much more collapsed than catenas in the drier climates. The high relief catena in Pretoriuskop was over 40 % collapsed in 5 of the six soils sampled representing over 90% (WH1, 70 % maximum collapse; to WH5, 40 % collapse) of the catena's extent. The last pedon sampled, DL6, almost experienced an expansion with the 4 % collapse (Fig. 1). In the middle relief catena, there was in excess of 50 % collapse in the greater extent of the hillslope (82 %), from WM1 with some 60 %

collapse to WM8 also attaining a 60 % collapse (Fig. 1). The only expanded pedon on WM was WM9 with a 44 % dilation, with soils below reverting to collapse in excess of 50 %. Finally, Pretoriuskop's low relief catena was characterized by wholesale collapse between 34 (in WL3) and 56 % (in WL5), but overall, as in the other catenas sampled, less collapsed soils occurred at the toeslope (Fig. 1).

3.2 Fate of Silica

Losses and gains of Si and other major elements were estimated with the equation

$$\tau_{j,w} = \left(\frac{C_{j,w}}{C_{j,p}} \times \frac{C_{i,w}}{C_{i,p}} \right) - 1$$

with zirconium as the index element as detailed in chapter 2. Soils in Shingwedzi had depth weighted average silica losses between 48 % and a 19 % net gain (Fig. 2). In the steepest catena, Si loss was most pronounced in the central pedon, DH2. Soils on either side of DH2 both had less Si losses, but due to completely different mechanisms. At the crest, losses were limited by a small contributing area while in DH3 at the toeslope, excessive losses were curtailed by augmentation with upslope-sourced Si. On DM, Si was lost from the crest to DM2 in about equal magnitudes, indicating that Si delivery into DM2 balanced the losses necessitated by increased contributing area. Downslope in clay-rich DM3, Si showed absolute gains which decreased sharply in the three distal soils. The low relief catena experienced Si loss at the crest, DL2 and peak Si loss in DL3. Some of the leached Si accumulated in DL4 which was the least Si-leached pedon. Losses continued progressively from DL4 right across the catena, presumably driven by moister conditions towards the toeslope.

Si loss was generally higher in Skukuza than in Shingwedzi, in the range 7 % to 76 %. On IH, Si loss peaked at the crest and decreased downslope suggesting that Si was translocated from points further upslope, but the pattern was not straightforward as evident in the erratic wavering about the range 38 % to 50 %. The middle relief catena, IM, had more pronounced Si augmentation in the clay-rich pedon, IM5, which had the least Si loss with about 90 % Si remaining (% remaining means 100 minus % lost, here and throughout). Below IM5, soils again experienced high losses of Si in the wetter sections of the catena. In the low relief catena, IL, Si was lost in excess of 34 % from the crest to IL3, the zone spanning IL4 to IL6 had reduced Si losses with 93 % Si remaining, while beyond IL6, Si was lost incrementally towards a 76 % peak loss in IL10.

Wet Pretoriuskop was even more Si-leached with losses ranging between 8 % and 81 %. The most highly leached soils occurred in the clay poor fractions of the three hillslopes in Pretoriuskop. Distal soils, through massive losses upslope and deposition downslope, were consequently less depleted in Si, but not sufficiently to impart net gains. The minimum loss of Si in Pretoriuskop occurred in WM9 with 92 % remaining, far greater retention of Si than other soils sampled in Pretoriuskop (Fig. 2).

3.3 Fate of Aluminium

The losses seen in silica were also experienced by aluminium, which closely resembled Si in its weathering trends along catenas. The main distinctions were in magnitudes of gains and losses rather than general patterns across catenas. On DH, for example, the Si (Fig. 2) and Al (Fig.3) curves were nearly identical in sign and trend but

were set apart by higher Al losses. Aluminum loss in excess of silica loss is an odd result since Al is conventionally held to be more recalcitrant than Si. In the soil environment of Shingwedzi's DH however, Si losses were off-set by much Si held in un-weathered quartz in the predominantly sandy soils of the catena. In DM, the role of clay in retaining Al was well displayed in the clay-rich pedon, DM3, where Al gain was greater than Si gain, despite higher Al losses in the surrounding soils, both upslope and downslope of DM3. In the low relief catena, DL, the loss of Al always exceeded Si loss except in the two clay-rich pedons furthest downslope.

Likewise in Skukuza and Pretoriuskop, Al loss was greater than Si loss, but trends were generally identical. The retention of Al in clay-rich soils was shown by less Al loss in WH6 and WM9 (where there was an actual Al gain against Si loss) (Fig. 3).

3.4 Fate of Calcium

Calcium was the most extensively leached element in the climate by relief matrix across Kruger (Fig. 4). It was almost completely removed from some pedons in wet Pretoriuskop with losses up to 99 %. In dry Shingwedzi, losses in DH were ≥ 50 % in all three soils sampled. Calcium lost from DM was less than that lost from DH, even though DM had moister soils due to a bigger catchment. Losses of Ca in DM occurred in the narrow range between 30 % and 46 %. The clay-rich DM3 did not experience Ca gain but had slightly reduced Ca loss (30 %) compared to other soils on the catena. Towards the toeslope on DM, calcium losses exceeded 30 % and peaked at 46 % in DM5. In the low relief catena, DL, calcium loss hovered around the 50 % mark from the crest to DL5,

with the remaining DL6 and DL7 experiencing less Ca loss (34 % and 46 % respectively).

Fractional losses of Ca in Skukuza exceeded those in Shingwedzi, and ranged between 66 % and 94 %. On IH, the loss of calcium was highest in the clay-poor pedons in the section between IH1 and IH3. Losses in the two most distal soils, IH4 and IH5, were subdued probably as a result of Ca translocated from the leached, upslope soils. In the middle relief catena, IM, Ca mass balance was dominated by wholesale losses throughout the catena, but slightly less losses in the clay-rich, central pedons, IM4 to IM6. In the low relief catena, losses were uniformly high with slight augmentation in the central pedons. Overall, Skukuza experienced high Ca losses and no gains with small variations about an essentially uniform pattern of high Ca loss.

The average Ca loss in Pretoriuskop ranged between a 99 % high and a low of 82 %. The distal sections of the three Pretoriuskop catenas were only sparingly augmented with upslope-derived Ca indicating exorbitant calcium leaching from all positions of the wet catenas (Fig. 4).

3.5 Fate of Potassium

More potassium was lost from Shingwedzi soils than either Si or Al, with absolute gains in DH1 and DL1, probably added by dust (Fig. 5). In detail, the fractional change in K on DH, the short catena, ranged between a gain of approximately 1 % on the crest to a maximum loss of 23 % in the central pedon. The middle relief catena, on the other hand, had K loss throughout, in the range 53 % in DM4 to 15 % in clay-rich DM3. Overall, K

losses in DM were relatively uniform and below losses recorded in DH. Like DH1, the crest on DL experienced K gain, also not very much at 8 %, with the rest of the catena losing K relative to rock concentrations up to a 61 % peak loss in DL7, the last soil sampled.

Higher rainfall in Skukuza led to more K loss than in Shingwedzi, between 50 % and 89 %. On IH, peak loss of K occurred in the crest while soils further downslope experienced less K loss. The middle relief catena had K loss in all pedons with the minimum in IM5, the clay rich pedon, wherein half the K originally in rock remained. In IL, K losses exceeded those in the shorter catenas of Skukuza. The losses therein were relatively uniform in the range 62 % to 89 % for the most part, with slightly less loss in the clay rich zone transecting IL4 and IL6.

In Pretoriusskop, K loss was massive, between 52 % and 91 %. Potassium loss in the high relief catena was 86 % and above for all soils sampled. Likewise in WM, losses were high except in the clay-rich soils which had only a 52 % K loss. The low relief catena was also extremely leached in K with faintly less losses at the toeslope (Fig. 5).

3.6 Fate of Sodium

As expected, the losses of Na were generally higher than the losses of both Si and Al (Fig. 6). In Shingwedzi, Na loss ranged between 28% and 71% without any gains. The shortest catena, DH, experienced Na loss with trends similar to those seen in Ca. With increased contributing area in DM, sodium, unlike Si and Al did not show absolute gains in DM3, the clay-rich pedon, but had minimum losses therein. Further downslope in the

wetter section of the catena, losses increased relative to those in the area between the crest and DM3. Patterns in the low relief catena of Shingwedzi, DL, reflected sodium's susceptibility to leaching with high losses all through the catena.

Strangely, increased rainfall in Skukuza led to somewhat less Na loss than in Shingwedzi, although the maximum Na loss was higher in Skukuza, 81 % versus 71 %. The high relief catena in Skukuza experienced Na losses of 52 % at the crest and 53 % in the most distal soil. Intervening soils had lower Na losses which increased monotonically from 37 % in IL2 to 47 % in IL4. The leaching of sodium in the middle relief catena was more varied in the range 7 % to 80 %. At the crest in IM, Na loss was 53 %, followed by a steady decrease in loss culminating in 93 % Na retention in IM5, the clay-rich pedon. The increased retention of sodium in the area between IM2 and IM5 was due to augmentation albeit not sufficient to yield a net gain in sodium. Below IM5 the trend of decreasing Na loss was reversed with increased losses in IM6 and IM7. In the low relief catena, there was actual gain in sodium. The gain occurred following increasingly less loss between the crest and IL3. Downslope the 10 % Na gain in IL3, there was progressive loss of Na from a net gain of 1 % in IL4 to a maximum loss of 81 % in IL10, the furthest downslope soil.

Similar to Ca and K, the Pretoriuskop Na pattern was much simpler and clearer; immense losses in the clay-poor soils from the crest and downslope through much of the hillslopes, and slightly reduced losses in distal soils with more clay (Fig. 6).

3.7 Fate of Phosphorus

The range of P loss in Shingwedzi was 47 % to 86 %, bizarrely far higher than all other elements considered (Fig. 7). Since plants utilize more P than all other rock-derived elements, P loss can be explained by incorporation into plant matter followed by combustion and associated loss of P with burnt plant material. In the short catena, DH, the loss of P increased progressively downslope from 61 % at the crest to 81 % in the toeslope. Losses of P were high still in the middle relief catena, with minimum loss in the clay rich pedon, DM3 at 63 % P loss, while soils further downslope experienced up to 86 % loss of P (in DM6). In the low relief catena, P losses were between 47 % and 67 %, and lacked a systematic trend across the catena.

Higher rainfall in Skukuza led to losses of P between 50 % and 98 %. The high relief catena, IH, had generally lower P losses in the distal soils with about 50 % P remaining and higher P losses in the zone between the crest (84 %) and IH3 (89 %). Moister conditions in the middle relief catena saw a much narrower range in P loss outside the crest (98 %) between 62 % and 83 %. The low relief catena had greater P retention than both IH and IM, with losses between 46 % and 80 %.

As with other elements, the loss of P was most pronounced in Pretoriuskop, between 40 % and 91 %. Most soils had high P loss except the clay-rich soils in toeslope positions of the three catenas (Fig 7).

3.8 Fate of Magnesium

Magnesium, unlike other base cations had net gains in Shingwedzi (Fig. 8). The fractional change in Mg across Shingwedzi catenas was from a maximum loss of 87 % to a maximum gain of 73 %. In DH, Mg was lost to a progressively greater extent with increased distance from the crest. With reduced relief in DM, the loss of Mg was above 50 % in the first two soils from the crest, to over 50 % gain in DM3, the clay-rich pedon, and near zero loss/ gain in the last three soils. The entire DL had less Mg loss than all of DH and the clay-poor section of DM.

Magnesium losses in Skukuza were between 44 % and 97 %. In the high relief catena (IH), there were relatively high Mg losses from the first three soils starting at the crest (between 82 % and 97 %) and less loss from the last two soils towards the toeslope (between 49 % and 59 %). For IM, magnesium experienced losses in excess of 70 % from the crest to IM4. In the clay-rich IM5, Mg loss was lowest at 44 %. Soils downslope from IM5 experienced more Mg loss than IM5 all the way towards the last soil, which had a 53 % Mg loss. In the low relief catena of Skukuza, Mg loss was very high in the greater proportion of the hillslope between the crest and IL5, with losses greater than 90 % throughout that zone. Soils from IL6 to IL10 had less Mg loss (58 % to 81 %).

By the peak rainfall in Pretoriuskop, Mg was completely annihilated from most of the catenas to almost 100 % depletion in some soils. Only soils in the distal locations were spared Mg losses over 90 % (Fig. 8).

3.9 Fate of Iron

The Shingwedzi catenas generally gained Fe compared to those in wetter climates. The fractional change in Fe in all Shingwedzi catenas ranged from a 40 % loss to a gain of 184 % (Fig. 9). On DH, iron experienced net losses in the three low-clay soils between 22 % and 40 %. In the middle relief catena, iron was gained in all but DM2 with a 19 % loss against concentrations in the parent material. Gains at the crest were small (8 %) with DM3 gaining the most iron calculated at 184 %. Iron was highly variable on the low relief catena, with losses peaking at 31 % and up to a 160 % gain. The oscillations and crossovers in the magnitude and sign of Fe gain/ loss may result from alternating zones of reducing and oxidizing conditions on the catena. The redox dynamics, together with aeolian inputs, may have played big roles in Fe release and mobilization on DL and the Shingwedzi area in general.

In Skukuza, Fe was lost in all pedons between a high of 84 % and a low of 15 %. The high relief catena had Fe losses between 28 % (IH3) and 84 % (IH4) with reduced losses in the distal soils. Iron mobilization on the middle relief catena was characterized by high losses in the clay-poor soils and greater iron conservation in the clay-rich soils, especially IM5 with an iron loss of 23 % compared to losses in excess of 70 % in the soils upslope of it. A pattern identical to IM was identified in IL as well; high Fe losses in skeletal soils with low clay and reduced Fe loss in the distal soils with more clay. As with other elements, loss of Fe in Pretoriuskop was immense, up to 92 % in one pedon. And iron, much like Ti and unlike Al, was gained substantially in WH6 and WM9, and so appeared to be less mobile than Al (Fig. 9).

4. DISCUSSION

In this section, I discuss the strain and mass losses of elements in relation to the amount of clay in the soil, since clay was advocated as a master soil property from which other soil properties can be inferred (Chapter 3). Elemental losses and gains will be examined in terms of the clay forming elements (Si, Al, Fe, and Ti) and the base cations (Ca, Mg, Na, K). The evaluation will be in three parts: (1) the relative position of the maximum retention of an element on each catena in relation to the maximum retention of other elements (2) the relative position of an element's maximum retention point evaluated against relief class in a climate zone; and (3) the relative position of an element's maximum retention point evaluated against increasing effective rainfall within relief classes.

4.1 Strain – collapse and dilation of profiles

The relative location of maximum strain, whether negative (least collapse) or positive (most dilation) and maximum clay % on catenas across relief class in each climate zone were 5 % (dilation, where X percent represents the proportion of hillslope relative to the crest where the crest is 0 % of the hillslope), 60 % (dilation) and 1 % (dilation) in Shingwedzi; 81 % (collapse), 37 % (dilation) and 61 % (dilation) in Skukuza; and 99 % (collapse), 82 % (dilation) and 87 % (collapse) in Pretoriuskop (Fig. 10). All maximum dilations in Skukuza and Pretoriuskop catenas coincided – within

reason – with maxima in clay. In Shingwedzi, only DM had peak dilation and peak clay in the same pedon, while on both DH and DL maximum strain and maximum clay were decoupled (Fig. 10).

The overlap in locations of maximum strain and maximum clay confirms that where strain was high, material generally accumulated, some in the form of clay. This means material translocated from points upslope at least partly compensated for weathering and leaching driven losses downslope. Where maxima in strain and clay fell in different parts of the catena it is likely that additions of dust and carbon assimilation were more important than material redistribution. This was particularly the case in the Shingwedzi catenas.

Turning to peak strain in relation to relief and climate, starting with relief. In Shingwedzi, maximum strains on the high and low relief catenas (both dilations) occurred at the crest (Fig. 10). Therefore, dust addition overwhelmed the weathering signal resulting in dilations at the crests despite lacking upslope contributing area. In Skukuza, maximum dilations shifted upslope between IH (81 %) and IM (37 %), then shifted downslope between IM and IL (61 %). This pattern is reminiscent of maximum clay extent in Skukuza, which peaked in the middle relief catena (Chapter 3). Thus with strain, the maximum retention of weathered material occurred in the middle relief catena. Pretoriuskop catenas had patterns similar to those in Skukuza.

Moving on to the climatic imprint on strain. As stated in the previous chapter, dust likely falls everywhere but its fine particle size means that it is rapidly weathered in the wetter sites and persists as an identifiable influence on element mass balances only in dry Shingwedzi. The maximum strain location in Shingwedzi was therefore more

associated with dust addition than weathering. The trends between Skukuza and Pretoriuskop indicate that the point of maximum retention of weathering products shifted downslope with increased rainfall. Shifts were 81 – 99 % in high relief catenas, 37 – 82 % in middle relief catenas and 61 – 87 % in low relief catenas.

4.2 Clay forming elements

4.2.1 Shingwedzi

In DH, Silica and Al retentions peaked at the crest in conjunction with maximum dilation suggesting that the crest was the locus of the most intense dust accretion (Fig. 10). The Fe and Ti peaks were located further downslope the catena and coincided with peak clay. It appears that Fe and Ti were mobilized from the crest in association with clay in excess of Si and Al translocations. A reasonable explanation is addition of pre-weathered Fe and Ti minerals in much greater abundance than added Si and Al, followed by subsequent translocation downslope. In DM, the peak retention for all clay-forming elements co-occurred with maximum strain and maximum clay indicating that all contributed to the material build-up and high dilation in DM3. Similar to DH, DL's Fe and Ti maximum retentions were downslope of Si and Al's, and an identical process to DH's can be invoked *i.e.* excess addition of Fe-Ti and translocation downslope. In the relief space of Shingwedzi, patterns were confounded by dust addition thus obscuring the direct impact of increasing catena length on the locus of maximum retention of each element. Regardless, Fe and Ti experienced systematic shifts downslope as a function of

hillslope length. Silica and Al, on the other hand, essentially displayed shifts in response to dust dynamics rather than increasing water availability (Fig. 10). The Shingwedzi catenas were under conditions too dry to drive clear hillslope differentiation by material retranslocation.

4.2.2 Skukuza and Pretoriuskop

In both IH and IM, the location of the maximum retention of all clay-forming elements coincided with maximum strain in IH4 (81 %) and IM5 (47 %), respectively (Fig 10). In Pretoriuskop's WH and WM as well, there were overlapping occurrences of all clay-forming elements and strain, but there; the overlap was also in tandem with maximum clay (in WH6 (99 %) and WM9 (82 %), respectively). Unlike the high and middle relief catenas, the low relief catenas in the Skukuza-Pretoriuskop area presented slightly more complex patterns.

On IL in Skukuza, the only elemental overlap was between Fe and Ti with maximum clay in IL7 (69 %). Aluminium retention peaked in IL6 (61 %) in synch with peak dilation while peak Si retention was further upslope in IL4 (48 %). The downslope sequence of maximum retention was therefore Si, Al and Ti (and Fe) in the downslope direction from the crest. In magnitude terms the Ti peak tau was highest (net gain, in fact), next was Si, then Al. Since the accumulated Ti in IL7 was invariably sourced from upslope, and since Ti is more immobile than Si and Al, there must have been a time when the Si and Al tau peaks were at IL7 or further downslope. Thus the current distribution of the elements may be a vestige of past processes.

For Pretoriuskop's WL, the most distal soil sampled (WL6 in 99 % of the catena) was the locus of maxima in the retentions of Si, Fe and Ti; as well as maximum clay. The peak strain and peak retention of Al were 150 m upslope from the hotspot in WL6.

The increased rainfall between Skukuza and Pretoriuskop resulted in a downslope shift in the position of maximum retention of the respective elements (Fig. 10).

4.3 Base cations

4.3.1 Shingwedzi

In DH, Ca and Na were leached furthest downslope and did not contribute to the high strain experienced at the crest, only the Mg and K peak retentions coincided with peak strain (Fig. 11). Similar to clay-forming elements, all peak retentions for base cations co-occurred with the peak strain and peak clay in DM3. The low relief catena had overlapping peak retentions of Ca (net loss) and Mg (net gain), whereas peak K retention (net gain) was highest at the crest while that of Na (net loss) was in DM4. As a result of dust additions in Shingwedzi, it was difficult to evaluate weathering using the location of peak taus as a proxy for weathering strength and the extent to which base cations were leached. To illustrate, it would seem like the leaching extent of Na along Shingwedzi catenas was moving upslope with increased catchment area: from 97 % in DH, 60 % in DM and 31 % in DL. How can increasing water availability result in a crest-ward shift in the maximum retention of Na? Short of invoking dust as the scapegoat, other mechanisms can be postulated. First, it might be that the increasing hillslope length does not increase

water availability because nearly all the water is taken up by plants. Second, the shorter hillslope might have a longer effective length for water transport while the same length on a longer hillslopes yields little re-translocation.

4.3.2 Skukuza-Pretoriuskop

The maximum retention of Ca and Mg occurred at the toeslope of IH in concert with peak clay. Sodium and K peaks, on the other hand, occurred in IH2 (Fig. 11). In IM, peak retention of Ca was in IM4 (coinciding with peak clay) while the other bases peaked together in IM5. For the low relief catena, the peak taus for the divalent cations occurred in IL6 alongside the peak strain on the hillslope. The monovalent cations had peaks in IL4.

In Pretoriuskop, the peak retentions of Ca, K and Na were in WH5, while that of Mg overlapped with maximum strain and clay in WH6 (Fig. 11). With reduced steepness in WM, strain, clay, Mg, K and Na all peaked in WM9, with Ca outlying further downslope in WM10. In the low relief hillslope Ca and K co-occurred in WL3, strain and Mg in WL6, and Na and maximum clay in WL4.

5. CONCLUSIONS

The modes of element loss/gain differed most fundamentally on an element by element basis. The suites of element behavior in dry Shingwedzi included (1) moderate losses and some gain exemplified by Si and Al; (2) high losses typified by Ca, Na, K and

P; and (3) high net elemental gains seen in Ti, Fe and Mg. In the wetter climates of Skukuza and Pretoriuskop, elemental losses were generally greater and only exhibited characteristics of a leaching system with insignificant dust persistence.

The concentration of elements at any point in the landscape is subject to many influences including heterogeneity in the underlying rock, dust inputs and mass movements upon the slope. When weathering is limited by dry condition as in Shingwedzi, the expression of various parent materials in soil composition is not masked by a high degree of elemental losses. In wet soils, by contrast, the signal from various sources of soil is subdued by massive elemental losses.

This study presented an investigation into weathering and soil development across a wide range of catenas in different topo-climatic contexts, using geochemical mass balance. As far as I am aware, mine is a unique study of mass balance on a wide range of catenas as advocated by Sommer and Schlichting (1997) some ten years ago. Their appeal was that soil scientists should go beyond descriptions of catenas based on soil morphology and the distribution of soil types but should examine the actual processes that lead to the different soil types. This study is an attempt at that, albeit limited by being solely focused on elemental transfers across catenas. When combined with other work on soil morphology and properties in chapter 3, it provides a powerful foundation for further investigations into how catenas form and evolve.

List of figures

Figure 1. Depth-integrated zirconium-based strain in soil profiles of the relief-climate matrix of Kruger.

Figure 2. Depth weighted average net losses and gains of Si in soil profiles along catenas in Kruger's relief-climate matrix.

Figure 3. Depth weighted average net losses and gains of Al in soil profiles along catenas in Kruger's relief-climate matrix.

Figure 4. Depth weighted average net losses and gains of Ca in soil profiles along catenas in Kruger's relief-climate matrix.

Figure 5. Depth weighted average net losses and gains of Na in soil profiles along catenas in Kruger's relief-climate matrix.

Figure 6. Depth weighted average net losses and gains of K in soil profile along catenas in Kruger's relief-climate matrix.

Figure 7. Depth weighted average net losses and gains of P in soil profiles along catenas in Kruger's relief-climate matrix.

Figure 8. Depth weighted average net losses and gains of Mg in soil profiles along catenas in Kruger's relief-climate matrix.

Figure 9. Depth weighted average net losses and gains of Fe in soil profiles along catenas in Kruger's relief-climate matrix.

Figure 10. Relative (%) positions of maximum retention of clay-forming elements shown with maxima in strain and clay % for the nine boxes representing the relief-climate matrix sampled in Kruger. Signs represent dilation (+) and collapse (-).

Figure 11. Relative (%) positions of maximum retention of base cations shown with maxima in strain and clay % for the nine boxes representing the relief-climate matrix sampled in Kruger. Signs represent dilation (+) and collapse (-).

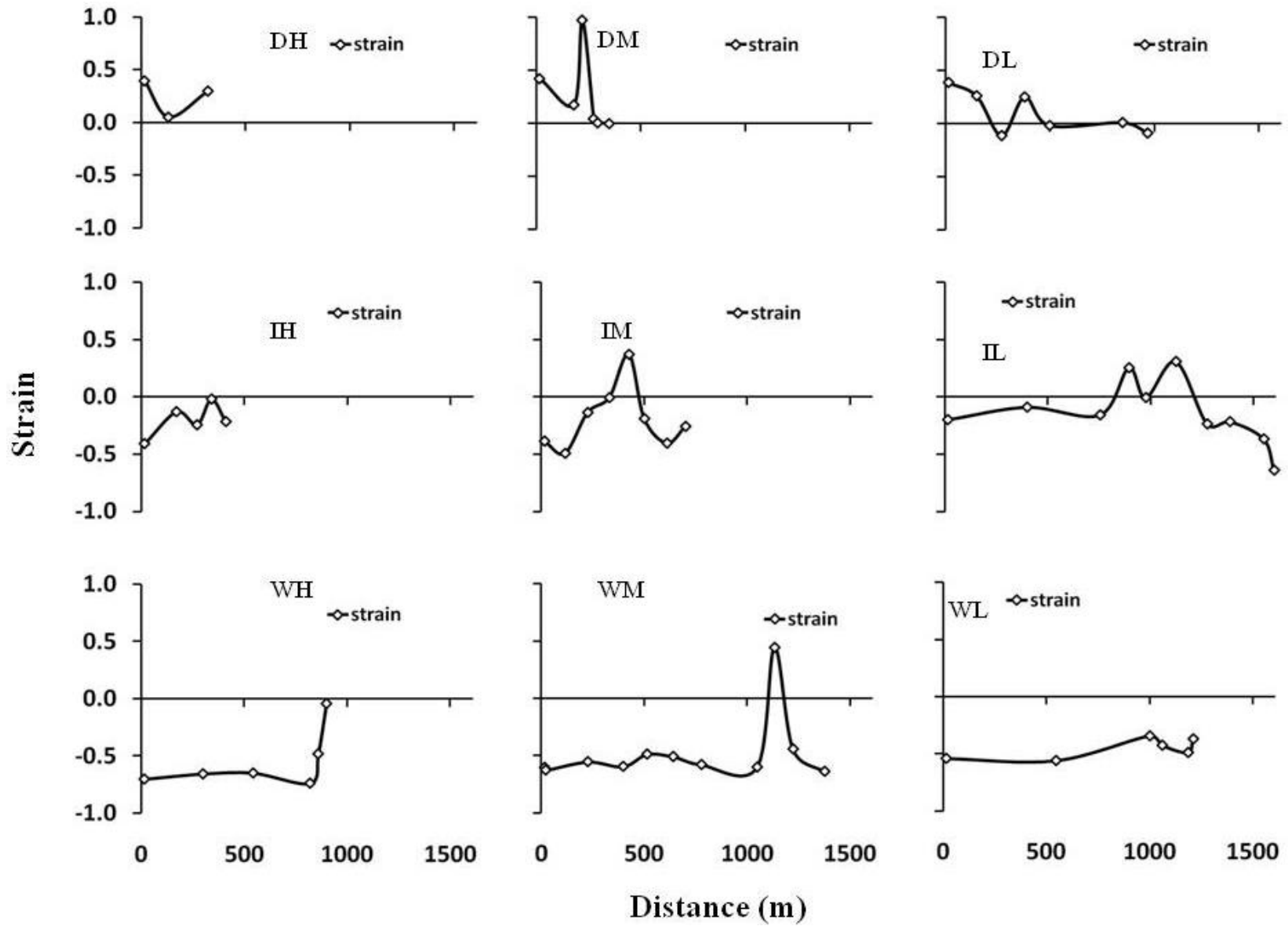


Figure 1. Depth-integrated zirconium-based strain in soil profiles of the relief-climate matrix of Kruger.

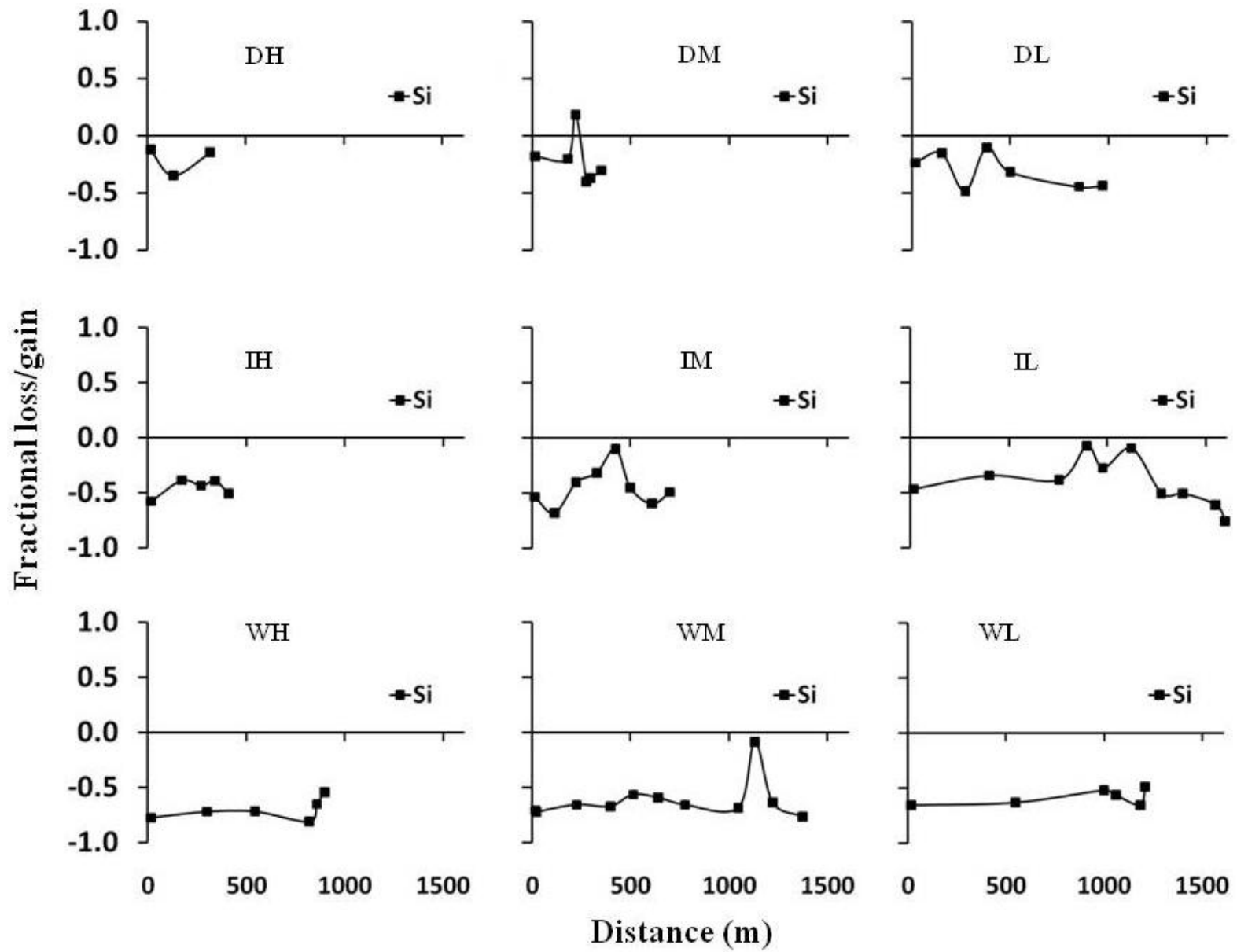


Figure 2. Depth weighted average net losses and gains of Si in soil profiles along catenas in Kruger's relief-climate matrix.

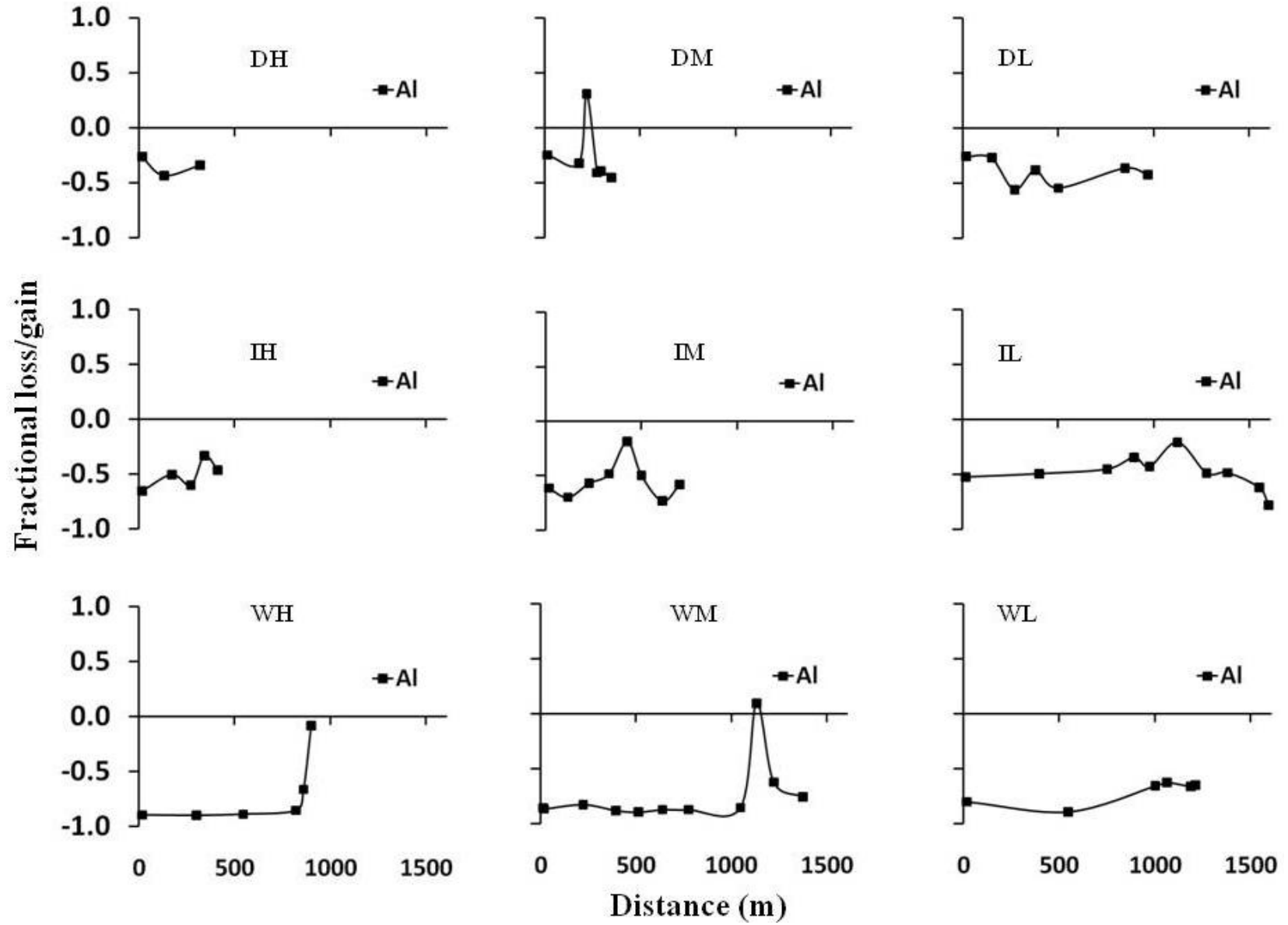


Figure 3. Depth weighted average net losses and gains of Al in soil profiles along catenas in Kruger's relief-climate matrix.

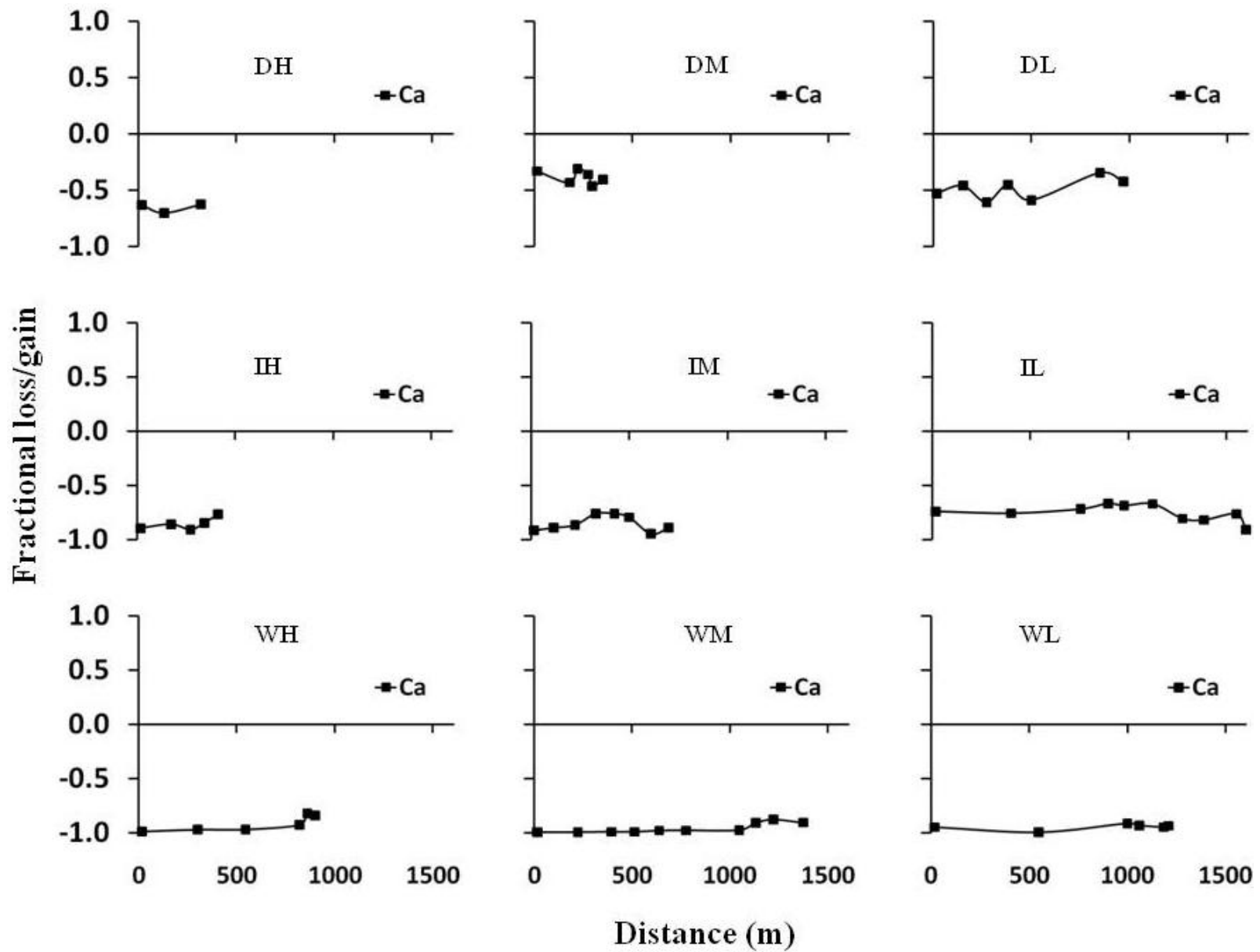


Figure 4. Depth weighted average net losses and gains of Ca in soil profiles along catenas in Kruger's relief-climate matrix.

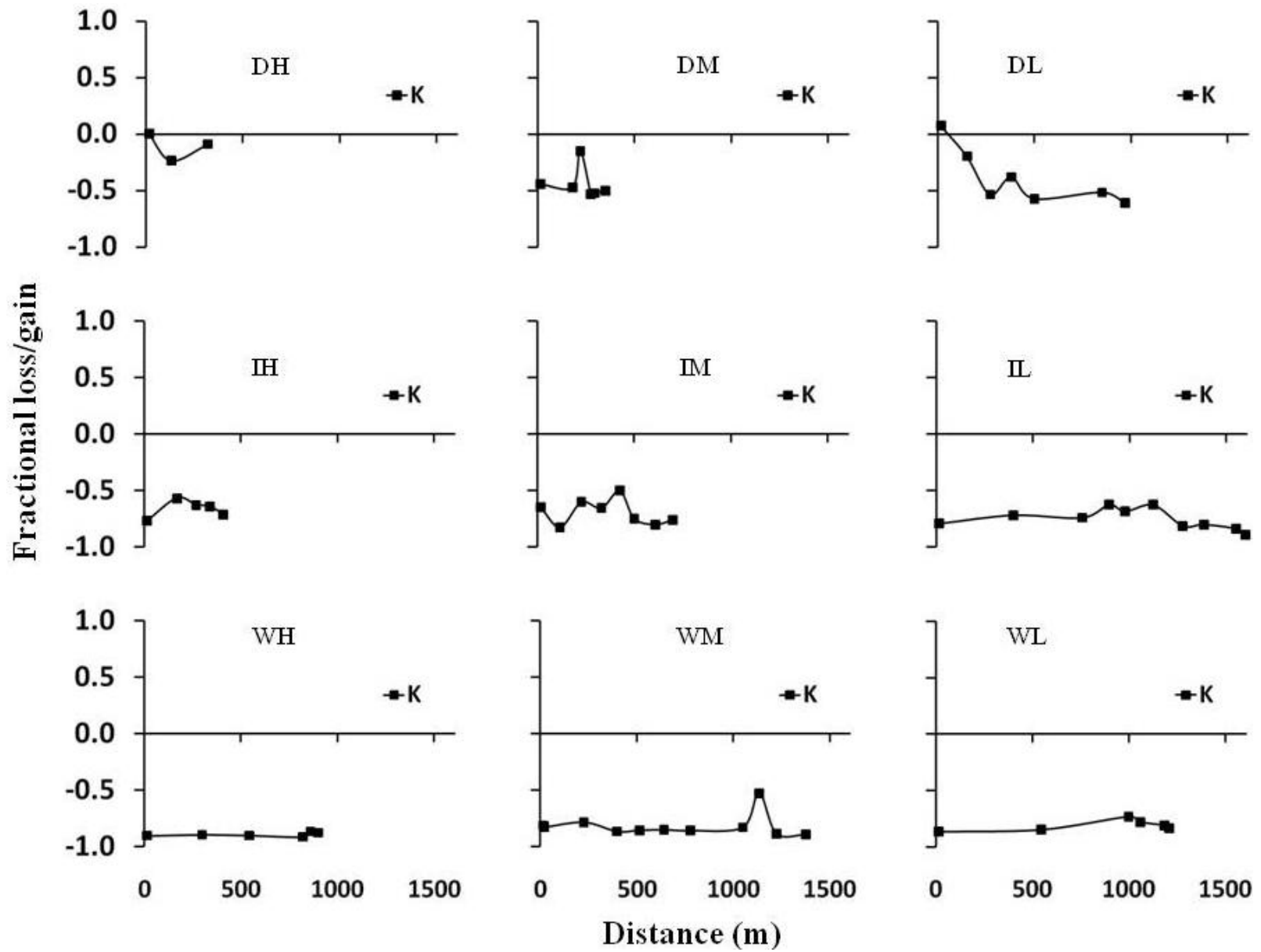


Figure 5. Depth weighted average net losses and gains of K in soil profiles along catenas in Kruger's relief-climate matrix.

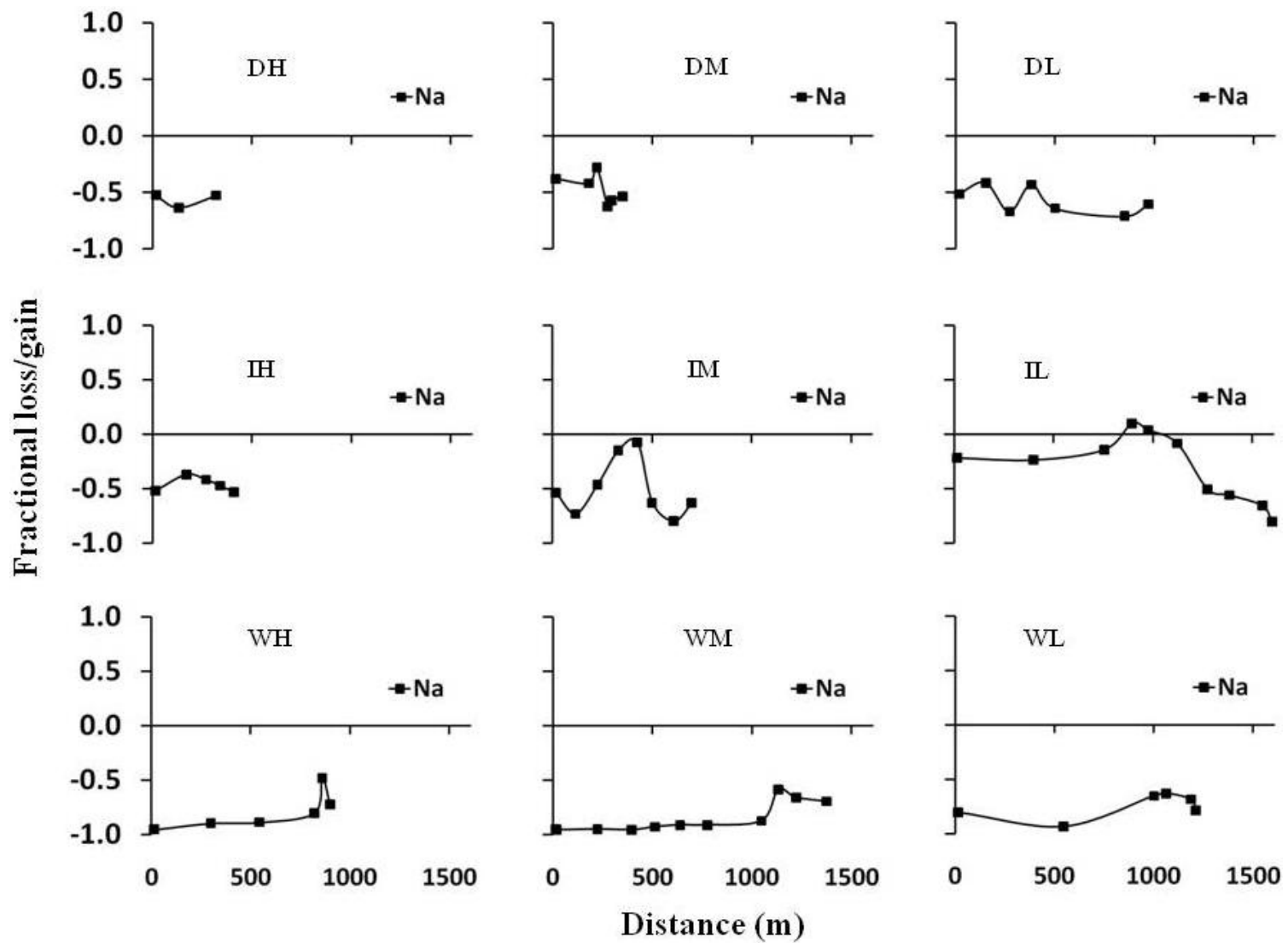


Figure 6. Depth weighted average net losses and gains of Na in soil profiles along catenas in Kruger's relief-climate matrix.

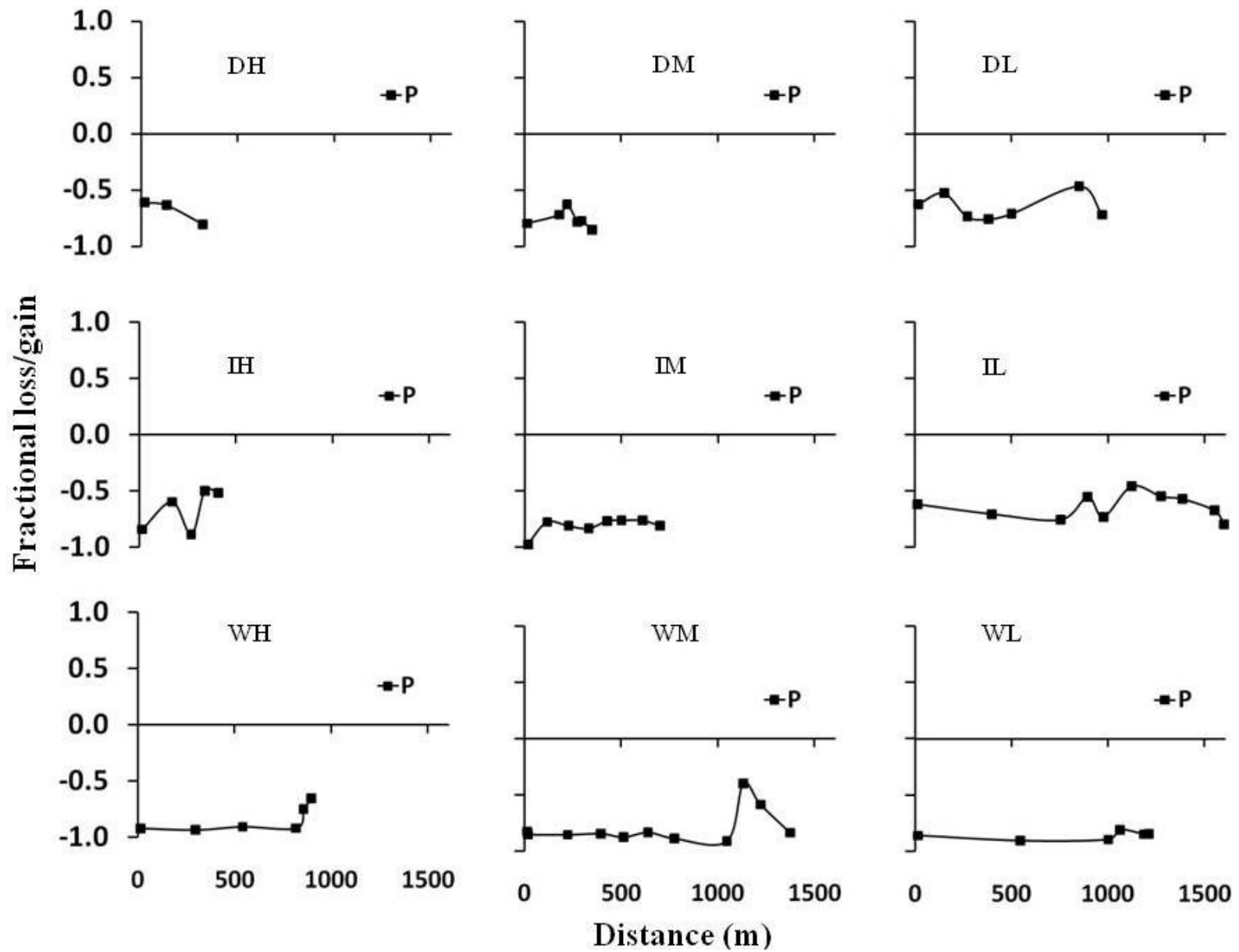


Figure 7. Depth weighted average net losses and gains of P in soil profiles along catenas in Kruger's relief-climate matrix

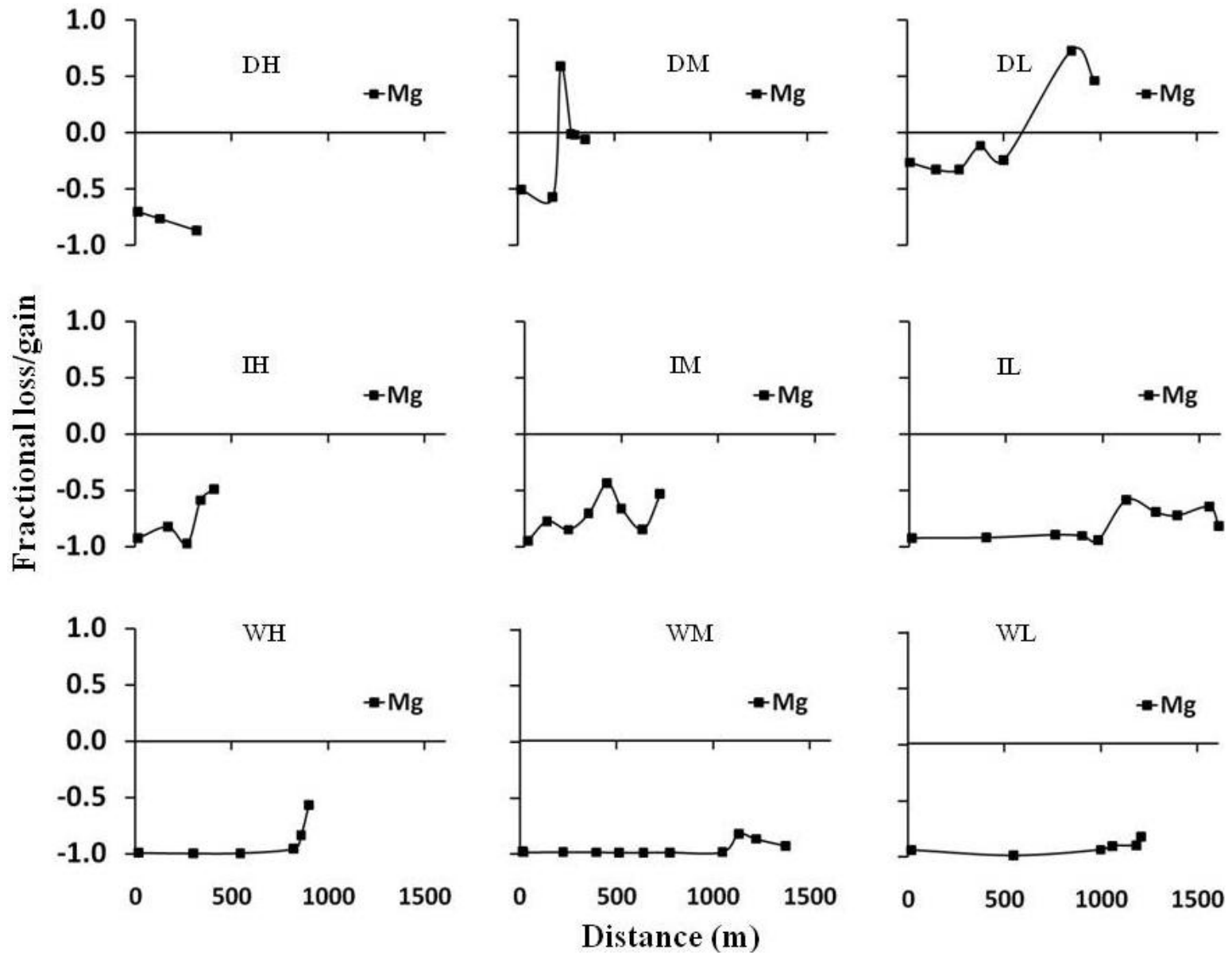


Figure 8. Depth weighted average net losses and gains of Mg in soil profiles along catenas in Kruger's relief-climate matrix

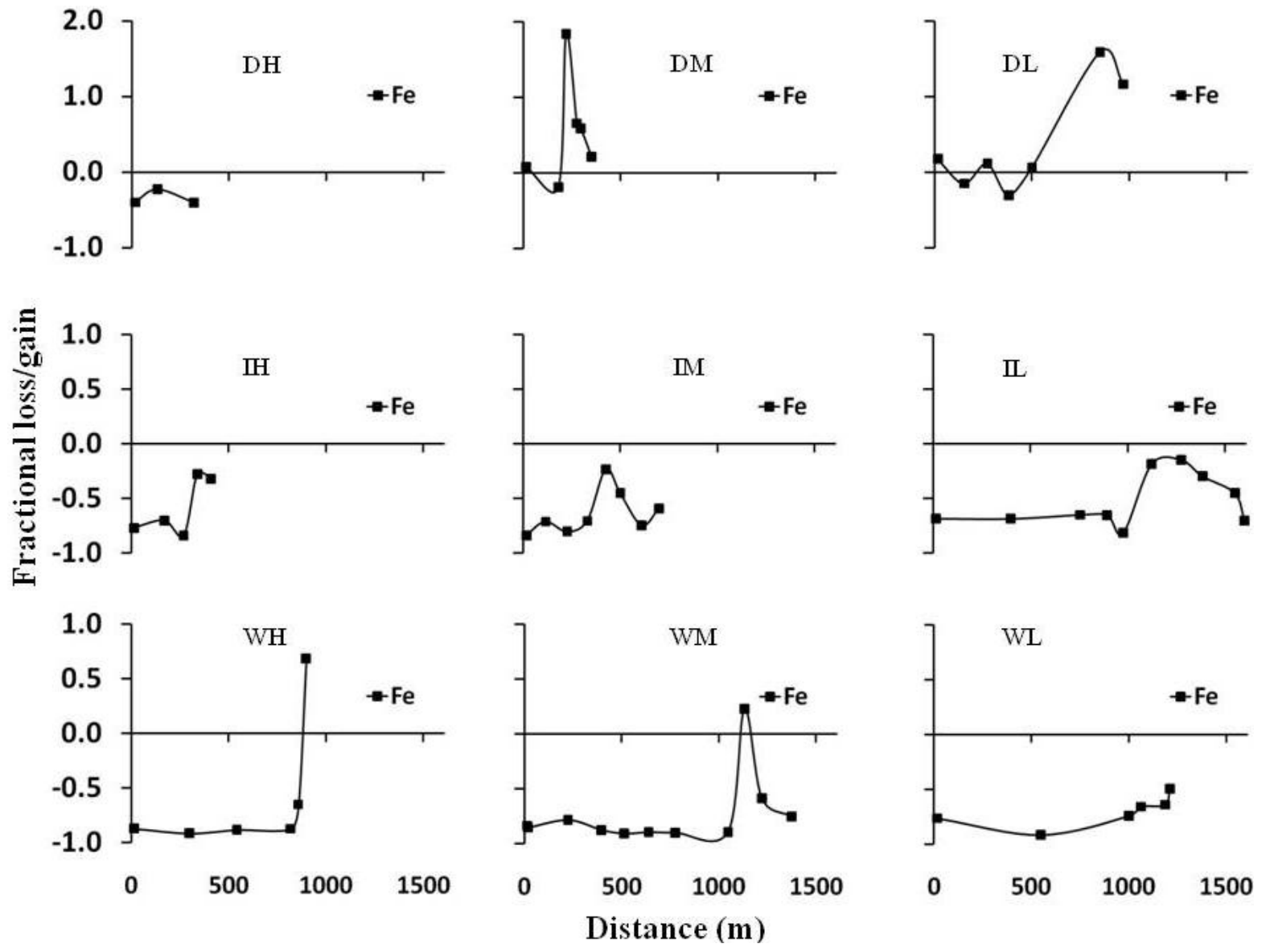


Figure 9. Depth weighted average net losses and gains of Fe in soil profiles along catenas in Kruger's relief-climate matrix.

5 (-) silicon	DH	5 Aluminium (-)	60 (+)	DM	60 (+)	31 (-)	DL	12 (-)
		39 – clay 5 – strain (+)		60 60 (+)			79 1 (+)	
39 – iron (-)		39 – titanium (+)	60 (+)		60 (+)	70 (+)		70 (+)
81 (-)		81 (-)	47 (-)	IM	47 (-)	48 (-)	IL	61 (-)
	IH				56 47 (+)		69 61 (+)	
81 (-)		81 (-)	47 (-)		47 (+)	69 (-)		69 (+)
99 (-)	WH	99 (-)	82 (-)	WM	82 (+)	99 (-)	WL	87 (-)
		99 99 (-)			82 82 (+)		99 87 (-)	

Figure 10. Relative (%) positions of maximum retention of clay-forming elements shown with maxima in strain and clay % for the nine boxes representing the relief-climate matrix sampled in Kruger. Signs represent dilation (+) and collapse (-).

97 Calcium (-)	DH	5 (-) magnesium	60 (-)	DM	60 (+)	70 (-)	DL	70 (+)
		39 – clay 5 – strain (+)			60 60 (+)		79 1 (+)	
97 – sodium (-)		5 – potassium (+)	60 (-)		60 (-)	31 (-)		1 (+)
98 (-)	IH	98 (-)	37 (-)	IM	47 (-)	61 (-)	IL	61 (-)
		98 81 (-)			56 47 (+)		69 61 (+)	
40 (-)		40 (-)	47 (-)		47 (-)	48 (+)		48 (-)
95 (-)	WH	99 (-)	88 (-)	WM	82 (-)	82 (-)	WL	99 (-)
		99 99 (-)			82 82 (+)		99 87 (-)	

Figure 11. Relative (%) positions of maximum retention of base cations shown with maxima in strain and clay % for the nine boxes representing the relief-climate matrix sampled in Kruger. Signs represent dilation (+) and collapse (-).

CHAPTER 6. CONCLUSIONS

The theoretical underpinnings of this study can be summarized in the conceptual model of soil formation in figure 1. This model applies to any point in a landscape. Thus in the nine-box conceptualization of catenas in Kruger National Park, the magnitudes of rainfall, hillslope length, dust accretion, *etc.* vary, leading to unique soil patterns at different points in the landscape. Also, from below ground, the degree of heterogeneity in rock changes depending on location.

The same set of processes illustrated in figure 1 has operated across all nine catenas studied here. Each catena was under a particular regime of soil forming factors and soil forming processes which determined the trajectory of weathering and soil development. In the first catena, DH, characterized by a dry climate and steep slope, limited water availability resulted in shallow depths, low clay and low concentrations of base cations (Fig. 2a). The distribution of rock-derived elements relative to their concentration in parent material also emphasized that the catena lacked a strong downslope transfer of water. Had more water been available to transfer mobile elements such as K and Mg, they would not have been most retained at the crest but would have accumulated further downslope. Elemental distributions do however suggest dust additions are a major influence on soil properties, as shown by large gains in Mg, Ti and Fe. Interestingly, it was only in the dry catenas that there was evidence of dust influence on the concentration and distribution of major elements. Dust influence was evident across all Shingwedzi catena, but was especially important on DH, where the leaching

driver was relatively attenuated. In the longer and wetter catenas of Shingwedzi, leaching effects occurred as evident in the emergence of clay-rich zones.

At the opposing end of DH in soil property space was WH in Pretoriuskop: a wet catena where the impact of dust were undetectable and near-complete mineral decomposition and strong leaching were the dominant modes of soil development (Fig. 2c.). In WH, the leaching power driven by high effective rainfall and the leaching intensity driven by the long residence time of Pretoriuskop's deep soils resulted in a catena far advanced in soil development. This "maturity" was seen most fervently expressed in the very thin extent of clay-rich soils on the catena – a mere 1 % of the entire hillslope. Other soil properties as well attested to the great leaching that had taken place on the catena. Most rock-derived elements and all exchangeable base cations were, like clay, preserved in the last possible point before being lost to the river. The clay mineralogy as well, showed that the catena was so well-leached that kaolinite occurred all through the catena, even in the most distal soil sampled, and smectite was absent in all sampled soils.

Outside the two extremes of DH and WH, the rest of the catenas exhibited behavior intermediate between the restricted soil development of DH and the highly weathered state of WH. In the Pretoriuskop area, WM and WL were also highly leached but not to the extent that WH was (Fig. 2c). Moreover, the extent of Bt horizons in WM and WL was more extensive than in WH; furthermore, smectite was present in WL; and lastly, major element and base cation losses were also not too excessive in WM and WL in comparison with WH. In the drier soils of Skukuza, patterns were like those observed in WM and WL, but again, the reduced moisture availability led to more extensive clay-

rich zone. Thus in the longer catenas of Pretoriuskop and all Skukuza catenas, the notion of clay-rich and clay-poor zones on the catenas was more convincing, while in WH it applied very marginally due to the very thin clay-rich zone.

6.1 Summary, limitations and final thoughts

I started this thesis with a framework for studying soils in an integrated and synthetic way, rather than in disaggregated means that serve narrow disciplinary biases. This was how pedology was researched by pioneers before evolutionary perspectives were overshadowed by agriculture in much of the last century. From the late 20th century until now, geology and geomorphology have re-surfaced to the pedological fore taking the study of soils beyond static description by asking the why and how of landscape structure. By posing why or how such a soil exists in some location forces answers that invoke processes and mechanism of landscape evolution. An evolutionary framework for pedology is much more likely to contribute significantly to Earth system science in general and biogeochemistry in particular. Using the catena as a concept as well as the fundamental unit of soil organization in field settings, my contribution to the process-based study of landscapes had three aims: first, I aimed to investigate the weathering and soil development on granite along a rainfall gradient. This task was undertaken without the added complication of topography; hence only crests were used. The second aim was the examination of soil patterns across catenas in different circumstances of rainfall and topography. While pioneer pedologists working in Africa specifically (see summary in Paton et al., 1995), but globally as well, have at best described special-case catenas,

catenas in this thesis are to my knowledge, the first exhaustive account of catenas in factorial space. Finally, in the last two chapters – which I think were the most valuable, geochemical mass balance was explored across catenas, challenging some basic assumptions of the method necessary when faced with old and heterogeneous landscapes.

Chapter 2 of the thesis was an analysis of soil properties on crests as they were influenced by climate with few other controlling influences. All measured soil properties in the crest soils including clay amount, clay mineralogy, exchangeable base cation concentrations and loss/ gain of major rock-forming elements showed that crests in Kruger are net exporters of rock-derived material. The amount exported depended on the rainfall, with the obvious relationship of increased material export with greater water availability. While it is certain that more rain leads to deeper soils, it is unclear whether greater leaching intensity in the wet soils was due to the wetness or soil antiquity. To cast the conundrum more clearly: what drives leaching intensity? Is it soil age which is a function of depth which is itself a function of rainfall intensity? More geomorphic work is required to decouple these variables and place weights on their importance in driving weathering intensity because all undoubtedly contribute. Beyond the unresolved issues in the crest analysis, it remains certain that massive losses occurred from every crest sampled in Kruger, even the dry ones. The losses were impressive relative to global records (Riebe et al., 2004), to the extent that they rivaled losses in areas up to ten times wetter.

The implications of these losses were explored in the third chapter where clay formation and distribution was used as the central thread in examining soil properties along catenas. There, I found context-dependency in the fate of material released from

the weathering of crest soils. This entailed correspondence between clay amount and the location of that clay on a hillslope, both being functions of rainfall and relief. Figure 2 summarizes the morphology of the 62 study pedons in nine catenas investigated in the thesis. Highlighted therein are occurrences of clay-rich horizons across the relief-climate matrix. Clearly, soils with high clay percentages occurred right across Kruger except in situations where weathering was severely limited, such as the high relief catena of Shingwedzi. Elsewhere, catenas had clay-poor skeletal soils in near-crest positions and clay-rich heavy soils near valleys. The clay chapter suffered the perennial problem in soil sampling: did I sample sufficiently? I am satisfied that the vertical dimension of the soils – surface to rock – was sampled effectively. The lateral aspect as well – crest to valley – was also sampled as best as was possible, but it could have been better. Definitely the most deficient aspect of the sampling was the restriction to nine catenas. The rainfall gradient in Kruger is continuous and hence could have been more populated than the three points investigated here. Perhaps I missed some threshold in rainfall due to the wide spacing of the climate zones. Less serious, the relief classes could have spanned a wider range so that in the end, I sampled a 5 by 5 relief-climate matrix instead of the 3 by 3. But then, sampling issues will always hound field-based soil research.

In the last two data chapters (4 and 5), I applied the same geochemical mass balance examined on crests in chapter 2 onto the nine catenas. The products of these analyses were fruitful: titanium was discounted as an index element for geochemical mass balance; and the importance of choosing the correct parent material was highlighted. The titanium result sets a precedent cautioning researchers who use Ti indiscriminately as a refractory element. But alas, zirconium itself might just be as bad,

and needs to be tested against other relatively immobile elements in the straightforward method used in this study. The fractionation of parent material during weathering was yet another previously unnoticed subtlety of how geochemical mass balance can go wrong. Thus studies on granitic substrate emplaced long ago and subsequently modified by geological agents to gneiss and migmatite should take heed to the findings in this thesis. Otherwise, estimates of elemental losses will be wrong. The synthetic parent material solution proposed for the problem of heterogeneity in parent material requires more refinement, but it is a step in the right direction.

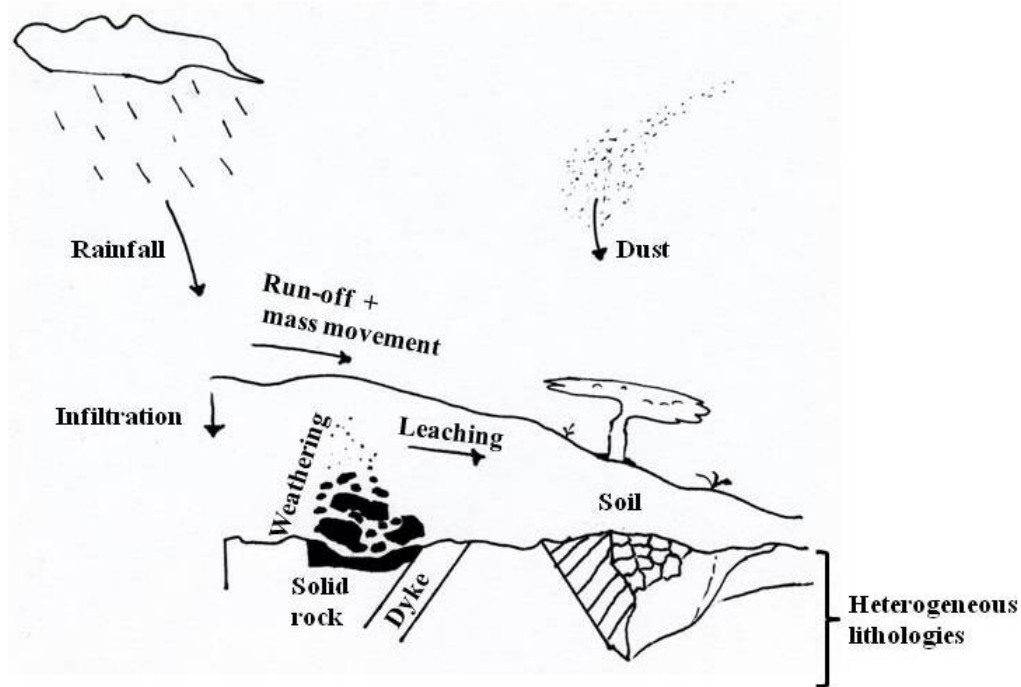


Figure 1. Conceptual links amongst soil forming processes and soil forming factors on a catena. Long-term and large-scale controls on weathering and soil properties are the rainfall and geology, these form the template upon which the soil forming processes act. Weathering releases material from primary minerals in rock and leaching can remove weathering products. The weathering and leaching intensity are rainfall dependent. Part of the rainfall infiltrates the soil, a subset of which is involved in weathering and another in leaching. Some of the rainfall may induce removal of surficial material through mass movement. Dust is added to a greater or lesser degree. All these interactions occur on catenas in various setting of climate and geology.

Figure 2. Depiction of variation in soil morphology among sampled catenas. Each box represents 20 cm, inside the box are horizons designations in order of appearance with depth, number at the bottom of cross is the relative distance of the pedon where 100 % is the toeslope and 0 % is the crest, shading marks clay-rich horizons. The locations of the maximum retention of elements by geochemical mass balance and the maximum strain along catenas are indicated by “Strain” and element symbols, location of maximum magnitudes of the base cations are indicated by xBase and the semi-quantitative amounts of smectite and kaolinite are also shown, (a) is Shingwedzi, (b) is Skukuza and (c) is Pretoriuskop.

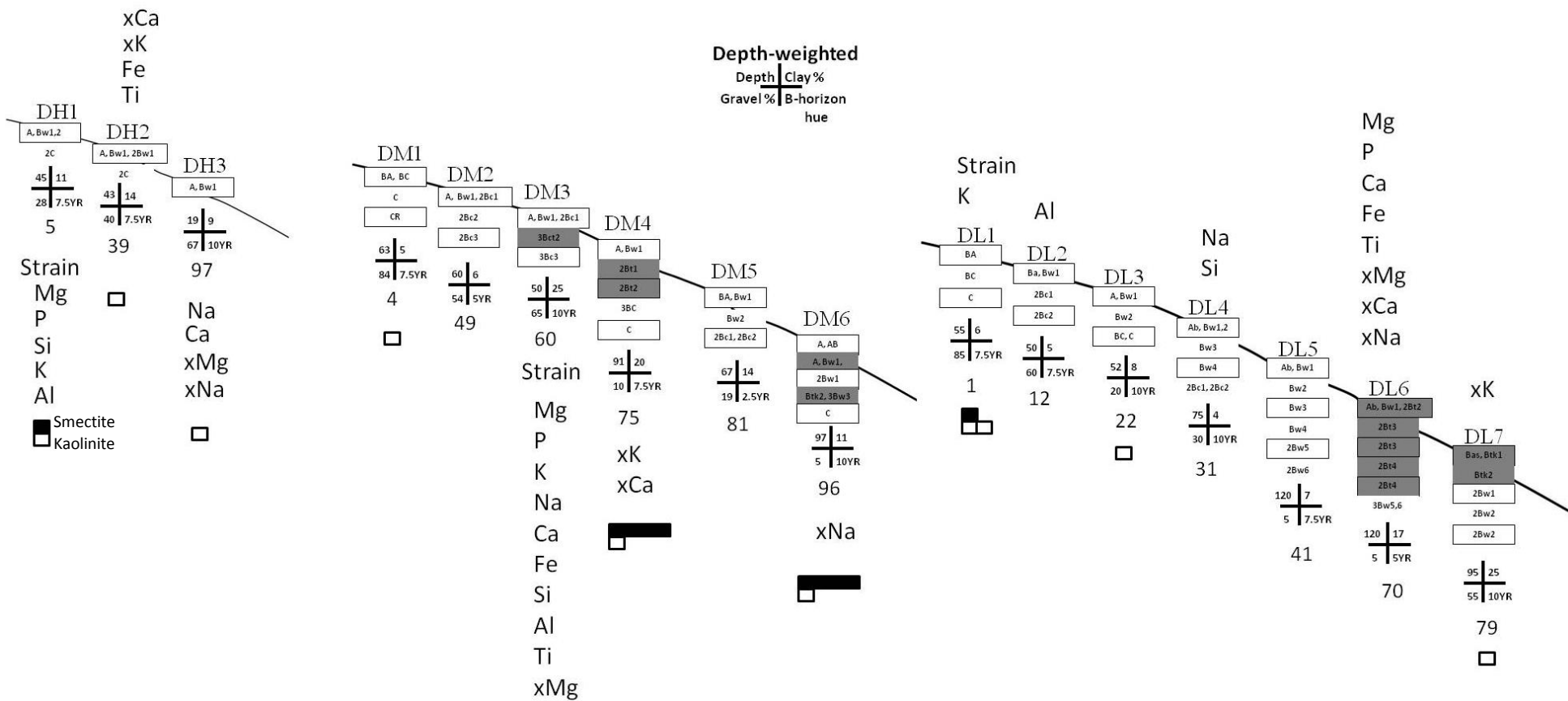


Figure 2a. Shingwedzi soil catenas.

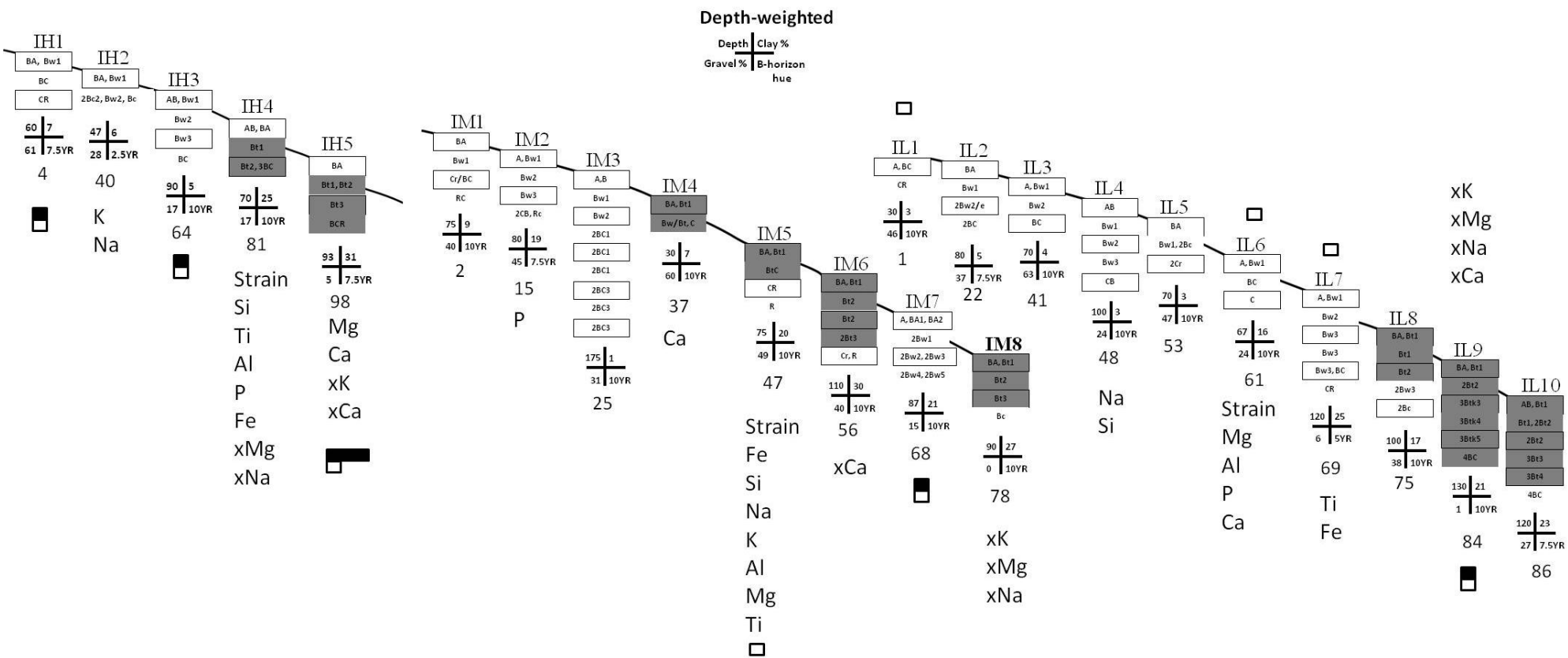


Figure 2b. Skukuza soil catenas.

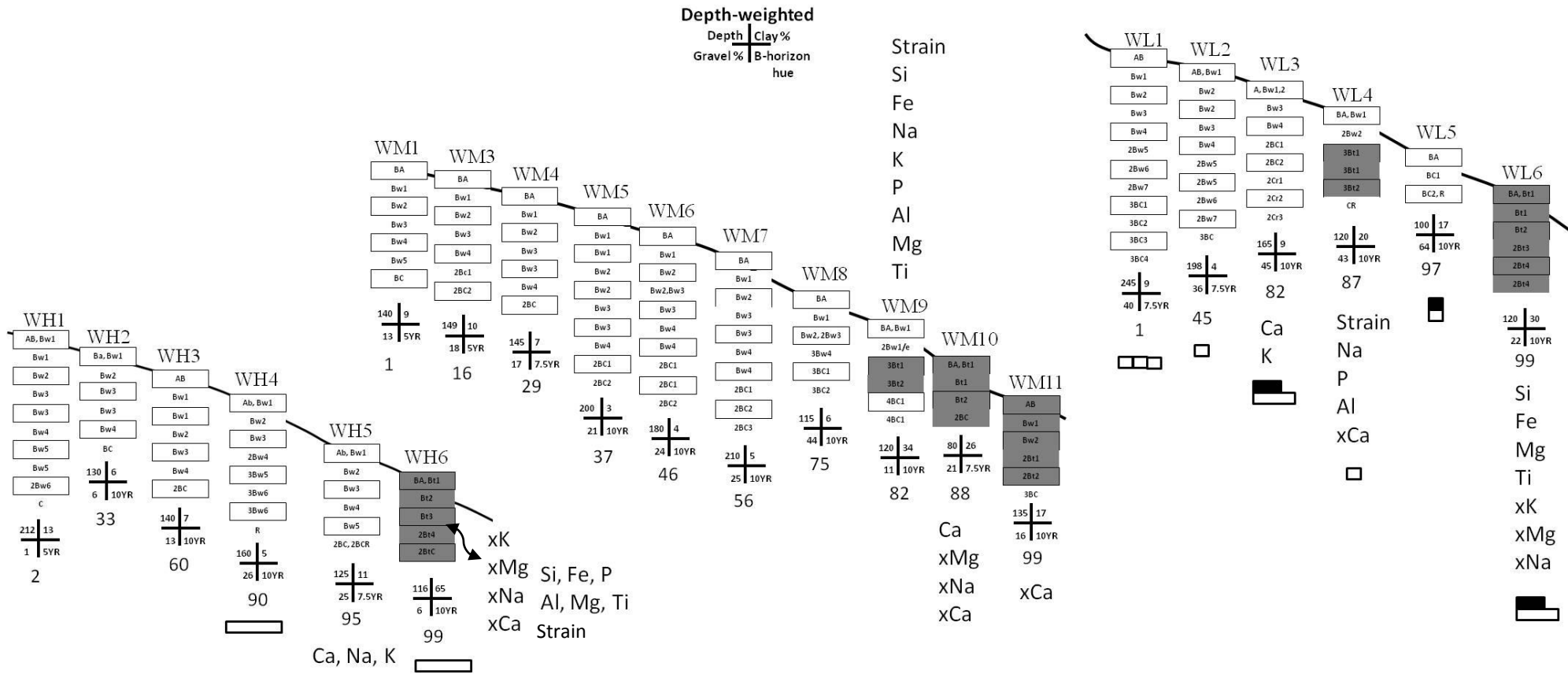


Figure 2c. Pretoriuskop soil catenas.

REFERENCES

- Ajmone Marsan, F., Bain, D.C. and Duthie, D.M.L., 1988. Parent material uniformity and degree of weathering in a soil chronosequence, northwestern Italy. *Catena*, 15: 507-517.
- Anonymous, 1940. Obituary notice. *Soils and Fertilizers*, 3(4): 147-148.
- Barton, J.M., Bristow, J.W. and Venter, F.J., 1986. A summary of the Precambrian granitoid rocks of the Kruger National Park. *Koedoe*, 29: 39-44.
- Bern, C.R., Porder, S. and Townsend, A.R., 2007. Erosion and landscape development decouple strontium and sulfur in the transition to dominance by atmospheric inputs. *Geoderma*, 142(3-4): 274-284.
- Bierman, P.R. and Clapp, E.M., 1996. Estimating geologic age from cosmogenic nuclides: an update. *Science*, 271(15 March 1996): 1606.
- Birkeland, P.W., 1999. *Soils and geomorphology*. Oxford University Press, Oxford.
- Birkeland, P.W., Berry, M.E. and Swanson, D.K., 1991. Use of soil catena field data for estimating relative ages of moraines. *Geology*, 19(3): 281-283.
- Botha, G. and Porat, N., 2007. Soil chronosequence development in dunes on the southeast African coastal plain, Maputaland, South Africa. *Quaternary International*, 162: 111-132.
- Brady, N.C. and Weil, R.R., 2002. *The nature and properties of soils*. Prentice hall, New Jersey.
- Brantley, S.L., Goldhaber, M.B. and Ragnarsdottir, K.V., 2007. Crossing disciplines and scales to understand the Critical Zone. *Elements*, 3(5): 307-314.
- Bravo, O., Blanco, M.D. and Amiotti, N., 2007. Control factors in the segregation of Mollisols and Aridisols of the semiarid-arid transition of Argentina. *Catena*, 70(2): 220-228.
- Bridges, E.M., 1978. *World soils*. Cambridge University Press, New York, 128 pp.

- Brimhall, G.H., Chadwick, O.A., Lewis, C.J., Compston, W., Williams, I.S., Danti, K.J., Dietrich, W.E., Power, M.E., Hendricks, D. and Bratt, J., 1991. Deformational mass transport and invasive processes in soil evolution. *Science*, 255(5045): 695-702.
- Brimhall, G.H. and Dietrich, W.E., 1987. Constitutive mass balance relations between chemical-composition, volume, density, porosity, and strain in metasomatic hydrochemical systems: results on weathering and pedogenesis. *Geochimica Et Cosmochimica Acta*, 51(3): 567-587.
- Brimhall, G.H., Lewis, C.J., Ague, J.J., Dietrich, W.E., Hampel, J., Teague, T. and Rix, P., 1988. Metal enrichment in bauxites by deposition of chemically mature aeolian dust. *Nature*, 333(6176): 819-824.
- Brown, D.J., 2006. A historical perspective on soil-landscape modeling. In: S. Grunwald (Editor), *Environmental soil-landscape modeling: geographic information technologies and pedometrics*. CRC/Taylor & Francis, Boca Raton, FL.
- Brown, D.J., Clayton, M.K. and McSweeney, K., 2004. Potential terrain controls on soil color, texture contrast and grain-size deposition for the original catena landscape in Uganda. *Geoderma*, 122(1): 51-72.
- Buhmann, C. and Kirsten, W.F.A., 1991. The mineralogy of five weathering profiles developed from Archaean granite in the eastern Transvaal, Republic of South Africa. *S. Afr. J. Plant Soil* 8: 146-152.
- Burbank, D.W. and Pinter, N., 1999. Landscape evolution: the interactions of tectonics and surface processes. *Basin Research*, 11(1): 1-6.

- Burt, T.P. and Park, S.J., 1999. The distribution of solute processes on an acid hillslope and the delivery of solutes to a stream: I. Exchangeable bases. *Earth Surface Processes and Landforms*, 24(9): 781-797.
- Carter, M.R., 1993. *Soil sampling and methods of analysis*. Lewis, Boca City.
- Chadwick, O.A. and Chorover, J., 2001. The chemistry of pedogenic thresholds. *Geoderma*, 100(3-4): 321-353.
- Chadwick, O.A. and Davis, J.O., 1990. Soil-forming intervals caused by aeolian sediment pulses in the Lahontan basin, northwestern Nevada. *Geology*, 18(3): 243-246.
- Chadwick, O.A., Gavenda, R.T., Kelly, E.F., Ziegler, K., Olson, C.G., Elliott, W.C. and Hendricks, D.M., 2003. The impact of climate on the biogeochemical functioning of volcanic soils. *Chemical Geology*, 202(3-4): 195-223.
- Chamran, F., Gessler, P.E. and Chadwick, O.A., 2002. Spatially explicit treatment of soil-water dynamics along a semi-arid catena. *Soil Sci. Soc. Am. J.*, 66: 1571-1583.
- Chappel, C., 1992. The ecology of sodic sites in the Eastern Transvaal Lowveld. M.Sc. thesis Thesis, University of the Witwatersrand, Johannesburg.
- Chittleborough, D.J., 1992. Formation and pedology of duplex soils. *Australian Journal of Experimental Agriculture*, 32(7): 815-825.
- Chittleborough, D.J. and Oades, J.M., 1980. The development of a red-brown earth 2: uniformity of the parent material. *Australian Journal of Soil Research*, 18(4): 375-382.
- Chittleborough, D.J., Oades, J.M. and Walker, P.H., 1984. Textural differentiation in chronosequences from eastern Australia 3: evidence from elemental chemistry. *Geoderma*, 32(3): 227-248.

- Chorover, J., Kretzschmar, R., Garcia-Pichel, F. and Sparks, D.L., 2007. Soil biogeochemical processes within the Critical Zone. *Elements*, 3(5): 321-326.
- Cockburn, H.A.P., Brown, R.W., Summerfield, M.A. and Seidl, M.A., 2000. Quantifying passive margin denudation and landscape development using a combined fission-track thermochronology and cosmogenic isotope analysis approach. *Earth and Planetary Science Letters*, 179(3-4): 429-435.
- Cockburn, H.A.P. and Summerfield, M.A., 2004. Geomorphological applications of cosmogenic isotope analysis. *Progress in Physical Geography*, 28(1): 1-42.
- Cornu, S., Lucas, Y., Lebon, E., Ambrosi, J.P., Luizao, F., Rouiller, J., Bonnay, M. and Neal, C., 1999. Evidence of titanium mobility in soil profiles, Manaus, central Amazonia. *Geoderma*, 91(3-4): 281-295.
- Cox, P.A., 1995. *The elements on Earth : inorganic chemistry in the environment*. Oxford University Press, Oxford.
- Dahlgren, R.A., Boettinger, J.L., Huntington, G.L. and Amundson, R.G., 1997. Soil development along an elevational transect in the western Sierra Nevada, California. *Geoderma*, 78(3-4): 207-236.
- Dollar, E.S.J., James, C.S., Rogers, K.H. and Thoms, M.C., 2007. A framework for interdisciplinary understanding of rivers as ecosystems. *Geomorphology*, 89(1-2): 147-162.
- ESRI, 2005. *ARC/Info*. ESRI, Inc, Redlands, CA.
- Ewing, S.A., Sutter, B., Owen, J., Nishiizumi, K., Sharp, W., Cliff, S.S., Perry, K., Dietrich, W., McKay, C.P. and Amundson, R., 2006. A threshold in soil formation at Earth's arid-hyperarid transition. *Geochimica Et Cosmochimica Acta*, 70(21): 5293-5322.

- Fleming, A., Summerfield, M.A., Stone, J.O., Fifield, L.K. and Cresswell, R.G., 1999. Denudation rates for the southern Drakensberg escarpment, SE Africa, derived from in-situ-produced cosmogenic Cl-36: initial results. *Journal of the Geological Society*, 156: 209-212.
- Gertenbach, W.P.D., 1980. Rainfall patterns in the Kruger National Park. *Koedoe*, 23: 35-43.
- Gertenbach, W.P.D., 1983. Landscapes of the Kruger National Park. *Koedoe*, 26: 9 - 121.
- Gessler, P.E., 1996b. Statistical soil-landscape modelling for environmental management. Dissertation Thesis, The Australian National University, Canberra, Australia.
- Gilchrist, A.R., Kooi, H. and Beaumont, C., 1994. Post-Gondwana geomorphic evolution of south-western Africa: implications for the controls on landscape development from observations and numerical experiments. *Journal of Geophysical Research-Solid Earth*, 99(B6): 12211-12228.
- Green, E.G., Dietrich, W.E. and Banfield, J.F., 2006. Quantification of chemical weathering rates across an actively eroding hillslope. *Earth and Planetary Science Letters*, 242(1-2): 155-169.
- Greene, H., 1947. Soil formation and water movement in the tropics. *Soil Fertility*, 10: 253-256.
- Guilfoyle, K.J., Althouse, M.L. and Chang, C.I., 2001. A quantitative and comparative analysis of linear and nonlinear spectral mixture models using radial basis function neural networks. *IEEE Transactions on Geoscience and Remote Sensing*, 39(10): 2314-2318.
- Gunn, R.H., 1974. Soil catena on weathered basalt in Queensland. *Australian Journal of Soil Research*, 12(1): 1-14.
- Heimsath, A.M., Dietrich, W.E., Nishiizumi, K. and Finkel, R.C., 1997. The soil production function and landscape equilibrium. *Nature*, 388(6640): 358-361.

- Heimsath, A.M., Dietrich, W.E., Nishiizumi, K. and Finkel, R.C., 1999. Cosmogenic nuclides, topography, and the spatial variation of soil depth. *Geomorphology*, 27(1-2): 151-172.
- Hobbs, J.E., Lindsay, J. and Bridgman, H.A., 1998. *Climates of the southern continents: present, past, and future*. John Wiley and Sons, New York.
- Hodson, M.E., 2002. Experimental evidence for mobility of Zr and other trace elements in soils. *Geochimica Et Cosmochimica Acta*, 66(5): 819-828.
- Humphreys, G.S. and Wilkinson, M.T., 2007. The soil production function: a brief history and its rediscovery. *Geoderma*, 139(1-2): 73-78.
- Jenny, H., 1941. *Factors of soil formation: a system of quantitative pedology*. McGraw-Hill, New York.
- Jones, J.A., 1990. Termites, soil fertility and carbon cycling in dry tropical Africa: a hypothesis. *Journal of Tropical Ecology*, 6: 291-305.
- King, L.C., 1944. Geomorphology of the Natal Drakensberg. *Transactions of the geological society of South Africa*, 47: 225-228.
- King, L.C., 1976. Planation remnants upon high lands. *Z. Geomorph. N.F.*, 20(2): 133-148.
- Kohl, C.P. and Nishiizumi, K., 1992. Chemical isolation of quartz for measurement of in-situ-produced cosmogenic nuclides. *Geochimica Et Cosmochimica Acta*, 56(9): 3583-3587.
- Kurtz, A.C., Derry, L.A. and Chadwick, O.A., 2001. Accretion of Asian dust to Hawaiian soils: isotopic, elemental, and mineral mass balances. *Geochimica Et Cosmochimica Acta*, 65(12): 1971-1983.
- Kurtz, A.C., Derry, L.A., Chadwick, O.A. and Alfano, M.J., 2000. Refractory element mobility in volcanic soils. *Geology*, 28(8): 683-686.

- Linacre, E.T., 1977. A simple formula for estimating evaporation rates in various climates, using temperature data alone. *Agricultural Meteorology*, 18: 409-424.
- Mabunda, D., Pienaar, D. and Verhoef, J., 2003. The Kruger National Park: a century of management and research. In: J.T. du Toit, K.H. Rogers and H. Biggs (Editors), *The Kruger experience: ecology and management of savanna heterogeneity*. Island Press, Washington, DC, pp. 3-21.
- Mason, J.A. and Jacobs, P.M., 1998. Chemical and particle-size evidence for addition of fine dust to soils of the midwestern United States. *Geology*, 26(12): 1135-1138.
- McCarthy, T.S. and Rubidge, B., 2006. *The story Of earth & life: a southern African perspective on a 4.6-billion-year journey*. Struik Publishers, Johannesburg.
- McClain, M.E., Boyer, E.W., Dent, C.L., Gergel, S.E., Grimm, N.B., Groffman, P.M., Hart, S.C., Harvey, J.W., Johnston, C.A., Mayorga, E., McDowell, W.H. and Pinay, G., 2003. Biogeochemical hot spots and hot moments at the interface of terrestrial and aquatic ecosystems. *Ecosystems*, 6(4): 301-312.
- Merrill, G.P., 1897. *A treatise on rocks, rock-weathering and soils*. Macmillan, New York, 411 pp.
- Milne, G., 1935. Some suggested units of classification and mapping, particularly for East African soils. *Soil Research*, 4: 183-198.
- Minnitt, R.C.A., 1975. *The geology of the eastern portion of the Murchison Range between the Quagga Camp Area and the Kruger National Park*. MSc Thesis, University of the Witwatersrand, Johannesburg.

- Mongelli, G., Cullers, R.L., Dinelli, E. and Rottura, A., 1998. Elemental mobility during the weathering of exposed lower crust: the kinzigitic paragneisses from the Serre, Calabria, southern Italy. *Terra Nova*, 10(4): 190-195.
- Moore, I.D., Grayson, R.B. and Ladson, A.R., 1991. Digital terrain modeling: a review of hydrological, geomorphological, and biological applications. *Hydrological Processes*, 5(1): 3-30.
- Muir, J.W. and Logan, J., 1982. Eluvial/illuvial coefficients of major elements and the corresponding losses and gains in three soil profiles. *J. Soil Science*, 33: 295-308.
- Munnik, M.C., Verster, E. and van Rooyen, T.H., 1990. Spatial pattern and variability of soil and hillslope properties in a granitic landscape 1. Pretoriuskop area. *South African Journal of Plant Soil*, 7(2): 121-130.
- Neaman, A., Chorover, J. and Brantley, S.L., 2006. Effects of organic ligands on granite dissolution in batch experiments at pH 6. *American Journal of Science*, 306(6): 451-473.
- Nesbitt, H.W. and Markovics, G., 1997. Weathering of granodioritic crust, long-term storage of elements in weathering profiles, and petrogenesis of siliciclastic sediments. *Geochimica Et Cosmochimica Acta*, 61(8): 1653-1670.
- Nikiforoff, C.C., 1949. Weathering and soil evolution. *Soil Science*, 67: 219-230.
- Nishiizumi, K., Kohl, C.P., Arnold, J.R., Klein, J., Fink, D. and Middleton, R., 1991. Cosmic-ray produced Be-10 and Al-26 in Antarctic rocks: exposure and erosion history. *Earth and Planetary Science Letters*, 104(2-4): 440-454.
- Nishiizumi, K., Winterer, E.L., Kohl, C.P., Klein, J., Middleton, R., Lal, D. and Arnold, J.R., 1989. Cosmic-ray production rates of Be-10 and Al-26 in quartz from glacially polished rocks. *Journal of Geophysical Research-Solid Earth and Planets*, 94(B12): 17907-17915.

- Nye, P.H., 1955a. Some soil forming processes in the humid tropics II: the development of the upper-slope member of the catena. *Journal of Soil Science*, 6(1): 48-62.
- Nye, P.H., 1955b. Some soil forming processes in the humid tropics, IV: the action of soil fauna. *Journal of Soil Science*, 6: 73-83.
- Parsons, A.J., 1977. A technique for the classification of hill-slope forms. *Transactions of the Institute of British Geographers*, 3: 432-444.
- Partridge, T.C. and Maud, R.R., 1987. Geomorphic evolution of southern Africa since the Mesozoic. *South African Journal of Geology*, 90(2): 179-208.
- Paton, T.R., Humphreys, G.S. and Mitchell, P.B., 1995. *Soils: a new global view*. Yale University Press, New Haven.
- Pickett, S.T.A. and Cadenasso, M.L., 1995. Landscape ecology: spatial heterogeneity in ecological systems. *Science*, 269(5222): 331-334.
- Porder, S., Hilley, G.E. and Chadwick, O.A., 2007. Chemical weathering, mass loss, and dust inputs across a climate by time matrix in the Hawaiian Islands. *Earth and Planetary Science Letters*, 258(3-4): 414-427.
- Porder, S., Paytan, A. and Vitousek, P.M., 2005. Erosion and landscape development affect plant nutrient status in the Hawaiian Islands. *Oecologia*, 142(3): 440-449.
- Railsback, L.B., 2003. An earth scientist's periodic table of the elements and their ions. *Geology*, 31(9): 737-740.
- Raymo, M.E. and Ruddiman, W.F., 1992. Tectonic forcing of late Cenozoic climate. *Nature*, 359(6391): 117-122.

- Riebe, C.S., Kirchner, J.W. and Finkel, R.C., 2003. Long-term rates of chemical weathering and physical erosion from cosmogenic nuclides and geochemical mass balance. *Geochimica Et Cosmochimica Acta*, 67(22): 4411-4427.
- Riebe, C.S., Kirchner, J.W. and Finkel, R.C., 2004. Erosional and climatic effects on long-term chemical weathering rates in granitic landscapes spanning diverse climate regimes. *Earth and Planetary Science Letters*, 224(3-4): 547-562.
- Robb, L.J., 1977. The geology and geochemistry of the archaean granite-greenstone terrane between Nelspruit and Bushbuckridge, Eastern Transvaal. MSc Thesis, University of the Witwatersrand.
- Robb, L.J., 1983. The nature, origin and significance of archaean migmatites in the Barberton mountaintailand: a new approach in the assessment of early crustal evolution. *Spec. Publ. Geol. Soc. S. Afr.*, 9: 81-101.
- Rosin, P.L., 2001. Robust pixel unmixing. *IEEE Transactions on Geoscience and Remote Sensing*, 39(9): 1978-1983.
- Rountree, M.R., Rogers, K.H. and Heritage, G.L., 2000. Landscape state change in the semi-arid Sabie River, Kruger National Park, in response to flood and drought. *South African Geographical Journal*, 82(3): 173-181.
- Sauve, S. and Hendershot, W.H., 1995. Cation selectivity coefficient variations in acidic forest soils in Sutton, Quebec. *Geoderma*, 68: 301-308.
- Schaetzl, R.J. and Anderson, S., 2005. *Soils: genesis and geomorphology*. Cambridge University Press, Cambridge.
- Schoeneberger, P.J., 1998. *Field book for describing and sampling soils*. National Soil Survey Center, Natural Resources Conservation Service, U.S. Dept. of Agriculture, Lincoln, NE.

- Schoeneberger, P.J., Wysocki, D.A., Benham, E.C. and Broderson, W.D., 2002. Field book for describing and sampling soils. Version 2.0. Natural Resources Conservation Service, United States Department of Agriculture, Lincoln, NE.
- Scholes, R.J., 1986. A guide to bush encroachment in the eastern Transvaal Lowveld. Resource ecology group, Witswatersrand University, Johannesburg.
- Scholes, R.J., 1987. Response of three semi-arid savannas on contrasting soils to the removal of the woody component. PhD Thesis, University of the Witwatersrand, Johannesburg.
- Scholes, R.J., Bond, W.J. and Eckhardt, H.C., 2003. Vegetation dynamics in the Kruger ecosystem. In: J.T. du Toit, K.H. Rogers and H.C. Biggs (Editors), Ecology and Management of Savanna Heterogeneity. Island Press, Washington, DC.
- Scholes, R.J. and Walker, B.H., 1993. An African savanna: a synthesis of the Nylsvley study. Cambridge University Press, Cambridge.
- Scholten, T., Felix-Henningsen, P. and Schotte, M., 1997. Geology, soils and saporlites of the Swaziland Middleveld. Soil Technology, 11(3): 229-246.
- Schulze, R.D., 1997. South African atlas of agrohydrology and climatology, Water Research Commission, Pretoria, Report TT82/96.
- Schutte, I.C., 1986. The general geology of the Kruger National Park. Koedoe, 29: 13-37.
- Scribner, A.M., Kurtz, A.C. and Chadwick, O.A., 2006. Germanium sequestration by soil: targeting the roles of secondary clays and Fe-oxyhydroxides. Earth and Planetary Science Letters, 243(3-4): 760-770.
- Simonson, R.W., 1995. Airborne dust and its significance to soils. Geoderma, 65(1-2): 1-43.
- Soil Survey Staff, 1996. Soil survey laboratory methods manual. Soil survey investigation report no. 42 Version 3.0, National Soil Survey Centre, Lincon, NE.

- Sommer, M., Halm, D., Weller, U., Zarei, M. and Stahr, K., 2000. Lateral podzolization in a granite landscape. *Soil Science Society of America Journal*, 64(6): 2069-2069.
- Sommer, M. and Schlichting, E., 1997. Archetypes of catenas in respect to matter: a concept for structuring and grouping catenas. *Geoderma*, 76(1-2): 1-33.
- Stiles, C.A., Mora, C.I. and Driese, S.G., 2003. Pedogenic processes and domain boundaries in a Vertisol climosequence: evidence from titanium and zirconium distribution and morphology. *Geoderma*, 116(3-4): 279-299.
- Still, C.J., Berry, J.A., Ribas-Carbo, M. and Helliker, B.R., 2003. The contribution of C-3 and C-4 plants to the carbon cycle of a tallgrass prairie: an isotopic approach. *Oecologia*, 136(3): 347-359.
- Taboada, T., Cortizas, A.M., Garcia, C. and Garcia-Rodeja, E., 2006. Particle-size fractionation of titanium and zirconium during weathering and pedogenesis of granitic rocks in NW Spain. *Geoderma*, 131(1-2): 218-236.
- Tarboton, D.G., 1997. A new method for the determination of flow directions and upslope areas in grid digital elevation models. *Water Resources Research*, 33(2): 309-319.
- Tardy, Y., Bocquier, G., Paquet, H. and Millot, G., 1973. Formation of clay from granite and its distribution in relation to climate and topography. *Geoderma*, 10(4): 271-284.
- Theissen, A.A. and Harwars, M.E., 1962. A paste method for preparation of slides for clay mineral identification by X-ray diffraction. *Proceedings of the soil science society of America*, 26: 90-91.
- Tilahun, K., 2006. The characterisation of rainfall in the arid and semi-arid regions of Ethiopia. *Water SA*, 32(3): 429-436.

- Tyson, P.D. and Partridge, T.C., 2000. Evolution of cenozoic climates. In: T.C. Partridge and R.R. Maud (Editors), Oxford monographs on geology and geophysics: The cenozoic of southern Africa. Oxford University Press, Cape Town.
- Venter, F.J., 1990. A classification of land for management planning in the Kruger National Park. PhD Thesis, University of South Africa.
- Venter, F.J. and Bristow, J.W., 1986. An account of the geomorphology and drainage of the Kruger National Park. *Koedoe*, 29: 117-124.
- Venter, F.J., Scholes, R.J. and Eckhardt, H.C., 2003. The Abiotic template and its associated vegetation pattern. In: J.T. du Toit, K.H. Rogers and H. Biggs (Editors), *The Kruger experience: ecology and management of savanna heterogeneity*. Island Press, Washington, DC, pp. 83-129.
- Vitousek, P.M., 2002. Oceanic islands as model systems for ecological studies. *Journal of Biogeography*, 29(5-6): 573-582.
- Vitousek, P.M., 2004. *Nutrient cycling and limitation: Hawaii as a model system*. Princeton University Press, Princeton.
- Vorster, C.J., 1979. Die geologie van die Klein-Letabagebied, noord-oos-Transvaal met spesiale verwysing na die granitiese gesteentes. MSc thesis, Rand Afrikaans University.
- Watson, J.P., 1964. Soil catena on granite in Southern Rhodesia I: field observations. *Journal of Soil Science*, 15(2): 239-257.
- White, A.F. and Blum, A.E., 1995. Effects of climate on chemical weathering in watersheds. *Geochimica Et Cosmochimica Acta*, 59(9): 1729-1747.

- Yoo, K., Amundson, R., Heimsath, A.M. and Dietrich, W.E., 2005. Process-based model linking pocket gopher (*Thomomys bottae*) activity to sediment transport and soil thickness. *Geology*, 33(11): 917-920.
- Yoo, K., Amundson, R., Heimsath, A.M., Dietrich, W.E. and Brimhall, G.H., 2007. Integration of geochemical mass balance with sediment transport to calculate rates of soil chemical weathering and transport on hillslopes. *Journal of Geophysical Research-Earth Surface*, 112(F2).
- Young, A., 1976. Tropical soils and soil survey. Cambridge geographical studies ; 9. Cambridge University Press, Cambridge, 468 p. pp.